Canadian
Journal of Chemistry

CORRECTIONS

Volume 38, 1960

Page 1135. In line 2 up, "N-dichloroacetyl chloride" should read "dichloroacetyl chloride".

Pages 1636, 1637. Subsequent to the earlier report (C. T. Bishop. Can. J. Chem. **38**, 1636 (1960)) on crystalline O-methyl ethers of D-galactitol, the author has learned that two of the derivatives described (2,4-di-O-methyl-D-galactitol and 2,3,4-tri-O-methyl-D-galactitol) were reported previously in the experimental section of a paper on the constitution of larch ϵ-galactan (G. O. Aspinall, E. L. Hirst, and E. Ramstad. J. Chem. Soc. 593 (1958)). The author sincerely regrets overlooking that report, which should be cited as the original reference to these two compounds.

THE HYDROGEN ISOTOPE EFFECT
IN THE PYROLYSIS OF CYCLOPROPANE[1]

ARTHUR T. BLADES

ABSTRACT

The hydrogen isotope effect in the thermal rearrangement of cyclopropane has been determined by the copyrolysis of cyclopropane and cyclopropane-d_6. The isotope effect in the temperature range 407–514° C and at pressures of about 60 cm Hg may be expressed by

$$k_H/k_D = 0.82 \exp (1300/RT).$$

The isotope effect is pressure dependent, decreasing from 1.98 at 76 cm Hg to 1.35 at 0.0178 cm Hg at 482° C.

The isotope effect and its temperature and pressure dependence are discussed in relation to the mechanism. The conclusion is reached that though trimethylene may be formed as an intermediate, the isotope effect is consistent only with an activated complex where a hydrogen atom is weakly bonded both to its original and ultimate carbon atoms, a situation which might also lead directly to propylene. A similar argument is presented to account for the previously described isotope effect in the decomposition of cyclobutane.

INTRODUCTION

The thermal rearrangement of cyclopropane to propylene is an unusually interesting reaction for a number of reasons. It is a unimolecular reaction wherein chain processes and heterogeneous behavior are readily eliminated, and·it is the simplest of a group of cycloalkane reactions which exhibit a quasi-unimolecular behavior at relatively high pressures. Two completely different mechanisms have been proposed (1) for the reaction, one involving the intermediate formation of trimethylene diradical, and the other, formation of a transition state wherein one hydrogen atom is in the act of transferring from one carbon atom to another as the carbon–carbon bond breaks. While both mechanisms have some merit in explaining the accumulated experimental data, the latter is greatly favored on the basis of the theoretical treatment of the reaction by Slater (2).

A study of the hydrogen isotope effect in this reaction provides an important clue to the sequence of events which ultimately leads to reaction. The effect of pressure on the isotope effect may contribute to the understanding of the quasi-unimolecular behavior of unimolecular reactions at low pressures.

The tritium isotope effect in this reaction has been examined by Weston (3) and by Lindquist and Rollefson (4) by comparing the tritium content of a mixture of cyclopropane and cyclopropane-t_1 with that of propylenes produced by its isomerization. Lindquist and Rollefson found a relative rate constant expression $k/k_1 = 0.63 \exp (825/RT)$ at a pressure of 200 mm Hg in the temperature range 447–555° C, the isotope effect being 6–27%. Weston reports $k/k_1 = 0.86 \exp (385/RT)$ at the same pressure in the temperature range 406–492° C with an isotope effect up to only 17% despite the lower temperatures used. Weston also measured the isotope effect down to 0.4 mm Hg where it had decreased to approximately zero. While both of these studies suffer from

the difficulty of tritium analysis, most uncertainty arises in the interpretation of the experimental results, i.e. the conversion of k/k_1 values to true isotope effects. Here the analysis by Weston seems preferable, but the temperature coefficients so obtained (5900 ± 2000 and 8300 cal/mole) are impossibly high, as he states. In his appraisal of the pressure effect, Weston attempted to fit the data to two simple models. Both assumed that the isotope effect had fallen to its low-pressure limit at zero effect and the data fit both equally well. He pointed out that the zero effect at low pressure as found was coincidental since the isotope effect at low pressure is expected to be temperature dependent.

More recently, Schlag and Rabinovitch (5) have reported an isotope effect of 1.22 from a comparison of the rates of isomerization of cyclopropane and cyclopropane-d_2 at 718° K. Using Weston's conversion technique, this gives ($k_H/k_D = 2.18$) but this value did not decrease appreciably with pressure.

The present paper reports a study of the isotope effect in cyclopropane-d_6 as a function of temperature and pressure.

EXPERIMENTAL

The cyclopropane was Ohio Chemical Anesthetic grade and the cyclopropane-d_6 was supplied by Merck & Co. Both contained small amounts of impurities, especially propylene, which were removed by vapor phase chromatography. The deuterated compound was 93% d_6, the remainder being mainly d_5 and d_4.

The two cylindrical aluminum (2S) pyrolysis furnaces, accommodating 18- and 875-cc Pyrex reaction cells, were heated by directly applied asbestos-insulated Chromel "A" resistance wire and were lagged with 1.5-in. Marinite asbestos board with additional thicknesses at the ends. In each furnace, the reaction cell was surrounded on the sides by 1 in. of aluminum and on the ends by 1.5 in. The temperature of the small reactor was taken from the surrounding aluminum and of the large reactor from an axial thermocouple well extending to the center of the reactor. Temperatures were measured on a calibrated Pt: Pt − 10% Rh thermocouple.

The vacuum system utilized silicone-greased stopcocks throughout. No correction was attempted for reactor dead space as this was an insignificant percentage of the reactor volumes.

If two molecular species are copyrolyzed so that both have the same time and temperature history and if both exhibit first-order kinetics, then

$$k_1/k_2 = f_1/f_2 \cdot \frac{1 + 1/2f_1 + 1/3f_1^2 \ldots}{1 + 1/2f_2 + 1/3f_2^2 \ldots}$$

where f_1 and f_2 are the fractional conversions, i.e. the ratio of rate constants is the ratio of the fractional conversions modified by a correction term. If the conversions are kept below 0.1, the correction term remains small and great precision is not required in the individual conversions; the ratio of the two may be accurately determined from the ratios of the reactants and of the products. For present purposes a stock mixture of the normal and deuterated cyclopropanes was prepared and used in all subsequent experiments.

Separations of the two propylene products from reactants were carried out on a 15-ft dodecyl phthalate vapor phase chromatographic column at room temperature with hydrogen as carrier gas. The propylenes were collected in liquid-air traps, measured, and examined on a mass spectrometer. Isotope analysis of the first part of a vapor phase

chromatographic peak of a propylene sample indicated some fractionation; care was subsequently taken to collect the total chromatographic "peak".

In the mass spectrometric analysis of the propylene, the parent ions at mass 48 ($C_3D_6^+$) and 42 ($C_3H_6^+$) were taken as indicative of the relative proportions of the two isotopic species. Since the ion $C_3D_3^+$ makes a significant contribution at mass 42 at 50 v, a correction factor was determined from a sample of propylene-d_6 produced by the rearrangement of 10% of a sample of the deuterated cyclopropane. This procedure was also carried out at an ionization potential of 12 v where these corrections are considerably reduced but no significant or systematic difference was noted between the two analyses.

A similar procedure was followed in the analysis of the stock mixture of cyclopropane and cyclopropane-d_6.

In the study of the temperature coefficient, the small reactor was used throughout, conventional techniques being employed for introducing and retrieving the reactants. In the study of the pressure effect, the small reactor was used down to 50 mm Hg and the large reactor for lower pressures. In the very low pressure range, the pressure was calculated from the quantity of reactants introduced to the reactor. In experiments below 1 mm Hg, several successive runs were combined to provide sufficient sample for isotope-ratio analysis of the products.

RESULTS

The effect of pressure on the isotope effect is shown in Fig. 1 where k_H/k_D at 482° C
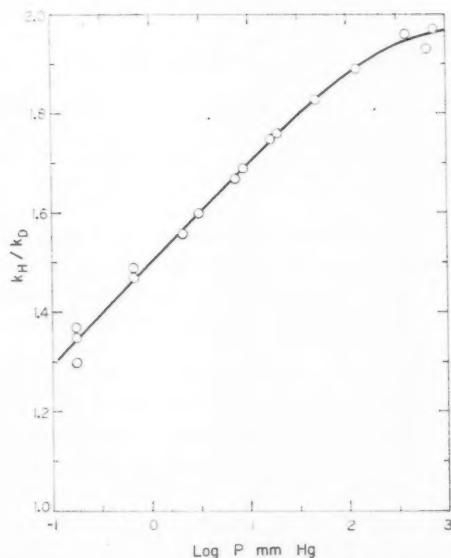
FIG. 1.   The effect of pressure on the isotope effect at 482° C.

is plotted against the logarithm of pressure for comparison with the similar plot by Weston (3). To determine the isotope effect at infinite pressure, the best plot was that suggested by Schlag and Rabinovitch (5), k_D/k_H vs. $p^{-1/2}$; the value so obtained at 482° C is 1.96.
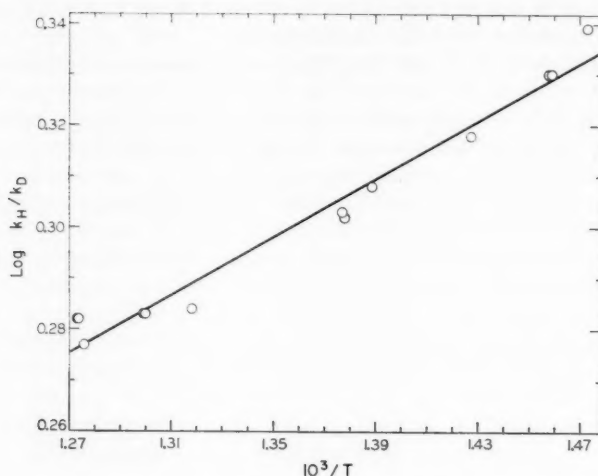
FIG. 2.   The temperature dependence of the isotope effect.

The effect of temperature on the isotope effect is illustrated in Fig. 2 and the pertinent data are presented in Table I. A least-squares treatment of these data gives an isotope effect expression.

$$k_H/k_D = 0.82 \exp (1300\pm150/RT)$$

TABLE I

Data for the relative rate constants at high pressure

Expt. No.	Pressure, cm Hg	Temperature, °K	Conversion correction	k_H/k_D
16	67.6	720.0	1.026	2.03
17	66.8	700.4	1.017	2.08
18	64.4	783.3	1.032	1.89
25	63.6	758.6	1.027	1.92
27	62.2	725.7	1.034	2.00
28	62.1	726.1	1.037	2.01
30	59.6	678.6	1.006	2.18
31	58.7	785.1	1.034	1.91
32	58.1	785.4	1.034	1.91
33	58.3	769.4	1.037	1.92
34	57.5	769.6	1.037	1.92
35	56.6	685.8	1.009	2.12
36	56.4	685.3	1.009	2.12

Since these data were obtained in the pressure range 56–68 cm Hg, it would be expected that the pre-exponential term for the isotope effect at infinite pressure would be slightly higher.

DISCUSSION

The high-pressure hydrogen isotope effect reported here (2.04 at 445° C) compares favorably with effects observed in other gas phase reactions at the same temperature, for example the ethyl–ethyl-d_5 acetate decomposition (2.23) (6) and the abstraction

reaction of CD_3 with acetone and acetone-d_6 (2.5) (7). The activation energy difference of 1300 cal/mole is slightly less than the values of 1515 cal/mole and 1670 cal/mole respectively for these two reactions but is still substantially above the maximum value of about 1150 cal/mole derivable from a single C—H stretching frequency being converted to a very weak vibration in the activated complex. It is therefore obvious that the hydrogen isotope effect in this reaction is a primary effect and that considerable carbon–hydrogen bond relaxation occurs during activation.

The decrease in the isotope effect with decreasing pressure confirms the observation of this same effect with cyclopropane-t_1 (3). Unlike that effect, which decreased to zero at 0.4 mm Hg, the present effect has not decreased to nearly the same extent at this pressure, nor is there any suggestion of its reaching a limiting value. Since this would happen only when the reaction has become truly second order, the present data must be considered as a more reliable measure of the variation of the effect with pressure.

Two quite distinct mechanisms have been proposed for the rearrangement of cyclopropane: the first, a mechanism wherein a hydrogen atom transfers from one carbon atom to another with the simultaneous breaking of the carbon ring; the second, involving the intermediate formation of a trimethylene diradical by the simple scission of the carbon ring, the propylene being subsequently formed by the transfer of a hydrogen atom from the middle carbon to a terminal one. This latter mechanism has recently been supported by the re-examination of data on the iodination of cyclopropane and on the rearrangement of cyclopropane-d_2 by Benson (8). Following the notation of Benson, the mechanism is given as

$$\triangle \underset{b}{\overset{a}{\rightleftharpoons}} T: \overset{c}{\rightarrow} P$$

and applying the steady-state treatment, the rate of formation of propylene becomes

$$\frac{dP}{dt} = \frac{k_a k_e}{k_b} \triangle \Big/ \left(1 + \frac{k_c}{k_b}\right).$$
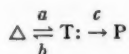
If the ratio k_c/k_b is small, then the over-all rate constant for the reaction becomes $k_a k_c/k_b$. Hence the hydrogen isotope effect observed must arise in one of these constants, and, since reaction (c) involves the transfer of a hydrogen atom, it must be assumed that k_c is the source of the primary effect, k_a and k_b probably having little, if any, isotope dependence.

The rate constant expressions derived by Benson for k_b and k_c indicate that at 444° C the reactions of trimethylene are so rapid that virtually no opportunity exists for collisions even at one atmosphere pressure. If true, this can only mean that the pressure effect in the isomerization occurs in the reaction (a), and, because the isotope effect is postulated to occur in (c) and not (a), then the isotope effect should not be pressure dependent. Since this is contrary to the experimental results, the mechanism must be incorrect unless either the instability of the trimethylene has been exaggerated, or the isotope effect in reaction (a) is of primary importance. Some assurance that the former is not the case may be gained from the results of Flowers and Frey (9), who found that at 100° C, trimethylene from the photolysis of cyclobutanone reacted with ethylene, but no such reaction occurred when cyclopropane was rearranged in the presence of excess ethylene. Both of these results are to be expected on the basis of half lives of the trimethylene radical at the two temperatures as calculated from Benson's rate-constant equations.

Two alternate interpretations may be put on a major isotope effect occurring in the reaction (a). It may be assumed that a transition state exists for the formation of trimethylene which involves a largely broken C—H bond, the hydrogen being in such a position as to considerably influence the carbon–carbon bond break. This would require that reactions (b) and (c) also have isotope effects and that they be of about the same magnitude. Since the geometric isomerization can be explained by the rotation in the trimethylene radical, it is unnecessary that the configuration of the activated complex allow for this alternate reaction. Secondly, it may be assumed that this transition state is such as to allow for geometric isomerism if it reverts to cyclopropane, and that it may go over directly to propylene. This would suggest an activated complex of the structure suggested by Smith (10) in which two hydrogens and the three carbon atoms are coplanar, with one of the hydrogens weakly bonded to its original carbon atom and to its ultimate acceptor. The postulate of a trimethylene intermediate from such a complex is unnecessary in explaining the experimental facts. The hydrogen isotope effect data does not conclusively decide between these two reaction schemes. It seems most reasonable to accept the latter, however, purely on the basis that, if the hydrogen does become bridged from one carbon to the next, as it must if it is to be of any assistance in the rupture of the carbon–carbon bond, then it will be most advantageous for it to continue on its path toward that carbon atom.

It is interesting to compare the isotope effect in this reaction with that observed for the decomposition of cyclobutane (11) to ethylene where the effect is 1.37 at 449° C, and the activation energy difference, 1400 cal/mole. The existence of this effect, despite the fact that the hydrogens do not transfer during the reaction, suggests that there is some similarity between the cyclopropane rearrangement and this decomposition. The similarity of the activation energy differences (1400 and 1300 cal/mole) suggests that the critical processes involved in reaching the activated complex are the same for each. If then, for the sake of argument, one proposes a mechanism for cyclobutane involving the tetramethylene diradical as an intermediate in the path to ethylene, and applies

$$\square \underset{b}{\overset{a}{\rightleftharpoons}} T \overset{c}{\rightarrow} 2E$$
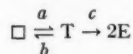
the same steady-state treatment as for cyclopropane, it must be true that reaction (a) is the isotope-dependent step since the effect is again pressure dependent. The reaction (c) in cyclobutane does not involve a hydrogen transfer and would not be expected to involve a hydrogen isotope effect. In reaction (b), however, the activated complex is the same as for the forward reaction, and a roughly equivalent C—H bond weakening must occur as in reaction (a); hence a fairly large activation energy difference would be expected. Since this would tend to cancel the energy difference in (a), a relatively small temperature coefficient would have been expected in the isotope effect. The experimental value does not support this thesis, and it therefore seems reasonable to suggest that the decomposition of cyclobutane involves a transition state in which the carbon–carbon bond split is assisted by the partial bonding of one hydrogen to its neighboring carbon atom.

If this is a reasonable description of the mechanism of the reaction, some correlation must exist between the critical difference between the cyclopropane and cyclobutane mechanisms, i.e. the transfer and non-transfer of hydrogen atoms, and the considerable difference in the isotope effects, i.e. 2.04 vs. 1.37. The fact that the ratio of these two numbers is about 1.5 suggests that this difference arises from that part of the isotope

effect which is due to the relative reduced mass ratio in the reaction co-ordinate in the region of the transition state, which, for hydrogen isotope effects, is about 1.4. This implies that the difference in these isotope effects arises not in the mode of formation of the activated complex nor of its geometry, but rather in the unique way in which the hydrogen atom is concerned in that degree of freedom of the complex which results in reaction.

ACKNOWLEDGMENTS

REFERENCES

1. T. S. CHAMBERS and G. B. KISTIAKOWSKY. J. Am. Chem. Soc. 56, 399 (1934).
2. N. B. SLATER. Proc. Roy. Soc. A, 218, 224 (1953).
3. P. E. WESTON, JR. J. Chem. Phys. 26, 975 (1957).
4. R. H. LINDQUIST and G. K. ROLLEFSON. J. Chem. Phys. 24, 725 (1956).
5. E. W. SCHLAG and B. S. RABINOVITCH. J. Am. Chem. Soc. 82, 5996 (1960).
6. A. T. BLADES and P. W. GILDERSON. Can. J. Chem. 38, 1407 (1960).
7. J. R. McNESBY, T. W. DAVIS, and A. S. GORDON. J. Am. Chem. Soc. 76, 823 (1954).
8. S. W. BENSON. J. Chem. Phys. 34, 521 (1961).
9. M. C. FLOWERS and H. M. FREY. J. Chem. Soc. 2758 (1960).
10. F. T. SMITH. J. Chem. Phys. 29, 235 (1958).
11. J. LANGRISH and H. O. PRITCHARD. J. Phys. Chem. 62, 761 (1958).

CONSTITUTION OF THE GALACTOMANNAN FROM THE KERNEL OF GREEN PALMYRA PALM NUT (BORASSUS FLABELLIFER LINN.)[1]

A. K. Mukherjee, D. Choudhury, and P. Bagchi

ABSTRACT

The water-soluble polysaccharide extracted from the kernel of green palmyra palm nut (*Borassus flabellifer* Linn.) was shown to be composed of D-galactose and D-mannose in the proportion of 1:2.4. Hydrolysis of the fully methylated galactomannan yielded 2,3,4,6-tetra-O-methyl-D-galactose, 2,3,6-tri-O-methyl-D-mannose, and 2,3-di-O-methyl-D-mannose in the molar ratio of 1:1.4:0.95. Partial hydrolysis of the galactomannan afforded 4-O-β-D-mannopyranosyl-D-mannose, 6-O-α-D-galactopyranosyl-D-mannose, and two trisaccharides. Based on these results a structural formula for the galactomannan has been proposed, additional evidence for which was adduced from periodate-oxidation studies.

In 1956 Subrahmanyan *et al.* (1) reported the isolation of a polysaccharide from the kernel by extraction with 10% sodium hydroxide which gave, on hydrolysis, D-galactose and D-mannose in the ratio of 1:2.9 approximately. However, no detailed investigations seem to have been carried out on its structure.

This paper reports the structural studies on the polysaccharide obtained by precipitating the aqueous extract of the soft kernel with ethanol. Hydrolysis of the polysaccharide, $[\alpha]_D^{30}$ +8.5° (in 4% sodium hydroxide solution) gave D-galactose and D-mannose in the molar proportion of 1:2.4 as estimated by the periodate method (2).

The galactomannan was methylated first by repeated treatment with methyl sulphate and alkali (3) and then by Purdie's method (4). The resulting methylated galactomannan, which showed no hydroxyl absorption band in the I.R. spectrum, was a glassy solid —OCH₃ 43.25%, $[\alpha]_D^{29}$ +29° (in chloroform). After methanolysis of the methylated polysaccharide and hydrolysis of the resulting mixture of methyl glycosides the mixture of methyl sugars, so obtained, on paper chromatographic examination using solvents B and D showed the presence of three methylated sugars together with a trace amount of another. The mixture of methylated sugars was separated on a cellulose column (5) using butanone–water azeotrope (6) as eluent.

Identification of the various methylated sugars obtained by column chromatography showed them to be 2,3,4,6-tetra-O-methyl-D-galactose (1 mole), 2,3,6-tri-O-methyl-D-mannose (1.35 moles), 2,3,6-tri-O-methyl-D-galactose (0.035 mole), and 2,3-di-O-methyl-D-mannose (1.03 moles).

The relative proportion of 2,3,4,6-tetra-O-methyl-D-galactose, 2,3,6-tri-O-methyl-D-mannose, and 2,3-di-O-methyl-D-mannose was estimated by hypoiodite titration (7) after separation on paper using solvent B and was found to be 1:1.4:0.95. This ratio is in good agreement with that obtained by weighing the different fractions obtained during column chromatographic examination of the mixture.

The tetra-O-methyl sugar fraction, $[\alpha]_D^{30}$ +109° (in water) obtained as a sirup, gave on demethylation (8) D-galactose only along with some partially demethylated sugars and was characterized to be 2,3,4,6-tetra-O-methyl-D-galactose through its anilide (9).

The tri-O-methyl-D-mannose $[\alpha]_D^{30}$ −9° (in water) was characterized as 2,3,6-tri-O-methyl-D-mannose through the crystalline 2,3,6-tri-O-methyl-D-mannose, 1,4-di-p-nitrobenzoate (10).

The fraction containing the trace quantity of the tri-O-methyl sugar gave D-galactose and D-mannose on demethylation and on paper chromatography using solvent B gave two spots corresponding to those of 2,3,6-tri-O-methyl-D-galactose and 2,3,6-tri-O-methyl-D-mannose the relative proportions of which were calculated from the observed specific rotation.

The dimethyl sugar fraction having $[\alpha]_D^{30}$ −16.4° (in water) was chromatographically pure and was characterized to be 2,3-di-O-methyl-D-mannose by conversion to 2,3-di-O-methyl-D-mannonic acid phenyl hydrazide (11).

From the above results it is possible to assign a structure to the galactomannan. Demonstration of the existence of 2,3,4,6-tetra-O-methyl-D-galactose alone in the tetra-methyl fraction of the hydrolyzate of the methylated polysaccharide shows that D-galactose in the pyranose form constitutes the non-reducing ends of the molecule.

That the backbone of the molecule is made up of $1 \rightarrow 4$-linked mannopyranose residues is proved by the characterization of 2,3,6-tri-O-methyl-D-mannose in the hydrolyzate of the methylated galactomannan.

The fact that 2,3-di-O-methyl-D-mannose is present in the hydrolyzate indicates that the polysaccharide is branched and that at branch points the mannose residues are linked through C_1, C_4, and C_6.

The trace amount of the tri-O-methyl-D-galactose might have originated from partial demethylation of the tetra-O-methyl-D-galactose fraction during methanolysis and hydrolysis of the methylated galactomannan (12) and is considered to have no structural significance.

Further support for the proposed structure for the galactomannan was obtained from the periodate oxidation of the galactomannan. It was found that one molar proportion of formic acid was liberated for every 3.7 hexose units in 25 hours and that 1.30 moles of periodate were consumed per hexose unit in 30 hours. If one galactopyranose residue is present as non-reducing terminal group for every 2.4 units of mannopyranose residues, on the average, in the chain, then theoretically the consumption of periodate works out to be 1.30 moles per hexose residue. The results of periodate uptake are thus in good agreement with the theoretically expected results.

When the periodate-oxidized polysaccharide was reduced with sodium borohydride and hydrolyzed, glycerol and erythritol were obtained from the non-reducing units and $1 \rightarrow 4$-linked mannose residues respectively in the molar proportion of 1:2.45. The linkages at the branch points through C_1, C_4, and C_6 as mentioned above were confirmed by the absence of mannose in this hydrolyzate. The length of the repeating unit (3.45) calculated from the amounts of glycerol and erythritol obtained is in good agreement with those obtained from methylation and periodate-oxidation studies.

In order to establish the stereochemistry of the linkages between the sugar units the galactomannan was subjected to graded hydrolysis. After separation by column and paper chromatography, two disaccharides, viz. 4-O-β-D-mannopyranosyl-D-mannose and 6-O-α-D-galactopyranosyl-D-mannose, and two trisaccharides, O-β-D-mannopyranosyl $(1 \rightarrow 4)$-O-β-D-mannopyranosyl$(1 \rightarrow 4)$-O-β-D-mannose and another triose having one galactose residue and two mannose residues with mannose residue at the reducing end, were isolated and, in pure form, studied.

The presence of mannobiose and mannotriose in comparatively larger amounts clearly shows a $1 \rightarrow 4$ β-linked mannose chain in the molecule. The existence of α-linked galacto-pyranose residues as non-reducing terminal units is confirmed by the isolation and characterization of 6-O-α-D-galactopyranosyl-D-mannose.

Based on the above results it can be concluded that the galactomannan has a structure of the following type:

$$-\overset{\beta}{}----\underset{4}{\text{Mp}}\overset{\beta}{\underset{1}{}}-----\overset{6'}{\underset{4}{\text{Mp}}}\overset{\beta}{\underset{1}{}}---\left[--\underset{4}{\text{Mp}}\overset{\beta}{\underset{1}{}}-\right]_{x}----\overset{6'}{\underset{4}{\text{Mp}}}\overset{\beta}{\underset{1}{}}-----\underset{4}{\text{Mp}}\underset{1}{}.....$$

(with Gap $\overset{1}{\underset{\alpha}{|}}$ attached above the two Mp residues)
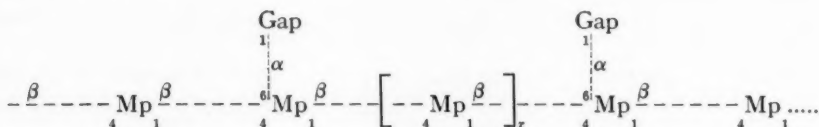
where x has the value of 1 in one segment and 2 in the next, Gap = galactopyranose residue, Mp = mannopyranose residue.

The low specific rotation (+8.5° in 4% sodium hydroxide) of the galactomannan indicates the presence of both α and β linkages in the molecule.

During purification of the galactomannan through copper complex (13a, 13b) it was observed that the proportion of galactose gradually decreased. The ratio of galactose to mannose was found to change from 1:2.4 to 1:3.4 during five treatments with Fehling's solution. It was also noticed that only galactose residues were released when the galactomannan was hydrolyzed under very mild condition employing 0.02 N oxalic acid. The resulting galactomannan after 4 hours had galactose-to-mannose ratio of 1:3.7. Hence the increase in the mannose content during purification through copper complex may be attributed to the fact that some of the α-linked galactose residues, which are more labile, were removed during the acid treatment employed for destruction of the copper complex.

The galactomannan was acetylated in the usual way (14, 15). The triacetate, which showed an increased mannose content, was fractionally precipitated from a solution of the substance in a solvent containing s-tetrachloroethane and 95% ethanol in the ratio of 9:1, by gradual addition of methanol. The different fractions after deacetylation and hydrolysis were found to have galactose-to-mannose ratios between 1:2.4 to 1:3.2. It is significant to note that none of the fractions had the ratio of galactose to mannose more than 1:2.4. One of these fractions (fraction 5) having galactose-to-mannose ratio 1:3.2 was methylated directly (14) first by treating a solution of the triacetate in dry tetrahydrofuran with solid sodium hydroxide and methyl sulphate and then by Purdie's method. The resulting fully methylated polysaccharide, —OCH₃, 43.05%, $[\alpha]_D^{25}$ +24° (in chloroform) was subjected to methanolysis and hydrolysis. The mixture of the methyl sugars obtained, on paper chromatography, showed the presence of 2,3,4,6-tetra-O-methyl-D-galactose, 2,3,6-tri-O-methyl-D-mannose, and 2,3-di-O-methyl-D-mannose in the ratio of 1:2.11:1.08 as estimated by alkaline hypoiodite method. The mixture (ca. 200 mg) was separated on Whatman No. 3MM papers and the individual sugars were identified as above.

The isolation and characterization of the same methylated sugars from this fraction show that the original material was essentially homogeneous and that during acetylation some of the labile α-linked galactose units were eliminated.

The molecular weight of the methylated galactomannan as determined by light-scattering method was found to be 1.39×10^5.

The galactomannan obtained from palm kernel is similar in the essential structure to those obtained from fenugreek seed (16), carob seed (11, 17), and guar seed (18, 19, 20) but differs from that obtained from the kernel of coconut (*Cocos nucifera*) (paper in press).

EXPERIMENTAL

All specific rotations are equilibrium values. Unless otherwise stated, all evaporations were carried out *in vacuo* at 30°–40° C. The solvent mixtures (v/v) used for partition chromatography of sugars and their derivatives were:

(A) ethyl acetate:pyridine:water (8:2:1);

(B) methyl ethyl ketone – water azeotrope;

(C) butanol:acetic acid:water (4:1:5) upper layer;

(D) butanol:ethanol:water (40:11:19);

(E) butanol:ethanol:water (4:1:5) upper layer;

(F) ethyl acetate:acetic acid:water (9:2:2).

Whatman No. 1 filter papers were used for paper partition chromatography. The spray reagents used were:

(*a*) aniline hydrogen oxalate (saturated aqueous solution);

(*b*) *p*-anisidine hydrochloride (3% solution in butanol);

(*c*) ammoniacal silver nitrate solution.

Isolation and Purification of the Galactomannan

The kernel obtained from the market was peeled and the soft fleshy material was macerated in a high-speed "Kenmix 55" blender for 2 minutes in the presence of ethanol. The resulting slurry was kept overnight under ethanol and then was filtered through cloth. The residue was freed from ethanol by squeezing and then dried in air. The material (50 g) so obtained was allowed to swell with water (1500 ml) for some time and heated, while being stirred, on a boiling-water bath for 5 hours. After being kept overnight in a refrigerator the slurry was diluted with water (1500 ml) and the coarse suspended material was removed by filtration through cloth. The filtrate was passed through Cepa supercentrifuge at 25,000–30,000 r.p.m. for further clarification. The clear liquid was slowly added, with stirring, to acidified (pH 4–5) 95% ethanol when a white fibrous precipitate appeared. This was separated by centrifuge and triturated five times with absolute ethanol and finally with ether. The product was dried in air and then *in vacuo*. It was a white amorphous powder, yield: 12 g, moisture 10.9%, ash 0.36%, $[\alpha]_D^{30}$ +8.5° (in 4% aqueous sodium hydroxide solution, *c*, 0.5), intrinsic viscosity 1.25 dl/g (in 4% sodium hydroxide solution), pentosan (21) 0.5%, methoxyl group (22) 0.3%, nitrogen 0.7%, uronic acid (23) negligible. D-Galactose and D-mannose were detected by paper chromatography in the hydrolyzate of the polysaccharide using solvent A. A small portion of the hydrolyzate was separated quantitatively by paper chromatography using solvent A. The zones corresponding to each sugar were eluted in the usual way and estimated by the periodate method (2). D-Galactose and D-mannose were found in the ratio of 1:2.4.

The galactomannan was purified by complexing (13*a*, 13*b*) with Fehling's solution. The galactomannan (10 g) was dissolved in 4% sodium hydroxide solution (1 l.) in an atmosphere of nitrogen, and freshly prepared Fehling's solution (500 ml) was added to it while it was stirred in a cold bath (10° C). The flocculent blue precipitate so obtained was filtered through a piece of fine nylon cloth and washed with water till the filtrate was colorless. The precipitate was suspended in water (500 ml) in a cold bath (10° C) and 2 N HCl was added dropwise with stirring till the mixture was just acidic. The stirring was continued for 2 hours more when a homogeneous dispersion was obtained. This was then added slowly, with stirring, to ethanol (800 ml) when a white fibrous

precipitate separated out. This was centrifuged, washed with a mixture of 80% ethanol: HCl (100:1), and triturated with ethanol till free from acid and finally with ether. Yield 8.75 g, $[\alpha]_D^{30}$ +9° (in 4% sodium hydroxide solution, c, 0.5). On hydrolysis of the purified polysaccharide D-galactose and D-mannose were obtained in the ratio of 1:2.6.

Each repetition of the process led to a product showing higher mannose content. After five precipitations the ratio of galactose to mannose was found to be 1:3.4.

Mild Hydrolysis of the Galactomannan with Oxalic Acid

The galactomannan (1 g) was dispersed in water (50 ml) to which 0.04 N oxalic acid (50 ml) had been added and was heated on a water bath (90°–95° C). At intervals of 1 hour aliquots (25 ml) were withdrawn and precipitated with ethanol (30 ml). The supernatant liquids were concentrated to sirups. Each of these on paper chromatographic examination using solvent A indicated the presence of D-galactose only. The precipitated polysaccharide from the fourth stage was washed with alcohol and then hydrolyzed with 2 N sulphuric acid. The hydrolyzate was treated in the usual manner and the resulting sirup had D-galactose and D-mannose in the ratio of 1:3.7.

Hydrolysis and Identification of D-Galactose and D-Mannose

The galactomannan (0.5 g) was kept with 72% sulphuric acid (24) at room temperature overnight and diluted with water to give normal acid solution. The solution was heated for 8 hours on a boiling-water bath when the hydrolysis, followed iodometrically (25), was complete. The solution obtained after neutralization with barium carbonate and filtration, was deionized by passage through Amberlite I.R. 120(H)* and Amberlite I.R. 45(OH)* and was concentrated to a sirup. A portion of this sirup (200 mg) was separated on a Whatman No. 3MM filter paper using solvent A. The strips corresponding to D-galactose and D-mannose were each eluted with water (20 ml) and evaporated to give sirups, D-galactose, $[\alpha]_D^{30}$ +79° (in water, c, 1) and D-mannose, $[\alpha]_D^{30}$ +14° (in water, c, 1). Each of these components were refluxed with p-nitroaniline in methanol acidified with hydrochloride acid (26). The galactose component gave p-nitro-N-phenyl-D-galactosyl amine, m.p. and mixed m.p. 217°–218° C, $[\alpha]_D^{30}$ −245° (in dry pyridine, c, 0.5), lit. (26) −248°. D-Mannose component gave p-nitro-N-phenyl-D-mannosyl amine, m.p. and mixed m.p. 217°–218°, $[\alpha]_D^{30}$ −325° (in dry pyridine, c, 0.5) lit. (26) −325°.

Methylation of the Galactomannan

The galactomannan (10 g) was methylated by treatment first with methyl sulphate and alkali and then with methyl iodide and silver oxide according to the method of Falconer and Adams (27a, 27b) to yield a methylated derivative (3.22 g) showing no hydroxyl absorption band in the infrared spectrum. It had intrinsic viscosity 0.267 dl/g in chloroform and $[\alpha]_D^{29}$ +28.7° (in chloroform, c, 1). (Anal. Calc. for $C_9H_{16}O_5$, —OCH$_3$ 44.7; found —OCH$_3$ 43.25%.)

Molecular-Weight Determination of the Methylated Galactomannan

All measurements of the intensity of scattered light for molecular-weight determination of the methylated galactomannan were carried out with a Brice Phoenix light-scattering photometer (Model OM 1000A) using semioctagonal cells. Intensities of scattered light at four angles (viz. 0°, 45°, 90°, and 135°) over a concentration range of 0.5 to 4.5×10⁻³ g/ml were measured and working standard method was used to calculate turbidity (τ). The solutions used for the measurement were taken from a stock solution of known

*A product of Rohm & Hass Company, Pennsylvania, U.S.A.

concentration in redistilled chloroform and diluted to a definite volume in a calibrated volumetric flask with the same solvent. Special precaution was taken to avoid dust and suspended particles by filtering the stock solution and solvent through sintered glass (G 4) and (G 5) respectively. The concentration of each solution was determined by dry-weight method. The refractive indices of the solutions were determined with Brice Phoenix differential refractometer at the same wave length and temperature. The turbidities and dissymmetries obtained by the above procedure were reproducible indicating absence of anomalous aggregation. The molecular weight of the methylated galactomannan was found to be 1.39×10^5 calculated by dissymmetry method (28a) assuming particle-scattering factor (P 90°) (28b, 28c) for random coil.

Methanolysis and Hydrolysis of the Methylated Galactomannan

The methylated galactomannan (1 g) was refluxed with 4% methanolic hydrogen chloride (100 ml) till the rotation reached a constant value (15 hours). The solution was evaporated to a sirup and the resulting mixture of methyl glycosides was hydrolyzed with N hydrochloric acid (75 ml) till the rotation reached constant value (14 hours). The hydrolyzate was neutralized (silver carbonate), filtered, and the resulting solution deionized by passage through Amberlite I.R. 120(H) and Amberlite I.R. 45(OH). The mixture of methylated sugars was evaporated to a sirup (0.85 g).

A preliminary analysis was made by paper partition chromatography using solvents B and D and spray reagent a. The following spots were identified.

Spot No.	R_f Solv. B	R_G* Solv. D	Sugars
1	0.69	0.91	2,3,4,6-Tetra-O-methyl-D-galactose
2	0.51	0.82	2,3,6-Tri-O-methyl-D-mannose
3	0.47	—	2,3,6-Tri-O-methyl-D-galactose (trace)
4	0.24	0.61	2,3-Di-O-methyl-D-mannose

*R_G values are with respect to n-tetra-O-methyl-D-glucose.

Separation of the Mixture of Methylated Sugars by Column Chromatography

The mixture of methylated sugars (825 mg) was separated on a cellulose column (5) (60×2.5 cm) using solvent B (6) on an automatic fraction collector. The total eluent was then divided into the following five fractions guided by the difference in the refractive indices of the solvent and solution in each test tube using a Brice Phoenix differential refractometer and also by examination by paper chromatography.

Fraction	Tube No.	Sugars	Molar ratio
A	21–25	2,3,4,6-Tetra-O-methyl-D-galactose	1
B	26	2,3,4,6-Tetra-O-methyl-D-galactose and 2,3,6-tri-O-methyl-D-mannose	
C	27–29	2,3,6-Tri-O-methyl-D-mannose	1.25
D	30–31	2,3,6-Tri-O-methyl-D-mannose and 2,3,6-tri-O-methyl-D-galactose	
E	35–44	2,3-Di-O-methyl-D-mannose	1.03

Identification of 2,3,4,6-Tetra-O-methyl-D-galactose

Fraction A on evaporation gave a sirup (245.7 mg) having $[\alpha]_D^{30}$ +109° (in water, c, 1) lit. (29) +109.5°. The sirup (5 mg) was demethylated (8) by heating for 5 minutes on a

boiling-water bath with 48% hydrobromic acid (2 ml) in a sealed tube in an atmosphere of nitrogen. The resulting solution after usual treatment gave a sirup, which on paper chromatographic analysis using solvent A, indicated the presence of D-galactose only along with some partially demethylated sugars. The identity of 2,3,4,6-tetra-O-methyl sugar was confirmed by preparing the N-phenyl-2,3,4,6-tetra-O-methyl-D-galactosyl amine in the usual way, m.p. and mixed m.p. 187° C, lit. 188°–190° C (8), 186°–188° (30); $[\alpha]_D^{30}$ +38° (in acetone), lit. +39° (8), +40.7° (31).

Examination of Fraction B

This fraction on evaporation yielded a sirup (53.3 mg) having $[\alpha]_D^{30}$ +5° (in water). Demethylation of a small portion of this fraction gave D-galactose and D-mannose along with partially demethylated sugars. Paper partition chromatography using solvent D with authentic samples indicated that the mixture contained 2,3,4,6-tetra-O-methyl-D-galactose and 2,3,6-tri-O-methyl-D-mannose by comparison with authentic samples. Specific rotation value showed that the tetramethyl galactose and the trimethyl mannose were present in the proportion of 1:7 approximately.

Identification of 2,3,6-Tri-O-methyl-D-mannose

The fraction C on evaporation gave a sirup (277 mg). This was chromatographically homogeneous and had $[\alpha]_D^{30}$ −9° (in water, c, 1) lit. −13° (9), −10° (11). It gave D-mannose along with some partially demethylated sugars on demethylation of a portion of it. The 2,3,6-tri-O-methyl-D-mannose was characterized through its crystalline 2,3,6-tri-O-methyl-D-mannose, 1,4-di-p-nitrobenzoate (10), m.p. and mixed m.p. 189°–190° C, lit. (9) 190°–191° C; $[\alpha]_D^{30}$ +32° (in chloroform), lit. (10) +33°.

Examination of Fraction D

This fraction yielded a sirup (33 mg) having $[\alpha]_D^{30}$ +13.5° (in water). Demethylation of a part of it yielded D-galactose and D-mannose along with other partially demethylated sugars. Examination of this sirup using solvent D with authentic samples indicated that it contained a mixture of 2,3,6-tri-O-methyl-D-galactose and 2,3,6-tri-O-methyl-D-mannose. Optical rotation value indicated that they were present in the ratio of 1:3 approximately.

Identification of 2,3-Di-O-methyl-D-mannose

Fraction E on evaporation gave a sirup (212.9 mg) having $[\alpha]_D^{30}$ −16° (in water) lit. (32) −15.8°. This fraction was chromatographically pure and gave D-mannose only along with partially demethylated sugars on demethylation of a part of it. The sirup (25 mg) was oxidized with bromine water at room temperature (10) for 68 hours. The bromine was removed by aeration and the solution after usual treatment yielded a thick sirup containing the lactone $[\alpha]_D^{29}$ +58° (in water, after 24 hours), which could not be induced to crystallization. This was converted to the phenylhydrazide by heating it with phenyl-hydrazine in ethanol on a boiling-water bath. The 2,3-di-O-methyl-D-mannonic acid phenylhydrazide was crystallized from methanol–ether (11), m.p. 158° C, lit. 156° (18), 168° C (10); $[\alpha]_D^{29}$ −24° (in water), lit. −24.2° (18), −25° (10).

Estimation of the Methyl Sugars

A small quantity of the mixture of methylated sugars (5 mg) was separated by paper chromatography using solvent B. Each sugar was eluted in the usual way and estimated by alkaline hypoiodite (7) method. The molar ratio of the different sugars found

were as follows: 2,3,4,6-tetra-*O*-methyl-D-galactose:2,3,6-tri-*O*-methyl-D-mannose:2,3-di-*O*-methyl-D-mannose as 1:1.4:0.95. The 2,3,6-tri-*O*-methyl-D-galactose was obtained in negligible amount.

Periodate Oxidation of the Galactomannan

The galactomannan (84.2 mg) was dispersed in water (50 ml) and oxidized by shaking with 0.1 M sodium metaperiodate (50 ml) in the dark at 15° C. The liberated formic acid and the amount of periodate consumed during the reaction were estimated in the usual way (33) at regular intervals of time. The liberation of formic acid became constant in 25 hours, 3.7 hexose residues liberating 1 mole of formic acid. The periodate uptake became constant after 30 hours corresponding to 1.30 moles of the oxidant per hexose residue.

Reduction of the Periodate-oxidized Galactomannan

The periodate-oxidized product (140 mg) was neutralized with barium hydroxide and filtered, and to the clear solution sodium borohydride (200 mg) was added. The reduction was allowed to proceed for 4 hours at room temperature. The resulting solution after usual treatment (34) yielded a sirup which, on paper chromatographic examination using solvent E and spray reagent *c*, indicated the presence of erythritol and glycerol.

The above sirup was separated on Whatman No. 3MM filter paper using solvent E. The zones corresponding to erythritol and glycerol were eluted and evaporated to sirups. They were characterized through their crystalline tetra- and tri-tosyl derivatives respectively. The tetratosyl erythritol had m.p. and mixed m.p. 163°–165° C, lit. (35) 165°–166°. The tritosyl glycerol had m.p. and mixed m.p. 102°–103° C, lit. (35) 103°–104° C.

Quantitative Estimation of the Polyhydric Alcohols

A small portion of the mixture was separated quantitatively by paper chromatography using solvent E, and the polyhydric alcohols were estimated by the method of Lambert and Neish (36). The ratio of glycerol to erythritol was found to be 1:2.45.

Acetylation of the Galactomannan

The galactomannan (8 g) was dispersed by stirring for 5 hours in formamide (100 ml). To this dispersion pyridine (150 ml) was added followed by the dropwise addition, with stirring, of acetic anhydride (120 ml) for a period of 4 hours at 20°. The stirring was continued for 3 days at room temperature and the galactomannan acetate was precipitated by pouring the dark viscous material into ice-cold water. The precipitate was washed first with water, then with methanol, and finally with ether. Completely dried material was once again acetylated by dissolving it in pyridine (150 ml) and adding acetic anhydride (120 ml) in a dropwise manner and then proceeding as above. Yield 6.8 g, $[\alpha]_D^{30}$ +11° (in chloroform, *c*, 1), intrinsic viscosity 5.65 dl/g (in chloroform), acetyl content (37) 43.07%. On deacetylation (38) and hydrolysis D-galactose and D-mannose were obtained in the ratio of 1:2.6.

Fractionation of the Acetylated Galactomannan

The acetylated galactomannan was fractionated according to the method of Hamilton and Kircher (14). The material (5.95 g) was dissolved in a solvent containing *s*-tetrachloroethane:95% ethanol in the ratio of 9:1 and fractionally precipitated by the gradual addition of methanol. Seven fractions could be collected in this way. The last two fractions

were obtained on concentration of the solution after the fifth precipitation and after addition of petroleum ether. The results of studies on each of these fractions are shown in the following table.

Sample	Wt. (g)	$[\alpha]_D^{30°}$ in CHCl₃	I.V. (dl/g) in CHCl₃	Acetyl content (%)	Gal:Man
Original galactomannan acetate	5.95	+11°	5.65	43.07	1:2.6
Fraction 1	0.345	+11°	3.4	39.1	1:2.4
" 2	0.136	+11°	4.7	39.7	1:2.5
" 3	0.988	+11°	7.2	42.2	1:2.5
" 4	1.460	+11°	7.8	43.5	1:2.6
" 5	2.240	+12°	6.3	44.2	1:3.2
" 6	0.233	+11.5°	2.1	42.3	1:3
" 7	0.081	+11.5°	1.0	42.8	1:3

Methylation of the Acetylated Galactomannan (Fraction 5)

The fraction 5 (2 g) of the galactomannan triacetate was dissolved in dry tetrahydrofuran (40 ml) and methylated directly with methyl sulphate (35 ml) and solid sodium hydroxide (30 g) according to the method of Hamilton and Kircher (14). The product was methylated twice by Purdie's method. Yield 0.85 g, —OCH₃, 43.05%, $[\alpha]_D^{20}$ +24° (in chloroform).

Methanolysis and Hydrolysis of the Methylated Galactomannan

The methylated galactomannan was methanolyzed and the mixture of methyl glycosides was hydrolyzed as described earlier. On paper partition chromatography using solvent B the mixture of methyl sugars gave only three spots corresponding to 2,3,4,6-tetra-O-methyl-D-galactose, 2,3,6-tri-O-methyl-D-mannose, and 2,3-di-O-methyl-D-mannose. They were isolated and characterized as described earlier.

A portion of this mixture was quantitatively separated by paper chromatography using solvent B and each component estimated by the alkaline hypoiodite method (7). The 2,3,4,6-tetra-O-methyl-D-galactose, 2,3,6-tri-O-methyl-D-mannose, and 2,3-di-O-methyl-D-mannose were found in the molar ratio of 1:2.11:1.08.

Graded Hydrolysis of the Galactomannan

The galactomannan (15 mg) was dispersed in water (750 ml), 0.4 N sulphuric acid (750 ml) was added and the mixture was heated on a boiling-water bath for 2 hours. The solution was filtered and the residue was again hydrolyzed with 0.2 N sulphuric acid for 2 hours. The two solutions were combined and neutralized, filtered, and passed through ion exchange resins I.R. 120(H) and I.R. 45(OH). The resulting mixture of sugars was concentrated to 50 ml. Paper partition chromatography using solvent F indicated the presence of D-galactose, D-mannose, two disaccharides, and two trisaccharides.

Spot	R_{Gal} (in solvent F)	Sugars
1	0.62	4-O-β-D-Mannopyranosyl-D-mannose
2	0.54	6-O-α-D-Galactopyranosyl-D-mannose
3	0.34	A triose
4	0.30	O-β-D-Mannopyranosyl-(1 → 4) O-β-D-Mannopyranosyl-(1 → 4) O-β-D-Mannose

Separation of the Oligosaccharides by Column Chromatography

The sugar mixture was allowed to soak into the top of a cellulose–charcoal (60–80 mesh) (39) column (35×4.2 cm). The column was first eluted with water and then subjected to stepwise elution (40) using 2.5%, 5%, 7.5%, and 10% aqueous ethanolic solutions successively. Eight liters of each fraction was collected and each was concentrated to small volume. The monosaccharides were eluted with water and the di- and oligo-saccharides with aqueous ethanol. All the alcoholic eluates were found to contain mixtures.

The mixture was separated on Whatman No. 3MM filter papers using solvent F into chromatographically pure fractions and the corresponding di- and tri-saccharide fractions were combined and evaporated to sirups. Thus two disaccharides and two trisaccharides were collected.

Identification of 4-O-β-D-Mannopyranosyl-D-mannose

The sirup (243.7 mg) having $[\alpha]_D^{30}$ $-8° \rightarrow -7°$ (in water), lit. $[\alpha]_D^{23}$ $-7.7 \rightarrow 2.2$ (19), $[\alpha]_D^{25}$ $-8.13° \rightarrow -7.4°$ (14), $-4.4°$ (41), gave on hydrolysis D-mannose only. The molecular weight determined by the alkaline hypoiodite method was found to be 329 (calc. for $C_{12}H_{22}O_{11}$, 342). The oxidation of mannobiose (65 mg) with 0.3 M sodium metaperiodate (10 ml) made up to 50 ml with water was followed by determining the formic acid liberated and uptake of periodate at various intervals of time. The corresponding values are 1.35 moles (10 hours), 2.45 moles (20 hours), and 2.90 moles (30 hours) and 2.40 moles (10 hours), 3.90 moles (20 hours), and 4.91 moles (35 hours). But when the same oxidation was carried out in acetate buffer (pH 3.7) the disaccharide (50 mg) consumed 4.06 moles of the oxidant per mole of the disaccharide in 3 hours (constant value). The periodate-oxidized product was freed from the oxidant in the usual way and reduced with sodium borohydride. After hydrolysis and usual treatments the mixture was found to contain glycerol and erythritol on paper chromatographic examination using spray reagent c.

A small portion of the disaccharide (30 mg) was converted to the phenylhydrazone in the usual way to give yellow crystals having m.p. 198°–199° C, lit. (42) 200°–201° C.

Identification of 6-O-α-D-Galactopyranosyl-D-mannose

The fraction 2 on evaporation gave a sirup (114.7 mg) having $[\alpha]_D^{30}$ $+124°$ (in water), lit. (41) $+123°$. On hydrolysis it afforded D-galactose and D-mannose in equal proportion and the hydrolyzed sirup had $[\alpha]_D^{30}$ $+49°$ (in water, c, 1). Hydrolysis of a portion after reduction with sodium borohydride indicated the presence of only D-galactose. The disaccharide (36 mg) was oxidized with sodium metaperiodate and the liberation of formic acid and consumption of periodate were recorded at various intervals of time. The corresponding values per mole of the disaccharide are, 1.95 moles (10 hours), 4.0 moles (20 hours), and 4.93 moles (30 hours) and 3.05 moles (10 hours), 4.75 moles (20 hours), and 5.95 moles (30 hours) respectively. On oxidation in the presence of acetate buffer (pH 3.7), however, the disaccharide (25 mg) consumed 5.14 moles of the oxidant per mole of the disaccharide in 2.5 hours (constant value). The oxidized product was reduced and hydrolyzed as before and the mixture was found to contain only glycerol. The 6-O-α-D-galactopyranosyl-D-mannose was characterized by preparing its phenylhydrazone, m.p. 168°–169° C, lit. (41) 170° C.

Examination of Fraction 3

This fraction on evaporation gave a sirup (48.3 mg) having $[\alpha]_D^{30}$ $+33°$ (in water, c, 1).

On hydrolysis it afforded D-galactose and D-mannose in the proportion of 1:2. On reduction and hydrolysis it indicated the presence of D-galactose and D-mannose on a paper chromatogram using spray reagent a indicating the presence of mannose residue at the reducing end. A portion (25 mg) was oxidized with sodium metaperiodate in acetate buffer (pH 3.7) and was found to consume 6.12 moles of the oxidant per mole of the sugar. The sugar thus seems to be a trisaccharide containing 1 mole of D-galactose residue and 2 moles of D-mannose residues.

Identification of the Mannotriose

This fraction yielded a sirup (82.6 mg) having $[\alpha]_D^{30}$ $-15°$ (in water, c, 1), lit. $-16°$ and $-22°$ (41), $-15°$ (19), $-24.7° \rightarrow -23.3$ (43), $-15.7° \rightarrow -20.2°$ (42). On hydrolysis it afforded only D-mannose. The molecular weight of this sugar was determined by the alkaline hypoiodite method and was found to be 488 (calc. for $C_{18}H_{32}O_{16}$, 504). A portion of this fraction (30 mg) was oxidized with sodium metaperiodate in acetate buffer (pH 3.7). One mole of the trisaccharide was found to consume 5.08 moles of the periodate.

REFERENCES

1. V. Subrahmanyan, G. S. Bains, C. P. Natarajan, and D. S. Bhatia. Arch. Biochem. Biophys. **60**, 27 (1956).
2. E. L. Hirst and J. K. N. Jones. J. Chem. Soc. 1659 (1949).
3. W. N. Haworth. J. Chem. Soc. **107**, 8 (1915).
4. T. Purdie and J. C. Irvine. J. Chem. Soc. **83**, 1021 (1903).
5. L. Hough, J. K. N. Jones, and W. H. Wadman. J. Chem. Soc. 2511 (1949).
6. L. Boggs, L. S. Cuendet, I. Ehrenthal, R. Koch, and F. Smith. Nature, **166**, 520 (1950).
7. E. L. Hirst, L. Hough, and J. K. N. Jones. J. Chem. Soc. 928 (1949).
8. L. Hough, J. K. N. Jones, and W. H. Wadman. J. Chem. Soc. 1702 (1950).
9. N. Prentice, L. S. Cuendet, W. F. Geddes, and F. Smith. J. Am. Chem. Soc. **81**, 684 (1959).
10. P. A. Rebers and F. Smith. J. Am. Chem. Soc. **76**, 6097 (1954).
11. E. L. Hirst and J. K. N. Jones. J. Chem. Soc. 1278 (1948).
12. K. Freudenberg and H. Boppel. Ber. **73**, 609 (1940).
13a. S. K. Chanda, E. L. Hirst, J. K. N. Jones, and E. G. V. Percival. J. Chem. Soc. 1289 (1950).
13b. C. P. J. Glaudemans and T. E. Timell. J. Am. Chem. Soc. **80**, 1209 (1958).
14. J. K. Hamilton and H. W. Kircher. J. Am. Chem. Soc. **80**, 4703 (1958).
15. J. F. Carson and W. D. Maclay. J. Am. Chem. Soc. **68**, 1015 (1946).
16. P. Andrews, L. Hough, and J. K. N. Jones. J. Chem. Soc. 2744 (1952).
17. F. Smith. J. Am. Chem. Soc. **70**, 3249 (1948).
18. C. M. Rafique and F. Smith. J. Am. Chem. Soc. **72**, 4634 (1950).
19. R. L. Whistler and J. Z. Stein. J. Am. Chem. Soc. **73**, 4187 (1951).
20. Z. F. Ahmed and R. L. Whistler. J. Am. Chem. Soc. **72**, 2524 (1950).
21. C. Dorée. The methods of cellulose chemistry. 2nd ed. Chapman & Hall Ltd., London. 1947. p. 381.
22. E. P. Clark. Semimicro quantitative organic analysis. Academic Press, Inc., New York. 1943. p. 68.
23. C. Dorée. The methods of cellulose chemistry. 2nd ed. Chapman & Hall Ltd., London. 1947. p. 391.
24. J. K. Hamilton and E. V. Partlow. J. Am. Chem. Soc. **80**, 4880 (1958).
25. F. L. Baker and H. F. E. Halton. Biochem. J. **14**, 754 (1920).
26. F. Weygand, W. Perkow, and P. Kuhner. Chem. Ber. **84**, 594 (1951).
27a. E. L. Falconer and G. A. Adams. Can. J. Chem. **34**, 338 (1956).
27b. G. A. Adams. Can. J. Chem. **36**, 755 (1958).
28a. P. Debye. J. Phys. Chem. **51**, 18 (1947).
28b. G. Oster. Chem. Revs. **43**, 352 (1948).
28c. P. Doty and R. F. Steiner. J. Chem. Phys. **28**, 1211 (1950).
29. J. C. Irvine and A. Cameron. J. Chem. Soc. **85**, 1071 (1904).
30. R. Johnston and E. G. V. Percival. J. Chem. Soc. 1994 (1950).
31. W. N. Haworth and G. C. Leitch. J. Chem. Soc. **113**, 188 (1918).
32. G. J. Robertson. J. Chem. Soc. 330 (1934).
33. P. Fleury and J. Lunge. J. pharm. chim. **17**(8), 107 (1933).
34. F. Smith and H. C. Srivastava. J. Am. Chem. Soc. **81**, 1715 (1959).
35. J. K. Hamilton and F. Smith. J. Am. Chem. Soc. **78**, 5907 (1956).
36. M. Lambert and A. C. Neish. Can. J. Research, B, **28**, 83 (1950).
37. J. B. Niederl and V. Niederl. Methods of quantitative organic analysis. 2nd ed. John Wiley & Sons, Inc., New York. 1948. p. 252.
38. F. C. Peterson, A. J. Barry, H. Unkauf, and L. E. Wise. J. Am. Chem. Soc. **62**, 2361 (1940).
39. R. L. Whistler. Science, **26**, 899 (1954).
40. A. Tiselius. Endeavour, **11**(41), 5 (1952).
41. M. F. Henderson, L. Hough, and T. J. Painter. J. Chem. Soc. 3519 (1958).
42. G. O. Aspinall, R. B. Rashbrook, and G. Kessler. J. Chem. Soc. 215 (1958).
43. R. L. Whistler and C. G. Smith. J. Am. Chem. Soc. **74**, 3795 (1952).

THE MERCURY-PHOTOSENSITIZED OXIDATIONS
OF HYDROCARBONS

PART I. INTERACTION OF MERCURY WITH PRODUCTS FORMED
IN THE REACTING MIXTURE[1]

K. M. BELL[2] AND C. A. McDOWELL

ABSTRACT

The interaction of mercury with two hydrocarbon oxidation systems, namely those of oxygen and cyclohexene, and oxygen and isobutane, has been studied at 30° C in a conventional static photochemical apparatus. The removal of mercury from the gas phase in the mercury-photosensitized oxidation of isobutane is attributed to a reaction with ozone,

$$Hg + O_3 \rightarrow HgO + O_2,$$
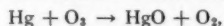
whilst interaction with an intermediate of the oxidation chain is responsible for mercury removal in the cyclohexene oxidation reaction:

$$Hg + RO_2 \rightarrow HgO + RO.$$

INTRODUCTION

Several workers have observed the interaction of mercury with oxidation chain systems. Marshall (1), while studying the mercury-photosensitized hydrogen and oxygen reaction, found that HgO was deposited simultaneously on the vessel walls with the formation of water and hydrogen peroxide. Later Small and Ubbelohde (2) found the yield of peroxides in the thermal oxidation of n-hexane to be greatly reduced by the addition of small amounts of mercury vapor. Mercuric oxide was observed by Gray (3) to be deposited on the vessel walls during a study of the mercury-photosensitized oxidation of ethane, in a flow system at 25° C. Studying the same reaction in a similar manner Watson and Darwent (4) found that mercuric oxide was formed at 25° C, but that none was detected when the temperature was raised to between 40 and 45° C. Callear, Patrick, and Robb (5) have recently reported the removal of mercury as mercuric oxide from Hg–O$_2$ mixtures on illumination with 2537-Å radiation at 25° C.

In any mercury-photosensitized hydrocarbon oxidation system there are clearly two main possibilities for interaction of mercury with the products formed in the reacting mixture. It may react (i) with the products from the excited oxygen molecule reactions, or (ii) with the intermediates or final products of the hydrocarbon oxidation chain.

Two systems, isobutane–oxygen–mercury and cyclohexene–oxygen–mercury have been studied and found to illustrate these two types of interaction.

EXPERIMENTAL

A conventional static photochemical apparatus was used. A Cintel QVA 39 phototube, with a quartz envelope, was used in conjunction with a potentiometer circuit to give relative intensity variations in the parallel beam of radiation, transmitted through the reaction mixture. The reactions were carried out in a cylindrical quartz cell of 2-cm light path and 4-cm diameter. The light source was a water- and air-cooled Hanovia low-pressure mercury arc lamp, emitting 85–90% of its radiation at 2537 Å as determined by filters and the known spectral response characteristics of the phototube. Phillips

Petroleum Company cyclohexene of 99.98% purity was freed from peroxide by refluxing with copper stearate and subsequent distillation under nitrogen. The same firm also supplied Research Grade isobutane. Oxygen was piped from a cylinder to a storage bulb through a spiral cooled to $-78°$ C.

Mercury vapor was introduced into a selected hydrocarbon–oxygen mixture by alternately raising and lowering the level of mercury in a premixing vessel several times. The reactants were passed into the evacuated cell through two U tubes, packed with small glass helices, surrounded by ice. The procedure of mixing and admittance to the cell was standardized, and reproducible light absorptions could be obtained. Results using greater than 24 mm Hg pressure of cyclohexene were obtained by dispensing with the traps cooled to $0°$ C.

PHOTOMETRY

The intensities of light transmitted through the reaction cell were related to the resistance needed to balance a potentiometer circuit, and calibrated by comparison with the potassium ferrioxalate actinometer of Hatchard and Parker (6).

If

I_t = intensity of transmitted radiation

I_o = intensity of incident radiation

I_a = intensity of radiation absorbed by reactants in the cell,

then

$$I_t/I_o = \exp\{-\epsilon[\text{Hg}]l\}$$

and by differentiation

$$-d[\text{Hg}]/dt = \frac{1}{\epsilon l}\frac{d\{\log(I_t/I_o)\}}{dt},$$

where ϵ = extinction coefficient and l = light path. If the quantum yield of mercury removal is Φ, then we have

$$\Phi = -\frac{\Delta[\overline{\text{Hg}}]}{\Delta t}\cdot\frac{1}{I_a}$$

that is

$$\Phi = \frac{1}{\epsilon l}\frac{\Delta\log(I_t/I_o)}{\Delta t}\cdot\frac{1}{I_a}.$$

I_t and I_o were measured at the beginning of each experiment. As the concentration of mercury vapor [Hg] was known, it was possible to calculate the value of the extinction coefficient ϵ. Since Δt and I_a were known for each kinetic run, it was possible to calculate Φ. It was found that Φ was a useful parameter to give a measure of the interaction of mercury with the reactive species in the system, having a constant value ($\pm5\%$), while more than 50% of the mercury vapor reacted. The measurable range of values for using the full intensity of the lamp ($\sim 3\times10^{14}$ quanta/sec) was from 1×10^{-4} to 9×10^{-3}.

RESULTS

The results of typical experiments are presented in Fig. 1. In the series of experiments using C_4H_{10}–O_2–Hg, Φ decreases from 7×10^{-3} to 9×10^{-4} in the isobutane pressure range 0–25 mm Hg (Fig. 2). The relative quenching cross sections of isobutane and oxygen are such that oxygen quenches more than 90% of the 6^3P_1 excited mercury atoms for partial pressures of isobutane of less than 25 mm Hg with $P_{O_2} = 100$ mm Hg.
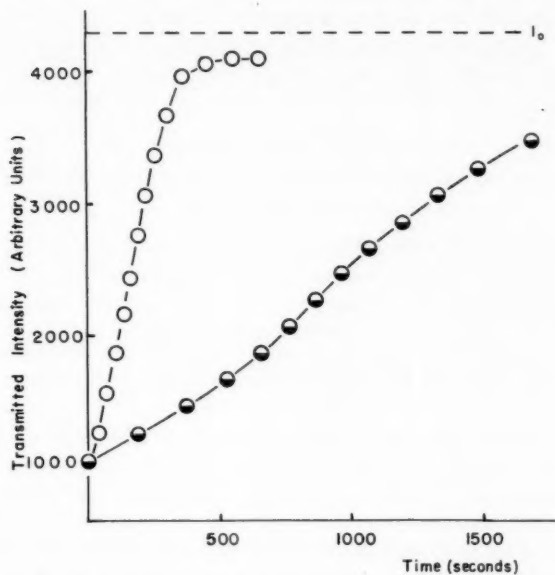
FIG. 1.   Typical experiments showing variation in rate of removal of excited 6^3P_1 mercury atoms in the isobutane/oxygen and cyclohexene/oxygen systems at 30° C. ○ $p_{C_6H_{10}} = 24$ mm Hg; $p_{O_2} = 200$ mm Hg. ◑ $p_{C_4H_{10}} = 50$ mm Hg; $p_{O_2} = 100$ mm Hg. Arbitrary intensity units = potentiometer ohms.
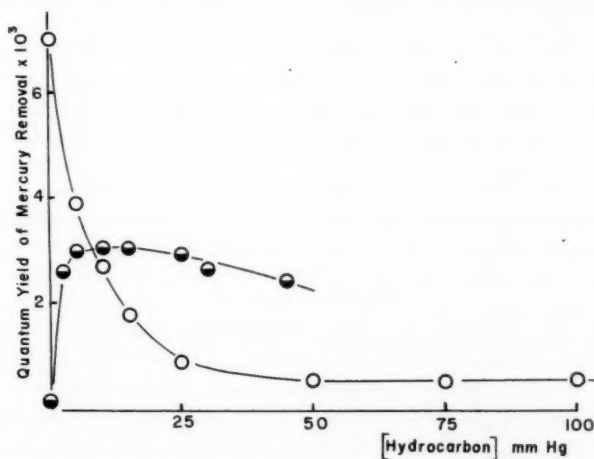
FIG. 2.   Quantum yield of mercury removal as a function of partial pressure of hydrocarbon at constant oxygen pressure at 30° C. ○ Isobutane series $p_{O_2} = 100$ mm Hg. ◑ Cyclohexene series $p_{O_2} = 200$ mm Hg.

Mercury and oxygen react rapidly in a clean reaction vessel ($\Phi = 7$–10×10^{-3}), but if an experiment using oxygen and mercury alone is performed after several using cyclohexene, oxygen, and mercury, the mercury–oxygen reaction is inhibited ($\Phi \sim 2 \times 10^{-4}$) presumably by involatile products having been deposited on the walls. In the presence of an increasing concentration of cyclohexene, Φ rapidly increases to a maximum value of 3×10^{-3} (Fig. 2).

DISCUSSION

The interaction of oxygen and mercury on illumination with 2537-Å radiation has recently been interpreted by Callear, Patrick, and Robb (5) in terms of the following series of equations [1]–[5]:

$$O_2 + Hg(6^3P_1) \rightarrow O_2{}^* + Hg(6^1S_0) \tag{1}$$

$$O_2 + O_2{}^* \rightarrow O_3 + O \tag{2}$$

$$O_2 + O_2{}^* \rightarrow O_2 + O_2 \tag{2'}$$

$$O + O_2 + M \rightarrow O_3 + M \tag{3}$$

$$O_3 + Hg \rightarrow HgO + O_2 \tag{4}$$

$$O + O_3 \rightarrow O_2 + O_2. \tag{5}$$
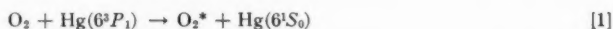
In the presence of hydrocarbon, the products formed by the reactions indicated by equations [2] and [3] will react rapidly with the hydrocarbon, presumably by the following processes:

$$RH + O_3 \rightarrow RO + HO_2 \tag{6}$$

$$RH + O \rightarrow R + OH. \tag{7}$$

There will thus be a competition between the hydrocarbon molecules and mercury atoms for reaction with ozone. This will result in the observed decrease in Φ for increasing partial pressure of isobutane, since the rate of ozone production will not be appreciably altered on using a large excess of oxygen. Under the conditions of a large excess of isobutane ($p_{C_4H_{10}}/p_{O_2} = 600/30$), $\Phi < 2\times10^{-4}$, whilst the peroxide quantum yields were about 0.85, indicating a negligible interaction between mercury and the intermediates or final products of the reaction.

As mentioned earlier the mercury–oxygen reaction, i.e. reaction [4], seems to be inhibited in a vessel which has been used for several experiments with cyclohexene. This is illustrated in Fig. 2 from which we see that, under the circumstances mentioned, the quantum yield for the disappearance of mercury vapor in the presence of 200 mm Hg of oxygen has an initial value of about 2×10^{-4}. On adding cyclohexene the value of Φ increases until it reaches a maximum of about 3×10^{-3}. This maximum occurs when the pressure of cyclohexene is approximately 10 mm Hg. The reasons for the initial inhibition of the mercury–oxygen reaction are not clear. Reaction [4] would be expected to take place to some extent, but apparently the HgO is not stabilized on the walls of the reaction vessel after these have been exposed to the products from the cyclohexene reaction. Were this the case then it would, of course, be easy to understand the initial low value observed for Φ. The addition of increasing amounts of cyclohexene would reduce the rate of diffusion of the HgO to the walls of the vessel, and so we thus have some of the features of a wall-inhibited reaction. In this type of kinetic system, i.e. one with a step which is wall-inhibited, the rate of the over-all process studied increases with pressure because at the higher pressures the inhibiting influence of the walls becomes less important owing to the rate of diffusion of the active species being smaller at the higher pressures. The shape of the curve in Fig. 2 showing the variation of Φ with increasing cyclohexene pressure is in agreement with these requirements and so the suggested explanation would appear to be a reasonable one.

Since mercury does not react with cyclohexene in the absence of oxygen, our results suggest that the mercury vapor is removed by reaction with some product, or intermediate, of the oxidation. If the lamp was shielded midway through a run, the light

absorption was the same on reillumination as it was immediately prior to shielding, indicating that the mercury reacts with an active intermediate rather than a final product. Radicals produced in reaction [7], or by direct cleavage of the R—H bond in the hydrocarbon, will react rapidly with oxygen according to equation [8].

$$R \cdot + O_2 \rightarrow RO_2 \cdot \tag{8}$$
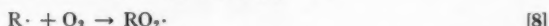
The subsequent reaction of the peroxy radical with mercury as indicated in equation [9]

$$RO_2 + Hg \rightarrow HgO + RO \cdot \tag{9}$$

seems reasonable. This reaction was postulated by Small and Ubbelohde (2) as being responsible for the reduction of peroxide yield in the presence of mercury for the oxidation of n-hexane. Reaction [9] does not, however, necessarily lead to removal of $RO_2 \cdot$ from the system if $RO \cdot$ reacts by the following scheme.

$$RO \cdot + RH \rightarrow ROH + R \cdot \tag{10}$$

$$R \cdot + O_2 \rightarrow RO_2 \cdot \tag{8}$$
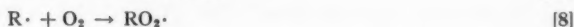
In the cyclohexene oxidation, low quantum yields of peroxide were obtained (< 0.08). The final amounts of products were very low owing to the limited period of initiation resulting from the rapid removal of mercury, the original concentration of which was about 5×10^{-10} g-mole liter^{-1}. As the quantities of products produced were extremely small the only analysis done was for peroxide. A modification of the sensitive ferrous thiocyanate method of Young et al. (8) was used. Cyclohexene will probably have a higher quenching cross section for excited 6^3P_1 mercury atoms than oxygen, and the decrease in Φ towards higher cyclohexene values where the cyclohexane is quenching an appreciable fraction of the excited mercury, suggests that each C_6H_{10}-Hg* quenching process has a lower radical-producing efficiency than the corresponding O_2-Hg* quenching process. The final radical yield would then be expected to be low since the yield of ozone in the O_2-Hg reaction was determined by Callear, Patrick, and Robb to be 0.14 (5). The final peroxide yield will also be low since the work of Burgess and Robb (7) indicates that it is unlikely that a hydrocarbon peroxide chain will be operative at 30° C.

REFERENCES

1. A. L. MARSHALL.   J. Phys. Chem. **30**, 34 (1926).
2. N. J. H. SMALL and A. R. UBBELOHDE.   J. Chem. Soc. 4619 (1952).
3. J. A. GRAY.   J. Chem. Soc. 3150 (1952).
4. J. S. WATSON and B. de B. DARWENT.   J. Phys. Chem. **61**, 577 (1957).
5. A. B. CALLEAR, C. R. PATRICK, and J. C. ROBB.   Trans. Faraday Soc. **55**, 280 (1959).
6. C. G. HATCHARD and C. A. PARKER.   Proc. Roy. Soc. (London), A, **235**, 518 (1956).
7. R. H. BURGESS and J. C. ROBB.   Trans. Faraday Soc. **54**, 1015 (1958).
8. C. A. YOUNG, R. R. VOIGT, and J. A. NIEULAND.   Ind. Eng. Chem. Anal. Ed. **8**, 198 (1936).

MERCURY-PHOTOSENSITIZED OXIDATIONS OF HYDROCARBONS

PART II. THE MERCURY-PHOTOSENSITIZED OXIDATION OF ISOBUTANE[1]

K. M. BELL[2] AND C. A. McDOWELL

ABSTRACT

The mercury-photosensitized oxidation of isobutane has been studied over a wide range of pressures of the hydrocarbon and oxygen, in a conventional static photochemical apparatus at the temperatures of 30° C and 100° C. The main products of the reaction are tertiary butyl hydroperoxide, together with tertiary butyl alcohol, acetone, and corresponding small quantities of formaldehyde and methyl alcohol. Isobutyraldehyde was also detected; ditertiary butyl peroxide being notably absent. Peroxide yields suggest that a reaction between an excited isobutane molecule and oxygen is important in the initiation processes and that peroxide is formed in the reaction

$$RO_2 + HO_2 \rightarrow ROOH + O_2.$$

INTRODUCTION

The mercury-photosensitized oxidations of methane, ethane, and propane have previously been studied in flow systems (1, 2, 3). The original classical concept of the peroxide chain reaction

$$RO_2\cdot + RH \rightarrow ROOH + R \qquad [19]$$

occurring at 25° C was modified in the most recently published work of this type by Watson and Darwent (4), who explained the low yields of peroxide obtained in the ethane oxidation by suggesting the following reaction

$$RO_2\cdot + HO_2 \rightarrow ROOH + O_2 \qquad [3]$$

as the source of hydroperoxide rather than reaction [19]. These workers found that the yields of peroxide decreased on raising the reaction temperature or on lowering the flow rate. They attributed these effects to thermal and photochemical decomposition of the peroxide. The hydroperoxide was characterized as ethyl hydroperoxide by Gray (1), and so this work provides no evidence on the nature of the mutual interaction of HO_2 radicals.

In an effort to elucidate further the nature of certain aspects of hydrocarbon oxidation mechanisms we have studied the mercury-photosensitized oxidation of isobutane in a static photochemical apparatus employing low light intensities.

EXPERIMENTAL

The apparatus and photochemical techniques employed were the same as those described in Part I (K. M. Bell and C. A. McDowell. Can. J. Chem. This issue). Using a modification of the ferrous thiocyanate method of Young, Voigt, and Nieuland (5), 5×10^{-9} mole of peroxides could be determined. The method is non-stoichiometric, and a calibration curve was prepared using purified solutions of tertiary butyl hydroperoxide. The hydroperoxide was also determined gas chromatographically, dinonyl phthalate on chromosorb being used as the column material. The other products were determined and identified by their characteristic elution times on different columns. Formaldehyde

was estimated by the method of Bricker and Johnson (6). In all cases the final yield of product was limited by the slow removal of the mercury vapor (see Part I). The rate of removal was greater at 30° C than 100° C. For a mixture of 50 mm Hg of isobutane and 100 mm Hg of oxygen, Φ (the quantum yield of *removal* of excited 6^3P_1 Hg atoms) was 6×10^{-4} at 30° C and 2×10^{-4} at 100° C.

RESULTS

The main product of the oxidation was tertiary butyl hydroperoxide, together with smaller yields of tertiary butyl alcohol, acetone, methyl alcohol, formaldehyde, and iso-butyraldehyde. Evidence was also obtained for a trace of isobutyl alcohol. Tests were specifically made for ditertiary butyl peroxide but none could be detected under conditions where the lower limit of detection corresponded to a quantum yield of 0.02. It is also to be noted that we were unable to detect isobutylene oxide despite several attempts using our gas chromatographic apparatus. Close agreement was obtained between the total peroxide determined colorimetrically, and tertiary butyl hydroperoxide determined gas chromatographically.

The yield of peroxide was directly proportional to the integrated absorbed light intensity (Fig. 1) for constant incident intensity, and also to the average absorbed
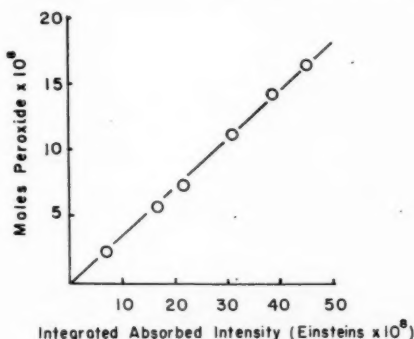

FIG. 1.   Yield of peroxide as a function of the integrated absorbed intensity, for constant incident intensity, in the mercury-photosensitized oxidation of isobutane at 30° C, $p_{O_2} = p_{C_4H_{10}} = 100$ mm Hg.

intensity when a given isobutane–oxygen mixture was illuminated for a given time (500 seconds) at varying light intensities (Fig. 2). The integrated absorbed light intensity was obtained from the sum of the average numbers of quanta absorbed between deter-mined short time intervals during the course of the reaction (see Part I). The time of illumination (500 seconds) for the intensity variation was the minimum required to obtain an accurately determinable quantity of peroxide at the lowest intensity, so minimizing the change in absorbed intensity, which in no case was greater than 15% of the total.

The quantum yield of peroxide was constant for a given isobutane–oxygen ratio for oxygen pressures in excess of 30 mm Hg, but increased as the fraction of isobutane in the mixture increased (Fig. 3). The yield of tertiary butyl alcohol underwent the same variation with varying light intensity as the peroxide (Fig. 4), and was constant in the region of constant peroxide (Fig. 5). The total yield of (tertiary butyl alcohol + acetone) was approximately proportional to the corresponding yield of peroxide (Fig. 6).
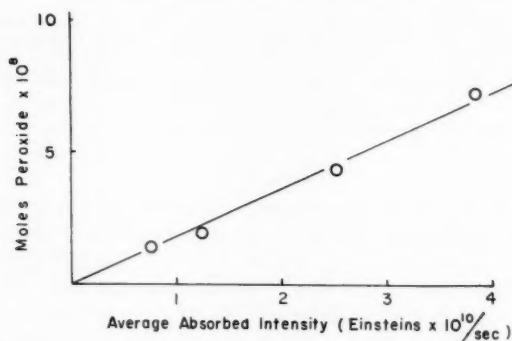
Fig. 2. Yield of peroxide as a function of the average absorbed intensity, varying the incident intensity and illuminating for constant time (500 seconds), in the mercury-photosensitized oxidation of isobutane at 30° C, $p_{O_2} = p_{C_4H_{10}} = 100$ mm Hg.
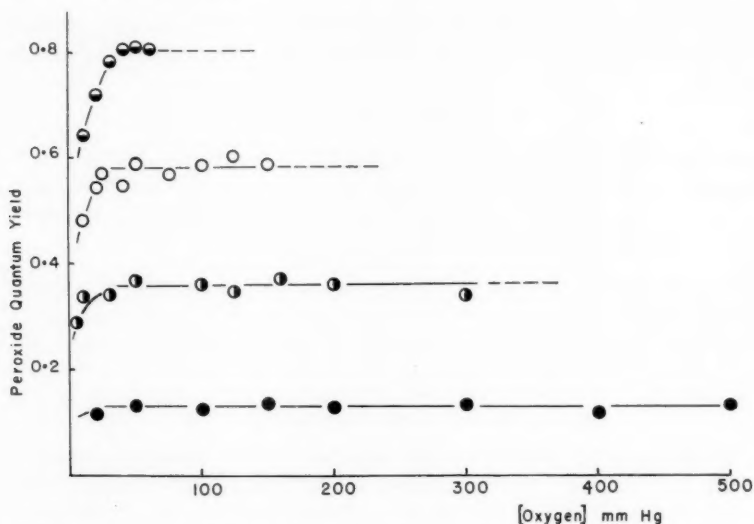

Fig. 3. Peroxide quantum yield as a function of the concentration of reactants at fixed hydrocarbon–oxygen ratios, in the mercury photosensitized oxidation of isobutane at 30° C. ◑ $p_{C_4H_{10}}:p_{O_2} = 10:1$; ○ $p_{C_4H_{10}}:p_{O_2} = 3:1$; ◐ $p_{C_4H_{10}}:p_{O_2} = 1:1$; ● $p_{C_4H_1}:p_{O_2} = 1:10$.

At 100° C an almost identical set of results was obtained (Tables I and II), modified

TABLE I

Quantum yields of products in the isobutane mercury-photosensitized oxidation at 30° C

$p_{C_4H_{10}}/p_{O_2}$		% Hg(6^3P_1) quenched by C_4H_{10}	Total perioxide	t-BuOOH	t-BuOH	Acetone	Isobutyraldehyde
(ratio)	(mm Hg)						
1/10	40/400	3	0.13	N.D.	0.065	N.D.	0.08
1/1	220/220	24	0.36	0.33	0.12	0.02	0.12
3/1	330/110	48	0.58	0.55	0.23	0.03	0.09
10/1	400/40	76	0.80	0.76	0.36	0.06	0.05
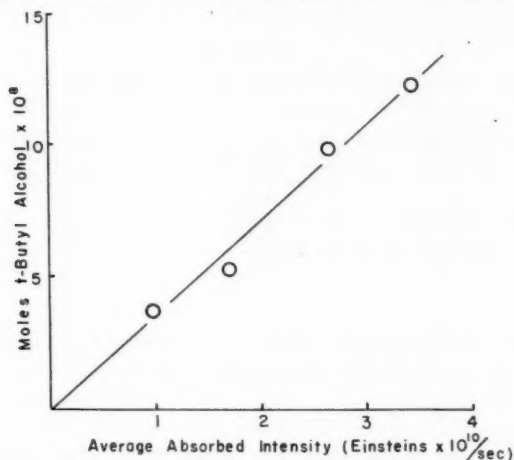
FIG. 4. Tertiary butyl alcohol as a function of the average absorbed intensity, varying the incident intensity and illuminating for constant time (1000 seconds), in the mercury-photosensitized oxidation of isobutane at 30° C, $p_{C_4H_{10}} = 400$ mm Hg; $p_{O_2} = 40$ mm Hg.
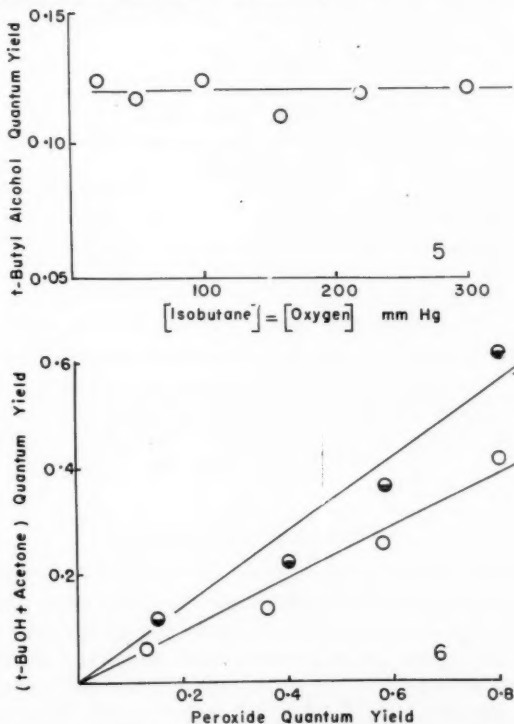
FIG. 5. Tertiary butyl alcohol quantum yield as a function of the concentration of reactants at fixed hydrocarbon–oxygen ratio = 1:1 in the mercury-photosensitized oxidation of isobutane at 30° C.

FIG. 6. Quantum yields of (t-butyl alcohol + acetone) as a function of tertiary butyl hydroperoxide quantum yield in the mercury-photosensitized oxidation of isobutane. ○ 30° C; ◑ 100° C.

TABLE II

Quantum yields of products in the isobutane mercury-photosensitized oxidation at 100° C

| $p_{C_4H_{10}}/p_{O_2}$		% Hg(6^3P_1) quenched by C_4H_{10}	Total peroxide	t-BuOOH	t-BuOH	Acetone	CH_3OH	CH_2O	Isobutyr-aldehyde
(ratio)	(mm Hg)								
1/10	40/400	3	0.15	0.12	0.04	0.08	N.D.	0.07	0.06
1/1	220/220	24	0.40	0.38	0.08	0.14	N.D.	0.12	0.09
3/1	330/110	48	0.58	0.55	0.13	0.24	N.D.	0.16	0.07
10/1	400/40	76	0.80	0.75	0.20	0.42	0.17	0.23	0.035

only by an increased yield of acetone relative to tertiary butyl alcohol, and an increased total yield of (tertiary butyl alcohol + acetone). With the increase in acetone, methanol and formaldehyde were detected. The variation with conditions for all products was the same at 100° C as at 30° C. Small quantum yields of isobutyl alcohol verging on the lower limit of detection ($\phi \approx 0.02$–0.03) were observed at the higher isobutane–oxygen ratios.

Results showing the thermal stability of the peroxide to both homogeneous and heterogeneous decomposition during the course of an experiment, are given in Table III, the

TABLE III

Thermal stability of peroxide at 30° C and 100° C
($p_{O_2} = p_{C_4H_{10}} = 100$ mm Hg)

Period of illumination (seconds)	Period of shielding (seconds)	Peroxide	Temp. (°C)
500	—	0.36	30
500	1000	0.35	30
500	—	0.40	100
500	1000	0.39	100

products being left in the reaction cell for 1000 seconds, with the lamp shielded, after a 500-second period of illumination. The hydrocarbon conversion was never greater than 1%, and in the case of the colorimetric peroxide determination often less than 0.1%, thus minimizing photochemical decomposition with subsequent reaction of intermediate and final products.

DISCUSSION

Variation of the concentrations of the reactants in a mercury-photosensitized oxidation will possibly have an effect on the initiation reactions. The rate of initiation will depend upon the relative quenching cross sections of the two gases and also upon the numbers of radicals produced as a result of each quenching process. Values of the quenching cross section of oxygen have been variously reported in the literature lying in the range 13.2–19.9 Å^2 (7, 8). Burgess and Robb in a recent paper (9) adopted a value for $\sigma^2_{O_2.Hg(6^3P_1)}$ of 17.2 Å^2 and for $\sigma^2_{C_4H_{10}.Hg(6^3P_1)}$ of 6.9 Å^2, both determined in the same way. Using these values the number of excited mercury atoms quenched by each gas is given by

$$\frac{Z_{O_2, Hg(6^3P_1)}}{Z_{C_4H_{10}, Hg(6^3P_1)}} = 3.2 \frac{n}{(1-n)}$$

where n is the mole fraction of oxygen in the mixture (see Table I).

Radicals are produced from the hydrocarbon quenching reaction [a],

$$Hg(6^3P_1) + RH \rightarrow Hg(6^1S_0) + R + H. \qquad [a]$$
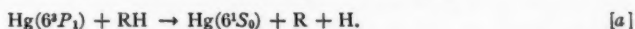
Radical yields in mercury-photosensitized decompositions are usually below unity. For isobutane a yield of 0.2 radicals has been determined by Darwent and Winkler (10), indicating that reaction [b] must occur.

$$RH^* + M \rightarrow RH + M \qquad [b]$$

In this equation RH^* represents an excited RH molecule.

In the presence of oxygen it is possible that reaction [c] will occur.

$$RH^* + O_2 \rightarrow R + HO_2 \qquad [c]$$

Burgess and Robb (9) postulated that each O_2-Hg quenching collision led to three radicals in the sequence of reaction [d] to [i] since reaction [e] was stated to have an efficiency close to unity.

$$Hg(6^3P_1) + O_2 \rightarrow O_2^* + Hg(6^1S_0) \qquad [d]$$
$$O_2^* + O_2 \rightarrow O_3 + O \qquad [e]$$
$$RH + O_3 \rightarrow RO + HO_2 \qquad [f]$$
$$RO + RH \rightarrow ROH + R \qquad [g]$$
$$RH + O \rightarrow R + OH \qquad [h]$$
$$RH + OH \rightarrow R + H_2O \qquad [i]$$

In a subsequent paper Callear, Patrick, and Robb (11) while studying the O_2-Hg(6^3P_1) reaction found the net efficiency of process [e] including reaction [j]

$$O + O_2 + M \rightarrow O_3 + M \qquad [j]$$

to be 0.14, due to deactivation of the active species in reaction [k]

$$O_2^* + O_2 \rightarrow O_2 + O_2. \qquad [k]$$

This seems to contradict the value adopted in their earlier paper. In hydrocarbon–oxygen mixtures the reactions [l] and [m]

$$RH + O_2^* \rightarrow R + HO_2 \qquad [l]$$

and

$$RH + O_2^* \rightarrow RO + OH \qquad [m]$$

are also possibilities.

The situation is obviously complex since efficiencies cannot be accurately assigned to all the above reactions. One simplification which can be made is to operate at a constant ratio of hydrocarbon to oxygen. Under these conditions the rate of initiation should not vary, provided the over-all gas pressures are adequate to provide complete quenching of all the excited mercury atoms. Using different ratios it is possible to assign efficiencies to some of the above reactions.

The fact that the quantum yields of peroxide were below unity and independent of

the hydrocarbon-concentration variation in a mixture containing a fixed hydrocarbon-oxygen ratio (Fig. 3) indicates the absence of a peroxide chain reaction at the temperatures studied. The operation of the simple mechanism below:

$$RH \xrightarrow{R_1} R + H \tag{1}$$

$$R + O_2 \xrightarrow{k_2} RO_2 \tag{2}$$

$$H + O_2 \xrightarrow{k_2'} HO_2 \tag{2'}$$

$$RO_2 + HO_2 \xrightarrow{k_3} ROOH + O_2 \tag{3}$$

leads, on applying the stationary state hypothesis, to the kinetic equation

$$d[ROOH]/dt = R_1 = \phi I_a$$

where ϕ is the effective primary radical yield in all initiation processes.

For a given hydrocarbon–oxygen ratio the total yield of peroxide should be proportional to the absorbed light intensity as observed (Fig. 2). Yields of tertiary butyl alcohol vary in a manner parallel to those of the hydroperoxide (Figs. 4 and 5) suggesting that the tertiary butoxy radical, which must be the immediate precursor of the alcohol, in the absence of ditertiary butyl peroxide, originates in reaction [4]

$$RO_2 + RO_2 \rightarrow 2RO\cdot + O_2 \tag{4}$$

with subsequent hydrogen abstraction from the parent hydrocarbon as follows,

$$RO + RH \rightarrow ROH + R. \tag{5}$$

Reaction [4] is not a terminating step and, therefore, does not affect the rate equation for peroxide production. In addition to reaction [5] a similar type of process, namely [3'], merits some consideration.
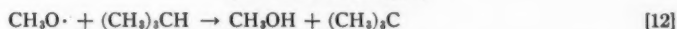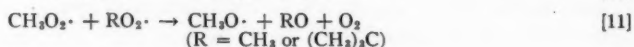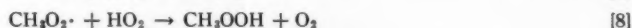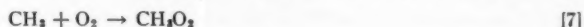
$$RO + HO_2 \rightarrow ROH + O_2 \tag{3'}$$

It is difficult to decide definitively between the two reactions [3'] and [5]. If [3'] is assumed to be the process leading to the production of tertiary butyl alcohol this would imply a primary radical yield of greater than unity for those mixtures with an isobutane–oxygen ratio of 10:1, since [3'] is a terminating reaction. The value of 0.8 found for the quantum yield of tertiary butyl hydroperoxide suggests that [3] alone is the main terminating reaction. For these reasons, reaction [5] would seem to be a better suggestion for the production of tertiary butyl alcohol. Figure 5, however, shows that the quantum yield of tertiary butyl alcohol is constant and independent of pressure for a fixed ratio of isobutane–oxygen and this is predicted by equation [3']. The inclusion of equation [5] and omission of [3'] would lead to a decrease in alcohol and an increase in acetone production for lower values of isobutane in the fixed isobutane–oxygen ratio. Either equation [5] or [3'] leads to the same expected change in the rate of formation of alcohol and acetone with variation in light intensity. The kinetic data we have obtained is in favor of reaction [3'] as being the process responsible for the formation of the tertiary butyl alcohol. It would, however, also be reasonable to include reaction [5] on the basis of the values and trends observed for the quantum yields of tertiary butyl alcohol. It must, however, be pointed out that the constant value found for the ratio tertiary butyl alcohol – acetone for varying values of the ratio [isobutane]–[oxygen] (see Table II) is predicted

by neither [3'] nor [5] if either is in competition with equation [6], which is obviously the source of the acetone found.

$$(CH_3)_3CO \rightarrow CH_3COCH_3 + CH_3 \tag{6}$$

However, the process represented by equation [6] may not necessarily be so simple as there indicated. Should equation [6] be more complex than indicated it is possible that the inclusion of equation [5] may give the correct form of the variation of the quantum yields of tertiary butyl alcohol with hydrocarbon concentration.

The decomposition of the tertiary butoxy radical indicated in equation [6] is almost complete at temperatures about 190° C, even in the presence of an excess of a hydrocarbon containing a weak R—H bond (13, 14, 15, 16). At room temperature, it appears that the abstraction predominates because it requires a much lower activation than the decomposition. At 100° C the increasing yields of acetone are a measure of increasing extent to which the decomposition reaction [6] occurs. There is much uncertainty regarding the reaction of the resulting methyl radicals with oxygen to form methyl alcohol and formaldehyde (1, 16, 17, 18, 19, 20, 21). Below are listed some of the reactions considered possible at 100° C in the absence of significant yields of methyl hydroperoxide.

$$CH_3 + O_2 \rightarrow CH_3O_2 \tag{7}$$

$$CH_3O_2 \cdot + HO_2 \rightarrow CH_3OOH + O_2 \tag{8}$$

$$CH_3O_2 \cdot \rightarrow CH_2O + OH \tag{9}$$

$$CH_3OOH \xrightarrow{\text{surface}} CH_3O \cdot + OH \tag{10}$$

$$CH_3O_2 \cdot + RO_2 \cdot \rightarrow CH_3O \cdot + RO + O_2 \tag{11}$$
$$(R = CH_3 \text{ or } (CH_3)_3C)$$

$$CH_3O \cdot + (CH_3)_3CH \rightarrow CH_3OH + (CH_3)_3C \tag{12}$$

$$CH_3O + O_2 \rightarrow CH_2O + HO_2 \tag{13}$$

It is not, of course, possible to assign individual efficiencies to reactions [7]–[13] given above. Tables I and II show that the peroxide yields and the variations of these with the composition of the reactants are about the same at 30° and 100°. Similar reactions as indicated in [7]–[13] must have about the same efficiencies at both these temperatures.

Close agreement between the total peroxide and tertiary butyl hydroperoxide indicates that neither the mutual interaction of hydroperoxy radicals nor abstraction from the parent hydrocarbon to form hydrogen peroxide occurs to any appreciable extent. The exothermicity for abstraction by the tertiary butyl peroxy radical from the isobutane molecule, equation [5']

$$RO_2 + RH \rightarrow RO_2H + R, \tag{5'}$$

is about 1.5 kcal mole^{-1}, and the activation energy has been determined by Burgess and Robb (9) to be 16 kcal mole^{-1}, thus accounting for the radical–radical reaction at 30° C. Abstraction from the isobutane molecule by the tertiary butoxy radical, equation [5], is exothermic by about 16 kcal mole^{-1}, and the activation energy is presumably less than for the peroxy abstraction, equation [5'], being sufficiently low to exclude the occurrence of the radical–radical reaction at 30° C.

The above isobutane–oxygen reaction scheme predicts that, providing $[HO_2] = [RO_2]$, the quantum yield of peroxide should be proportional to the sum of the reactions involving the RO · radical, i.e. tertiary butyl alcohol + acetone. Figure 6 shows that this is what our experimental results indicate.

The yields of peroxide which are formed in the main terminating reaction [3] increase with the increasing role of hydrocarbon in the excited mercury quenching processes (Tables I and II) and suggest that reaction [c] in the initiation processes has an efficiency close to unity. Low peroxide yields ($\phi < 0.15$) for the oxygen–isobutane = 10:1 mixtures are attributed to a low efficiency of reaction [e]. The value for ϕ in this case is close to that determined by Callear, Patrick, and Robb (11) for the oxygen–mercury reaction.

The detection of small yields of isobutyraldehyde was surprising. This is regarded as being formed from the isobutoxy radical according to equation [14]

$$(CH_3)_2CHCH_2O + O_2 \rightarrow (CH_3)_2CHCHO + HO_2. \tag{14}$$
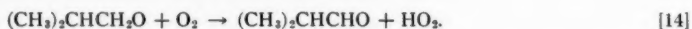
In the absence of significant quantities of the corresponding hydroperoxide the isobutoxy radicals will probably be formed as primary products without going through the isobutyl peroxy stage, where the opportunity for formation of the hydroperoxide exists. The data in Table II show that the ratio isobutyraldehyde – tertiary butyl peroxide increases with the increase in the percentage of the excited mercury atoms quenched by molecular oxygen. This suggests that the reactions [15] and [16] may be of some importance:

$$(CH_3)_2CHCH_3 + O_3 \rightarrow (CH_3)_2CHCH_2O + HO_2 \tag{15}$$

$$(CH_3)_2CHCH_3 + O_2{}^* \rightarrow (CH_3)_2CHCH_2O + OH. \tag{16}$$

Both of these are very exothermic.

The occurrence of [14] and [15] maintains the balance of hydroperoxy radicals at high oxygen–hydrocarbon ratios where each effective oxygen quenching process has the potentiality of producing three $RO_2 \cdot$ radicals and only one HO_2 radical (reactions [c] to [i]).

Hydrogen abstraction by oxygen from the isobutoxy radical must have a lower activation energy than abstraction by the isobutoxy radical from the parent hydrocarbon, in view of the low yields of isobutyl alcohol found. Hydrogen abstraction from the tertiary butoxy radical by oxygen does not occur to any extent because the product of this reaction, namely isobutylene oxide, was not detected. A small fraction of the formaldehyde yields is attributable to decomposition of the isobutoxy radical occurring at 100° C where the quantum yields of the aldehyde are lower. The over-all increase in the yield of (acetone + t-butyl alcohol) at 100° C suggests reaction [4] may have a small activation energy. The slight increase in peroxide at 100° C for oxygen-rich mixtures is explained if the efficiency of [e] increases with increasing temperature.

A pressure of ~ 3 mm Hg of oxygen will give complete quenching in a system containing mercury vapor at its room temperature equilibrium vapor pressure. The tail-off in peroxide yield at oxygen pressures below 30 mm Hg may be attributable to a competition between deactivation processes and reaction with oxygen for removal of active isobutane molecules as portrayed by equations [17] and [18]

$$C_4H_{10}{}^* \rightarrow C_4H_{10} \tag{17}$$

$$C_4H_{10}{}^* + O_2 \rightarrow C_4H_9 + HO_2. \tag{18}$$

The slow, absolute rate of reaction of mercury with the isobutane oxidation system will not be significant in reducing the rate of production of radicals in the initiation processes (see Part I).

ACKNOWLEDGMENTS

REFERENCES

1. J. A. GRAY.   J. Chem. Soc. 3150 (1952).
2. A. B. NALBANDYAN.   Doklady Akad. Nauk, S.S.S.R. **66**, 413 (1949).
3. A. B. NALBANDYAN and N. V. FOK.   Doklady Akad. Nauk, S.S.S.R. **86**, 589 (1952).
4. J. S. WATSON and B. de B. DARWENT.   J. Phys. Chem. **61**, 577 (1957).
5. C. A. YOUNG, R. R. VOIGT, and J. A. NIEULAND.   Ind. Eng. Chem. Anal. Ed. **8**, 198 (1936).
6. C. E. BRICKER and H. R. JOHNSON.   Anal. Chem. **17**, 400 (1945).
7. W. A. NOYES, JR. and P. A. LEIGHTON.   Photochemistry of gases.   Reinhold. 1941. p. 221.
8. A. C. G. MITCHELL and M. W. ZEMANSKY.   Resonance radiation and excited atoms. Cambridge 1934. p. 204.
9. R. H. BURGESS and J. C. ROBB.   Trans. Faraday Soc. **54**, 1015 (1958).
10. B. de B. DARWENT and C. A. WINKLER.   J. Phys. Chem. **49**, 150 (1945).
11. A. B. CALLEAR, C. R. PATRICK, and J. C. ROBB.   Trans. Faraday Soc. **55**, 280 (1959).
12. N. A. MILAS and D. M. SURGENOR.   J. Am. Chem. Soc. **68**, 205 (1946).
13. L. M. DORFMAN and Z. W. SALSBURG.   J. Am. Chem. Soc. **73**, 255 (1951).
14. J. MURAWSKI, J. S. ROBERTS, and M. SZWARC.   J. Chem. Phys. **19**, 698 (1951).
15. G. McMILLAN and M. J. H. WIJEN.   Can. J. Chem. **36**, 1227 (1958).
16. E. R. BELL, J. H. RALEY, F. F. RUST, F. H. SEUBOLD, and W. E. VAUGHAN.   Discussions Faraday Soc. **10**, 242 (1951).
17. J. R. BATES and R. SPENCE.   J. Am. Chem. Soc. **53**, 381, 1689 (1931).
18. W. J. BLAEDEL, R. A. OGG, JR., and P. A. LEIGHTON.   J. Am. Chem. Soc. **64**, 2500 (1942).
19. D. E. HOARE and A. D. WALSH.   Trans. Faraday Soc. **53**, 1102 (1957).
20. F. B. MARCOTTE and W. A. NOYES, JR.   Discussions Faraday Soc. **10**, 236 (1951).
21. P. L. HANST and J. G. CALVERT.   J. Phys. Chem. **63**, 71, 104 (1959).

METAL OXIDE ALKOXIDE POLYMERS

PART I. THE HYDROLYSIS OF SOME PRIMARY ALKOXIDES OF ZIRCONIUM[1]

D. C. BRADLEY[2] AND D. G. CARTER[3]

ABSTRACT

Ebulliometric studies have been made on the hydrolysis of some zirconium alkoxides, $Zr(OR)_4$ where R = Et, Pr^n, Bu^i, and Bu^n. The variation of the degree of polymerization of the zirconium oxide alkoxides so produced was determined as a function of the degree of hydrolysis. The results are interpreted in terms of structural models based on octahedrally 6-co-ordinated zirconium.

INTRODUCTION

It is well established (1) that zirconium alkoxides $Zr(OR)_4$ are polymeric compounds involving metal–oxygen co-ordinate bonds. Although these alkoxides hydrolyze with great facility it is possible under rigorously controlled conditions to isolate the intermediate oxide alkoxides $ZrO_x(OR)_{4-2x}$. These products are of particular interest from the structural viewpoint because they may involve both condensation polymerization (giving ZrOZr systems) and co-ordination polymerization. In addition they are of interest as inorganic polymers which are intermediate between the relatively small polymers of the tetraalkoxide and the macromolecular metal oxide. Studies on the hydrolysis of titanium alkoxides (2, 3, 4) led to the suggestion of structural models for the titanium oxide ethoxides based on octahedrally 6-co-ordinated titanium. Since titanium exhibits a maximum co-ordination number of 6 but zirconium may expand its co-ordination to 7 or 8 it was important to determine whether or not the zirconium oxide alkoxides conformed to the same structural models as the corresponding titanium compounds. We now report the results of an ebulliometric study of the hydrolysis of four primary alkoxides of zirconium in which the degree of polymerization was determined as a function of the degree of hydrolysis.

EXPERIMENTAL AND RESULTS

Zirconium Alkoxides

These were prepared and analyzed using previously described (1) methods. The compounds were distilled at 0.1 mm pressure prior to the hydrolysis experiments.

Zirconium isobutoxide had not previously been described and it was prepared as follows. Freshly distilled zirconium tetraisopropoxide (9 g) was caused to react with isobutanol (125 cc), and the liberated isopropanol removed by fractional distillation. The solution was concentrated to ca. 30 cc and a mass (9 g) of crystals of the *solvate* $Zr(OBu^i)_4,Bu^iOH$ was deposited on cooling. At 100° C at 0.1 mm the crystals softened and lost isobutanol, and the tetraisobutoxide was distilled at 213° C at 0.3 mm. The gummy solid (found: Zr, 24.5; $Zr(OBu^i)_4$ requires: Zr, 23.8%) was recrystallized from isobutanol to reform the *solvate*. Found: Zr, 20.2. $Zr(OBu^i)_4,Bu^iOH$ requires: Zr, 19.9%. Heated under atmospheric pressure the *solvate* softened at 146° C and melted with dissociation at 154° C.

1434

Ebulliometry

An all-glass ebulliometer, similar to that already described (5) and incorporating a differential water thermometer, was used. About 20 cc of dry alcohol was distilled into the ebulliometer in each experiment, the exact amount being determined by weighing to 0.01 g. The water levels in the differential thermometer were read to 0.01 mm using a travelling microscope. About 20 minutes were required after each addition of solute for thermal equilibrium to be re-established.

The following procedure was adopted for the ebulliometric hydrolysis studies. First a series of additions of weighed amounts (Δm) of zirconium alkoxide was made and the corresponding elevations of the boiling point (ΔT) were recorded. The slope of the linear plot of ΔT versus Δm was then found graphically. Next, several weighed amounts of the pure standard (either fluorene or azobenzene) were added and the ΔT's again plotted against weight of solute. The molecular weight of the zirconium compound was then calculated from a knowledge of the two slopes and the molecular weight of the standard. Finally, a series of additions of known aqueous alcohol were made. These solutions contained less than 10% w/w of water and were made up gravimetrically. The addition of aqueous alcohol caused an immediate decrease in the boiling point elevation due to the increase in molecular weight caused by hydrolysis of the zirconium compound. To obtain the correct degree of polymerization of the hydrolysis product an allowance was made for the additional solvent added, and for the amount of alcohol liberated by hydrolysis. These experiments were of several hours' duration and the ebulliometer was weighed at the end of the experiment to determine whether solvent had been lost by evaporation. The process being studied may be depicted by the following equation:

$$[ZrO_{x_1}(OR)_{4-2x_1}]n_1 + (n_2x_2 - n_1x_1)H_2O \rightarrow n_1/n_2[ZrO_{x_2}(OR)_{4-2x_2}]n_2 + 2(n_2x_2 - n_1x_1)ROH$$
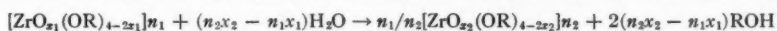
where $n_2 > n_1$ and $x_2 > x_1$. In fact the system may contain a distribution of polymer sizes and the values of n determined are number-average degrees of polymerization. The degree of hydrolysis, namely the ratio of gram-molecules of water added per gram-atom of zirconium, is designated by h. In principle h may be varied from 0 to 2 but some experiments were terminated when insoluble products appeared in the ebulliometer.

Zirconium Ethoxide

Experiments were made at three initial concentrations of zirconium ethoxide. The results are given in the following tables.

(*a*) Initial concentration of $Zr(OEt)_4$: 0.186 g-mol./kg ethanol.

TABLE I

h	0.00	0.01	0.10	0.22	0.38	0.52	0.69	0.92	1.16	1.49	1.63	(1.87)
n	2.10	2.15	2.42	2.70	3.18	3.68	4.53	6.55	9.39	9.97	11.4	(10.9)

Precipitation of a white solid occurred 5 minutes after the addition corresponding to $h = 1.87$.

(*b*) Initial concentration of $Zr(OEt)_4$: 0.409 g-mol./kg ethanol.

TABLE II

h	0.000	0.060	0.148	0.273	0.422	0.630	0.825	1.027	(1.229)
n	2.17	2.47	2.83	3.12	3.60	4.81	6.65	10.3	(13.3)

Opalescence in the solution was just perceptible at $h = 0.630$ and became appreciable

at $h = 1.229$. The hydrolysis was continued to $h = 1.433$ before allowing the system to cool when about 0.1 g solid was deposited.

(c) Initial concentration of $Zr(OEt)_4$: 0.723 g-mol./kg ethanol.

TABLE III

h	0.000	0.037	0.080	0.121	0.182	0.248	0.344	0.463	0.612	0.766
n	2.24	2.42	2.61	2.81	3.01	3.22	3.54	3.94	4.66	5.79

Opalescence was first detected at $h = 0.612$ and became appreciable at $h = 0.888$.

Zirconium n-Propoxide

The concentration of $Zr(OPr^n)_4$ was 0.147 g-mol./kg *n*-propanol.

TABLE IV

h	0.000	0.159	0.400	0.711	1.118	1.469
n	2.44	2.79	3.30	4.21	7.27	13.9

The experiment was terminated at $h = 1.814$ because the thermometer reading was unsteady. This behavior is believed to indicate the presence of water in the system.

Zirconium n-Butoxide

The concentration of $Zr(OBu^n)_4$ was 0.0707 g-mol./kg *n*-butanol.

TABLE V

h	0.000	0.483	0.953	1.671
n	1.77	2.46	3.81	9.39

The experiment was terminated by fluctuations in the thermometer reading at $h = 2.606$.

Zirconium Isobutoxide

The concentration of $Zr(OBu^i)_4$ was 0.0766 g-mol./kg isobutanol.

TABLE VI

h	0.000	0.223	0.506	0.882	1.403	1.845
n	1.52	1.61	1.71	2.03	2.50	3.31

DISCUSSION

Before discussing the structural implications of the results on zirconium oxide alkoxides it is necessary to recapitulate briefly the structural models considered by Bradley, Gaze, and Wardlaw (3, 4) to explain the behavior of titanium oxide alkoxides. Three structural models were proposed, each involving 6-co-ordinated titanium. Model I was based on the unsolvated trimeric alkoxide $Ti_3(OR)_{12}$ (Fig. 1) and gave a series of trilinear polymers, e.g. $Ti_6O_4(OR)_{16}$ (Fig. 2) and the infinite polymer $[Ti_3O_4(OR)_4]_\infty$ (Fig. 3). These structures all fitted the general relationship $n = 12/(4-3h)$, where $h = 0$ to 1.333. A feature of the system is the fact that the number-average degree of polymerization n is uniquely determined by h and is thus independent of the distribution of polymer sizes. Model II was based on a solvated dimeric species $Ti_2(OR)_8,2ROH$ (Fig. 4) and gave bilinear

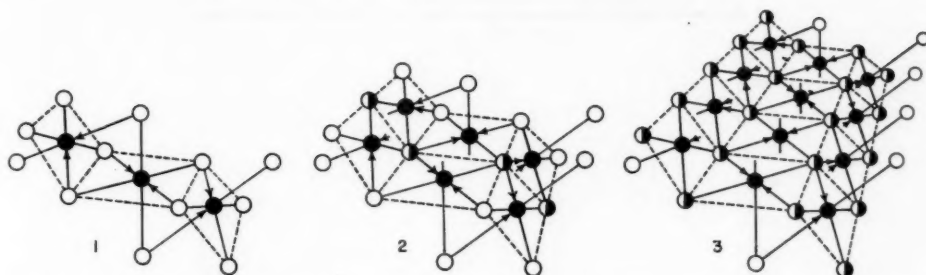FIG. 1. $Ti_3(OR)_{12}$.   ● = Ti; ○ = oxygen in OR groups; R groups omitted.
FIG. 2. $Ti_6O_4(OR)_{16}$.   ● = Ti; ◑ = oxygen in Ti.O.Ti; ○ = oxygen in OR (some OR groups omitted for clarity); R groups omitted.
FIG. 3.   Section of infinite trilinear polymer $Ti_{3(x+1)}O_{4x}(OR)_{4(x+3)}$.   ● = Ti; ◑ = oxygen in Ti.O.Ti; ○ = oxygen in OR (some OR groups omitted for clarity); R groups omitted.

polymers (Fig. 5) corresponding to $n = 6/(3-2h)$, $h = 0$ to 1.5. A third model was based on a monomeric solvated species $Ti(OR)_4,2ROH$. This gave rise to the relation $n = 3/(3-h)$.
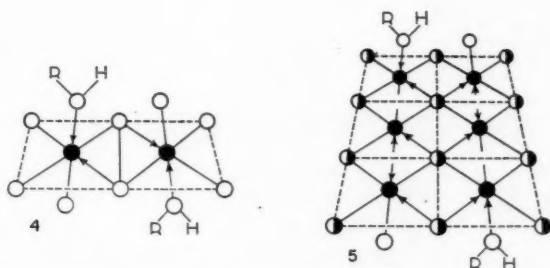
FIG. 4.   Solvated dimer $Ti_2(OR)_8,2ROH$.   ● = Ti; ○ = oxygen in OR.
FIG. 5.   Section of infinite bilinear solvated polymer $Ti_2O_2(OR)_2,2ROH$.   ● = Ti; ◑ = oxygen in Ti.O.Ti; ○ = oxygen in OR (some OR and R omitted for clarity); some ROH molecules omitted for clarity.

Accordingly, if the oxide alkoxides of zirconium conform to the same structural series, based on octahedrally 6-co-ordinated zirconium, then we should expect the variation of n with h to resemble one of the predicted relationships. For example, if the original alkoxide is trimeric in its boiling alcohol it should follow the requirements of model I and so forth.

Zirconium Oxide Ethoxides

In Fig. 6 we show a comparison between the experimental data for $Zr(OEt)_4$ and the predicted curves for models I and II. Two features are immediately apparent. Firstly it is noteworthy that practically all of the experimental points lie between the predicted curves for models I and II. Secondly it is clear that in the initial stages experimental points drift closer to the curve I, then remain fairly constant in distance from the curve before deviating towards curve II at h values >1.0. This general behavior is reminiscent of that shown by the hydrolysis products of $Ti(OEt)_4$ (3) and it seems reasonable to apply the principles developed by Bradley, Gaze, and Wardlaw. For a system containing species belonging to models I and II, if the degree of hydrolysis h is
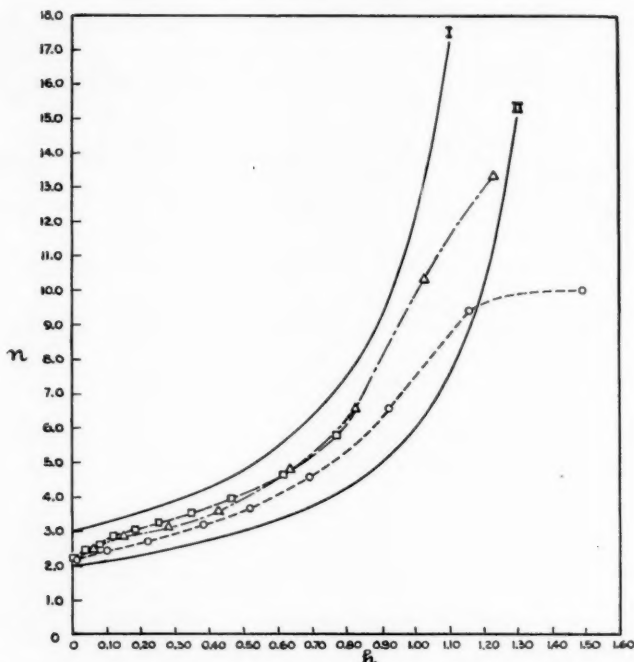
FIG. 6. The hydrolysis of $Zr(OEt)_4$ in boiling ethanol. $\square$ = initial concentration 0.723 g-mol. $Zr(OEt)_4$/kg EtOH; $\triangle$ = initial concentration 0.409 g-mol. $Zr(OEt)_4$/kg EtOH; $\bigcirc$ = initial concentration 0.186 g-mol. $Zr(OEt)_4$/kg EtOH.

the same for each model, it is readily deduced that the fraction of zirconium atoms in model I is α_I, where $\alpha_I = n_I(n - n_{II})/n(n_I - n_{II})$. In this expression n_I is the degree of polymerization if all the zirconium were in model I and n_{II} if all were in model II. In Fig. 7 is shown the variation of α_I with h for each experiment. Bearing in mind the sensitivity of α_I to experimental error the data still show clearly the rapid initial rise in α_I with increase in h followed by the attainment of a fairly constant value over a range of h and finally a decrease near the completion of the experiment. The latter phenomenon is probably the result of increasing solvation (model II) as the molar concentration of the polymeric species becomes low. This is a consequence of the experimental method since the mass of zirconium is constant throughout the experiment whereas the average molecular size of the zirconium oxide ethoxide species increases steadily with increasing degree of hydrolysis. The striking increase in α_I in the early stages of hydrolysis is more difficult to explain. Thus it is tempting to suggest that the original zirconium ethoxide ($h = 0$) exhibits a low value of n due to the steric effect of the ethyl groups opposing co-ordination polymerization. Then as hydrolysis proceeds and ethoxide groups are removed, co-ordination polymerization develops more fully. However, studies in the alkoxide field have shown (1) that n-alkyl groups exert relatively small steric effects in metal tetraalkoxides and it is surprising that such a large change could be due to this effect. Another puzzling feature is that zirconium ethoxide exhibits a slightly lower degree of polymerization in boiling ethanol than titanium ethoxide but a higher value in boiling benzene. In other words, in boiling ethanol, zirconium apparently has a greater
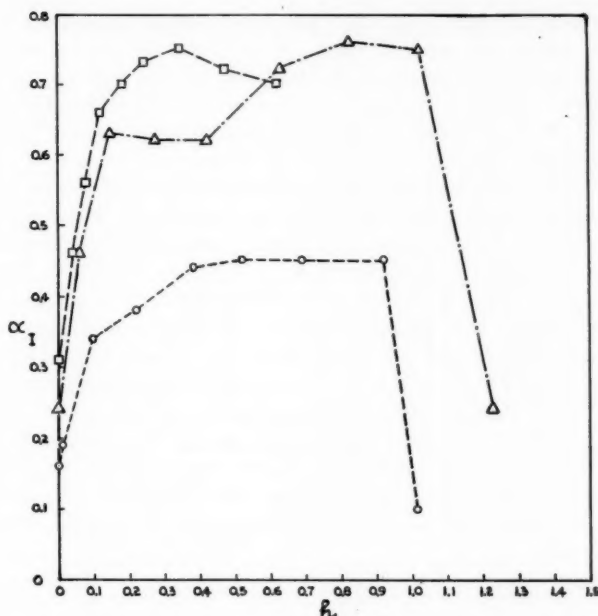
FIG. 7.   The variation of α_I with h for zirconium oxide ethoxides. $\square$ = initial concentration 0.723 g-mol. Zr(OEt)$_4$/kg EtOH; $\triangle$ = initial concentration 0.409 g-mol. Zr(OEt)$_4$/kg EtOH; $\bigcirc$ = initial concentration 0.186 g-mol. Zr(OEt)$_4$/kg EtOH.

tendency to obtain 6-co-ordination by co-ordination with alcohol rather than by polymerization of the ethoxide. The electronic factors involved in bonding in these polymers must also be considered. For example, we should expect that the electron density on the oxygen will be greater for the oxygen in a ZrOZr system than in ZrOEt or EtOH because zirconium is more electropositive than hydrogen or carbon. Therefore the ZrOZr oxygen should be a stronger donor than ZrOEt or EtOH oxygens. Hence as hydrolysis is increased and the proportion of ZrOZr groups becomes significant this may lead to the favoring of polymerization at the expense of solvation and thus a change from model II to model I. The alternative polymers for $h = 1.0$ illustrate this point. In the molecule Zr$_{12}$O$_{12}$(OEt)$_{24}$ (model I) one half of the ZrOZr oxygens are utilized in co-ordination polymerization but in Zr$_6$O$_6$(OEt)$_{12}$,6EtOH (model II) only one third of the ZrOZr oxygens are so used. These proportions remain constant throughout the oxide ethoxide series and accordingly it would be expected that the values of α_I would rise rapidly at the initial stages of hydrolysis and then remain sensibly constant over a range of h values. Nevertheless, calculations show that this suggestion does not fully account for the rise in α_I with increase in h from 0.0 to 0.5. We are forced to conclude that zirconium tetraethoxide in boiling ethanol is not in true equilibrium with regard to trimer (unsolvated) and dimer (solvated) species but that the oxide ethoxide molecules act as catalysts in bringing the system nearer to equilibrium. There is other evidence which points to the suggestion that solutions of Zr(OEt)$_4$ in boiling ethanol are not in true equilibrium. For example in determining the molecular weight of Zr(OEt)$_4$ a number of additions of solute are made over a range in concentration yet the plot of ΔT (elevation of boiling point) vs. concentration of solute is linear, although a non-integral value for n suggests that more than one

polymer species is present and hence the molecular weight should be concentration dependent. On the other hand we find that the elevation of boiling point at a given concentration remains constant over a period of hours suggesting that a pseudo equilibrium is set up. The sudden decline in α_I at $h > 1.0$ may be a dilution effect (decrease in polymer concentration) which favors solvation or alternatively it could be caused by the presence of ZrOH groups.

The structural model I reaches a limiting, infinite trilinear polymer at $h = 1.333$ and it would be expected that such a polymer would be insoluble. Our ebulliometric experiments were in fact limited by the onset of turbidity in the system. In the case of the experiment at the intermediate concentration of $Zr(OEt)_4$ a slight opalescence was detected at $h = 0.63$ and the experiment was terminated when precipitation occurred at $h = 1.43$. The precipitate was isolated and analysis showed that its composition was near to that for the infinite polymer $[Zr_3O_4(OEt)_4]_\infty$. Found: Zr, 51.2; EtO, 36.3. $Zr_3O_4(OEt)_4$ requires: Zr, 52.8; EtO, 35.0%. The degree of hydrolysis in the solid product corresponded to $h = 1.28$ and this would give a polymer with a number-average degree of polymerization of $\sim$90. It is not surprising that such a large molecular species was sparingly soluble. However, it is interesting that it corresponded to a slightly lower degree of hydrolysis than that calculated from the known addition of water. This lends further support to the suggestion that hydrolysis may not be quantitative in the later stages of the experiment.

Zirconium Oxide n-Propoxides

The variation of n with h in this system is shown in Fig. 8. No precipitation occurred up to $h = 1.469$ but following the next addition of water (to $h = 1.814$) the behavior of the water thermometer suggested that hydrolysis was no longer quantitative. The shape of the hydrolysis curve suggests that polymers of the models I and II are present in the early stages of hydrolysis but for $h > 1.0$ solvation becomes more effective as the molar concentration of polymers decreases and hence the polymers are based on models II and III. In Table VII we report the values for α_I, $1 - \alpha_I$, α_{II}, and $1 - \alpha_{II}$ as a

TABLE VII

h	α_I	$1 - \alpha_I$	α_{II}	$1 - \alpha_{II}$	c
0.000	0.54	0.46	—	—	0.0602
0.159	0.72	0.28	—	—	0.0532
0.400	0.48	0.52	—	—	0.0445
0.711	0.24	0.76	—	—	0.0349
1.118	—	—	0.98	0.02	0.0197
1.469	—	—	0.88	0.12	0.0101

function of h and the average molar concentration of polymers c (g-mol./kg). α_{II} is defined by $\alpha_{II} = n_{II}(n - n_{III})/n(n_{II} - n_{III})$ where n_{II} and n_{III} are the calculated degrees of polymerization for models II and III respectively.

The interesting point about these data is the small rise in α_I in the early stages (compared with the zirconium oxide ethoxide system) and thereafter the steady increase in proportion of the more solvated species of models II and III. The relatively small rise in α_I at first suggests that the initial solution of $Zr(OPr^n)_4$ in boiling n-propanol is nearer to the true equilibrium between polymer species than was the solution of $Zr(OEt)_4$ and this may be due to the higher boiling point of n-propanol. The higher boiling point of the alcohol is probably responsible for the more rapid onset of solvation in the zirconium
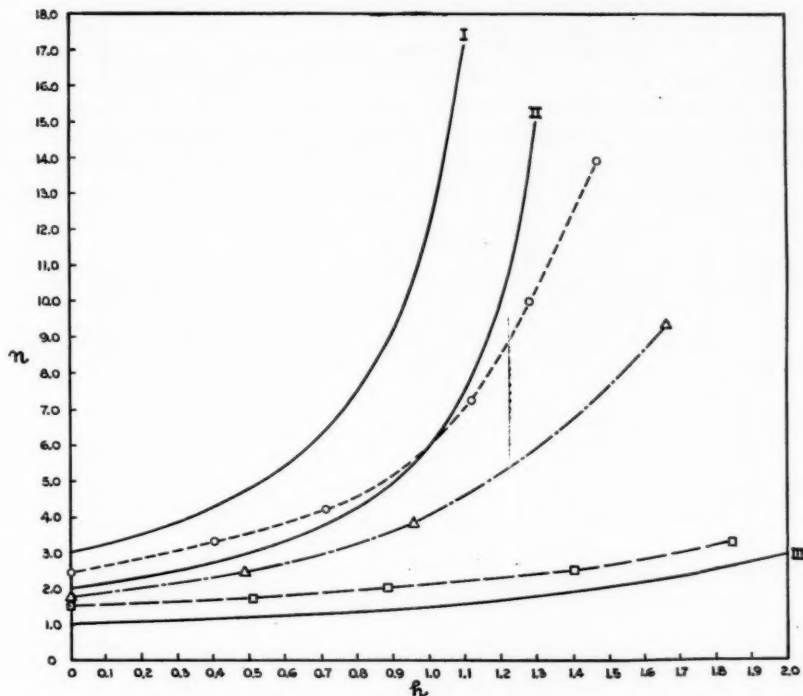
FIG. 8. The hydrolyses of $Zr(OPr^n)_4$, $Zr(OBu^n)_4$, and $Zr(OBu^s)_4$ in their respective alcohols. $\bigcirc$ = $Zr(OPr^n)_4$, initial concentration 0.147 g-mol./kg ROH; $\triangle$ = $Zr(OBu^n)_4$, initial concentration 0.0707 g-mol./kg ROH; $\square$ = $Zr(OBu^s)_4$, initial concentration 0.0766 g-mol./kg ROH.

oxide n-propoxide system. Thus Bradley, Gaze, and Wardlaw (4) suggested that solvation of the polymeric species would be promoted both by a decrease in molar concentration of polymer species and by increase in temperature. The data in Table VII suggest that the presence of polymers based on model III becomes increasingly significant with increase in h for $h > 1.0$. It is especially noteworthy that according to model III the highest polymer (at $h = 2.0$) possible is the trimer, whereas models I and II predict infinite linear polymers at $h = 1.33_4$ and 1.50 respectively. In our experiment no precipitation was observed although the reaction was terminated at $h = 1.814$ due to the presence of residual water in the system. The absence of a precipitate is thus in agreement with the presence of polymers based on model III in the final stages of hydrolysis. However, the presence of water at $h = 1.814$ also suggests that hydrolysis may be reversible at this stage due to the presence of Zr—OH groups and this offers an alternative means of producing low polymers.

Zirconium Oxide n-Butoxides

The high boiling point of n-butanol should promote the solvation process even more than n-propanol. The variation of n with h for the $Zr(OBu^n)_4$ system, shown in Fig. 8, agrees with this supposition. It appears that the polymeric species involve models II and III (with II predominating) and the dependence of α_{II} on h is shown in Fig. 9. It is extremely interesting to note that there is only a small initial rise in α_{II} at the early stages of
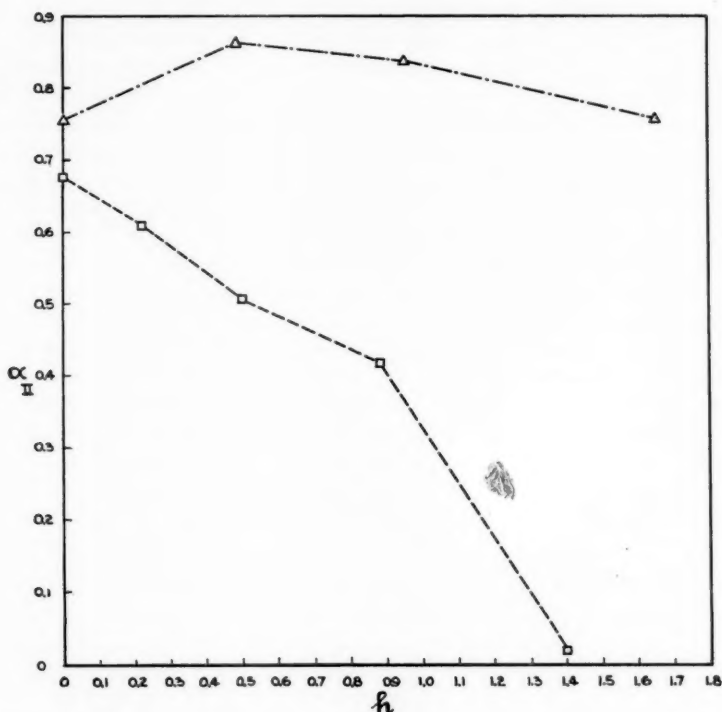
FIG. 9.   The variation of α_{II} with h for zirconium oxide n-butoxides and zirconium oxide isobutoxides.
$\triangle$ = Zr(OBu^n)$_4$, initial concentration 0.0707 g-mol./kg ROH; $\square$ = Zr(OBu^i)$_4$, initial concentration 0.0766 g-mol./kg ROH.

hydrolysis, followed by a steady decline in α_{II} as the decrease in polymer concentration with increase in n favors the model III species. No precipitation was observed and this suggests the predominance of model III in the final stages of hydrolysis. However, the detection of residual water at $h > 1.671$ means that hydrolysis may be reversible and incomplete in this region.

Zirconium Oxide Isobutoxides

The interesting feature of this system is that in spite of the lower boiling point of isobutanol compared with n-butanol, the solvation of Zr(OBu^i)$_4$ appears to be greater than for Zr(OBu^n)$_4$. This may well be due to the greater steric effect of the isobutoxide groups. It is well established (1) that branching of the alkyl groups in zirconium alkoxides opposes the formation of Zr—O intermolecular bonds and thus prevents co-ordination polymerization. The zirconium is thus forced to achieve its higher co-ordination by the process of solvation. Striking evidence in support of the preferential solvation of Zr(OBu^i)$_4$ was the isolation of the relatively stable solvate Zr(OBu^i)$_4$,Bu^{i}OH, in contrast to Zr(OBu^n)$_4$, which does not form a solvate. The variation of n with h for Zr(OBu^i)$_4$ is shown in Fig. 8. In Fig. 9 we show the steady decrease of α_{II} with increase in h, which suggests that model III species become favored as hydrolysis becomes extensive. No precipitation occurred up to $h = 1.845$ and this is in agreement with the predominance of model III species. Above $h = 1.845$ residual water was detected and this suggests that hydrolysis is reversible in this region.

CONCLUSIONS

The zirconium oxide alkoxides $ZrO_z(OR)_{4-2z}$, where R = Et, Pr^n, Bu^i, and Bu^n, exhibit low number-average molecular weights in solution in their progenitive alcohols at the boiling point. The variation of degree of polymerization with degree of hydrolysis is reasonably explained in terms of structural models based on 6-co-ordinated zirconium. With the exception of the ethoxides the zirconium compounds exhibited a greater degree of co-ordination polymerization than the corresponding titanium compounds.

REFERENCES

1. D. C. BRADLEY, R. C. MEHROTRA, J. D. SWANWICK, and W. WARDLAW.   J. Chem. Soc. 2025 (1953).
2. D. C. BRADLEY, R. GAZE, and W. WARDLAW.   J. Chem. Soc. 721 (1955).
3. D. C. BRADLEY, R. GAZE, and W. WARDLAW.   J. Chem. Soc. 3977 (1955).
4. D. C. BRADLEY, R. GAZE, and W. WARDLAW.   J. Chem. Soc. 469 (1957).
5. D. C. BRADLEY, W. WARDLAW, and A. WHITLEY.   J. Chem. Soc. 5 (1956).

THE INFLUENCE OF HYDROGEN ION CONCENTRATION
ON THE MYOSIN-CATALYZED HYDROLYSIS OF
ADENOSINE TRIPHOSPHATE[1]

GÉRARD E. PELLETIER[2] AND LUDOVIC OUELLET

ABSTRACT

The Michaelis constants for the system myosin–ATP have been measured at 5° C and 15° C from pH 7.0 to pH 10.5, in the presence of 0.4 M potassium chloride and 0.005 M calcium chloride. The experimental data point to the presence, in the active center, of two ionizable groups, with experimental acid pK of 7.35 and 8.6 respectively at 15° C. The apparent heats of ionization of these groups are about 9 kcal/mole for the first one and close to zero for the second. These data are interpreted as indication of the presence in the active center of myosin of a histidyl and a sulphydryl residue. A mechanism is proposed for the hydrolysis of ATP in the presence of myosin.

The kinetics of hydrolysis of adenosine triphosphate (ATP) in the presence of myosin has been described under several of its aspects. The reaction follows the Michaelis–Menten law. The influence of concentration of substrate, activator ions, ionic strength, and dielectric constants have been reported and have been summarized by Laidler (1). Recently Nihei and Tonomura (2) have observed an increase in the Michaelis constant at pH around 6.8. Blum (3) has also mentioned the variation of the Michaelis constant with the concentration of p-chloromercuribenzoate, an inhibitor probably reacting with sulphydryl residues.

The present paper describes the variation of the Michaelis constant of myosin as a function of the pH at two temperatures. The data so obtained will be used as information on the nature of the active groups of myosin.

DESCRIPTION OF THE DATA

The data reported in this paper were collected in terms of the usual system describing the influence of hydrogen ions on the rate of an enzymatic reaction. As the work progressed, however, it became evident that the simple usual scheme had to be modified to describe the experimental results.

The fundamental scheme is represented in Fig. 1. The enzyme is assumed to exist in
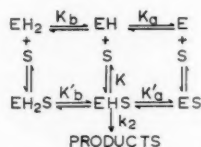

FIG. 1. Scheme representing the ionization states of an enzyme E and the enzyme substrate complex when the active center includes two acid groups.

three different ionic states EH_2, EH, E, in equilibria one with the other. The ionization constants K_b and K_a describe the ionization equilibrium. The charges and the hydrogen ions participating in the equilibrium have been left out. In the general case, these three

enzymic forms react with a substrate molecule S to give the complexes EH_2S, EHS, and ES. The complex EHS is usually assumed to give products.

Assuming the above system to be in equilibrium, the rate of hydrolysis V is given by the Michaelis–Menten equation:

[1] $$V = \bar{V}_m[S]/(\bar{K}_m + [S])$$

where $\bar{V}_m$, the rate at very high substrate concentration, assuming no substrate inhibition, is given by:

[2] $$\bar{V}_m = V_m \left/ \left(1 + \frac{[H^+]}{K_b{}'} + \frac{K_a{}'}{[H^+]}\right) \right.$$

and $\bar{K}_m$, the Michaelis constant, is:

[3] $$\bar{K}_m = K_m \left(1 + \frac{K_a}{[H^+]} + \frac{[H^+]}{K_b}\right) \left/ \left(1 + \frac{K_a{}'}{[H^+]} + \frac{[H^+]}{K_b{}'}\right) \right. .$$

The variation of $\bar{V}_m$ and $\bar{K}_m$ with pH provides information on the values of K_a, K_b, $K_a{}'$, and $K_b{}'$. The techniques suggested by Dixon (5) and Massey and Alberty (6) have been used to estimate the ionization constants from the experimental data.

For a discussion of the various hypotheses involved in this representation, one is referred to Laidler (4).

EXPERIMENTAL PART

Myosin of the Weber–Edsall type (7) was used. Adenosine triphosphate (ATP) was the crystalline sodium salt purchased from Pabst Laboratories. All the other reagents were reagent grade.

In the determination of the Michaelis constants, all rates were measured by an electrometric titration method, as the hydrolysis of ATP liberates phosphoric acid according to the following equation.

$$ATP^{-4} + H_2O \rightarrow HPO_4{}^- + ADP^{-3} + H^+ \qquad [4]$$
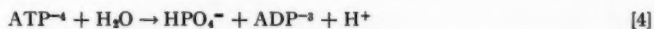
By continuously titrating standard alkali into the reaction mixture to maintain the pH constant, it is possible to follow the rate of formation of the acid.

The apparatus used consisted of a titrator (type TTT 1b) equipped with glass and calomel electrodes, a titrigraph (type SBR2b), and syringe microscrew burette (type SBU1a), from Radiometer (Copenhagen).

Nineteen milliliters of a 0.4 M solution of potassium chloride containing the required amount of ATP and calcium chloride (0.005 M) was pipetted into a double-jacketed reaction vessel. Circulation of water from a constant-temperature bath maintained the temperature within 0.1° C. Stirring was provided magnetically.

To minimize absorption of carbon dioxide from the atmosphere, air which had been twice washed in 30% potassium hydroxide solutions, followed by washing in water at the experimental temperature, was circulated over the surface of the reaction mixture. This proved effective up to pH 10, where a small blank correction was applied. One milliliter of the enzyme solution was injected to the above reaction mixture. The amount of alkali added was recorded as a function of time by the titrigraph. The total volume of sodium hydroxide added never exceeded 2% and was usually less than 1% of the reaction volume.

The rate at high substrate concentration was obtained from a series of runs, made in

1 day at one enzyme concentration. The results so obtained were then multiplied by $(\bar{K}_m + [S])/[S]$. At pH lower than 8, the rate at high concentration of substrate was obtained from analyses for orthophosphate by a colorimetric method (8).

<div align="center">RESULTS</div>

Influence of pH on $\bar{V}_m$

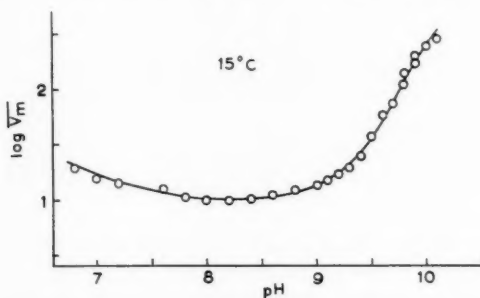Figure 2 shows the results obtained when the logarithm of the apparent maximum

FIG. 2.   Plot of the logarithm of the rate of hydrolysis of ATP at high concentration of substrate, $\bar{V}_m$, as a function of pH, at 15.1° C. The rates are in arbitrary units.

rate $\bar{V}_m$ was plotted against the pH at 15.1° C. The curve passes through a minimum in the neighborhood of pH 8.2. No true maxima could be obtained on the alkaline side of these curves, due in part to precipitation in the system and myosin inactivation (9). At 5.2° C, the alkaline branch of the curve was displaced toward higher pH values. Those results are consistent with observations reported by other investigators. Mommaerts and co-workers (10) as well as Tonomura and co-workers (11) have traced $\bar{V}_m$-vs.-pH curves under different conditions of temperature and ionic strength. In general, the curves passed through a minimum at low pH and reached a maximum in the vicinity of pH 9–10, after which a sharp drop resulted. By light-scattering experiments Blum (12) showed that this last phenomenon was due to an irreversible inactivation of the enzyme. Morales (13) has further shown that the concentration of calcium ions affects the position of the alkaline part of the curve, the curve shifting to lower pH values as the concentration of calcium ions is increased.

As no true maximum can be observed under our conditions, these curves cannot be used to estimate the pK of ionization of the myosin–ATP complex. All the experimental data pertaining to the ionization have perforce been obtained from a study of the variation of the Michaelis constant with pH.

The experimental Michaelis constants $\bar{K}_m$ were determined at two different temperatures over a range extending from pH 6.7 to 10.0 at 15.1° C and pH 7.0 to 10.4 at 5.2° C. Figure 3 represents examples of Lineweaver–Burk (14) plots of the reciprocal of the rate against the reciprocal of the ATP concentration. Each Michaelis constant was determined on the same day to eliminate errors due to possible loss in enzyme activity. The Michaelis–Menten law was found to hold under all the conditions studied. The usual determinations of $\bar{K}_m$ covered a ratio of 20 to 50 in concentrations of substrate.

Influence of pH on $\bar{K}_m$

For purposes of interpretation, the influence of pH on the apparent Michaelis constant is usually represented in the form of plots of $p\bar{K}_m$ ($-\log \bar{K}_m$) against pH. Figure 4
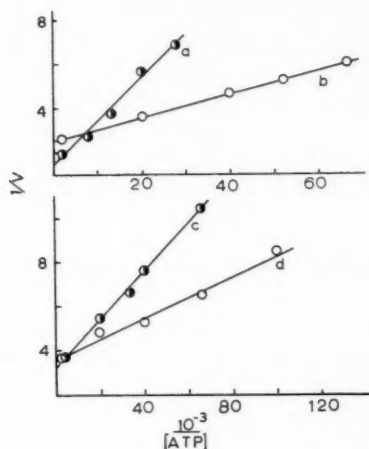
Fig. 3. Lineweaver–Burk plots of the reciprocal of the rate of hydrolysis in arbitrary units as a function of the reciprocal of the ATP concentration at 15.1° C. pH: $a = 9.8$; $b = 7.2$; $c = 7.0$; $d = 8.0$.
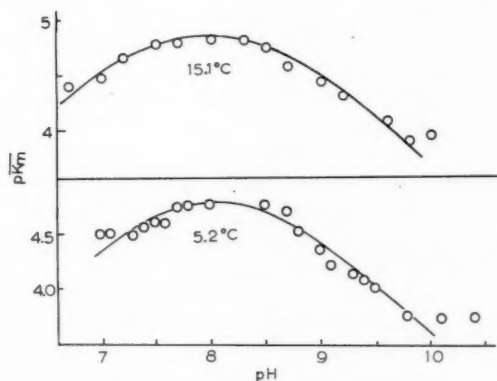

Fig. 4. Plots of $p\bar{K}_m$ ($-\log \bar{K}_m$) as a function of pH. The curves are theoretical curves drawn assuming $K_b' \gg K_b$ and $K_a' \ll K_a$ in equation [3] and $pK_a = 8.6$, $pK_b = 7.34$ at 15.1° C and $pK_a = 8.6$, $pK_b = 7.6$ at 5° C.

represents such plots at 15.1 and 5.2° C. Classical bell-shaped curves were obtained in both cases. These results are consistent with the observations of Nihei and Tonomura (2), who found that in buffered solutions containing 0.08 M THAM–maleate under two different ionic strength conditions, $\bar{K}_m$ hardly changed in the range of pH between pH 6.7 and 8.0 but increased with decreasing pH below 6.7. The ionization constants were calculated from these data by the method developed by Massey and Alberty (6). One assumes that the top part of the curve down to a point 0.3 $p\bar{K}_m$ units below the maximum is unaffected by any complication, and can be described by two ionization constants. Plots of $\bar{K}_m$ as a function of hydrogen ion concentrations or reciprocal of hydrogen ion concentrations, Figs. 5 and 6, gave approximately the same results, which have been tabulated in Table I.
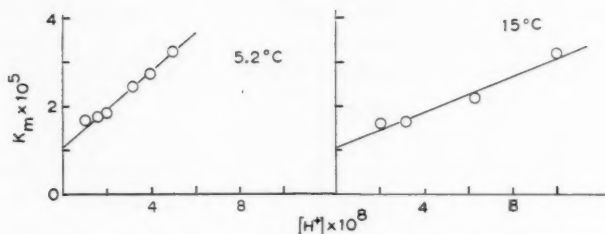
FIG. 5.   Plots of $\bar{K}_m$ as a function of the hydrogen ion concentration.
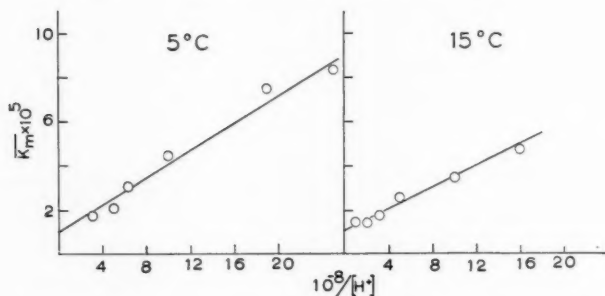
FIG. 6.   Plots of K_m as a function of the reciprocal of hydrogen ion concentration.

TABLE I

pK_a and pK_b values for the active center of myosin at 15.1 and 5.2° C

	Temperature	pK_a	pK_b
Alberty and Massey's equation	5.2	8.60	7.60
	15.1	8.60	7.34
$\bar{K}_m$ vs. [H⁺] or 1/[H⁺]	5.2	8.53	7.60
	15.1	8.62	7.34

The two methods give similar values and an inspection of Fig. 4 indicates that these pK's correspond to pH where there are definite changes in direction in the $p\bar{K}_m$–pH curves (5).

The apparent heat of ionization of the group identified by pK_b is about 9 kcal/mole while that of the group identified by pK_a is close to zero with an indication that it might be an exothermic quantity.

The data represented in Figs. 5 and 6 show that the value of the pH-independent Michaelis constant is the same at 5.2 and 15.1° C at 1.05×10^{-5} mole/liter. This would suggest that the formation of the myosin–ATP complex is athermic, and is accompanied by an increase in entropy of about 23 e.u.

At high pH, the curves of $p\bar{K}_m$ vs. pH level off. Normally, this would be interpreted as a contribution of an ionizable group in the complex to the function representing $\bar{K}_m$. Such a function does not appear in the rate at high substrate concentration (Fig. 2), as there is no indication of a leveling of the curve. The experiments could not be carried to higher pH because of myosin inactivation (9).

DISCUSSION

The data presented in this paper do not follow the pattern expected from a simple system like the one suggested in the description of the data. No really satisfactory explanation has been given for the minimum in the rate-vs.-pH curve (Fig. 2). Two possibilities will be mentioned here.

The description of the rate as a function of pH can be handled by assuming several complexes like EH_2S, EHS, ES, all yielding products. From a purely formal point of view, one can easily show that $\bar{K}_m$ is still described by equation [3]. On the other hand $\bar{V}_m$ can be described accurately, if one uses three complexes. One can criticize that hypothesis from two different points of view. First, it is evident that the inclusion of a sufficient number of constants will allow a good description of the data. The constants used, in our opinion, cannot be interpreted to give any information on the process. Second, the hypothesis implies several mechanisms in parallel for the transformation of one substrate into given products by one enzyme. So the hypothesis should not be considered, except as an explanation available if no other one is justified.

One may rather assume that the active complex is unique (e.g. EHS) and that the odd behavior of $\bar{V}_m$ as a function of pH is due to the influence of other factors, probably the electrostatic charge. It can certainly be argued that the presence of a negative ion such as ATP in the active center can reduce considerably the tendency of hydrogen ion to leave the protein molecule. This could move pK_B from about 7.3 in the enzyme, to values higher than 10 in the enzyme–substrate complex and inactivation becomes important before it can be determined. The fact that the rate of the hydrolytic reaction does not vary with the pH could then be explained by the variation of the ionization constant K_B with pH. As will be seen later, such an explanation assumes that the charge of the complex varies with pH. No data are available on that particular point.

Other hypotheses, such as acid–base catalysis of the hydrolysis of the complex, have been considered. In all cases it appeared impossible to obtain information on the ionizing groups in the active center from the rate at high substrate concentration.

According to Dixon (5), concave bends in the $p\bar{K}_m$-vs.-pH plots are due to ionizing groups of either the enzyme or the free substrate. Investigations on the calcium activation of ATPase (15) suggest that the substrate of ATPase is the calcium salt of adenosine triphosphate, $ATPCa^{-2}$, for which Smith and Alberty (16) have reported a pK_a value of 5.3 at 0.2 ionic strength at 25° C. In the present experiments the pK appearing in the maxima of the $p\bar{K}_m$-vs.-pH graphs are all above 7 and are therefore too high to be due to the substrate in the form of $ATPCa^{-2}$. Nihei and Tonomura (2) have, however, interpreted their results on the pH-dependence of $\bar{K}_m$, which indicated a pK in the neighborhood of 6.8 at 25° C, by assuming that the "true" substrate is ATP^{-4} since, according to Smith and Alberty (16), this substance has a pK of 6.95 at 25° C and 0.2 ionic strength. The pK of ionization which we have estimated from Nihei and Tonomura's data at 25° C is not inconsistent with our data at 5 and 15° C, although using it in the calculations would give a heat of ionization of about 12 kcal/mole. However, Alberty et al. (17) report pK values for ATP^{-4} of 6.48 at 25° C and 6.50 at 38° C in 0.15 M sodium chloride, giving a negligible heat of ionization. It therefore seems that the interpretation given by Nihei and Tonomura is incorrect and that the substrate of ATPase is the calcium salt form of ATP. On this basis, we can conclude that the dissociation constants appearing in the maxima in the $p\bar{K}_m$-vs.-pH curves refer to the enzyme and not to the substrate.

The simplest description of the curve of $p\bar{K}_m$ vs. pH (Fig. 4) involves two ionization constants, K_a and K_b. As equation [3] contains ionization constants of the enzyme in the

numerator and ionization constants of the enzyme–substrate complex in the denominator, the possibility of a third group of the active center ionizing within the pH area considered is not eliminated. In order to describe the experimental data, with three groups, the third one with a pK around 9, one has only to assume that pK_b' is also about 9. This type of evidence cannot be used to show the existence of three ionizable groups in the active center, but it shows that our data are not sufficient to eliminate the possibility that three, maybe more, acid groups participate in the catalyzed reaction.

Alternate Dissociation Paths

In the presence of two acid groups, there are two ionization paths, as suggested by Alberty (18).
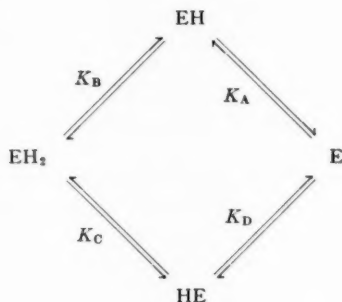
If K_a and K_b are experimental constants, they are related to the true constants by:

[5]
$$1/K_a = 1/K_A + 1/K_D$$

[6]
$$K_b = K_B + K_C.$$

In the simplest case of no interaction between the acid groups, i.e. if $K_A = K_C$ and $K_B = K_D$

[7]
$$K_{A \text{ or } B} = \frac{K_b \pm \sqrt{(K_b^2 - 4K_b K_a)}}{2}.$$

This equation imposes a minimum value of 4 to the ratio K_b/K_a, giving identical true ionization constants, $K_A = K_B$. This case has been reported by Alberty (18) in the fumarase case where, in acetate buffer, pK's of 5.9 and 6.5 are found.

If the ionization of one group does not affect the ionization of the other group, equation [7] gives at 5.2° C p$K_B = 7.65$ and p$K_A = 8.55$, while at 15° C p$K_B = 7.37$ and p$K_A = 8.57$. The correction on the pK is, however, within the limits of the experimental error and the hypothesis of no interaction possibly renders it insignificant. The important conclusion to be drawn from consideration of the alternate paths is that the actual nature of the ionized group is not known, that is, the one with a low pK could be unionized and the one with a high pK ionized in the most "stable" complex.

Electrostatic Effects

The influence of the electric charge of the molecule on the ionization process is much more important than the effects discussed above.

The two groups ionizing in the active center could be identical, if they are close so that the electrostatic charge developed on the ionized group reduces the tendency of the

second one to lose a proton. Differences of 1 and 1.3 are observed between the pK of symmetric dicarboxylic acids such as glutaric and succinic acids (19). In the case of myosin, it could be argued that a distance of about 7 Å between protons, based on the distance calculated from electrostatic effects in glutaric acid (19), is a reasonable quantity. However, the fact that the two groups have different heats of ionization, or that the difference between the pK of ionization varies with temperature, would suggest that the groups are of a different nature.

In order to estimate the influence of the electrostatic charge the following data on myosin are to be considered. According to Mihalyi (20), myosin has an isoionic point of about 5.75 in potassium chloride. At 15° C the molecule has lost 33 hydrogen ions on the average at pH 8.6 while at 5° C it has lost 30.5 hydrogen ions at the same pH. At pH 7.6, at 5° C, it has lost 25.2 protons and 24.5 at pH 7.35 at 15° C. All these data are reported to a weight of 10^5 grams of protein.

On the other hand, Lewis and Saroff (21) have found that most of the hydrogen ions are replaced by potassium ions at concentrations higher than 0.1 M of potassium chloride. The protein is, under these conditions, negatively charged if the pH is higher than about 5.8 (19, 21). In the presence of calcium chloride, electrophoresis experiments show that the protein is positively charged at pH 8.7 in 0.06 M calcium chloride (22). Under our conditions 0.01 M calcium chloride, 0.4 M potassium chloride, the charge on myosin is probably small, although it could be either positive or negative.

A semiquantitative treatment of the influence of the electrostatic charge Z on the ionization constant of an acid group on a protein is given by Scatchard (23).

[8] $$\mathrm{p}K = \mathrm{p}K_0 - 2wZ/2.3,$$

where w is given by

$$w = \frac{e^2}{2DkT}\left(\frac{1}{b} - \frac{\kappa}{1+\kappa a}\right).$$

The expression for w involves e the electronic charge, D the dielectric constant of the medium, k the Boltzman constant, T the absolute temperature, b the radius of the protein molecule assumed to be a sphere, and $\kappa/(1 + \kappa a)$ is a Debye–Hückel term including ionic strength effects. The quantity pK_0 is the pK at charge zero.

In the case of myosin, the correction is probably small, as the charge is small.

However, this effect explains the low value of the apparent heat of ionization for the group with a pK of 8.6. Myosin has a large number of ϵ amino residues with a heat of ionization of about 11 kcal/mole, and a pK around 10 at 25° C (24). At pH 8.6 these groups contribute to the charge of the proteins. If the temperature is raised 10° C the pK of a lysyl ϵ amino group is lowered by about 0.3 pK units, making the protein molecule more negative, at pH 8.6. If a group in the active center, with a pK at 8.6, has a heat of ionization of 6 to 7 kcal/mole, its pK is displaced by 0.15 to 0.18 pK unit for the same rise in temperature. But at the pH equal to the new pK, the charge of the protein is more negative, increasing the pK of ionization, following equation [8]. In the case of myosin, it appears that the lowering of the pK of ionization due to rise in temperature from 5 to 15° C is compensated by an increase in negative charge (or decrease in positive charge) due to ionization of ϵ amino groups.

The above interpretation requires that the heat of ionization of the group with a pK at 8.6 be smaller than that of ϵ amino groups. A value of 6 to 7 kcal/mole would be reasonable. The fact that the mobility of the protein is small in electrophoresis experiments would indicate a small charge on the enzyme and, probably, a small variation of

Z with pH in the region of pH 8.6. At pH 10, the increase in negative charge could be sufficient to eliminate the influence of pH on $p\bar{K}_m$, as the pK of ionization could well increase as fast as the pH. Erdös (24) has reported that in the presence of 0.1 M calcium chloride the electrophoretic mobility of myosin becomes suddenly negative as the pH is increased above 9.3 at an unspecified temperature.

Around pH 7.3, at 15° C, carboxylate groups affect the charge and the same effect probably contributes a rise in the heat of ionization. According to Mihalyi (20), the average heat of ionization of groups in myosin at pH 7.5 at 10° C, is very slightly above 5 kcal/mole, that is, lower than the value for histidyl (24) or sulphydryl (26) residues. Then, as the temperature is increased, the charge would have a tendency to become more positive as the pK is lowered, increasing the apparent temperature effect. This would lead to a true heat of ionization somewhat smaller than 9 kcal/mole for the group with a pK of 7.34 at 15° C.

Group in the Active Center

The suggestions on the nature of the groups in the active center of myosin will use the following conclusions. The first ionizable group has a pK of 7.34 at 15° C (7.1 at 25° C) and a heat of ionization smaller than 9 kcal/mole. As the charge on the protein is probably small, this value would be close to pK_0. Such values could well be attributed to the imidazole group of histidine, which has a pK_0 of ionization of 7.0 and a heat of ionization of 7 kcal/mole at 25° C (23).

The second group, with a pK of 8.6 and a heat of ionization significantly lower than 11 kcal/mole, would be attributed to a sulphydryl residue of cysteine. In cysteine itself, the pK of ionization of the —SH group is 8.5 for the species carrying no net charge (26). The heat of ionization of the —SH group of thioglycolic acid has been given as 7 kcal/mole (26). This identification would take into account the fact that p-chloromercuribenzoate, one of the best —SH inhibitors, inhibits myosin ATPase activity (27, 3) and that cysteine has been separated recently from the active center of myosin (28).

Suggestion of a Mechanism

Taking into account the fact that the substrate at very high concentration inhibits myosin, the above two groups, and a mechanism recently proposed by Krupka and Laidler (29) for the action of cholinesterase, we would like to suggest the following mechanism. ATP is bound in a regular Michaelis complex to an imidazole group and an unionized sulphydryl group of myosin. In the following step, the unionized SH group of myosin is phosphorylated to give enzyme – S – PO_3^-. This intermediate is then hydrolyzed with the participation of the imidazole group. This step is required to take substrate inhibition into account together with the large increase in pK_b observed when the substrate is attached to the enzyme. The hydrolysis of enzyme – S – PO_3^- intermediate would be rate limiting.

CONCLUSION

The influence of hydrogen ion concentration on the rate of hydrolysis of ATP in the presence of myosin suggests that the active center of the enzyme is made of at least one imidazole and one sulphydryl group. A two-step mechanism similar to that proposed for the enzyme cholinesterase would explain the experimental results presented.

ACKNOWLEDGMENTS

One of us (G. E. P.) wishes to acknowledge the award of a Cominco and a Shell Oil Co. scholarship during the time this work was carried out.

REFERENCES

1. K. J. LAIDLER.   The chemical kinetics of the enzyme action. Oxford, 1958. p. 280.
2. T. NIHEI and Y. TONOMURA.   J. Biochem. (Tokyo), **46**, 305 (1959).
3. J. J. BLUM.   Arch. Biochem. Biophys. **87**, 104 (1960).
4. K. J. LAIDLER.   The chemical kinetics of enzyme action. Oxford, 1958. p. 117.
5. M. DIXON.   Biochem. J. **55**, 161 (1953).
6. R. A. ALBERTY and V. MASSEY.   Biochem. et Biophys. Acta, **12**, 347 (1954).
7. J. BOTTS and M. F. MORALES.   J. Cellular Comp. Physiol. **37**, 27 (1951).
8. C. H. FISKE and J. SUBBAROW.   J. Biol. Chem. **81**, 629 (1929).
9. G. E. PELLETIER and L. OUELLET.   Can. J. Chem. **39**, 265 (1961).
10. F. W. H. M. MOMMAERTS and I. GREEN.   J. Biol. Chem. **208**, 833 (1954).
11. Y. TONOMURA, S. WATANABE, and K. YAGI.   J. Biochem. (Tokyo), **40**, 27 (1953).
12. J. J. BLUM.   Arch. Biochem. Biophys. **43**, 176 (1953).
13. M. L. MORALES, A. J. OSBAHR, H. L. MARTIN, and R. W. CHAMBERS.   Arch. Biochem. Biophys. **72**, 54 (1957).
14. H. LINEWEAVER and D. BURK.   J. Am. Chem. Soc. **56**, 658 (1934).
15. G. E. PELLETIER and L. OUELLET.   Can. J. Chem. **36**, 896 (1958).
16. R. M. SMITH and R. A. ALBERTY.   J. Am. Chem. Soc. **78**, 2376 (1956).
17. R. A. WEBER, R. M. SMITH, and R. M. BOCK.   J. Biol. Chem. **193**, 425 (1951).
18. R. A. ALBERTY.   J. Cellular and Comp. Physiol. **47**, 245 (1956).
19. E. H. WESTHEIMER and M. W. SHOOKHOFF.   J. Am. Chem. Soc. **61**, 555 (1939).
20. E. MIHALYI.   Enzymologia, **14**, 224 (1950).
21. M. W. LEWIS and H. A. SAROFF.   J. Am. Chem. Soc. **79**, 2112 (1957).
22. T. ERDÖS and O. SNELLMAN.   Biochim. et Biophys. Acta, **2**, 672 (1948).
23. G. SCATCHARD.   Ann. N.Y. Acad. Sci. **51**, 660 (1949).
24. E. J. COHN and J. T. EDSALL.   Proteins, amino acids and peptides. Reinhold Publishing Corp., New York. 1943. p. 445.
25. T. ERDÖS.   Acta Physiol. Acad. Sci. Hung. **7**, 1 (1955).
26. R. E. BENESCH and R. BENESCH.   J. Am. Chem. Soc. **77**, 5877 (1955).
27. E. S. G. BARRON and T. P. SINGER.   J. Biol. Chem. **157**, 221 (1945).
28. O. SNELLMAN.   Acta Chem. Scand. **12**, 503 (1958).
29. R. M. KRUPKA and K. J. LAIDLER.   Trans. Faraday Soc. **56**, 1467 (1960).

THE EFFECT OF INITIAL ACID CONCENTRATION ON THE LIGNIN
ISOLATED BY THE ACIDOLYSIS OF ASPEN WOOD[1]

J. M. PEPPER AND M. SIDDIQUEULLAH[2]

ABSTRACT

A further study has been made of the isolation, by acidolysis, of lignin from aspen wood meal (*Populus tremuloides* Michx.) using a dioxane–water (9:1) solvent medium containing hydrogen chloride and a low extraction temperature of $87 \pm 2°$ for a short extraction time of 0.5 hour. Lignins so isolated included those: (*a*) under different initial acid concentrations of 0.0, 0.05, 0.1, 0.2, 0.3, 0.4, 0.5, 0.6, 0.8, and 1.7 equivalents of HCl/liter of solvent medium; (*b*) from successive extractions under increasing initial acid concentrations of 0.2, 0.4, 0.8, and 1.6 equivalents/liter; and (*c*) from successive extractions under constant initial acid concentrations of 0.2 equivalent/liter.

All the lignin fractions so isolated were studied with respect to their yield, methoxyl content, infrared absorption spectra, and the yields of vanillin and syringaldehyde obtained from them by oxidation using alkaline nitrobenzene.

Evidence is presented in support of the non-homogeneity of the whole protolignin. This may be the result of the presence of possibly two basic types. One fraction, comprising around 70–85%, is most readily extracted, has a consistently high methoxyl content (ca. 21%), and is capable of being oxidized to give high yields of syringaldehyde and vanillin in a ratio close to 2.5:1. The second fraction is characterized by a greater difficulty of extraction, lower methoxyl content, and significantly lower yields of the aldehydes in a ratio closer to 1:1.

In a previous communication, Pepper, Baylis, and Adler (1) reported a study of the effect of extraction time on the isolation and properties of the lignin fraction obtained by the acidolysis of spruce and aspen wood meals. The extractions were carried out under reflux for periods ranging from 0.5 to 48 hours using a constant initial hydrochloric acid concentration, namely 0.2 N with respect to the dioxane–water (9:1) solvent medium. As the time of extraction was increased, the yields of the isolated lignin fractions also increased, but the yields of phenolic aldehydes (vanillin from spruce or a mixture of vanillin and syringaldehyde from aspen) obtained from them by alkaline nitrobenzene oxidation gradually decreased. It was also shown that with increasing time of acidolysis of the aspen wood, a rise in the carbon-methyl to methoxyl ratio was observed for the isolated lignins. A similar finding had been made earlier for spruce lignin isolated under the same conditions (2). As a result of these studies, it was suggested that such a lignin fraction isolated under conditions of 1-hour extraction with the 0.2 N acid solvent may be only mildly modified during extraction and hence suitable for subsequent chemical investigation.

This report deals with a study of the effect of the initial acid concentration on the yield and nature of the lignin isolated by a similar acidolysis of aspen wood.

An extraction time of 0.5 hour was chosen and all extractions were effected at $87 \pm 2°$, which represented a simmering state for all media. The lignin fractions so isolated are named by means of their association with the initial acid strengths of the solvent media, which were 0.0 N, 0.05 N, 0.1 N, 0.2 N, 0.4 N, 0.5 N, 0.6 N, 0.8 N, and 1.7 N expressed as equivalents of dry hydrogen chloride per liter of solvent medium. The yields of the lignins so isolated by this acidolysis procedure are given in Table I.

TABLE I

Effect of initial acid concentration on the isolation of aspen lignin*

Initial HCl (N)	Lignin recovery†	Initial HCl (N)	Lignin recovery†
0.0	1.6	0.4‡	63.0
0.05	17.1	0.5	69.4
0.1	22.2	0.6	72.9
0.2	44.0	0.8	74.8
		1.7	89.6

*Pre-extracted wood meal (25 g); dioxane–water (9:1) (500 ml); temperature, 87±2°; time, 0.5 hour, under nitrogen.
†Expressed as percentage of Klason lignin.
‡Media of concentrations of 0.4 and higher were two-phase systems at room temperature.

These results indicate that approximately 70–75% of the lignin is comparatively easily recoverable at lower acid concentrations, but that the isolation of the remainder requires higher initial acid concentrations. To study further the behavior of isolation of the lignin, extraction experiments were carried out along the following two lines: (1) lignin was isolated from the same wood meal by successive extractions under increasing initial acid concentrations (see Table II), and (2) lignin was isolated from the same wood meal by successive extractions under constant initial acid concentrations (see Table III).

TABLE II

Lignin isolation by successive extractions under increasing initial acid concentrations*

Initial HCl (N)	Isolated lignin	Recovery† (%)	Combined recovery† (%)
0.2	Lignin A	45.7	45.7
0.4	Lignin B	43.2	88.9
0.8	Lignin C	6.9	95.8
1.6	Lignin D	1.2	97.0

*Pre-extracted aspen wood meal (25 g) was successively extracted with increased normality of HCl in dioxane–water (9:1) (500 ml), at 87±2°, each extraction for 0.5 hour.
†Expressed as percentage of Klason lignin.

TABLE III

Lignin isolation by successive extractions under constant initial acid concentrations*

Isolated lignin	Recovery (%)†	Total combined recovery (%)†
Lignin A_1	43.2	43.2
Lignin A_2	12.1	55.3
Lignin A_3	4.4	59.7
Lignin A_4	1.2	60.9

*Pre-extracted wood meal (25 g) was successively extracted with 0.2 N HCl in dioxane–water (9:1) (500 ml), at 87±2°, each extraction for 0.5 hour.
†Expressed as a percentage of original Klason lignin.

General Description of Isolated Lignins

It was quite evident that as the conditions of isolation became more drastic the isolated lignin fractions showed progressive deterioration of color, ranging from a light tan-colored, 0.2 N lignin to a dark brown, 1.7 N lignin. The explanation of this change is not clear, but there is good evidence that under increasing initial conditions of acidity

a dark-colored material is isolated, in increasing amounts, which may be of rather different chemical composition* to the major lignin fraction (3). It is very probable that this change is caused by increasing condensation of the lignin.

A similar color change had been noted in the lignins isolated under similar acidolysis conditions with increasing time of extraction, and also in those lignin samples which were isolated originally by a 1-hour extraction and subsequently treated under similar conditions for varying times (1). This color change is not associated with any significant loss of methoxyl, but the conclusion that either some structural change is occurring or that lignin fractions having different structures are being isolated is borne out by the steadily decreasing yields of vanillin and syringaldehyde that are obtained by the alkaline nitrobenzene oxidation of these lignins.

Using approximately two milligrams of sample per 4 milliliters of solvent as a criterion of solubility, all the isolated lignins were found to be soluble in dioxane, glacial acetic acid, 80% ethanol, 80% methanol, and 80% acetone but insoluble in carbon tetrachloride, chloroform, acetone, ethanol, methanol, carbon disulphide, acetonitrile, and nitromethane. The various lignin samples were tested using the color reaction reported by Gierer (4) involving the coupling with quinone monochloroimide. An intense green-blue coloration, indicative of the presence of the p-hydroxybenzyl alcohol grouping, was obtained in all cases except for the 1.7 N lignin, lignin C, and lignin D. For these samples the test was very weak, or, if positive, was masked by the reddish-brown coloration of the original solution.

From the results of these isolation studies some conclusions may be drawn regarding the nature of the protolignin in the wood. From Table III, it is apparent that with successive extractions of wood meal using constant initial acid concentrations, the yields of recovered lignin decreased until on the fourth extraction only 1.2% of the original lignin was so recovered. It may be argued that if the protolignin were homogeneous, both with respect to its chemical structure and linkage to other cell components, and if no change were being effected under the conditions of isolation, a much more equal recovery by each extraction would have been expected. For aspen wood it may be that about seventy-five per cent of the total lignin is comparatively easily recoverable (see Tables I and III) but that the remaining part requires more drastic conditions for isolation. It is known that lignin is located both in the middle lamella and in other layers of the cell wall. According to Ritter (5) about seventy-five per cent is associated with the middle lamella and twenty-five per cent elsewhere. Even though this latter figure may be appreciably high, it is quite reasonable that the more easily isolated part, as obtained in these extraction experiments, may be the middle lamella lignin whilst the cell-wall lignins, if they are more intimately linked with carbohydrate, require the more drastic conditions for isolation.

All the isolated lignins described in Tables I, II, and III were analyzed for their methoxyl content and some representative samples were analyzed for carbon and hydrogen. These results are given in Table IV.

These few carbon and hydrogen analyses are sufficient to indicate that as the conditions of isolation become increasingly more drastic, the isolated lignins have increasing percentages of carbon and lower percentages of hydrogen. This is most simply explained by an increasing extent of an inter- or intra-molecular dehydration, but may in part

*It may be significant that these products had a methoxyl content ranging from 9.7 to 10.6%, which is half of that reported for the isolated lignins.

TABLE IV

Analyses of isolated lignins

Isolated lignin	Methoxyl (%)	Isolated lignin	Methoxyl (%)
0.05 N lignin	20.3	Lignin A (0.2 N)§	21.2
0.2 N*	20.7	B (0.4 N)‖	21.2
0.4 N	20.7	C (0.8 N)	18.5
0.5 N	20.5	D (1.6 N)	16.6
0.6 N	20.5	Lignin A$_1$	21.2
0.8 N†	20.5	A$_2$	20.9
1.7 N‡	19.1	A$_3$	20.7
		A$_4$	20.1

*C, 57.9; H, 6.31; ash, ca. 1%. †C, 59.9; H, 5.71; ash, ca. 1%. ‡C, 60.2; H, 5.58%. §C, 58.9; H, 6.02%. ‖C, 59.7; H, 5.96; ash, ca. 0.5%.

be due to the extraction of increasing amounts of a second lignin-like component having a higher carbon percentage.

The consistently high methoxyl content (av. 20.7%) obtained for all lignins except 1.7 N lignin, lignin C, and lignin D is in general agreement with the values of 19.8 and 21.5% methoxyl reported for native aspen lignin (6) and milled wood aspen lignin (7) respectively, both of which are considered to be representative lignins. It must be realized that the methoxyl content alone serves only to show that other non-lignin components are absent and is not necessarily a good criterion of the unchanged quality of the lignin. For example Klason aspen lignin, although drastically modified chemically as shown by the only trace amounts of vanillin and syringaldehyde obtainable by alkaline nitro-benzene oxidation, has a methoxyl content of 21.4%. The significantly lower methoxyl content of the 1.7 N lignin and lignins C and D may best be explained by the presence of either non-lignin (carbohydrate) residues carried by the lignin through chemical bondage or lower methoxyl-containing lignins such as those mentioned earlier. If this is so then the ability to isolate at least seventy-five per cent of the protolignin with a constant methoxyl content supports the belief that the major part of the lignin is of a higher methoxyl content than the remainder. This distinction may be related to the observation discussed earlier concerning the ease of isolation from which a similar con-clusion was drawn.

From a survey of recent studies (8, 9, 10) it would appear that the major infrared investigations on lignin have been carried out to evaluate lignins obtained from the same species by different processes or from different species by the same process. No detailed spectroscopic investigation has been conducted for a study of the lignin fractions obtained from a particular species using the same general extraction procedure but under a variety of conditions. This would permit of a better understanding of the changes taking place in the same lignin substance as a result of the controlled changes in reaction conditions. Once the nature of the major functional groups present and the changes undergone by them are known, a clearer interpretation with respect to the structure of the lignin molecule may be made.

With this general objective, the infrared absorption spectra were determined on all the isolated lignins described in Tables I, II, and III, as well as those described previously (1), which had been isolated from aspen wood at constant initial acid concentrations (0.2 N) under increasing times of reactions from 0.5 hour through 48 hours. For purposes of comparison, spectra were also obtained on both aspen and spruce Klason lignins. Since

the spectra were determined on a qualitative basis only, minor variations, slight lessening or strengthening in the intensity of peaks, were not considered since they could arise due to the variation in the concentration of the sample. In their general nature all spectra for the hardwood (aspen) lignins were basically similar but were distinctly different from the spectrum of a typical softwood (spruce) lignin. This is in agreement with their known chemical differences and therefore adds support to the belief that an interpretation of such spectra may reveal chemical changes taking place in the lignin substance as a result of any series of studies on the effect of various chemical treatments such as those described in this investigation.

The sharpness of the strong, characteristic, aromatic ring vibrations absorption bands near 1600 cm^{-1} and 1500 cm^{-1} progressively decreased as the conditions of lignin isolation became more severe, until for the 48-hour lignin and for the aspen Klason lignin the bands had become distinctly broad. This indicates that a significant change is occurring involving the substitution pattern associated with the aromatic nuclei and is in agreement with the analytical data already discussed and with the decreasing yields of phenolic aldehydes obtained by alkaline nitrobenzene oxidation to be discussed later. A similar conclusion could be drawn regarding the observed progressive lessening in intensity of the 1225–1235 cm^{-1} band attributed to the aryl C—O (phenolic) stretching mode (10), indicative of some condensation involving phenolic hydroxyl groups.

The significant differences between the aspen and spruce infrared spectra are associated principally with the carbonyl band and the aromatic substitution pattern. For the spruce lignin a weak, broad band at 1660–1670 cm^{-1} was present but absent in all the aspen lignins, whilst the 1710–1725 cm^{-1} band was distinctly stronger for spruce than for aspen. These two bands have been associated with carbonyl groupings, the first according to Herger (10) being, "a ketone carbonyl alpha to an aromatic ring, with the *para*-position etherified and with an oxygen atom (as a hydroxyl group or etherified) in the two-position" and the second, a non-conjugated carbonyl group. Distinct, weak bands occurred in the spruce lignin spectrum at 855 cm^{-1} and 810–820 cm^{-1} and are characteristic of the guaiacyl nucleus and due to the monohydrogen and two adjacent ring hydrogen out-of-plane deformations respectively. For the aspen lignin, which contains both the syringyl (with only a monohydrogen deformation possible) and the guaiacyl nuclei, it is not surprising that only a weak, broad band at 830–850 cm^{-1} appeared as a result of a combination of the two types of nuclei.

All the isolated lignins recorded in Tables I, II, and III were oxidized using alkaline nitrobenzene and the yields of vanillin and syringaldehyde are recorded in Table V. The quantitative analytical procedure of Stone and Blundell (11) was used. It has been reported previously that the possible interference of acetovanillone and acetosyringone in the chromatographic procedure did not exist due to the absence of these compounds in the products obtained at 180° (12). No *p*-hydroxybenzaldehyde was detected in the lignin oxidation products.

Further evidence is hereby presented for the marked decrease in the percentage recoveries of both vanillin and syringaldehyde obtained by the oxidation of wood meal and calculated on the basis of the Klason lignin content. Some possible explanations of this observation have been discussed (13) but none is entirely satisfactory. Experimental evidence does support the belief that protolignin itself, or that lignin substance formed at the moment of liberation from its close association, either physical or chemical, with other cell-wall constituents, is very reactive and rapidly undergoes side-chain rearrangements and/or intramolecular condensations. The ease of such rearrangements in isolated

TABLE V

Alkaline nitrobenzene oxidation of isolated lignins

Lignin substance	Yield of oxidation products*†		
	Vanillin (V) (%)	Syringaldehyde (S) (%)	Molar ratio (S/V)
0.1 N lignin	8.0	19.7	2.1
0.2 N	6.7	19.3	2.4
0.4 N	6.7	19.9	2.5
0.5 N	6.3	19.4	2.6
0.6 N	5.7	17.3	2.5
0.8 N	5.6	16.4	2.4
1.7 N	5.3	14.8	2.3
Lignin A	6.7	21.7	2.7
Lignin B	6.7	17.5	2.2
Lignin C	5.3	7.3	1.1
Lignin D	4.8	5.8	1.0
Pre-extracted aspen wood‡	11.5	29.1	2.1

*Reported values are means of two separate analyses.
†Percentage yields calculated on a weight basis.
‡Percentage yields calculated on the basis of the Klason lignin content.

lignins whereby C-methyl groups are produced has been reported (1, 2). Such changes can be envisioned to destroy, at least in part, the linkages which give rise to the aldehydic group on oxidation. On the other hand, the rather consistent yields of both vanillin and syringaldehyde (Table V) obtained from those lignins isolated under increasing strengths of initial acid concentrations, at least up to until about seventy per cent of the lignin has been removed, suggest that, in the protolignin, two different structural units are present. Both such linkages may be cleaved to yield the phenolic aldehydes under the conditions of alkaline nitrobenzene oxidation but only one is destroyed by the more common processes of lignin isolation. Support for this suggestion is found in the decreasing yields of the phenolic aldehydes obtained from the 0.6 N, 0.8 N, and 1.7 N lignins and even more definitely in the yields obtained from lignins B, C, and D isolated by successive extractions under increasing initial acid concentrations (Table II).

Of equal interest and structural significance are the molar ratios of syringaldehyde to vanillin reported in Table V. For those fractions representing a total recovery of lignin of 80–85% (previously suggested as the middle lamella lignin) an average molar ratio of about 2.5 (2.1–2.7) is found; whereas for the remainder (previously suggested as cell-wall lignin) an average ratio of close to 1 is found. In a previous communication (1) the ratio of the yields of the phenolic aldehydes obtained by the oxidation of lignin samples isolated under increasing times of reaction using an initial acid concentration of 0.2 N have been reported. If these yields are calculated on a molar basis, similar ratios (2.0–2.6) to those found in this investigation are obtained. It was therein pointed out that it is difficult to correlate the average methoxyl content of approximately twenty-one per cent of at least the major part of the isolated lignin with this molar ratio of syringaldehyde to vanillin obtained by oxidation of these same lignins. On the basis of the widely believed assumption that hardwood lignin is of a complex polyconiferyl alcohol – polysinapyl alcohol nature, a molar ratio of these two different nuclei of from 2:1 to 1:1, depending on the extent of side-chain oxidation, would be required to analyze for about twenty-one per cent methoxyl. This is in direct contrast to the actual ratio of the phenolic aldehydes produced by oxidation. It may be that as a result of the chemical reactions occurring

during isolation, a greater proportion of vanillin-yielding nuclei than syringaldehyde-yielding nuclei are destroyed. However, the consistency of these experimental observations suggests that these ratios are of real structural significance. An attempt to correlate some of these data will be made in a forthcoming publication.

EXPERIMENTAL

Pre-extracted (alcohol–benzene) aspen sapwood meal (*Populus tremuloides* Michx.) similar to that in the work reported by Pepper, Baylis, and Adler (1) was used. It was dried to constant weight over P_2O_5. Anal: Klason lignin, 18.2%; methoxyl, 5.13%.

All dioxane was purified according to Fieser (14). All water was purified and carefully freed of oxygen prior to use. Gaseous hydrogen chloride was used to prepare the extraction solvents, the strength of the acidic media being obtained by titration against standard carbonate-free sodium hydroxide. All dioxane–water systems were prepared on a 9:1 v/v basis.

Lignin Isolation under Different Initial Acid Concentrations

Pre-extracted, vacuum-dried aspen wood meal (25 g) was placed in a 1-liter, four-necked, round bottom Pyrex flask, fitted with a reflux condenser, nitrogen inlet, dropping funnel, thermometer, and a three-way stopcock to a water pump. The flask was then evacuated. A pressure of 10–15 mm of mercury was maintained in the flask for 15–20 minutes. Then the stopcock leading to the pump was closed and the solvent (500 ml) was added from the dropping funnel slowly with caution so that no air entered the flask. When about half of the solvent had been added, the pressure was restored by slowly introducing nitrogen. The remaining half of the solvent was added. The contents of the flask were gradually heated over a period of 15–20 minutes with stirring to $87 \pm 2°$. This temperature was maintained for 30 minutes. A slow stream of nitrogen, at the rate of 80–100 bubbles/minute was maintained throughout the period of heating and subsequent cooling.

After the reaction mixture had cooled down to 35–40°, it was filtered under a stream of nitrogen. The wood residue was washed with neutral dioxane–water (9:1) until the washings were colorless. The filtrate and washings were combined.

This red-brown filtrate was neutralized with solid sodium bicarbonate with stirring. It was then concentrated to 30–40 ml by distillation under reduced pressure (10–15 cm) to yield a dark syrupy liquid. The concentrate containing the bicarbonate sludge was transferred to a separatory funnel fitted to a 1-liter suction flask containing 500 ml of a 1% Na_2SO_4 solution in oxygen-free water.

By applying suction to the flask a partial vacuum was maintained inside it. The concentrate along with the sludge was then allowed to drop slowly into the sodium sulphate solution which was kept vigorously stirred. After the whole concentrate had been added, the precipitated lignin was recovered by centrifugation. It was then washed several times with a large excess of oxygen-free water until the washings were free from inorganic salts. Finally it was dried, while still lying in the centrifuge tubes, under vacuum over phosphorus pentoxide. It was then transferred to a weighing bottle and weighed.

Following this general procedure, lignin was isolated at the different initial acid concentrations of the solvent of 0.0 N, 0.05 N, 0.1 N, 0.2 N, 0.4 N, 0.5 N, 0.6 N, 0.8 N, 1.7 N.

Lignin Isolated by Successive Extractions under Increasing Initial Acid Concentrations

Pre-extracted wood meal (25 g) was first extracted with 0.2 N solvent and the lignin was recovered according to the procedure described above. The wood residue left after the precipitated lignin had been washed with neutral dioxane–water (9:1) was transferred to the previously used reaction flask. Again suction was applied for about thirty minutes and then the 0.4 N solvent was added and the extraction of the lignin and its recovery was carried out as usual. The wood residues were successively extracted in a similar fashion with the 0.8 N solvent and the 1.6 N solvent.

Lignin Isolation by Successive Extractions under Constant Initial Acid Concentrations

Pre-extracted wood meal (25 g) was successively extracted four times in a fashion similar to that described immediately above. In this case the initial concentration of the solvent for each extraction was the same (0.2 N).

Analytical Procedures

The methoxyl analyses were determined using the procedure of Gran (15). The infrared spectra were obtained using a Perkin–Elmer Model 21 spectrophotometer with sodium chloride optics and Nujol mulls. The alkaline nitrobenzene oxidations and quantitative estimations of the phenolic aldehydes were conducted according to the procedure of Stone and Blundell (11) with the recent modifications of Pepper and Siddiqueullah (12).

ACKNOWLEDGMENTS

REFERENCES

1. J. M. PEPPER, P. E. T. BAYLIS, and E. ADLER.   Can. J. Chem. **37**, 1241 (1959).
2. E. ADLER, J. M. PEPPER, and E. ERIKSOO.   Ind. Eng. Chem. **49**, 1391 (1957).
3. J. M. PEPPER and M. SIDDIQUEULLAH.   Unpublished results.
4. J. GIERER.   Acta Chem. Scand. **8**, 1319 (1954).
5. G. J. RITTER.   Ind. Eng. Chem. **17**, 1194 (1925).
6. M. A. BUCHANAN, F. E. BRAUNS, and R. L. LEAF.   J. Am. Chem. Soc. **71**, 1297 (1949).
7. A. BJÖRKMAN.   Ind. Eng. Chem. **49**, 1395 (1957).
8. F. F. NORD and W. J. SCHUBERT.   Tappi, **40**, 285 (1957).
9. R. A. DURIE, B. M. LYNCH, and S. STERNHILL.   Australian J. Chem. **13**, 156 (1960).
10. H. L. HERGERT.   J. Org. Chem. **25**, 405 (1960).
11. J. E. STONE and N. J. BLUNDELL.   Anal. Chem. **23**, 771 (1951).
12. J. M. PEPPER and M. SIDDIQUEULLAH.   Can. J. Chem. **38**, 2324 (1961).
13. J. M. PEPPER.   Tappi, **42**, 793 (1959).
14. L. F. FIESER.   Experiments in organic chemistry. 3rd ed. D. C. Heath & Co. 1955.
15. G. GRAN.   Svensk Papperstidn. **55**, 255 (1952).

THE FIVE-COMPONENT SYSTEM: LITHIUM–SODIUM–POTASSIUM–SULPHATE–CHLORIDE–WATER, AT 25° C[1]

A. N. CAMPBELL, E. M. KARTZMARK, AND H. M. HUTTON[2]

ABSTRACT

The system consisting of the ions Li_2^{++}, Na_2^{++}, K_2^{++}, Cl_2^{-}, SO_4^{-}, and water at 25° C has been investigated by the chemical analysis of the solutions and of the wet residues. In the solid model eight volumes were found where the following solid phases were in equilibrium with solution: $Li_2SO_4.H_2O$, K_2SO_4, $Na_2SO_4.10H_2O$, $K_3Na(SO_4)_2$, $KLiSO_4$, solid solution of Na_2SO_4 and Li_2SO_4, KCl, and NaCl. Anhydrous Na_2SO_4 was found to exist only as a surface in the solid diagram. Another volume, $LiCl.H_2O$, was not obtained experimentally owing to its close proximity to the LiCl corner of the diagram.

Five invariant points were discovered. No ternary salt was found to exist in the interior of the phase model at the temperature of this study, 25° C.

This paper marks the completion of a study of Campbell, Kartzmark, and their associates of the five-component system named in the title. Hitherto no such complete study has existed. Earlier papers (1) have dealt with the subsystems which had not previously been studied. All the component binary, ternary, and quaternary systems, including the reciprocal salt pairs, are now known at 25° C. There remained only the five-component system proper, represented graphically by the interior of the solid model.

EXPERIMENTAL PROCEDURE

Since the five quaternary subsystems were now completed and represented as the five surfaces (two triangular and three rectangular) of the Jänecke prism, the procedure adopted was to trace the paths of univariant curves from the corresponding quaternary invariant points on the outside surfaces till they met in quinquenary invariant points in the body of the diagram. This was accomplished experimentally by saturating with the phases of the quaternary invariant equilibrium, then adding increasing quantities of ions not participating in the quaternary equilibrium, and thus delineating the space curves. Since quinquenary invariant points mark the intersection of four curves (four solid phases), it was possible to check all these invariant points by approaching them along independent curves and this was always done. The experimental test for invariance was found in the sudden occurrence of a new ion in the solid phase, which was, of course, analyzed every time. The occurrence in large amount of a fresh ion is definitive, except for the change of sodium sulphate decahydrate to anhydrous sulphate, but here the change of water content was conclusive.

As an aid to clear thinking we constructed, while the experimental work was in progress, a solid model of stout wire, and suspended our analyzed points in the body of the model at the appropriate distances from the ends of the prism. In this way the direction of a line in space could be visualized.

As to the technique of solubility work, this has been too frequently described for mention here. Chloride ion was determined gravimetrically as silver chloride but the direct determination of sulphate ion as barium sulphate was avoided since we have found this to be completely inaccurate in the presence of alkali metal ions. Sulphate ion was determined solely by difference. Flame photometry was used to determine the alkali metal cations: our instrument was the Perkin–Elmer flame photometer. The accuracy of cation estimation was about two per cent but this is much better than can be attained by any other method of alkali determination in mixtures of alkali cations.

Since it is important to know the nature of the solid phases in contact with saturated solutions, it would be very desirable to have unequivocal methods of doing this but the usual methods, viz. X-ray powder photography or measurement of optical properties could not be applied because of the necessity of keeping the solid phase wet with equilibrium solution. If the solid phases are allowed to dry, phase change may occur, even at room temperature. Furthermore, the strongest X-ray reflections of sodium chloride and of sodium sulphate happen to be very close together, so that the X-ray method is less sensitive than usual. Consequently, we were forced to rest our determinations of the nature of solid phases entirely on the identification of the new phase which appeared at an invariant point. When a new ion suddenly appears, in quantity, in the solid phase, there is usually no question regarding the nature of the new phase. Moreover, the intersection of two or more solubility curves left little doubt about the nature of the four solid phases present at the invariant point.

EXPERIMENTAL RESULTS

The experimental results are given in Table I, which gives the mole % of each of Li_2^{++}, Na_2^{++}, K_2^{++}, $Cl_2^{=}$, and $SO_4^{=}$ in both the solid phase and the liquid phase, as well as m, the number of moles of water per "mole" of salt, and the nature of the solid phase.

Pictures of the equilibrium diagrams are shown in Fig. 1, with the invariant points marked as outlined in the caption. These are the solids in equilibrium with solution at 25° C. The photographs in Fig. 1 show the approximate positions of the quinquenary invariant points. To help differentiate the various lines in the prism, the quaternary lines on the surface are grey, while the quinquenary lines inside the prism are black. Picture (a) is shown with the K_2SO_4 corner nearest the right front; in picture (b) the NaCl corner is forward, presenting a view diagonally opposite to the first picture. Due to the difficulties in assembling this solder-and-wire diagram, the lines and invariant points are positioned only approximately. With the experimental data obtained, the invariants marked 2 and 4 in the photographs, Fig. 1, should be closer than indicated, actually almost touching.

One other invariant point, $LiCl.H_2O$, $Li_2SO_4.H_2O$, NaCl, KCl, in equilibrium with solution, exists in this system, but could not be obtained experimentally or even represented on this diagram. It is situated in the LiCl corner of the prism and theoretically is represented by the expanded diagram, Fig. 2.

The small volume which the lithium chloride salt occupies is the result of the powerful action of this chloride in displacing other salts from solution. This was expected from the data of the quaternary systems.

To illustrate the existence of the volumes indicating solution saturated with one salt, approximate cross sections at constant anion composition were drawn, using the three-dimensional wire model as a guide. The 16 diagrams are represented in Figs. 3–18.

Figure 3 is the sulphate end of the prism. In this system all the sulphates, $Li_2SO_4.H_2O$, K_2SO_4, and $Na_2SO_4.10H_2O$, are present with Na_2SO_4 anhydrous represented by the lines ab, and ab'. Only two addition compounds, $KLiSO_4$ and $K_3Na(SO_4)_2$, exist; at this temperature solid solution occurs between the lithium and sodium sulphates. Figures 4 and 5 show the change of the $Li_2SO_4.H_2O$, solid solution, and $Na_2SO_4.10H_2O$ areas. In Fig. 6, at the quinquenary invariant point (No. 5), where $K_3Na(SO_4)_2$, $KLiSO_4$, Na_2SO_4, $Na_2SO_4.10H_2O$ are the solids in excess in solution, another small wedge of solid solution appears: Na_2SO_4 anhydrous is still represented on the surface of the solid solution, that is ab, ab', and ab''. Past this quinquenary invariant, in Fig. 7, $Na_2SO_4.10H_2O$

TABLE I

No.	Mole per cent solid phase					Mole per cent liquid phase					Water content*	Nature of solid phase
	Li_2^{++}	Na_2^{++}	K_2^{++}	Cl_2^-	SO_4^-	Li_2^{++}	Na_2^{++}	K_2^{++}	Cl^-	SO_4^-		
1	5.0	10.6	33.7	0.7	50.0	23.3	8.7	17.3	9.8	40.9	24.2	K_2SO_4, $K_2Na(SO_4)_2$, $KLiSO_4$
2	24.1	6.9	17.4	10.8	40.8	22.1	8.8	19.8	21.7	27.6	20.0	K_2SO_4, $K_2Na(SO_4)_2$, $KLiSO_4$
3	16.4	4.9	27.6	4.6	46.5	16.0	13.3	20.0	45.7	5.0	17.3	K_2SO_4, $K_2Na(SO_4)_2$, $KLiSO_4$, KCl
4	14.5	0.2	35.6	22.6	27.1	21.6	4.3	24.3	45.7	4.1	18.4	K_2SO_4, $KLiSO_4$, KCl
5	19.1	3.7	26.7	3.4	47.1	18.0	14.6	21.4	41.9	4.2	18.2	K_2SO_4, $K_2Na(SO_4)_2$, $KLiSO_4$, KCl
6	28.8	11.3	11.0	13.7	35.2	3.2	15.3	31.4	48.1	2.9	18.5	K_2SO_4, $K_2Na(SO_4)_2$, KCl
7	1.2	10.5	39.9	12.3	36.1	7.5	14.2	29.7	45.7	2.9	18.4	K_2SO_4, $K_2Na(SO_4)_2$, KCl
8	1.0	7.8	43.6	23.2	24.4	12.0	11.0	27.3	45.7	4.0	17.7	K_2SO_4, $K_2Na(SO_4)_2$, KCl
9	1.0	11.6	40.3	14.3	32.8	14.3	12.5	24.0	45.3	3.9	17.0	K_2SO_4, $K_2Na(SO_4)_2$, KCl
10	0.2	1.9	43.9	37.1	11.0	16.3	13.1	21.8	45.1	3.7	17.8	K_2SO_4, $K_2Na(SO_4)_2$, $KLiSO_4$, KCl
Average invariant point #1						17.0	13.9	20.7	43.8	4.6		
11	0.4	36.1	14.9	40.0	8.6	5.8	31.0	14.4	45.9	2.9	14.4	$K_2Na(SO_4)_2$, KCl, $NaCl$
12	9.5	31.7	9.6	33.2	16.0	18.1	21.5	11.9	46.5	2.0	14.4	$K_2Na(SO_4)_2$, KCl, $NaCl$
13	11.2	29.1	9.1	33.9	16.7	23.7	16.4	10.1	47.7	2.2	14.3	$K_2Na(SO_4)_2$, KCl, $NaCl$
14	20.7	9.8	19.2	26.7	23.6	25.9	14.9	10.2	47.4	1.6	14.3	$K_2Na(SO_4)_2$, KCl, $NaCl$
15	10.7	30.8	9.1	32.7	15.9	37.5	6.8	6.9	48.1	1.4	13.0	$KLiSO_4$, $NaCl$, KCl
16	9.6	31.0	9.1	36.3	14.0	36.1	7.3	6.9	48.5	1.2	13.4	$KLiSO_4$, $NaCl$, KCl
17	26.2	11.2	10.7	24.4	27.5	33.5	9.9	6.2	47.2	3.2	15.6	$KLiSO_4$, $NaCl$, KCl
18	6.9	34.2	9.1	38.7	11.1	30.8	11.6	7.5	47.7	2.4	22.5	$KLiSO_4$, $NaCl$, KCl
19	9.5	34.4	8.6	32.4	15.1	28.4	12.3	8.0	48.9	2.4	14.1	$KLiSO_4$, $K_2Na(SO_4)_2$, KCl, $NaCl$
20	11.0	0.9	37.1	26.9	24.1	21.0	12.5	16.4	46.1	4.0	16.5	$KLiSO_4$, $K_2Na(SO_4)_2$, KCl
21	24.9	0.9	24.7	3.3	6.2	25.3	12.9	12.5	46.5	2.8	16.1	$KLiSO_4$, $K_2Na(SO_4)_2$, KCl, $NaCl$
22	18.4	7.5	20.1	31.2	22.8	28.2	12.5	8.4	48.5	2.4	14.0	$KLiSO_4$, $K_2Na(SO_4)_2$, KCl, $NaCl$
Average invariant point #2						28.3	12.4	8.2	48.7	2.4	14.1	$KLiSO_4$, $K_2Na(SO_4)_2$, KCl, $NaCl$
23	28.8	0.2	21.2	23.9	25.9	40.9	3.0	6.1	48.5	1.5	25.6	$KLiSO_4$, $Li_2SO_4 \cdot H_2O$, KCl
24	25.0	7.3	17.4	27.4	22.9	39.5	4.3	5.1	49.9	1.2	12.5	$KLiSO_4$, $Li_2SO_4 \cdot H_2O$, KCl
25	20.2	18.9	9.5	32.8	18.6	38.4	5.2	5.6	49.1	1.7	12.9	$KLiSO_4$, $Li_2SO_4 \cdot H_2O$, KCl
26	22.5	10.0	17.3	21.6	28.6	38.6	5.6	5.9	48.7	1.2	12.8	$KLiSO_4$, $Li_2SO_4 \cdot H_2O$, KCl, $NaCl$
27	20.7	19.4	10.2	27.9	21.8	38.7	6.8	5.4	47.7	1.4	12.8	$KLiSO_4$, $Li_2SO_4 \cdot H_2O$, KCl, $NaCl$
28	38.4	6.4	5.5	2.6	47.1	43.5	6.3	1.1	12.8	36.3	16.9	$KLiSO_4$, $Li_2SO_4 \cdot H_2O$, solid solution
29	32.9	8.9	8.2	6.3	43.7	41.2	7.3	1.3	30.2	20.0	18.0	$KLiSO_4$, $Li_2SO_4 \cdot H_2O$, solid solution
30	31.4	10.4	8.9	11.9	37.4	41.2	7.0	1.8	37.2	12.8	17.8	$KLiSO_4$, $Li_2SO_4 \cdot H_2O$, solid solution
31	32.3	10.0	8.0	17.0	32.7	39.6	7.8	2.4	43.3	6.9	16.8	$KLiSO_4$, $Li_2SO_4 \cdot H_2O$, solid solution
32	27.8	13.3	11.8	12.0	35.1	40.2	4.8	5.3	47.3	2.4	14.6	$KLiSO_4$, $Li_2SO_4 \cdot H_2O$, $NaCl$, KCl
33	13.2	28.1	8.4	38.8	11.5	38.9	5.1	5.6	48.3	1.4	12.7	$KLiSO_4$, $Li_2SO_4 \cdot H_2O$, $NaCl$, KCl
Average invariant point #3												

TABLE I (*Concluded*)

No.	Mole per cent solid phase					Mole per cent liquid phase					Water content*	Nature of solid phase
	Li++	Na₂++	K₂++	Cl₂⁻	SO₄⁻	Li++	Na++	K₂++	Cl⁻	SO₄⁻		
34	16.8	25.6	7.9	36.6	13.1	42.3	2.8	3.9	50.2	0.8	11.9	Li₂SO₄.H₂O, NaCl, KCl
35	15.7	23.9	8.7	39.7	12.0	46.1	0.9	2.5	50.1	0.4	10.0	Li₂SO₄.H₂O, NaCl, KCl
36	1.5	33.7	13.7	26.7	24.4	6.5	36.4	5.7	37.8	13.6	14.3	K₂Na(SO₄)₂, NaCl, solid solution
37	13.7	28.7	7.8	23.9	25.9	13.1	30.2	6.9	43.4	6.4	15.3	K₂Na(SO₄)₂, NaCl, solid solution
38	14.0	30.4	6.2	28.4	21.0	21.5	23.4	5.1	46.1	3.9	15.4	K₂Na(SO₄)₂, NaCl, solid solution
39	16.0	27.2	5.9	30.2	20.7	30.6	14.3	5.2	47.5	2.4	14.8	K₂Na(SO₄)₂, Li₂SO₄.H₂O, KLiSO₄, NaCl
40	23.9	24.1	2.0	25.5	24.5	34.4	15.1	1.0	44.7	4.9	15.0	Li₂SO₄.H₂O, NaCl, solid solution
41	25.4	20.5	4.7	23.9	25.5	35.1	15.5	1.0	44.4	4.0	14.9	Li₂SO₄.H₂O, NaCl, solid solution
42	27.9	14.5	9.6	14.6	33.4	31.5	15.9	3.4	45.5	3.7	15.8	Li₂SO₄.H₂O, NaCl, solid solution
43	22.8	14.1	10.4	14.7	38.0	29.8	15.3	4.3	47.7	2.9	15.2	Li₂SO₄.H₂O, K₂Na(SO₄)₂, KLiSO₄, NaCl
Average invariant point #4						30.2	14.8	4.8	47.6	2.6	15.0	Li₂SO₄.H₂O, K₂Na(SO₄)₂, KLiSO₄, NaCl
44	26.1	12.5	10.7	10.6	40.1	29.9	13.1	6.2	46.1	4.7	16.4	K₂Na(SO₄)₂, KLiSO₄, solid solution
45	24.8	13.7	10.5	11.8	39.2	29.8	16.6	4.0	44.1	5.5	17.0	K₂Na(SO₄)₂, KLiSO₄, solid solution
46	26.2	13.0	10.9	6.4	43.5	29.7	14.7	6.5	38.0	11.1	19.1	K₂Na(SO₄)₂, KLiSO₄, solid solution
47	25.5	15.3	10.6	4.6	44.0	22.7	24.0	3.6	26.3	23.4	18.4	K₂Na(SO₄)₂, KLiSO₄, solid solution
48	17.2	22.7	10.2	3.1	46.8	10.2	33.4	6.9	29.1	20.4	15.9	K₂Na(SO₄)₂, KLiSO₄, solid solution
49	5.9	42.3	2.1	1.1	48.6	4.3	41.6	5.1	17.7	31.3	15.1	K₂Na(SO₄)₂, Na₂SO₄.10H₂O
50	5.9	33.7	8.9	1.7	49.8	4.2	40.3	5.1	18.5	31.9	15.3	K₂Na(SO₄)₂, Na₂SO₄.10H₂O
51	12.3	38.5	1.6	0.9	46.7	8.2	35.1	6.3	17.5	32.9	16.1	K₂Na(SO₄)₂, Na₂SO₄.10H₂O
52	9.6	32.6	8.6	1.7	47.5	9.5	34.5	6.5	16.9	32.6	16.6	K₂Na(SO₄)₂, Na₂SO₄.10H₂O, KLiSO₄
53	0.8	41.5	8.8	0.4	48.5	7.9	35.1	6.4	4.6	46.0	15.8	K₂Na(SO₄)₂, Na₂SO₄.10H₂O
54	1.4	21.2	29.3	0.6	47.5	8.1	37.1	5.6	6.6	42.6	15.1	K₂Na(SO₄)₂, Na₂SO₄.10H₂O
55	7.8	31.1	10.5	0.6	50.0	8.1	35.7	6.1	9.3	40.8	15.6	K₂Na(SO₄)₂, Na₂SO₄.10H₂O
56	8.6	34.7	6.5	1.5	48.7	9.6	34.0	6.4	18.2	31.8	16.3	K₂Na(SO₄)₂, KLiSO₄, Na₂SO₄.10H₂O
57	22.8	15.0	12.2	0.6	49.4	20.5	24.5	4.6	4.9	45.5	16.5	K₂Na(SO₄)₂, KLiSO₄, Na₂SO₄
58	24.4	16.0	10.4	2.0	47.2	19.5	27.3	3.5	9.4	40.3	17.2	K₂Na(SO₄)₂, KLiSO₄, Na₂SO₄
59	19.3	15.5	14.8	1.8	48.6	10.3	34.5	5.8	17.3	32.1	16.2	K₂Na(SO₄)₂, KLiSO₄, Na₂SO₄, Na₂SO₄.10H₂O
Average invariant point #5						9.8	34.3	6.2	17.5	32.2	16.4	K₂Na(SO₄)₂, KLiSO₄, Na₂SO₄, Na₂SO₄.10H₂O

*Moles of water per mole of salt.
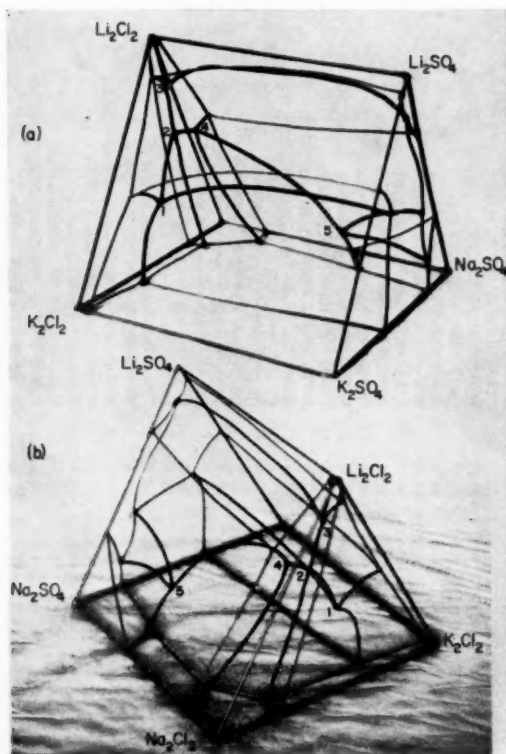
FIG. 1. 1. K_2SO_4, $K_3Na(SO_4)_2$, $KLiSO_4$, KCl
2. $KLiSO_4$, $K_3Na(SO_4)_2$, KCl, $NaCl$
3. $KLiSO_4$, $Li_2SO_4 \cdot H_2O$, $NaCl$, KCl
4. $Li_2SO_4 \cdot H_2O$, $K_3Na(SO_4)_2$, $KLiSO_4$, $NaCl$
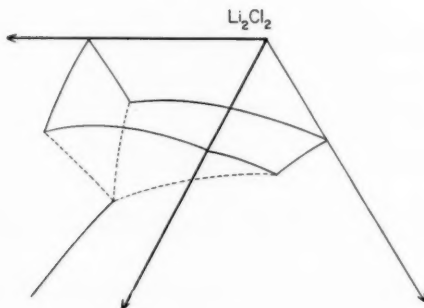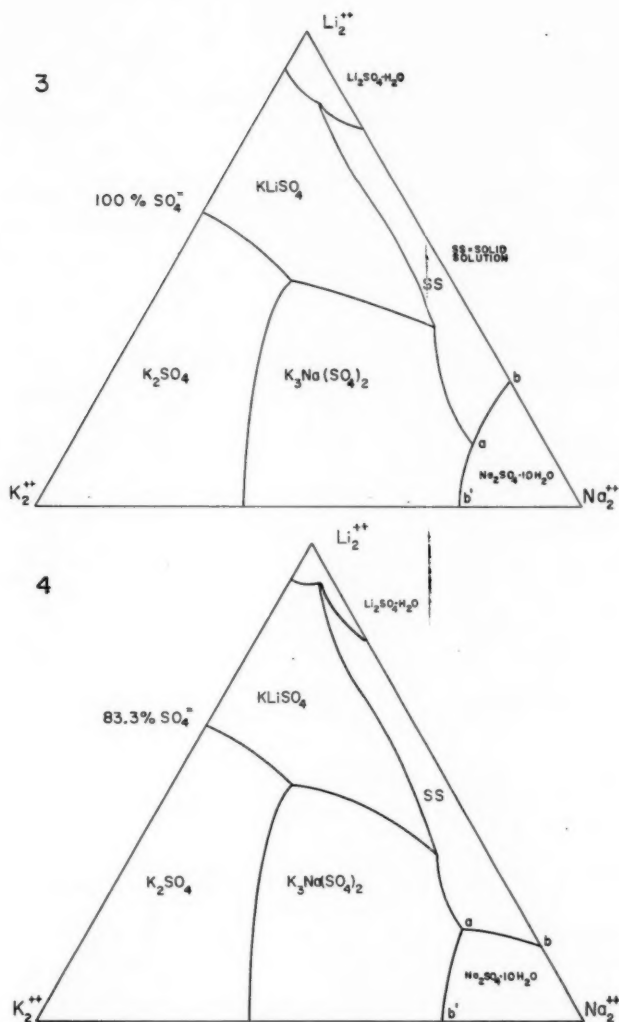5. $K_3Na(SO_4)_2$, $KLiSO_4$, Na_2SO_4, $Na_2SO_4 \cdot 10H_2O$

FIG. 2.

Figs. 3 and 4.

is still evident, with the anhydrous form existing on the base below the solid solution. Finally in Fig. 8 the decahydrate volume has vanished. In this interval the $KLiSO_4$–$K_3Na(SO_4)_2$ surface has been tilted upward at the $KLiSO_4$ – $K_3Na(SO_4)_2$ – solid solution line, as evident in Fig. 9. The first appearance of a chloride, $NaCl$, is observed in Fig. 10, its area increasing in Figs. 11 and 12, at the expense of the solid solution region. Figure 13
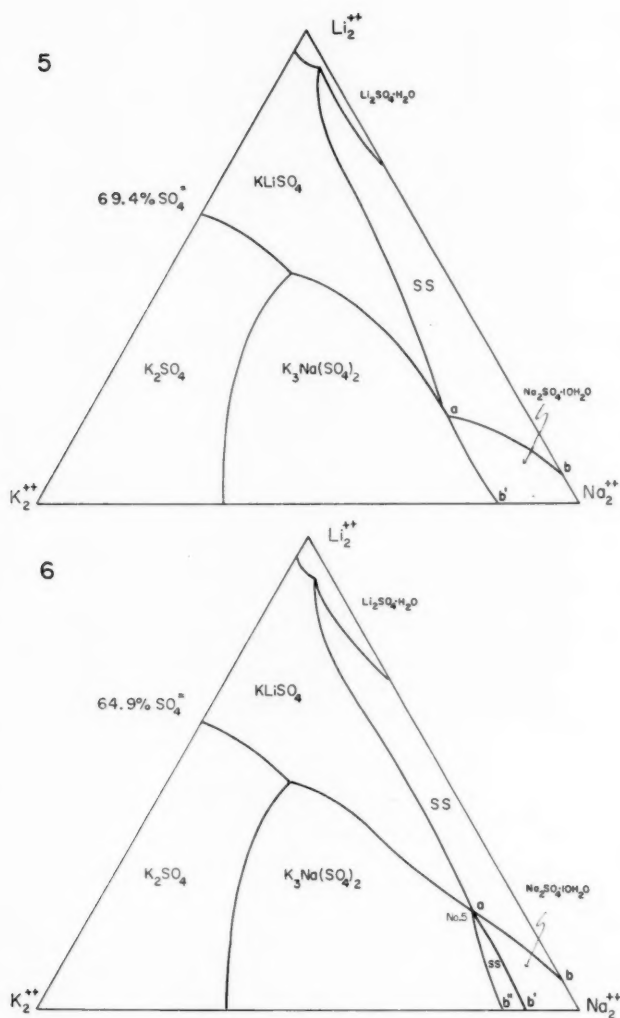
Figs. 5 and 6.

is drawn through the quaternary invariant point $Li_2SO_4.H_2O$, solid solution, NaCl in the lithium–sodium–chloride–sulphate–water system. Solid solution here is completely in the body of the diagram and in Fig. 14 it is quickly disappearing as another quinquenary invariant is approaching. Figure 14 also represents the quinquenary invariant (No. 1) $KLiSO_4$, $K_3Na(SO_4)_2$, K_2SO_4, KCl; KCl appears for the first time, but cannot
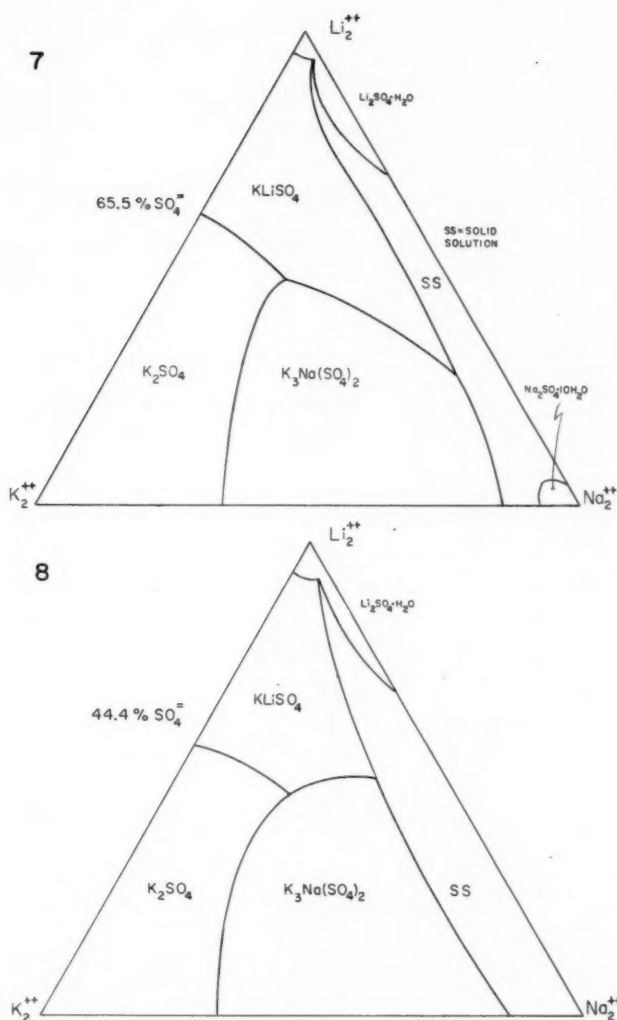
FIGS. 7 AND 8.

be represented since it is on the plane immediately behind Fig. 14. In Fig. 15, the invariant $K_3Na(SO_4)_2$, $KLiSO_4$, Li_2SO_4, $Li_2SO_4 . H_2O$, NaCl (No. 4) has been reached, this being one extremity of solid solution, that is, lithium sulphate; K_2SO_4 has all but disappeared. This surface represents the last plane of existence of the double salts $KLiSO_4$ and $Na_3K(SO_4)_2$. Between Figs. 15 and 16, the $Li_2SO_4 . H_2O$ – NaCl line has moved rapidly
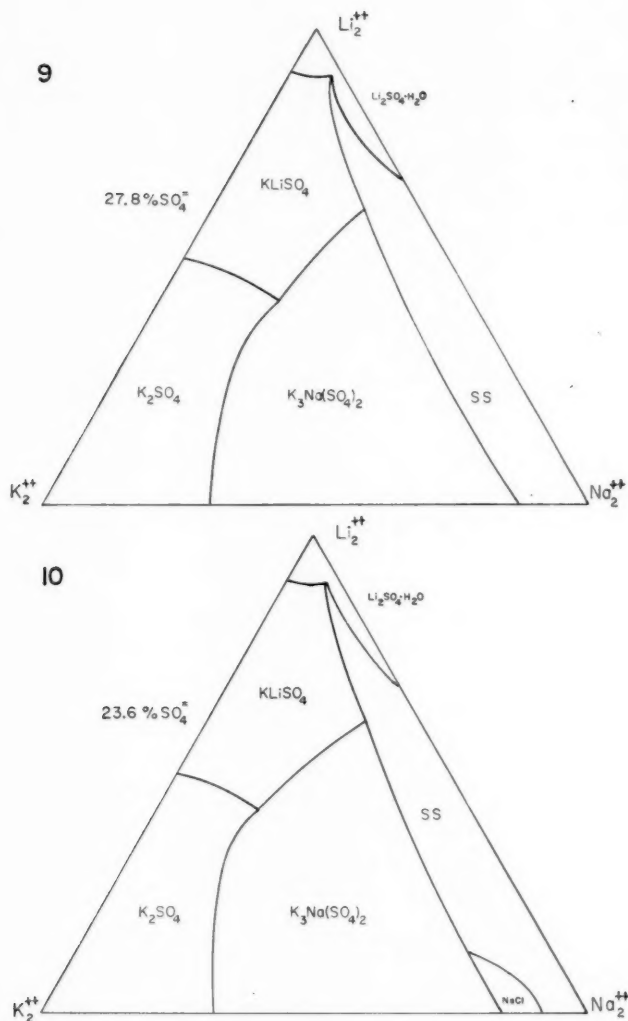
FIGS. 9 AND 10.

upward. Two quinquenary invariants are evident in Fig. 16: the $Li_2SO_4 \cdot H_2O$, $KLiSO_4$, NaCl, KCl (No. 3) and $Na_3K(SO_4)_2$, $KLiSO_4$, NaCl, KCl (No. 2) invariants, although not all the salts can be represented. Figure 17 shows the existence of the chlorides of sodium and potassium and the sulphate of lithium. The last, Fig. 18, where only the chlorides are present, represents only the sodium and potassium chlorides. Lithium
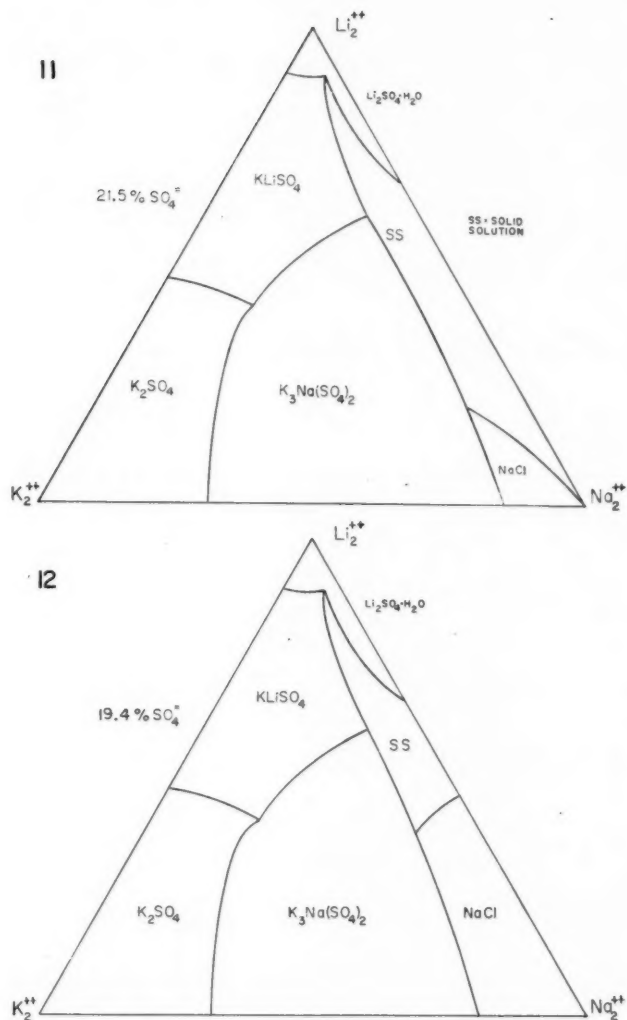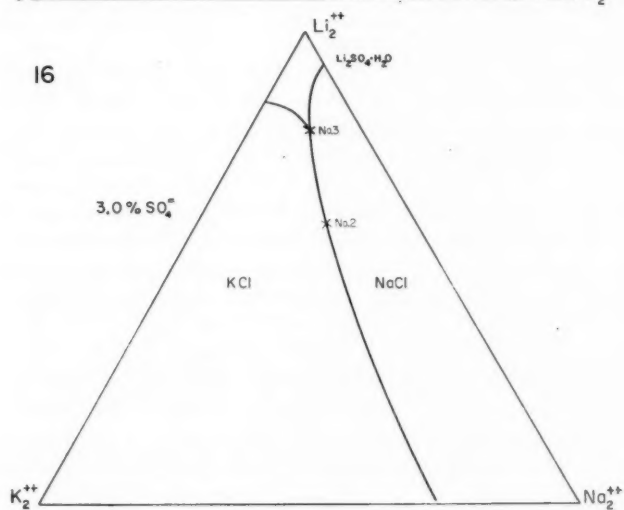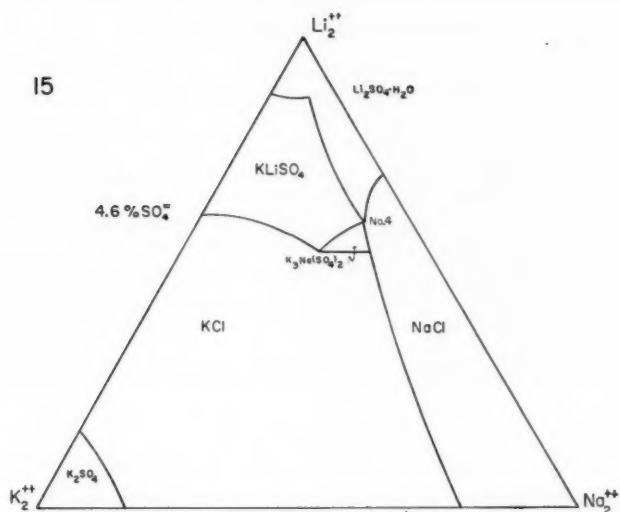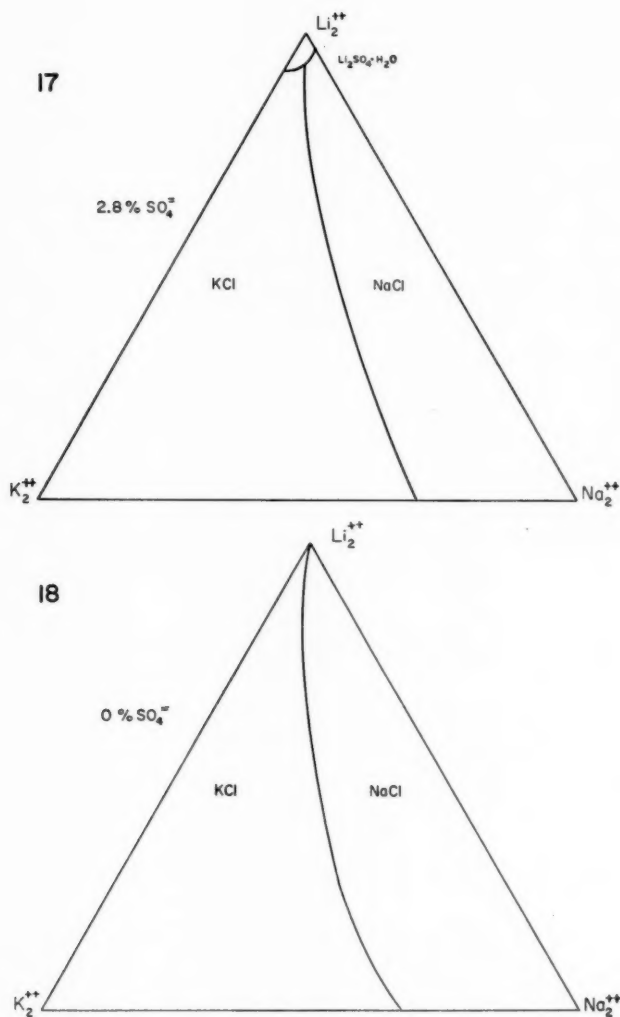
FIGS. 11 AND 12.

chloride so strongly displaces other salts from solution that its area of existence cannot be indicated on the diagram with the scale used. The other quinquenary invariant point $Li_2SO_4 \cdot H_2O$, $LiCl \cdot H_2O$, $NaCl$, KCl was not represented due to its position extremely close to the LiCl corner of the prism.
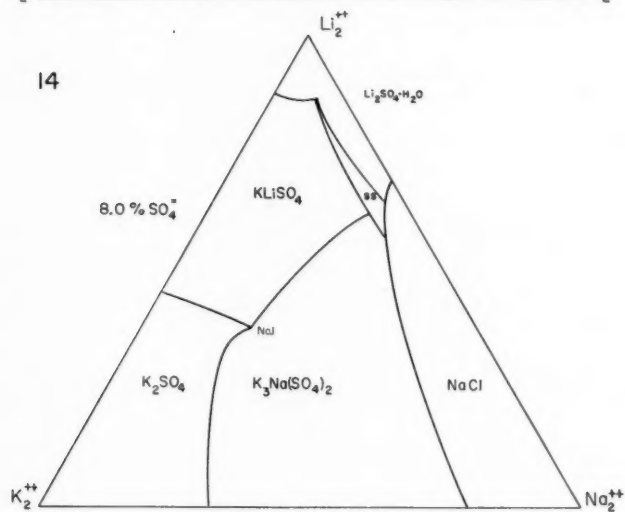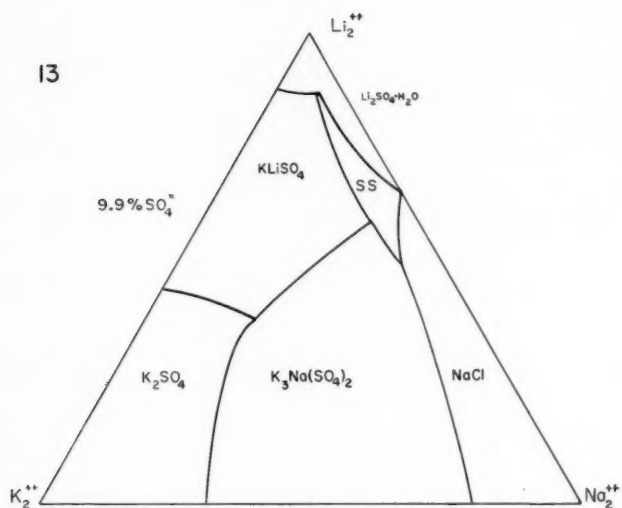
FIGS. 13 AND 14.

FIGS. 1 AND 16.

FIGS. 17 AND 18.

REFERENCES

1. A. N. CAMPBELL and E. M. KARTZMARK. Can. J. Chem. **34**, 672 (1956); **36**, 171 (1958); **37**, 1409
(1959). A. N. CAMPBELL, E. M. KARTZMARK, and E. LOVERING. Can. J. Chem. **36**, 1511 (1958).

EFFECT OF AMBIENT OXYGEN ON THE SEMICONDUCTIVITIES OF EVAPORATED FILMS OF MESONAPHTHODIANTHRENE AND MESONAPHTHODIANTHRONE[1]

H. Kuroda[2] and E. A. Flood

ABSTRACT

The electrical conductivity of an "evaporated" film of mesonaphthodianthrene increases when the film is exposed to oxygen. The increase in conductivity is associated with changes in the semiconductivity activation energies. The activation energy for the oxygen-free anthrene (bulk conduction) is 0.74 ev while that associated with oxygen adsorption (surface conduction) is 0.40 ev. In marked contrast, the conductivity of an evaporated film of meso-naphthodianthrone decreases when exposed to oxygen. An oxygen-free film of the anthrone has different activation energies in different temperature regions, the activation energies being 0.73 ev and 0.43 ev in the higher and lower temperature regions, respectively. The conduction associated with the lower activation energy decreases when the film is exposed to oxygen.

The effect of oxygen on the semiconductivities of mesonaphthodianthrene and mesonaph-thodianthrone are compared with the effect of oxygen on their electron spin resonance spectra.

INTRODUCTION

The adsorption of gas molecules on the surface of metals and semiconductors modifies the electrical properties associated with the surface (e.g. work function, contact potential, surface conductance, etc.) especially when the surface reaction involves an electron-transfer mechanism. While in the case of inorganic semiconductors there is a large body of scientific literature dealing with such effects, in the case of organic semiconductors comparatively few papers exist, in spite of the fact that adsorption on organic crystal surfaces can also involve electron-transfer mechanisms. Pick and Wissman observed that the electrical conductivity of a napthalene single crystal was affected markedly by ambient oxygen (1). The influence of ambient oxygen on the photoconductivity of the anthracene crystal has been studied by many investigators (2, 3, 4). The effect of oxygen on the photoconductivity of phthalocyanine is also known (5).

Recently Matsunaga found that a sharp absorption peak appeared in the electron spin resonance spectrum of mesonaphthodianthrene powder when it was exposed to air (6). This suggests that some kind of electron transfer is taking place between the hydro-carbon crystal and oxygen molecules adsorbed on the surface. It seemed, therefore, interesting to investigate the influence of ambient oxygen on the electrical conductivities of thin films formed by evaporation (evaporated films) of these compounds. A brief account of our findings on this subject has been presented in a previous note wherein it was pointed out that ambient oxygen does indeed exert an influence on the electrical conductivities of such films (7).
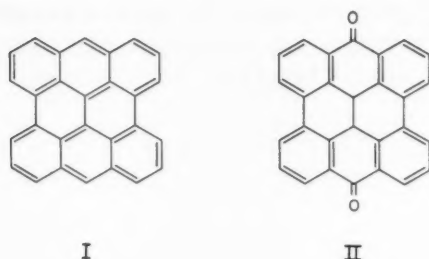
EXPERIMENTAL

Mesonaphthodianthrene (I) and mesonaphthodianthrone (II) were both purified by repeated sublimation in a high vacuum. Immediately after the final sublimation, a small amount of the powder of the sample was sealed in the conductivity apparatus,

I   II

which is schematically shown in Fig. 1. The powder of the sample was placed at the bottom of the small tube A. The cell was evacuated by means of a two-stage mercury diffusion pump together with two liquid nitrogen traps. The whole vacuum system except the region containing the sample was baked during the evacuation. The final vacuum attained after a long evacuation was 10^{-6} mm Hg. The sample was first evaporated to the upper part of the tube A and then re-evaporated from there to the flat surface B, which was equipped with two electrodes of platinum foil embedded in the glass as shown in Fig. 1. It was found necessary to carry out the sublimation rather
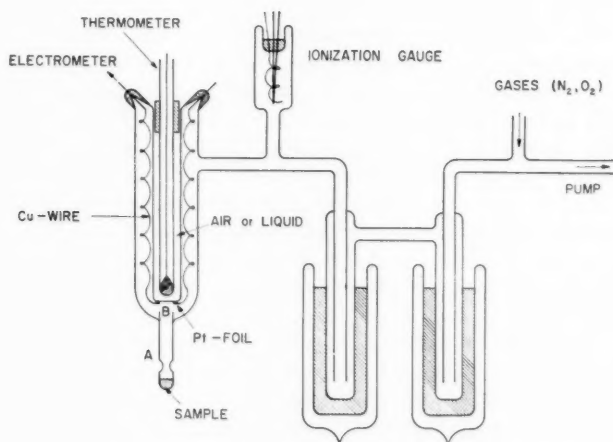

FIG. 1.   The apparatus for the measurement of the conductivity.

slowly, in order to obtain a coherent film. The films so obtained were transparent and the order of $1\,\mu$ in thickness. The electrical conductivities of the oxygen-free films were studied immediately after the preparation of the films, without breaking the high vacuum.

Conductivity measurements were made using a d-c. method. Direct-current voltage of 135 v was applied between the two electrodes by means of dry cells. The distance between the two electrodes was 1–3 mm. The current through the film was measured with a Hewlett and Packerd DC Micro-volt-ammeter Model 425. The output of the electrometer was connected to a Varian G-10 recorder. The conductivity change was followed by the change in current.

RESULTS

(a) Mesonaphthodianthrene Film

The temperature dependence of the conductivity of a film of mesonaphthodianthrene is shown in Fig. 2. The current, i, through the film is plotted in logarithmic scale against $(1/T)$. In order to avoid any permanent change due to the evaporation of the compound from the film, the temperature of the measurement was not raised to more than 150° C when the measurement was made in vacuum. With an oxygen-free film a linear relation is obtained between log i and $(1/T)$. There is no appreciable deviation between the curve for the heating process and that for the cooling process.
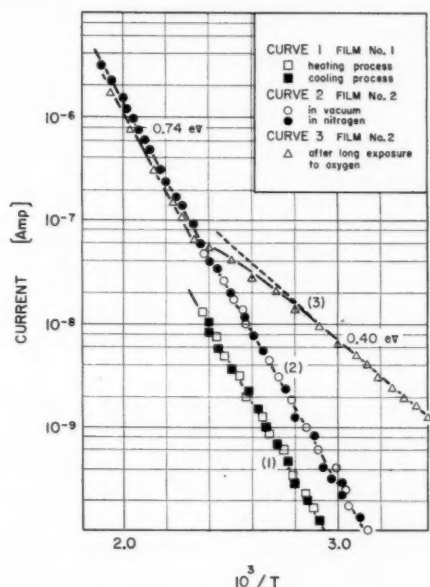

FIG. 2.   Temperature dependence of the current through mesonaphthodianthrene films.

The temperature dependence of the conductivity in nitrogen was measured using the same film as that used previously for measurements in vacuum. The results are shown in Fig. 2, curve 2. The temperature range of the measurement was extended up to 250° C. The plot of log i vs. $(1/T)$ gives again a straight line, which coincides with the results measured in vacuum at temperatures below 150° C. This indicates that nitrogen does not influence the electrical conductivity of the film appreciably. The temperature dependence described above can be expressed by an exponential function as is usually found with semiconductors,

[1] $$i = i_0 \exp{(-E/kT)}$$

where E is the activation energy for the semiconductivity. The value of E determined from the experimental results is 0.74 ev.

If an evaporated film of mesonaphthodianthrene is kept in oxygen or air for a long period, it shows quite a different behavior in respect to the temperature dependence of the electrical conductivity (cf. curve 3 of Fig. 2). In this case the slope of the log i vs. $(1/T)$ curve in the lower-temperature region differs distinctly from that in the higher-temperature region. The latter coincides exactly with the curve obtained in nitrogen.

The slope of the curve in the lower-temperature region corresponds to a smaller activation energy, 0.40 ev. At lower oxygen pressures the semiconductivity of the "anthrene" as a function of temperature shows considerable hysteresis due to adsorption–desorption effects.

If the evaporated film is placed in contact with oxygen at room temperature the conductivity increases gradually with time. The conductivity change at 24° C is shown in Fig. 3. This is a very slow process. The rate of the conductivity change is dependent upon
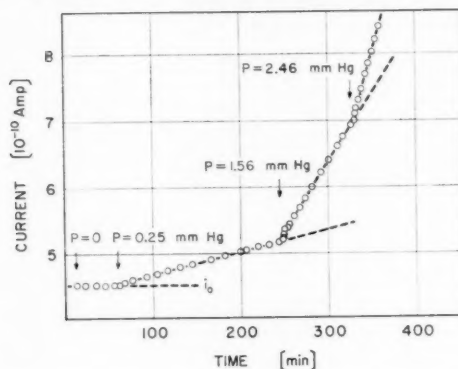

FIG. 3. Variation of the current through a mesonaphthodianthrene film in lower pressures of oxygen at 24° C.

the pressure of the ambient oxygen, being nearly proportional to the pressure when it is less than a few millimeters of mercury. This is illustrated in Fig. 4. If the pressure is high, the conductivity increases rapidly during a short initial period, after which the rate of increase falls off and the conductivity approaches constant values.

At a pressure about 100 mm Hg, the change in the conductivity practically ceases after a few days. When oxygen is pumped off, the conductivity of the film decreases slowly. This again is a very slow process. The change described above is evidently associated with the adsorption of oxygen molecules, and is reversible to a large extent.
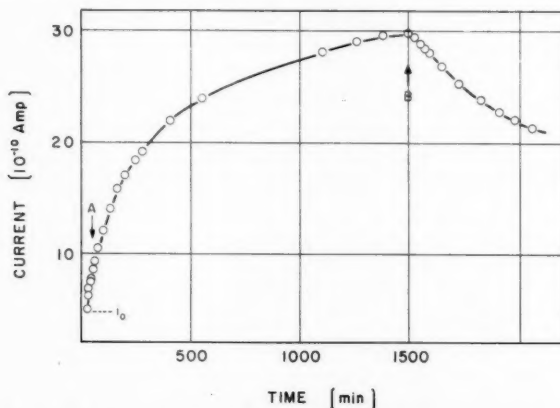

FIG. 4. Variation of the current through a mesonaphthodianthrene film in oxygen (10 mm Hg) at 24° C. The ambient oxygen is introduced into the cell at point A and pumped off at point B.

The temperature dependence of the electrical conductivity was measured at different stages of the oxygen adsorption although some difficulties due to temperature adsorption–desorption effects were encountered. It was found that the rate of the conductivity increase associated with the oxygen adsorption, as well as that of the reverse change, is faster at higher temperatures. Accordingly, the measurements were made as quickly as possible at temperatures below 40° C, and reproducible results were obtained. The results are shown in Fig. 5 and indicate clearly that the conduction mechanism associated with the lower activation energy is the one which is created by oxygen adsorption. The log i vs. $(1/T)$ curve is not a straight line when the amount of adsorbed oxygen is small. The slope of the curve at the high-temperature end is almost equal to that of the oxygen-free film, and the slope at the low-temperature end corresponds to the activation energy of 0.40 ev. As the amount of oxygen adsorption increases, the region in which the activation energy is 0.40 ev becomes predominant at temperatures below 40° C.
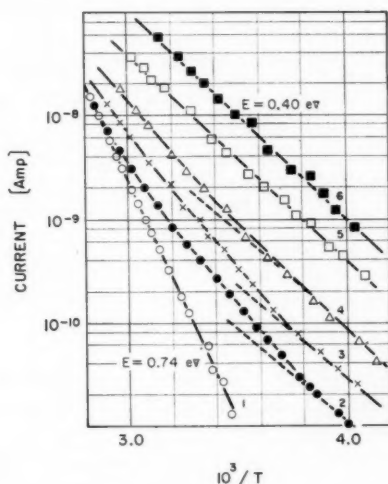

FIG. 5.   Temperature dependence of the current through a mesonaphthodianthrene film which has been exposed to oxygen at various pressures for different lengths of time. (1) Oxygen-free state; (2) 1 mm Hg, $\frac{1}{2}$ hr; (3) 3 mm Hg, $\frac{1}{2}$ hr; (4) 10 mm Hg, $\frac{1}{2}$ hr; (5) 50 mm Hg, 1 hr; (6) 300 mm Hg, 2 hr.

(b) Mesonaphthodianthrone Film

The temperature dependence of the conductivity of a mesonaphthodianthrone film is shown in Fig. 6. In marked contrast to the behavior of the mesonaphthodianthrene film, the activation energy of the oxygen-free film of mesonaphthodianthrone in the higher-temperature region differs distinctly from that in the lower-temperature region. In the latter region the activation energy is 0.43 ev while in the former it is 0.73 ev. Further if the film is exposed to air or oxygen the low-temperature activation energy of 0.43 ev disappears from the log i vs. $(1/T)$ curve, the activation energy becoming the same as at the higher temperature, i.e. it becomes 0.73 ev over the whole range thus resembling the oxygen-free anthrene.

The conductivity change due to ambient oxygen at 24° C is shown in Fig. 7 in which i_0 denotes the current in high vacuum; oxygen is introduced into the cell at point A and pumped off at point B. The conductivity of a mesonaphthodianthrone film decreases
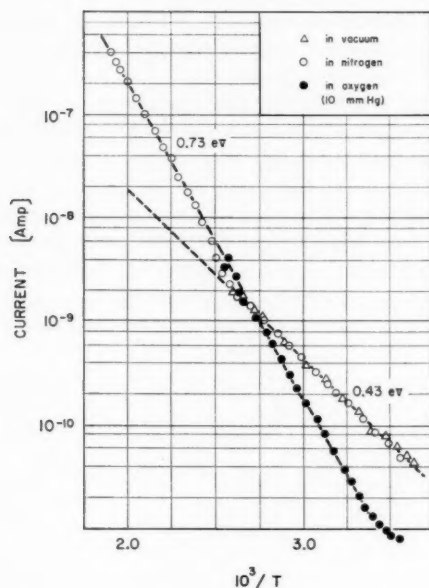
FIG. 6. Temperature dependence of the current through a mesonaphthodianthrone film.
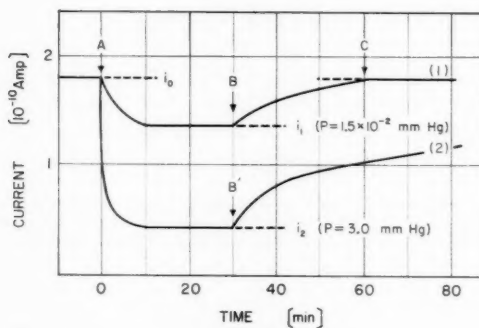

FIG. 7. Variation of the current through a mesonaphthodianthrone film caused by exposure to oxygen. Oxygen is introduced into the cell at point A and pumped off at point B (240° C).

rather rapidly when the film is exposed to oxygen, usually becoming constant within 10 minutes. As oxygen is pumped off the conductivity increases gradually with time, and goes back to the original value after evacuation during a long period. The magnitude of the conductivity at the equilibrium state is dependent upon the pressure of the ambient oxygen, as illustrated in Fig. 8 in which the current through a film with a constant applied potential difference is plotted against the pressure of oxygen.
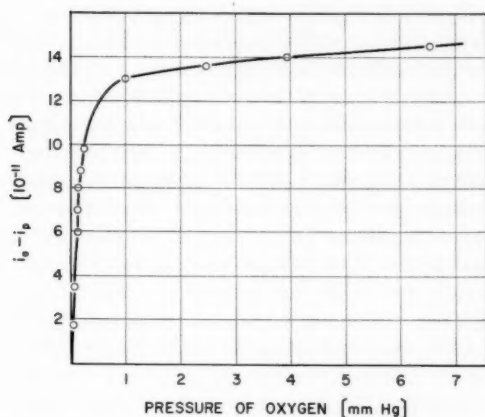
FIG. 8.   Current through a mesonaphthodianthrone film at the equilibrium state in oxygen as a function of the oxygen pressure (24° C).

DISCUSSION

From the results described above it is evident that there are at least two mechanisms involved in the electrical conduction of mesonaphthodianthrene films as well as in the conduction of mesonaphthodianthrone films. One of them, in each case, is dependent upon the ambient oxygen while the other is independent. The oxygen-sensitive conduction is associated with a lower activation energy. It is known that the conductivity of the intrinsic semiconductor can be described by the following equation,

[2] $$\sigma = \sigma_0 \exp\left(-\epsilon/2kT\right),$$

where σ_0 is a constant dependent upon the concentration of the electronic states and the mobility of the carrier, and ϵ is the energy gap in the band structure of the semiconductor. The semiconductivities of these compounds have been studied by Inokuchi using compressed-powder specimens (8). The energy gaps were estimated from the equation given above as 1.2 ev and 1.3 ev for mesonaphthodianthrene and mesonaphthodianthrone, respectively. Applying the same equation to our results the energy gaps corresponding to the two activation energies of the semiconductivity of mesonaphthodianthrene film are estimated as 1.48 ev and 0.80 ev, while those of the mesonaphthodianthrone film are 1.46 ev and 0.86 ev.

It is difficult to distinguish between bulk and surface conductivities where data refer to net conductivities of either compressed powders or to evaporated films, both of which may have fairly large surfaces. Surface effects might be expected to be particularly significant in the case of very thin evaporated films; of course surface states can control the semiconductivity. However, our results suggest that the activation energy, which is independent of the ambient oxygen, the higher activation energy, is associated with bulk conduction, i.e. independent of the surface.

The data given in Fig. 5, the temperature dependence of the electrical conductivity of mesonaphthodianthrene film in oxygen, can be described quite well by the following equation,

[3] $$\sigma = \sigma_1 \exp\left(-E_1/kT\right) + \sigma_2 \exp\left(-E_2/kT\right),$$

where E_1 is 0.74 ev and E_2 is 0.40 ev. The value of σ_1 remains constant for all curves while σ_2 increases as the amount of oxygen adsorbed increases. The values of σ_1 and σ_2 are dependent upon the mobility of the charge carrier and the concentration of the electronic states, i.e. the concentration of the impurity levels in the case of extrinsic semiconduction. As is well known, the surface state can contribute to the electrical conductivity either by forming a surface band through which charge carriers can move, or by behaving as an impurity level which provides the charge carriers to the bulk conduction. It seems probable in the present case that the electron-acceptor levels are created by oxygen adsorption on the surface and that the increase in the magnitude of σ_2 is due to the increase in the concentration of such acceptor levels. According to this model, 0.80 ev is the energy gap between the acceptor level and the lower band.

According to Matsunaga (6), mesonaphthodianthrene powder shows an electron spin resonance spectrum with a fine structure consisting of at least seven peaks separated by 4.4 oersted when it is detected in vacuum. The spin concentration corresponding to this electron spin resonance is 3×10^{21} per mole, g-value being 2.0024. If the powder is exposed to air the central peak of the electron spin resonance spectrum grows slowly reaching the maximum intensity after a few days. The spin concentration corresponding to this sharp absorption is about one tenth of that of the broad absorption mentioned above. The intensity of the sharp absorption decreases with time when air is pumped off. This change is evidently due to the interaction between oxygen and mesonaphthodianthrene crystals. Matsunaga also studied the electron spin resonance of mesonaphthodianthrone powder. It gives an electron spin resonance spectrum similar to that of the hydrocarbon, its spin concentration being about one third of that of the latter. In this case, however, the oxygen effect was not detected.

It is interesting to compare the effect of oxygen on the electrical conductivity with that on the electron spin resonance. In the first place, both effects take place very slowly at room temperature, taking a few days to reach the equilibrium state in air, and both are reversible. In the second place, the creation of the acceptor level and that of the spin center are caused by the ambient oxygen only in the case of the hydrocarbon. These facts suggest that the impurity level created as a result of oxygen adsorption is associated with the formation of a free radical on the surface of the hydrocarbon crystal.

The change in the electrical conductivity of mesonaphthodianthrene film in oxygen is accelerated if the film is illuminated with visible light. Photooxidation is known to occur with anthracene, tetracene, and some other hydrocarbons when oxygen-containing solutions of these hydrocarbons are illuminated with ultraviolet light (9). The molecular structures of these photooxides are known, an oxygen molecule "bridging" two active positions of each hydrocarbon molecule. Since molecules are closely packed in the crystals of these hydrocarbons, it is hard for an oxygen molecule to penetrate into the crystal to form a photooxide. Thus photooxidation can not take place in the bulk of the crystal, as it is illuminated in the ambient oxygen. On the surface of the crystal, however, photooxidation can occur much more easily. The photoconductivity of anthracene increases remarkably in the presence of oxygen, and has been attributed to the formation of a peroxide layer on the surface of the anthracene crystal (2, 3, 4). A similar effect is expected with crystals of various aromatic hydrocarbons which have reactive positions for oxygen in the molecular structure. The two meso positions of the mesonaphthodianthrene molecule are generally considered to be strongly reactive toward oxygen. The photooxide of this hydrocarbon, however, has not been isolated from the solution illuminated with light (10). This might be due to the fact that the two reactive positions are too far apart

from each other for an oxygen molecule to "bridge" them without considerable strain, thus leading to a "photooxide" so unstable that it can not be isolated. However, this does not exclude the possibility of considerable photooxidation on the surface of the crystal since the photooxide could be stabilized by surface forces. It thus seems that the acceleration of the change in the electrical conductivity in oxygen, caused by the illumination with light, is due to photooxidation. We are not sure if this reaction product is a peroxide or not. Whatever the structure of the reaction product may be, the bond between the oxygen molecule and hydrocarbon molecule must be a loose one, since oxygen molecules can be liberated rather easily. Thus it seems probable that the reaction product is a molecular complex formed between an excited hydrocarbon molecule and an oxygen molecule.

A mesonaphthodianthrone molecule is not markedly reactive to oxygen, no oxygen effect having been detected by electron spin resonance. The presence of the oxygen-sensitive mechanism of conduction in the oxygen-free film of this quinone indicates that the surface state of the crystal of the quinone itself is making an important contribution to the electrical conduction. An oxygen molecule behaves generally as an electron acceptor. Thus, if the semiconductor is p-type, the conductivity would be expected to increase in oxygen. While we do not know the nature of the charge carrier in the semiconduction of this quinone, it appears possible that the conduction associated with the activation energy of 0.43 ev is due to a surface conduction in which the majority of carriers are electrons. While this would be consistent with our experimental results, evidently a good deal more experimental data are needed concerning the very interesting reaction of oxygen with the surfaces of quinones. Some interesting recent papers germane to these problems are listed in References (11, 12, 13, 14).

ACKNOWLEDGMENT

REFERENCES

1. H. PICK and W. WISSMAN. Z. physik. Chem. **138**, 436 (1954).
2. A. G. CHYNOWETH. J. Chem. Phys. **22**, 1029 (1957).
3. A. BREE, D. J. CARSWELL, and L. E. LYONS. J. Chem. Soc. 1728 (1955).
4. T. C. WADDINGTON and W. G. SCHNEIDER. Can. J. Chem. **36**, 789 (1958).
5. A. T. VARTANYAN. J. Phys. Chem. (U.S.S.R.), **22**, 769 (1948).
6. Y. MATSUNAGA. Can. J. Chem. **38**, 323 (1960).
7. H. KURODA and E. A. FLOOD. J. Chem. Phys. **33**, 952 (1960).
8. H. INOKUCHI. Bull. Chem. Soc. Japan, **24**, 222 (1951).
9. CH. DUFRAISSE and I. GILLET. Compt. rend. **225**, 191 (1947).
10. M. G. SAUVAGE. Compt. rend. **225**, 247 (1947).
11. D. BIJL, H. KAINER, and A. C. ROSE-INNES. J. Chem. Phys. **30**, 765 (1959).
12. M. M. LABES, R. SEHR, and M. BOSE. J. Chem. Phys. **33**, 868 (1960).
13. J. KOMMANDEUR and F. R. HALL. J. Chem. Phys. **34**, 129 (1961).
14. L. S. SINGER and J. KOMMANDEUR. J. Chem. Phys. **34**, 133 (1961).

RADIOIODINE EXCHANGE BETWEEN IODOSTEARIC ACID MONOLAYERS AND SUBSTRATE IODIDE. III[1]

J. M. RAMARADHYA[2] AND R. F. ROBERTSON[3]

ABSTRACT

Further studies have been made of the isotopic exchange reaction between monolayers at the air/water interface of I^{131}-α-iodostearic acid and KI substrates. The dependence of the exchange velocity on substrate iodide ion concentration has been examined by employing KCl–KI mixtures of constant over-all molarity to minimize possible variations in film characteristics with substrate salt concentration. The order in substrate I^- ion concentration was found to be fractional at pH 2 and indeterminate at pH 3. The velocity of exchange at all KI concentrations was increased when KCl was added to the substrate. Surface potential measurements showed α-iodostearic acid to have a negative surface potential at high molecular areas which decreased to zero as the film was compressed. The apparent negativity of the surface potential increased as salt was added to the substrate. The surface potential was found to vary with the substrate pH, passing through a maximum between pH 2 and 3. The isotopic exchange velocity and the surface potential were found to be closely related. The variation of the surface potential with time during isotopic exchange has been examined both for monolayers and for collapsed films.

INTRODUCTION

The present investigation is an extension of earlier studies (1, 2) of the homogeneous isotopic exchange reaction

$$CH_3(CH_2)_{15}CHI^*COOH + KI \rightarrow CH_3(CH_2)_{15}CHICOOH + KI^*$$

occurring between I^{131}-labeled α-iodostearic acid, spread as a monolayer at the air/water interface, and iodide ion in the substrate.

In the earlier papers the temperature dependence of the reaction and the possible influence of film characteristics on the exchange rate were reported. The reaction was found to be first-order in surface concentration of film molecules but of indeterminate order in concentration of substrate KI. The impossibility of establishing the order of the exchange reaction in substrate concentration was attributed to changes in the film characteristics of α-iodostearic acid as the concentration of KI in the substrate was varied (1). The influence of pH on the exchange rate was also studied in detail (2). The rate was found to decrease almost 20-fold as the pH of the substrate was varied from 1 to 10 pH units. Between pH 2 and 3 the rate plot passed through a maximum.

In the present paper, further studies are reported on the influence of substrate iodide ion concentration on the exchange reaction, under conditions of constant film characteristics. The surface potential technique of Schulman and Rideal (3) has been employed to study α-iodostearic acid films on various substrates and I^{131}-α-iodostearic acid films during exchange.

EXPERIMENTAL PART

The trough, barriers, and radiochemical counting equipment employed have been described elsewhere (1, 2). The surface balance was the automatic, self-compensating, self-recording, vertical pull instrument described in another paper (4). The experimental

techniques employed were essentially the same as in these earlier publications. However, the following changes in equipment and materials should be noted.

(1) The surface potential measuring equipment.—The air electrode was a 5 mc Po^{210}-plated source obtained from the Commercial Products Division, Atomic Energy of Canada. This electrode was used in conjunction with a standard calomel half-cell (Beckman) dipping into the film-free substrate solution behind a stationary barrier on the trough. The air electrode, when in use, was positioned approximately $\frac{1}{4}$ inch above the film surface. The potential was measured by a Beckman Model G pH meter connected to the electrodes by shielded and grounded leads. The trough was insulated from the supporting stand by a teflon sheet. The outer aluminum casing of the air bath served, when electrically grounded, as a most satisfactory Faraday screen.

(2) Radiochemically tagged I^{131}-α-iodostearic acid.—Some minor modifications in the preparation of I^{131}-α-iodostearic acid resulted in samples of consistently higher specific activity than obtained previously. A solution of 0.02 g of stock α-iodostearic acid in 5 ml of absolute ethanol was placed in the reaction flask described earlier (1), and 10 mc of carrier-free NaI^{131} in 1 ml of water was added to the solution with 2 drops of constant-boiling HCl. This solution was refluxed for $1\frac{1}{2}$–2 hours, allowed to cool, and 50–75 ml of 0.01 M HCl was added. The mixture was left for 10 to 12 hours to permit good crystal growth, filtered on a sintered glass filter, washed with 25 to 50 ml of 0.01 M HCl, and dried by suction for a further 12 hours. The spreading solution was prepared in a 10 ml volumetric flask by dissolving the acid from the filter with warm reagent grade benzene.

(3) Other materials.—The benzene, KCl, and KI employed were of reagent grade. Tests for surface-active contamination by the usual compression and surface pressure technique indicated these chemicals to be suitable for use without further purification. A trace of sodium bisulphite was added in the trough to all KI substrate solutions to remove any iodine formed by air oxidation.

RESULTS

1. The Effect of Substrate KI Concentration on the Isotopic Exchange Rate

Studies of the π–A isotherms of α-iodostearic acid on KI substrates (2) and on KCl substrates indicated that the curves were identical for the two salts at the same substrate concentration. Substrates of KCl–KI mixtures should then give isotherms characteristic of the total substrate molarity and independent of the relative amounts of the two salts present. Isotopic halogen exchange reactions examined on such substrates could be assumed to be studied under conditions of constant film characteristics for any given total substrate molarity.

Solutions were prepared by the addition of the appropriate amounts of dry KI and KCl to distilled water to give two series of substrate solutions. One series was of unit over-all molarity in KCl and KI but 0.25, 0.5, 0.75, and 1.0 M in KI alone and the other, 2 M in over-all molarity but 0.25, 0.5, 0.75, 1.0, 1.5, and 2 M in KI. Exchange reactions were studied on these substrate solutions at 25° C and at pH 2 and 3. The film of α-iodostearic acid was maintained at a constant surface pressure of 4 dynes/cm during the exchange. After the appropriate background corrections were made, the ratio of the initial count rate at time $t = 0$, $C(0)$, to the count rate at time $t = t$, $C(t)$, was determined from the paper trace of the surface count rate against time. A plot of log $C(0)/C(t)$ vs. time was made for each exchange experiment. The typical linear semilogarithmic plots obtained in all these experiments are illustrated in Fig. 1 for the 2 M KI–KCl mixture at
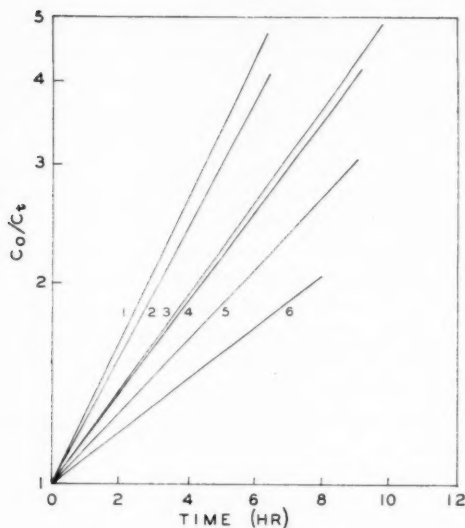
Fig. 1. Semilogarithmic plot of relative count rate against time at 25° C and pH 2 for substrates of variable composition. Curve (1) 2.0 M KI; (2) 1.5 M KI, 0.5 M KCl; (3) 1.0 M KI, 1.0 M KCl; (4) 0.75 M KI, 1.25 M KCl; (5) 0.5 M KI, 1.5 M KCl; (6) 0.25 M KI, 1.75 M KCl.

pH 2. The pseudo-first-order isotopic exchange rate constant, k', as defined previously (1) by the equation

$$k' = \frac{2 \cdot 303}{t(\text{min})} \log \frac{C(0)}{C(t)}$$

was calculated from the slope of each rate plot. The values of k' so obtained are collected in Table I for 1.0 M and 2.0 M substrates respectively.

TABLE I

Variation of the first-order isotopic exchange rate constant with substrate composition
(Temp. 25° C, $\pi = 4$ dynes/cm)

Substrate composition, moles/liter			$10^4 k'$, min^{-1} pH 2	$10^4 k'$, min^{-1} pH 3
KI	KCl	Total		
0.25	0.75	1	11.21	10.62
0.50	0.50	,,	17.70	13.00
0.75	0.25	,,	23.10	19.60
1.00	0.00	,,	24.00	23.90
0.25	1.75	2	15.15	10.25
0.50	1.50	,,	20.50	16.30
0.75	1.25	,,	26.30	25.22
1.0	1.00	,,	27.10	25.60
1.5	1.50	,,	37.18	25.60
2.0	0.00	,,	40.80	34.34

The equation for the specific rate constant, k_s, of the exchange reaction was given in the original paper (1) by the equation

$$V = k_s n \, m^y$$

where n is the surface concentration of monolayer; m, the concentration of I$^-$ in the substrate; and y, the order of the reaction in substrate iodide ion. A plot of log k' vs. log m should be a straight line of slope y. Figure 2 gives these plots for 1 and 2 M sub-
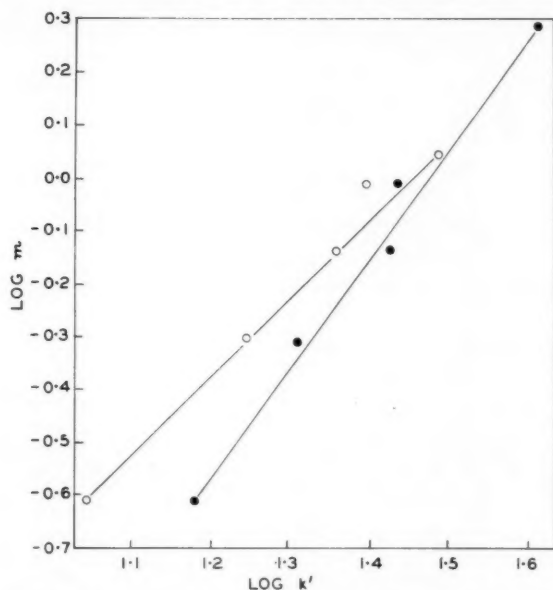

FIG. 2. Plot of logarithm of substrate KI concentration against logarithm of isotopic exchange rate constant. Temperature 25° C, substrate pH 2. Total molarity of substrate in KI and KCl: 1 M, open circles; 2 M, closed circles.

strates at pH 2. A value of y of 0.67 for 1.0 M and 0.48 for 2 M solution is calculated from these slopes. At pH 3 marked deviations from linearity appeared in the plot and calculations of the order could not be made (Table I).

2. The Surface Potential and the Isotopic Exchange Reaction

In an earlier publication (2) it was noted that in the range of pH 2 to pH 5 for 1 M KI substrates, the π–A isotherms of α-iodostearic acid remained essentially constant but the isotopic exchange rate varied markedly. Films of α-iodostearic acid were examined by the surface potential technique in this pH range to elucidate any relation between the surface potential (ΔV) and the rate constant for exchange.

The π–A–ΔV plots for 0.01 M HCl substrates are given in Fig. 3 and the corresponding plots for 1.0 M KI substrates at different values of the pH are given in Fig. 4. At both 17.5° C and 25° C the surface potential of the α-iodostearic acid monolayers on 0.01 M HCl was negative at high molecular areas and approached zero as the film was compressed to smaller areas per molecule. In the range 75 to 80 sq. Å/molecule the plot of ΔV vs. area showed a sudden increase in slope at both temperatures although no change in the
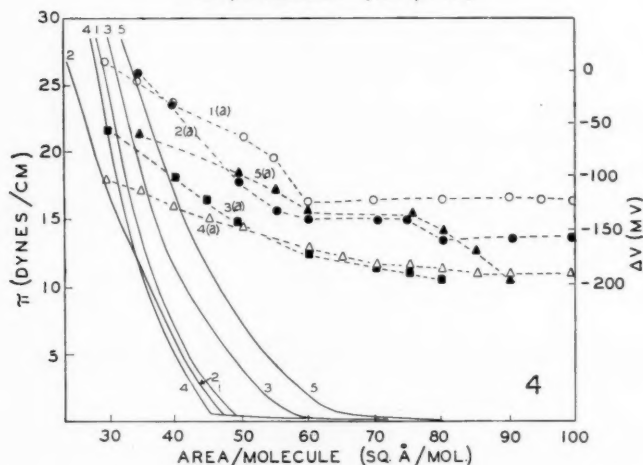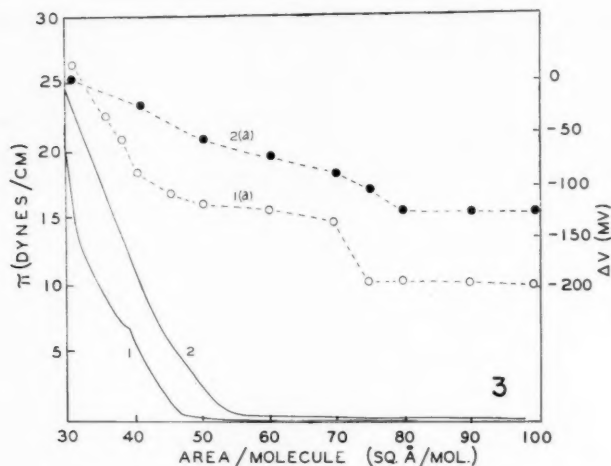
FIG. 3.   Pressure–area isotherms and surface potential – area plots for α-iodostearic acid on 0.01 M HCl substrates. Curve (1) π–A isotherm 17.5° C; (2) π–A isotherm 25° C. Curves 1a, 2a, corresponding ΔV–A plots.

FIG. 4.   Pressure–area isotherms and surface potential – area plots for α-iodostearic acid on 1.0 M KI substrates at 25° C. Curve (1) π–A, pH 1.2; (2) π–A, pH 2.0; (3) π–A, pH 2.8; (4) π–A, pH 3.2; (5) π–A, pH 3.8. Curves 1a, 2a, 3a, 4a, 5a, corresponding ΔV–A plots.

slope of the π–A isotherms could be detected in this region of molecular area. The transition to a liquid condensed film at 40 sq. Å/molecule in the 17.5° isotherm on 0.01 M HCl was markedly reflected in the ΔV-vs.-area plot. The surface potential approached zero very rapidly during compression once the transition point was crossed. The surface potentials of monolayers spread on 1.0 M KI substrates (Fig. 4) were decidedly more negative than for 0.01 M HCl at all values of the pH above 1.2. The same discontinuous change in slope of the ΔV-vs.-area plot was observed for all the isotherms on KI as on 0.01 M HCl except at pH 2.8 and 3.2. The range of area/molecule at which this discontinuity in slope appeared was considerably wider on KI substrates.

The variations of ΔV with pH are given in Fig. 5 for constant molecular areas of 100, 75, 50, and 35 sq. Å/molecule. Surface potential measurements made on I^{131}-α-iodostearic acid monolayers during exchange are given in Fig. 6 for a substrate pH of 2 and at 25 and 17.5° C with the corresponding semilogarithmic plots for the exchange reaction. The surface potential and semilogarithmic plots of an exchange reaction at 25° C in a collapsed film are also included in this figure.
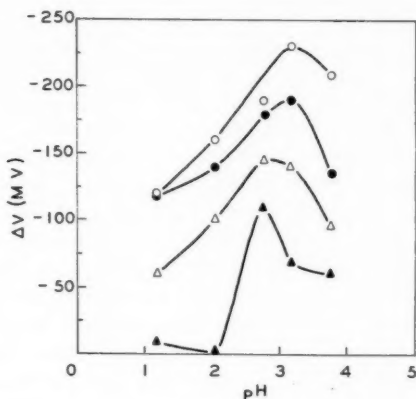

FIG. 5. Surface potential of α-iodostearic acid monolayer on 1 M KI at 25° C as a function of substrate pH at 35 sq. Å/molecule (▲); 50 sq. Å/molecule (△); 75 sq. Å/molecule (●); 100 sq. Å/molecule (○).
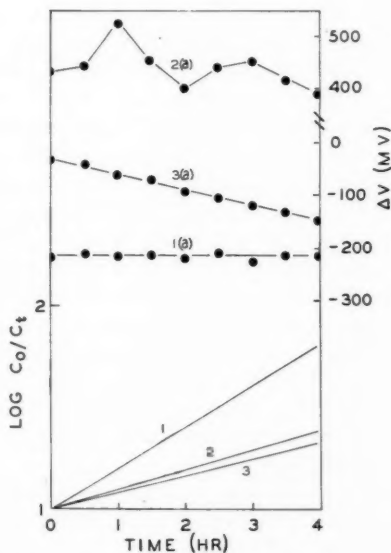

FIG. 6. Semilogarithmic plot of relative surface count rate against time and ΔV–time plot for I^{131}-α-odostearic acid during exchange on 1 M KI at pH 3. Curve (1), $\pi = 4$ dynes/cm, 25° C; (2) collapsed film 25° C; (3) $\pi = 4$ dynes/cm, 17.3° C. Curves 1a, 2a, 3a, corresponding ΔV– time plots.

DISCUSSION

The pseudo-first-order rate constants obtained in the presence of KCl at KI concentrations of 1.0 M or less were consistently higher than those obtained in KI substrates of the same molarity but with no KCl present (1). Since no exchange occurred on KCl substrates alone, the increase in the isotopic exchange rate in the presence of KCl is difficult to explain. Kinetic salt effects which have been reported for other monolayer reactions (5) seem hardly to be applicable to an exchange reaction of the type being studied. The kinetic accessibility of the I^- in the substrate to the I^{131} atom in the α-iodostearic acid monolayer can be assumed to remain constant on substrate solutions of constant total molarity in KCl and KI. No changes occur in the $\pi-A$ isotherms for such substrates and consequently no reorientation of the film molecules would be expected which could change the accessibility and hence the rate of exchange. Possibly the addition of KCl to the substrate may increase the effective concentration of I^- in the surface region below the monolayer. The more rapid exchange on substrates 2 M in total salt concentration for all KI concentrations would tend to support this view.

The failure to determine the order in substrate I^- concentration at pH 3 might be related to the apparent discontinuity found in the Arrhenius plot for the activation energy at this same pH (2). Both the apparent discontinuity in the activation energy and the apparent deviations from linearity at pH 3 in the plots for the reaction order in substrate I^- may have a common origin in undetected minor variations of the pH, since close control of this factor in the monolayer trough is most difficult. It has been shown (2) that the isotopic halogen exchange rate constant becomes markedly sensitive to pH near the maximum of the pH-vs.-k' plot. Since this maximum occurs near pH 3, small changes in the pH could lead to significant variations in the reaction velocity and thus to the results observed in the activation energy and substrate I^- order plots.

The negative value of the surface potential obtained for α-iodostearic acid monolayers on HCl substrates is similar to that obtained by Frumkin (6) with monolayers of ω-bromohexadecanoic acid. This negative surface potential suggests that the negative end of the vertical component of the dipole moment of the molecule is uppermost. The iodine atom is then above the carboxyl group in the monolayer surface. On compressing the iodostearic acid monolayers the relative planes of the iodine atom and carboxyl group, parallel to the water surface, must approach one another on compression as the surface potential approaches zero. At higher molecular areas, the increased negativity of the surface potential as the temperature is lowered from 25° C to 17.5° C (-130 mv to -190 mv at 90 sq. Å/molecule) may be related to a decrease in the relative solubility of the film molecules in the substrate. This effect would tend to force the α-iodine atom to a position in the surface above the carboxyl group.

The surface potential of films on 1.0 M KI substrates at pH 2 (25° C) is more negative at all higher molecular areas than the corresponding curve on HCl substrates but the two curves approach one another as the area per molecule is decreased. The greater degree of negativity on KI substrates might be related to salting out of the film molecules on the addition of electrolyte to the substrate.

The variation of the surface potential with pH on 1.0 M KI substrates would be expected to be associated with the variation in the degree of dissociation of the carboxyl group of the monolayer acid as the acidity of the substrate is decreased. The surface potential would presumably increase as the degree of dissociation increased with numerically increasing pH. In the range of pH studied (1–5 pH units) the change in the

film characteristics of α-iodostearic acid is small, only a slight expansion being detectable (2). Consequently, in the absence of the characteristic marked expansion to a gaseous film which occurs as a monolayer acid approaches complete dissociation, only a small increase in the degree of dissociation must have occurred in traversing this pH range. Since the degree of dissociation can only increase with increasing pH, the maximum of Fig. 5, detectable over a wide range of molecular areas, cannot be accounted for on the basis of the degree of dissociation alone. It must be concluded that the variation of surface potential with pH must arise from other unknown factors as well as the degree of dissociation. That the maximum of Fig. 5 is real seems to be established when the rate constants for isotopic halogen exchange (2) and the present surface potential data are plotted against substrate pH as in Fig. 7. The similarity between the two curves is
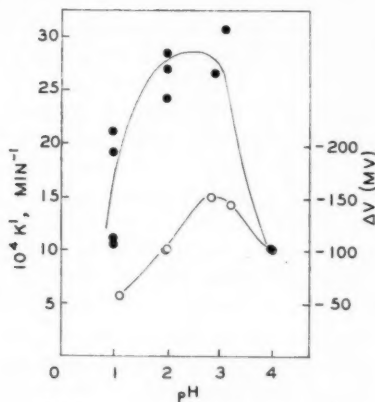

FIG. 7. Plot of isotopic exchange rate constant k' (closed circles) and ΔV (open circles) against substrate pH. Temperature 25° C, molecular area 35 sq. Å.

immediately evident, both the surface potential and the rate constant k' pass through a maximum near pH 3 for the same area/molecule in the monolayer. It seems reasonable to conclude that the variations in surface potential and k' with pH on 1.0 M KI substrates are closely related and are the result of changes in the degree of ionization of the stearic acid derivative and unknown changes, probably of both steric and electrical nature, occurring in the surface region.

The curves of the simultaneous relative surface count rate decrease and surface potential variations with time, taken during the course of an exchange reaction (Fig. 6) with I^{131}-α-iodostearic acid, indicate that at 25° C, pH 3, for a surface pressure of 4 dynes/cm, the surface potential remains essentially constant during the reaction and shows the same value of ΔV as obtained for the inactive films. When the temperature of exchange was lowered to 17.5° C, however, the surface potential was more erratic and slowly increased with time. At this temperature the apparent discontinuities appeared in the Arrhenius plot in earlier experiments and the liquid-intermediate monolayer was present in the π–A isotherms (1, 2). A progressive, slow change in the film characteristics of the monolayer itself might explain the variable surface potential and exchange rate constants in this region of temperature. The surface potential of the collapsed film changed from the negative or zero values found for homogeneous films to large positive

values. This probably indicates the formation of at least one layer of inverted α-iodo-stearic acid molecules above the original monolayer, out of the surface and, as indicated by the markedly reduced exchange rate, no longer available for exchange.

ACKNOWLEDGMENTS

REFERENCES

1. R. F. ROBERTSON, C. A. WINKLER, and S. G. MASON.   Can. J. Chem. **34**, 716 (1956).
2. W. RABINOVITCH, R. F. ROBERTSON, and S. G. MASON.   J. Colloid Sci. **13**, 600 (1958).
3. J. H. SCHULMAN and E. K. RIDEAL.   Proc. Roy. Soc. (London), A, **130**, 259 (1931).
4. W. RABINOVITCH, R. F. ROBERTSON, and S. G. MASON.   Can. J. Chem. **38**, 1881 (1960).
5. J. T. DAVIES and E. K. RIDEAL.   Proc. Roy. Soc. (London), A, **194**, 417 (1948).
6. A. FRUMKIN.   J. Chem. Phys. **4**, 624 (1936).

BACTERIOSTATS

V. THE PREPARATION AND BACTERIOSTATIC PROPERTIES OF AMIDINE DERIVATIVES[1]

D. L. Garmaise,[2] R. W. Kay,[2] R. Gaudry,[3] H. A. Baker,[3] and A. F. McKay[2]

ABSTRACT

A number of polyamidines, N-substituted amidines, and diamidines were prepared for evaluation as bacteriostats. N,N'-Bis-(3,4-dichlorobenzyl)-sebacamidine dihydrochloride was the most active compound prepared in this investigation.

Compounds with unsubstituted amidine groups have been employed as chemotherapeutic agents (1) but there have been relatively few investigations of N-substituted amidines. Some bacteriostatically active N-substituted monoamidines were found (2) to be too toxic for use in guinea pig infections. A series of N,N'-bis-(alkyl)-adipamidines and -sebacamidines has been patented (3) for use in disinfectant compositions, and high bacteriostatic activity has been claimed (4) for a number of polymeric amidines which were obtained by the reaction of diiminoethers with diamines. These polymers were highly toxic (5). The preparation and bacteriostatic evaluation of a number of N-substituted amidines, alkylenediamidines, arylenediacetamidines, and some new polyamidine hydrochlorides are described in the present paper.

The monosubstituted monoamides (Table I) were prepared by reaction of amines with iminoether hydrochlorides, while the condensation of amines with imidic chlorides was the most convenient method for the preparation of N,N'-disubstituted monoamidines (Table I) and N,N',N'',N'''-tetrasubstituted diamidines. The N,N'-bis-(aryl)-adipamidines (Table II) were readily prepared by condensation of adiponitrile with substituted aniline hydrochlorides, but no crystalline products could be obtained from the similar reaction of dinitriles with substituted benzylamine hydrochlorides.

The N,N'-bis-(benzyl)-diamidines (Table II) were prepared by heating dinitriles with benzylamine benzenesulphonic acid salts according to the general procedure described by Oxley and Short (6, 7). Conversion of the diamidine dibenzenesulphonates to the corresponding dihydrochlorides was accomplished by passing the dibenzenesulphonate in methanol through a column of Amberlite IRA-400 resin in the chloride form.

Three polyamidine salts (Table III) were prepared by the self-condensation of ω-aminonitrile hydrochlorides. The polymerization was effected by heating the molten hydrochloride in a nitrogen atmosphere until threads could be drawn from the melt. The polyamidine salts listed in Table IV were prepared in the same manner by heating hexamethylenediamine dihydrochloride with dinitriles. These polyamidine hydrochlorides with the exception of the polymer from 4-cyanobenzylamine hydrochloride, are water-soluble, hygroscopic solids with low melting points. The free polymeric bases could be precipitated from aqueous solutions of the hydrochlorides by addition of alkali.

The minimal growth inhibitory concentrations listed in Table V show that all the amidine derivatives are more effective against gram-positive than gram-negative organisms. In the polymeric series, the polymer derived from 10-cyanodecylamine hydrochloride was the most active. The β-(3,4-dichlorophenyl)-ethyl substituent was somewhat more effective than the 3,4-dichlorobenzyl group in the monoamidine derivatives.

TABLE I

N-Substituted amidines, $3,4\text{-}Cl_2C_6H_3(CH_2)_nC(NR')NHR$

R	R'	n	M.p. (°C)	Yield (%)	Formula	C		H		Cl		N	
						Calc.	Found	Calc.	Found	Calc.	Found	Calc.	Found
3,4-Dichloro-benzyl	H	1	96–98[a]	59	$C_{16}H_{12}Cl_4N_2$	49.75	49.85	3.34	3.33	39.17	39.16	7.74	7.54
			184–185[b]	100[c]	$C_{21}H_{15}Cl_4N_5O_7$	42.66	42.32	2.56	2.80	23.99	23.81	11.85	11.76
β-(3,4-Dichloro-phenyl)-ethyl	H	1	78–80[a]	45.6	$C_{16}H_{14}Cl_4N_2$	51.09	51.32	3.75	3.87	37.71	37.16	7.45	7.18
4-Chlorobenzyl	3,4-Dichloro-benzyl	0	121–123[a]	32.2	$C_{21}H_{16}Cl_5N_2$	53.37	52.98	3.20	3.34	37.52	37.64	5.93	5.91
3,4-Dichloro-benzyl	3,4-Dichloro-benzyl	0	117–118[a]	10.1	$C_{21}H_{14}Cl_6N_2$	49.74	49.54	2.78	2.87	41.95	42.25	5.53	5.59

[a]Crystallized from ether – petroleum ether.
[b]From aqueous ethanol.
[c]Picrate.

TABLE II

N,N'-Disubstituted alkylenediamines, $RNHC(NH)(CH_2)_nC(NH)NHR$

R	n	M.p. (°C)	Yield (%)	Formula	C Calc.	C Found	H Calc.	H Found	Cl Calc.	Cl Found	N Calc.	N Found
4-Chlorophenyl	4	247.5–248 (decomp.)[e]	17.4[k]	$C_{18}H_{22}Cl_4N_4 \cdot H_2O$	47.60	47.80	5.33	5.37	31.23	31.47	12.34	12.49
		179.5–180.5[b]	92.5[l]	$C_{30}H_{26}Cl_2N_{10}O_{14}$	43.86	44.17	3.19	3.31	8.63	8.77	17.08	17.02
3,4-Dichlorophenyl	4	243–244[c] (decomp.)	38.0[k]	$C_{18}H_{20}Cl_6N_4$	42.81	43.06	3.99	4.14	42.11	41.71	11.09	11.50
		181–182[b]	97.7[l]	$C_{20}H_{24}Cl_4N_{10}O_{14}$	40.47	40.80	2.72	2.72	15.93	15.57	15.73	16.05
4-Chlorobenzyl	4	194–196[c]	10.9[m]	$C_{32}H_{36}Cl_2N_4O_6S_2$[m]	54.30	54.34	5.13	5.24	10.03	9.63	7.92	7.83
		204–205[d]	42.0[k]	$C_{26}H_{26}Cl_4N_4 \cdot H_2O$	49.80	50.26	5.85	5.60	20.42	29.31	11.62	11.70
2,4-Dichlorobenzyl	4	197–198[d]	20.9[k]	$C_{22}H_{34}Cl_4N_4O_6S_2$[o]	49.50	49.55	4.41	4.40	18.26	18.45	7.22	7.48
		224–226[f]	80.8[k]	$C_{20}H_{24}Cl_6N_4$	45.06	45.07	4.54	4.41	39.89	39.84	10.51	10.23
3,4-Dichlorobenzyl	4	213.5–215.5[f]	11.4[m]	$C_{22}H_{34}Cl_4N_4O_6S_2$[p]	49.50	49.60	4.41	4.40	18.26	18.44	7.22	7.47
		242–244[f]	85.4[k]	$C_{20}H_{24}Cl_6N_4$	45.06	45.07	4.54	4.40	39.89	39.66	10.51	10.18
3,4-Dichlorobenzyl	6	197.5–198.5[a]	17.9[m]	$C_{34}H_{38}Cl_4N_4O_6S_2$[q]	50.75	50.73	4.76	4.50	17.63	17.59	6.96	7.13
		187–188[f]	88.4[k]	$C_{22}H_{28}Cl_6N_4$	47.09	47.38	5.03	5.15	37.90	37.64	9.98	10.02
3,4-Dichlorobenzyl	8	—[g,i]	68.0[k]	$C_{24}H_{32}Cl_6N_4$	48.92	49.41	5.47	5.73	36.11	35.44	9.50	9.23
3,4-Dichlorobenzyl	10	—[g,i]	54.0[k]	$C_{26}H_{36}Cl_6N_4$	50.58	50.99	5.88	6.07	34.47	34.31	9.07	9.52
3,4-Dichlorobenzyl	12	—[g,i]	61.5[k]	$C_{28}H_{40}Cl_6N_4$	52.11	52.43	6.25	6.57	32.96	32.45	8.68	8.93

[a]Crystallized from methanol-ether.
[b]From ethanol.
[c]From methanol.
[d]From ethanol – ethyl acetate.
[e]From water.
[f]From ethanol-ether.
[g]Non-crystalline solid.
[h]R_f 0.883 using butanol:acetic acid:water (50:40:10) on Whatman No. 1 filter paper.
[i]R_f 0.832.
[j]R_f 0.887.
[k]Dihydrochloride.
[l]Dipicrate.
[m]Dibenzenesulphonate.
[n]Calc.: S, 9.06%; found: S, 8.86%.

[o]Calc.: S, 8.25%; found: S, 7.92%.
[p]Calc.: S, 8.25%; found: S, 8.02%.
[q]Calc.: S, 7.97%; found: S, 7.88%.

TABLE III

Polymers from ω-aminonitrile hydrochlorides

Monomer	M.p. (°C)	Bath temp. (°C)	Time (hr)	Properties of polymer
6-Cyanohexylamine hydrochloride	—	215	1	Water-soluble sticky brown wax
10-Cyanodecylamine hydrochloride	55	223	13	Water-soluble yellow glass
4-Cyanobenzylamine hydrochloride	240–275	270–280	1	Water-soluble red-brown glass

TABLE IV

Polymers from dinitriles and hexamethylenediamine dihydrochloride

Dinitrile	M.p. (°C)	Bath temp. (°C)	Time (hr)	Properties of polymer
Succinonitrile	45–55	190	11	Water-soluble brown glass
Adiponitrile	50[a]	240–260	8	Water-soluble brown glass
Sebaconitrile	70	270	7	Brown glass, forms gel in water
p-Xylylenedicyanide	140	240–260	3	Water-soluble yellow-brown glass
N,N'-Di-(4-cyanobutyl-carbamyl)-hexa-methylenediamine	65	223	9	Water-soluble yellow glass
N,N'-Di-(10-cyanodecyl-carbamyl)-hexa-methylenediamine	90–100	223	9	Pale yellow glass, partially soluble in water

[a]Prepared by Hunt and Kirby (4).

In the alkylenediamidine series, N-aryl substituents were considerably less effective than N-benzyl groups. The 3,4-dichlorobenzyl derivative possessed the highest activity. A similar observation has been made in several other series of compounds (8). The most effective of the alkylenediamidines was N,N'-bis-(3,4-dichlorobenzyl)-sebacamidine dihydrochloride with a minimal growth inhibitory concentration of 1:5,120,000 for *Micrococcus pyogenes* var. *aureus* (penicillin resistant) and 1:10,240,000 for *Sarcina lutea*. Compounds possessing shorter or longer alkylene chains were less active. The introduction of additional 3,4-dichlorobenzyl substituents, as in N,N',N'',N'''-tetrakis-(3,4-dichloro-benzyl)-sebacamidine dihydrochloride, caused a reduction in activity. In the related series of arylenediacetamidines, N,N'-bis-(3,4-dichlorobenzyl)-toluene-2,4-diacetamidine dihydrochloride was found to be highly active.

In general, the diamidines retained a fair degree of their bacteriostatic effectiveness in the presence of 10% serum. The arylenediacetamidine derivative was more sensitive to deactivation by serum protein than the alkylenediamidines. Among the latter, serum deactivation had a leveling effect on the activity of members of the homologous series, and the relationship between chain length and optimum bacteriostatic activity, which was observed in the absence of serum, was no longer apparent.

EXPERIMENTAL[4]

N-(3,4-Dichlorobenzyl)-3,4-dichlorophenylacetamidine

A solution of 3,4-dichlorobenzyl cyanide (20.67 g, 0.11 mole) and anhydrous methanol (3.56 g, 0.11 mole) in anhydrous ether (250 ml) was saturated with hydrogen chloride at 0°. The solution was allowed to stand at 5° for 4 days. Methyl 3,4-dichlorophenyl-acetimidate hydrochloride, m.p. 105° (decomp.), was recovered by filtration, yield 18.0 g (63.6%).

[4]*All melting points are uncorrected. Microanalyses were performed by Micro-Tech Laboratories, Skokie, Ill.*

TABLE V

Bacteriostatic activities (M.I.C., $1/x.10^{-3}$)ᵃ of amidine derivatives

Product	M. pyogenes var. aureus (S)	M. pyogenes var. aureus (R)	Sarcina lutea	Streptococcus faecalis	Escherichia coli No. 198	Aerobacter aerogenes	Salmonella pullorum	Pseudomonas aeruginosa	Proteus mirabilis	Proteus vulgaris
Polymeric hexamethylenesuccinamidine dihydrochloride	1,280	160	160	80	160	20	40	10	20	10
Polymeric hexamethyleneadipamidine dihydrochlorideᵇ	160	160	1,280	40	160	160	160	80	160	80
Polymeric hexamethylenesebacamidine dihydrochloride	320	640	640	1,280	160	40	80	20	20	20
Polymeric hexamethylene p-phenylenediacetamidine dihydrochloride	160	80	80	40	320	80	80	80	160	80
Polymeric 10-cyanodecylamine hydrochloride	1,280	1,280	2,560	1,280	640	80	80	80	160	80
N-(4-Chlorobenzyl)-N'-(3,4-dichlorobenzyl)-3,4-dichlorobenzamidine	160	320	320	160	80	10	10	10	20	10
N,N'-Bis-(3,4-dichlorobenzyl)-3,4-dichlorobenzamidine	160	320	1,280	640	20	10	10	10	20	20
N-(3,4-Dichlorobenzyl)-3,4-trichlorophenylacetamidine	320	320	640	320	320	160	160	20	80	80
N-(β-(3,4-Dichlorophenyl)-ethyl)-3,4-dichlorophenylacetamidine	640	1,280	1,280	320	640	80	80	20	40	40
N,N'-Bis-(4-chlorophenyl)-adipamidine dihydrochloride	10	10	10	10	10	10	10	10	40	10
N,N'-Bis-(3,4-dichlorophenyl)-adipamidine	80	80	80	40	80	20	80	20	10	20
N,N'-Bis-(2,4-dichlorobenzyl)-adipamidine dihydrochloride	80	40	640	20	80	20	10	10	40	40
N,N'-Bis-(3,4-dichlorobenzyl)-adipamidine dihydrochloride	160	100	1,280	40	80	20	20	10	40	20
N,N'-Bis-(3,4-dichlorobenzyl)-suberamidine dihydrochloride	640	320	5,120	160	320	80	40	20	80	80
N,N'-Bis-(3,4-dichlorobenzyl)-sebacamidine dihydrochloride	320	640	5,120	320	160	40	40	20	40	20
In presence of 10% serum	160	160	5,120	40	160	40	40	20	40	20
N,N'-Bis-(3,4-dichlorobenzyl)-dodecanediamidine dihydrochloride	2,560	5,120	10,240	640	640	80	160	40	40	40
In presence of 10% serum	100	160	640	80	160	40	40	10	20	20
N,N'-Bis-(3,4-dichlorobenzyl)-tetradecanediamidine dihydrochloride	2,560	2,560	5,120	2,560	640	40	160	40	80	80
In presence of 10% serum	320	320	1,280	640	160	40	40	40	40	20
N,N',N'',N'''-Tetrakis-(3,4-dichlorobenzyl)-sebacamidine dihydrochloride	2,560	640	2,560	2,560	320	160	160	20	40	40
In presence of 10% serum	320	160	1,280	160	80	40	20	10	20	20
N,N'-Bis-(3,4-dichlorobenzyl)-p-phenylenediacetamidine dihydrochloride	320	160	1,280	1,280	160	40	20	10	20	40
N,N'-Bis-(3,4-dichlorobenzyl)-toluene-2,4-diacetamidine dihydrochloride	320	320	320	40	160	10	20	10	20	10
In presence of 10% serum	2,560	1,280	5,120	640	640	80	160	80	80	40
	80	80	640	20	20	20	20	10	10	10

ᵃMinimal inhibitory concentration determined by serial dilution tube technique, e.g., the value of 1,280 is equivalent to a concentration of 1 part in 1,280,000.
ᵇPrepared by Hunt and Kirby (4).

The iminoether hydrochloride (3.40 g, 0.00134 mole) and 3,4-dichlorobenzylamine (2.34 g, 0.00134 mole) were dissolved in anhydrous methanol (30 ml) and the solution was allowed to stand at room temperature for 4 days. The residue from evaporation of the solution was added to 0.1 N sodium hydroxide solution (147.4 ml) and ether (100 ml). The dried ether extract was concentrated to a small volume and diluted with petroleum ether to give N-(3,4-dichlorobenzyl)-3,4-dichlorophenylacetamidine, m.p. 94–97°, yield 2.86 g (59%). Recrystallization from ether – petroleum ether raised the melting point to 96–98°.

The iminoether hydrochloride on treatment with 2-(3,4-dichlorophenyl)-ethylamine (9) by the above procedure gave N-(β-(3,4-dichlorophenyl)-ethyl)-3,4-dichlorophenyl-acetamidine (Table I).

N-(3,4-Dichlorobenzyl)-3,4-dichlorobenzamide

Sodium hydroxide (8.0 g, 0.20 mole) in water (100 ml) was added dropwise to a stirred mixture of 3,4-dichlorobenzylamine hydrochloride (21.25 g, 0.10 mole) and 3,4-dichloro-benzoyl chloride (20.9 g, 0.10 mole) in water (250 ml) at 25°. After the addition period of 2 hours, the mixture was stirred for 6 hours. The crude product (m.p. 118–123°) was recovered by filtration, yield 28.6 g (82.0%). Crystallization from ethanol raised the melting point to 131–132.5°, yield 21.5 g (61.6%). Anal. Calc. for $C_{14}H_9Cl_4NO$: C, 48.18; H, 2.60; Cl, 40.64; N, 4.01%. Found: C, 48.36; H, 2.65; Cl, 40.65; N, 3.89%.

N,N'-Di-(3,4-dichlorobenzyl)-3,4-dichlorobenzamidine

A solution of N-(3,4-dichlorobenzyl)-3,4-dichlorobenzamide (10.4 g, 0.03 mole) and phosphorus pentachloride (6.24 g, 0.03 mole) in benzene (60 ml) was refluxed for 3 hours. Evaporation of the solvent yielded N-(3,4-dichlorobenzyl)-3,4-dichlorobenzimidic chloride as an oil which gradually solidified, m.p. 83–86°. 3,4-Dichlorobenzylamine (5.3 g, 0.03 mole) in ether (25 ml) was added, and the solution was allowed to stand for 3 days. The precipitate (2.8 g, m.p. 200–220°) was filtered, and the filtrate was shaken with 2 N hydrochloric acid (100 ml), giving an additional precipitate of 4.8 g, m.p. 210–230°. The combined solids were extracted with boiling water (25 ml) and the residue was recrystallized from dimethylformamide (30 ml). N,N'-Di-(3,4-dichlorobenzyl)-3,4-dichlorobenzamidine hydrochloride, m.p. 243–244.5°, was recovered in 15.1% yield (2.3 g).

A sample of the hydrochloride (1.6 g, 0.0032 mole) in dimethylformamide (15 ml) was added to 5% sodium hydroxide solution (100 ml) and chloroform (50 ml). The aqueous layer was extracted with chloroform (2×50 ml) and the combined chloroform extracts were washed with water, dried, and evaporated. The residue (1.3 g), m.p. 92–97°, was crystallized from ether – petroleum ether, giving the free base melting at 117–118°, yield 1.0 g (10.1% based on the amide).

Reaction between the imidic chloride and 4-chlorobenzylamine gave N-(4-chloro-benzyl)-N'-(3,4-dichlorobenzyl)-3,4-dichlorobenzamidine (Table I).

Preparation of Dinitriles

p-Xylylenedicyanide (m.p. 95–97°) was prepared in 60% yield from p-xylylenedi-bromide by the method of Titley (10).

Toluene-2,4-diacetonitrile

2,4-Di-(chloromethyl)-toluene (150 g, 0.79 mole) in ethanol (200 ml) was added, with stirring, to sodium cyanide (100 g, 2.04 moles) in water (90 ml) at 76–80° during a period of 30 minutes. The mixture was refluxed for 2 hours, and then cooled and filtered. Most

of the ethanol was removed by concentration of the filtrate at reduced pressure, and the oily residue was extracted with benzene (200 ml). The benzene layer was dried and evaporated, and the residue was distilled, giving the crude product, b.p. 162–170° at 0.1 mm, yield 91 g (68%).

The distillate was shaken with 50% sulphuric acid (100 ml) for 5 minutes, and the resulting emulsion was extracted with benzene (100 ml). The benzene layer was washed with sodium bicarbonate solution and water, dried, and evaporated. Distillation of the residue yielded the pure product, b.p. 182° at 0.7 mm, m.p. 38–42.5°, yield 64.8 g (49%). Anal. Calc. for $C_{11}H_{10}N_2$: C, 77.65; H, 5.88; N, 16.47%. Found: C, 77.73; H, 6.30; N, 16.43%.

1,12-Dicyanododecane

1,12-Dodecanedicarboxylic acid (20.7 g, 0.08 mole) was added to thionyl chloride (28.6 g, 0.24 mole) in benzene (100 ml) at room temperature. After being allowed to stand for 90 minutes, the solution was refluxed for 3 hours. The solvent and excess thionyl chloride were removed by concentration *in vacuo*, and the dark-brown residue was added dropwise to concentrated aqueous ammonia (67 ml) at 15°. The precipitated 1,12-dodecanedicarboxamide was recovered by filtration, m.p. 182–187°, yield 19.3 g (94.2%). After recrystallization from dimethylformamide, the diamide melted at 186–187°, resolidified, and remelted at 194–197°. Anal. Calc. for $C_{14}H_{28}N_2O_2$: C, 65.58; H, 11.01; N, 10.93%. Found: C, 65.44; H, 10.80; N, 10.79%.

The diamide (15.7 g, 0.061 mole) was refluxed with thionyl chloride (16.0 g, 0.134 mole) in benzene (100 ml) for 7 hours. The solution was evaporated and the residue was distilled, giving 1,12-dicyanododecane, b.p. 151–153° at 0.04 mm, m.p. 35.5–36°, yield 8.5 g (63.3%). Anal. Calc. for $C_{14}H_{24}N_2$: C, 76.31; H, 10.98; N, 12.71%. Found: C, 76.15; H, 10.83; N, 12.52%.

N,N'-Bis-(3,4-dichlorophenyl)-adipamidine Dihydrochloride

A mixture of 3,4-dichloroaniline hydrochloride (9.93 g, 0.05 mole) and adiponitrile 2.71 g, 0.025 mole) was heated to 210°. After 20 minutes at 205–210°, the melt solidified. Crystallization of the solid from hot water yielded material melting at 226–232° (decomp.), yield 8.62 g (68.2%). The pure dihydrochloride melting at 243–244° (decomp.) was obtained by recrystallization from methanol–ether solution, yield 4.82 g (38.0%).

N,N'-Bis-(4-chlorophenyl)-adipamidine dihydrochloride (Table II) was prepared by the same procedure.

N,N'-Bis-(3,4-dichlorobenzyl)-adipamidine

3,4-Dichlorobenzylamine (35.2 g, 0.20 mole) was added to a solution of benzenesulphonic acid (35.2 g, 0.22 mole) in methanol (600 ml). The solution was concentrated to 250 ml. 3,4-Dichlorobenzylamine benzenesulphonate (m.p. 244–248°) crystallized out on standing, yield 50.7 g (75.9%).

3,4-Dichlorobenzylamine benzenesulphonate (47.0 g, 0.141 mole) was stirred with adiponitrile (7.62 g, 0.0705 mole) at 235° for 35 minutes. The mixture was crystallized from methanol (150 ml) yielding some unchanged starting material (15.7 g, m.p. 206–235°). Concentration of the mother liquors yielded the crude product (14.7 g, m.p. 170–199°), which on recrystallization from water (600 ml), gave N,N'-bis-(3,4-dichlorobenzyl)-adipamidine dibenzenesulphonate (6.0 g, 11.4%), m.p. 210–213°. The analytical sample melted at 213.5–215° after recrystallization from methanol–ether solution.

A solution of the dibenzenesulphonate (3.83 g, 0.00493 mole) in methanol (80 ml) was passed through a column of Amberlite IRA-400 resin (50 ml), which had previously

been saturated with chloride ion. The column was washed with methanol (100 ml) and the combined eluates were evaporated, giving N,N'-bis-(3,4-dichlorobenzyl)-adipamidine dihydrochloride, m.p. 241–244°, yield 2.38 g (85.4%). Recrystallization from methanol–ether raised the melting point to 242–244°.

The other N,N'-diaralkyldiamidines described in Table II were prepared by the same method.

N,N'-Bis-(3,4-dichlorobenzyl)-p-phenylenediacetamidine

A mixture of p-xylylenedicyanide (14.3 g, 0.0915 mole) and 3,4-dichlorobenzylamine benzenesulphonate (61.3 g, 0.183 mole) was stirred in a nitrogen atmosphere at 230° for 90 minutes. The cooled reaction mixture was extracted successively with dimethylformamide (50 ml) and boiling methanol (100 ml), giving the product as the dibenzenesulphonic acid salt, m.p. 311–312°, yield 31 g (41%). The analytical sample melted at 313–314° after crystallization from dimethylformamide. Anal. Calc. for $C_{36}H_{34}Cl_4N_4O_6S_2$: C, 52.44; H, 4.16; Cl, 17.20; N, 6.74; S, 7.78%. Found: C, 52.30; H, 4.23; Cl, 17.45; N, 6.98; S, 7.88%.

The dibenzenesulphonate (30.0 g, 0.0364 mole) was dissolved in dimethylformamide (430 ml), and a solution of potassium hydroxide (30 g) in methanol (100 ml) was added. Dilution with water precipitated the product as the free base, m.p. 164–165°, yield 17.2 g (93%). The melting point was raised to 168–169° by recrystallization from dilute ethanol. Anal. Calc. for $C_{24}H_{22}Cl_4N_4$: C, 56.71; H, 4.36; Cl, 27.91; N, 11.02%. Found: C, 56.64; H, 4.68; Cl, 27.70; N, 10.77%.

N,N'-Bis-(3,4-dichlorobenzyl)-toluene-2,4-diacetamidine

Toluene-2,4-diacetonitrile (6.8 g, 0.04 mole) and 3,4-dichlorobenzylamine benzenesulphonate (26.8 g, 0.08 mole) were heated at 210–230° for 3 hours. The cooled mixture on crystallization from methanol and ether gave 8.4 g (31.4%) of unreacted 3,4-dichlorobenzylamine benzenesulphonate. Evaporation of the mother liquors yielded the product as an amorphous solid (yield 22 g, 66%) which gave a single spot, R_f 0.85, when chromatographed with butanol:acetic acid:water (50:40:10). A methanolic solution (200 ml) of the product was passed through a column of Amberlite IRA-400 resin (150 ml) in the chloride form, and the column was washed with methanol (200 ml). Evaporation of the eluate gave the product as the amorphous dihydrochloride (yield 14.7 g, 62%).

A sample of the dihydrochloride (4.5 g, 0.0086 mole) was added to fumaric acid (1.0 g, 0.0086 mole) in ethanol (30 ml). Addition of ether (20 ml) yielded the crystalline fumarate salt, m.p. 170–190°, which was recrystallized from dimethylformamide to a constant melting point of 190.5–193°, yield 1.95 g (35%). Anal. Calc. for $C_{29}H_{28}Cl_4N_4O_4 \cdot H_2O$: C, 53.06; H, 4.61; Cl, 21.61%. Found: C, 53.38; H, 5.13; Cl, 21.04%.

N,N'-Bis-(3,4-dichlorobenzyl)-sebacamide

Sebacyl chloride (23.9 g, 0.10 mole) in benzene (50 ml) was added dropwise to a solution of 3,4-dichlorobenzylamine (35.2 g, 0.20 mole) and pyridine (15.8 g, 0.20 mole) in dry benzene (300 ml) at 15–20° C. The solution was allowed to stand overnight and the precipitate was filtered and washed with water. Recrystallization from methanol gave the pure diamide, melting at 123–124°, resolidifying, and remelting at 135–136°, yield 38.0 g (69.5%). Anal. Calc. for $C_{24}H_{28}Cl_4N_2O_2$: C, 55.62; H, 5.44; Cl, 27.37; N, 5.41%. Found: C, 55.43; H, 5.50; Cl, 27.41; N, 5.37%.

N,N',N'',N'''-Tetrakis-(3,4-dichlorobenzyl)-sebacamidine

N,N'-Bis-(3,4-dichlorobenzyl)-sebacamide (5.18 g, 0.010 mole) was refluxed with phosphorus pentachloride (4.20 g, 0.020 mole) in dry benzene (70 ml) for 3.5 hours. The

benzene solution, after being decanted from the resinous by-products, was added to 3,4-dichlorobenzylamine (6.02 g, 0.040 mole), and the solution was allowed to stand for 2 hours.

The residue obtained on evaporation of the benzene was partitioned between ether (100 ml) and 2 N sodium hydroxide (100 ml). The ether solution was dried and evaporated, and the residue was extracted repeatedly with petroleum ether. The residual oil gave a single spot, R_f 0.93, in a paper chromatogram with the solvent system butanol:acetic acid:water (50:40:10).

The product was dissolved in ethanol (50 ml) and acidified with aqueous hydrochloric acid. Evaporation of the solution yielded the dihydrochloride as an amorphous solid which resisted all attempts at crystallization, yield 3.8 g (42%). Anal. Calc. for $C_{28}H_{40}Cl_{10}N_4$: C, 50.31; H, 4.44; N, 6.18%. Found: C, 49.54; H, 4.75; N, 5.58%.

Polyamidines

A mixture of succinonitrile (3.06 g, 0.382 mole) and hexamethylenediamine dihydrochloride (7.23 g, 0.382 mole) was heated, with stirring, in a nitrogen atmosphere until a homogeneous melt was obtained. Immersion in a bath at 245° for 15 minutes was required to melt the mixture. The bath temperature was lowered to 190° and the heating was continued for 10 hours. The pressure was reduced to 10 mm and the heating was continued for 1 hour. On cooling, the viscous mass solidified to a brown hygroscopic glass melting at 45–55°.

The other polymers described in Tables II and III were prepared in the same manner. In each case the mixture or the aminonitrile hydrochloride was first melted and then heated at the bath temperature noted in the tables until threads could be drawn from the polymeric mass. The pressure was reduced toward the end of the reaction to remove volatile impurities.

REFERENCES

1. H. GILMAN (*Editor*). Organic chemistry. An advanced treatise. Vol. III. John Wiley & Sons, Inc., New York. 1953. p. 486.
2. G. NEWBERRY and W. WEBSTER.   J. Chem. Soc. 738 (1947).
3. M. HUNT and J. E. KIRBY.   U.S. Patent No. 2,364,074 (1944).
4. M. HUNT and J. E. KIRBY.   U.S. Patent No. 2,310,789 (1943).
5. J. F. LONTZ.   U.S. Patent No. 2,310,799 (1943).
6. P. OXLEY and W. F. SHORT.   J. Chem. Soc. 147 (1946).
7. W. F. SHORT and P. OXLEY.   U.S. Patent No. 2,433,489 (1947).
8. A. F. McKAY, D. L. GARMAISE, R. GAUDRY, H. A. BAKER, G. Y. PARIS, R. W. KAY, G. E. JUST, and R. SCHWARTZ.   J. Am. Chem. Soc. **81**, 4328 (1959).
9. A. F. McKAY, D. L. GARMAISE, G. Y. PARIS, S. GELBLUM, and R. RANZ.   Can. J. Chem. **38**, 2042 (1960).
10. A. F. TITLEY.   J. Chem. Soc. 508 (1926).

INORGANIC SALTS DISSOLVED IN NON-AQUEOUS OR IN MIXED SOLVENTS

XIII. VISCOSITY STUDIES OF SnCl₄.5H₂O AND SnCl₂.2H₂O DISSOLVED SEPARATELY AND TOGETHER IN METHANOL – CARBON TETRACHLORIDE[1]

P. A. D. DE MAINE AND E. R. RUSSELL

ABSTRACT

Here is reported evidence from viscosity data for competitive, reversible complex formation between species of Sn(IV) or Sn(II) and Sn(IV) or methanol in methanol – carbon tetrachloride solutions of $SnCl_4.5H_2O$ and $SnCl_2.2H_2O$. Empirical relations between the viscosity parameter and the salt or methanol concentrations are also reported.

INTRODUCTION

Spectrophotometric and conductance data for $SnCl_4.5H_2O$ and $SnCl_2.2H_2O$ dissolved separately (1, 2, 3, 4, 5) and together (6, 7) in methanol or in methanol – carbon tetrachloride have shown that there is competitive, reversible complex formation between Sn(IV) and Sn(II) species, between two Sn(IV) species, between Sn(IV) species and methanol, and between Sn(II) species and methanol. The ratio, R (molar conductance at 45° C/molar conductance at 20° C), is independent of salt concentration for each solvent composition. Interactions between Sn(IV) species and Sn(II) or Sn(IV) species are favored by desolvation of methanolated Sn(IV) and Sn(II) (through elevation of the temperature or increase of the carbon tetrachloride concentration).

Here we report viscosity data for $SnCl_4.5H_2O$ and $SnCl_2.2H_2O$ dissolved separately and together in methanol – carbon tetrachloride at 25° and 45° C. These new data can be interpreted in terms of the four competitive, reversible complex formation modes noted in the preceding paragraph. Thus the spectral, conductance, and viscosity data all lead to the same interpretation.

EXPERIMENTAL

Fisher Spectrograde methanol and carbon tetrachloride were dispensed under an atmosphere of dry nitrogen (dew point less than −60° C). Fisher Certified Reagent Grade $SnCl_4.5H_2O$ and $SnCl_2.2H_2O$ were used without further purification. However analyses for tin and chlorine (4) showed that the actual composition of each salt is within 1% of the theoretical composition.

The techniques for preparation of solutions have been described (1, 6). Viscosities were measured with calibrated Ostwald–Fenske viscometers in thermostated baths at 25° and 45° C. Densities for each solution were calculated from density data for the pure solvents (8) and for tin chloride solutions of the highest concentrations, at both temperatures. In separate experiments we have shown that for methanol and methanol – carbon tetrachloride solutions of tin chlorides, densities calculated on the assumption of additive volumes agree to within 0.35% of actually measured densities over the range of concentrations used in this study.

Duplicated experiments showed that all measurements can be reproduced to better

TABLE I

Salt concentration ranges and composition of the methanol – carbon tetrachloride solvent for which viscosity data were recorded at 25 and 45° C
(All concentrations are moles/liter; in parentheses are the number of different salt concentrations for each range)

	CCl$_4$ concentration									
	0.000	1.029	2.058	3.087	4.116	5.145	6.174	7.203	8.235	9.261
	Salt concentration range									
SnCl$_2$·2H$_2$O	0.080–1.000 (13)	0.080–0.880 (11)	0.080–0.800 (10)	0.080–0.640 (8)	0.080–0.560 (7)	0.080–0.480 (6)	0.080–0.400 (5)	0.080–0.240 (3)	0.080–0.160 (2)	0.080 (1)
SnCl$_4$·5H$_2$O	0.100–1.000 (10)	0.100–0.900 (9)	0.100–0.800 (8)	0.100–0.500 (5)(a)	0.100–0.400 (4)(a)	0.100–0.200 (2)(a)	0.100 (1)(a)	0.100 (1)(a)	(a)	(a)
SnCl$_2$·2H$_2$O +SnCl$_4$·5H$_2$O	0.180–0.900 (5)	0.180–0.900 (5)	0.180–0.720 (4)	0.180–0.540 (3)	0.180–0.540 (3)	0.180–0.360 (2)	0.180–0.360 (2)	0.180 (1)(a)	(a)	(a)

NOTE: a denotes concentrations where systems formed two layers. Reference 4 is a study of these two-layer systems.

than 0.30% with another set of solutions. Table I indicates the ranges of solvent composition and salt concentration over which viscosity data was collected.

RESULTS

In this work we define salt molar viscosity (η_{salt}) thus:

$$\eta_{salt} = (\eta_s - \eta_0)/c = \eta_{sp}\eta_0/c$$

where η_s and η_0 are the measured viscosity coefficients of the solution and solvent respectively, η_{sp} is the specific viscosity coefficient, and c is the salt concentration in moles/liter.

Systems with $SnCl_4.5H_2O$ as Solute

For all salt concentrations and both temperatures, plots of viscosity coefficient versus carbon tetrachloride concentration, for solutions with fixed $SnCl_4.5H_2O$ concentration, are linear (Fig. 1).

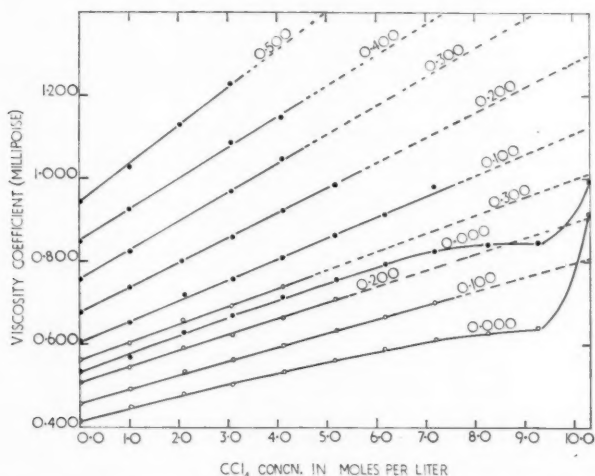FIG. 1. Viscosity coefficient for $SnCl_4.5H_2O$ – methanol – carbon tetrachloride solutions versus carbon tetrachloride concentration (moles/liter) at the indicated temperatures and molar salt concentrations. ● 25° C; ○ 45° C.

Plots of $SnCl_4.5H_2O$ molar viscosity (η_{IV}) versus salt concentration for solutions with fixed solvent composition and temperature are linear with positive slope (Fig. 2). The ratio B (η_{IV} at 25°/η_{IV} at 45° C) appears to be independent of the salt concentration. Average B values and the square-root-mean-square deviations are given in Table II.

Systems with $SnCl_2.2H_2O$ as Solute

Plots of viscosity coefficient for solutions with fixed $SnCl_2.2H_2O$ concentration versus carbon tetrachloride concentration are illustrated in Fig. 3. Here linearity in the plots was observed only for the higher salt concentrations at both temperatures. The $SnCl_2.2H_2O$ molar viscosity (η_{II}) appears to be independent of salt concentration at each temperature and solvent composition. The average η_{II} values do increase on addition of carbon tetrachloride (Table III, data for 25° C).
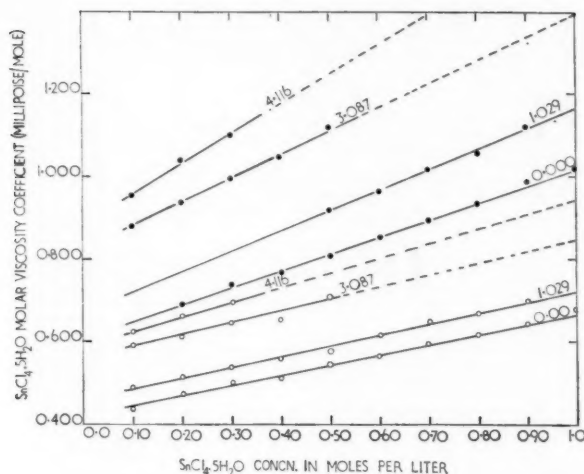
FIG. 2. $SnCl_4.5H_2O$ molar viscosity versus salt concentration at the indicated concentrations of carbon tetrachloride in moles/liter. ● 25° C; ○ 45° C.

TABLE II

Average values for B, B', and B'' (η_{salt} at 25°/η_{salt} at 45° C) for the indicated salts dissolved in methanol – carbon tetrachloride at the indicated concentration

(Below each ratio is given the square-root-mean-square deviation (SRMS) and in parentheses the number of averaged values)

		CCl$_4$ concentration (M)							
		0	1.029	2.058	3.087	4.116	5.145	6.174	7.203
SnCl$_4$.5H$_2$O	B SRMS	1.492 0.024 (7)	1.595 0.019 (8)	1.534 0.024 (4)	1.567 0.031 (4)	1.560 0.022 (3)	1.535 — (1)		
SnCl$_2$.2H$_2$O	B' SRMS	1.460 0.022 (12)	1.582 0.046 (8)	1.556 0.023 (7)	1.493 0.026 (5)	1.519 0.016 (4)	1.514 0.019 (4)	1.389 0.024 (3)	1.450 0.022 (2)
SnCl$_4$.5H$_2$O +SnCl$_2$.2H$_2$O	B'' SRMS	1.496 0.015 (4)	1.581 0.026 (4)	1.563 0.036 (4)	1.545 0.006 (2)	1.555 0.022 (3)	1.538 0.011 (2)	1.586 — (1)	

The ratio B' (η_{II} at 25°/η_{II} at 45° C) is independent of salt concentration for each solvent composition. B' does depend on solvent composition. Table II lists average B' values together with square-root-mean-square deviations and the number of values averaged.

Systems with SnCl$_4$.5H$_2$O and SnCl$_2$.2H$_2$O as Solute

For solutions with a constant total salt concentration, plots of viscosity coefficient versus carbon tetrachloride concentration are similar in form to the plots in Fig. 3. The increase in measured viscosity coefficient ($\eta_s - \eta_o$) on addition of the mixed salts to solvents of fixed composition and temperature is noted in Table IV. Also given are the sums of increments of viscosity for separate solutions of each salt at the concentrations and temperature of the corresponding mixed-salt system in the same solvent.

TABLE III

Salt molar viscosity values at 25° C for $SnCl_2 \cdot 2H_2O$ dissolved in methanol – carbon tetrachloride at the indicated carbon tetrachloride concentrations
(Average values and the square-root-mean-square deviations are given. Values not included in the average are denoted with a prime)

$SnCl_2 \cdot 2H_2O$ concn. (M)	CCl_4 concentration (M)									
	0	1.029	2.058	3.087	4.116	5.145	6.174	7.203	8.235	9.261
0.080	0.263'	—	—	0.375	0.400	—	0.463	0.425'	0.580	0.625
0.160	0.294	0.388'	—	0.363	0.388	0.431	0.406'	0.506	0.581	
0.240	0.283	0.362	—	0.354	0.396	0.421	0.462	0.500		
0.320	0.284	0.347	0.319	0.372	0.394	—	0.447			
0.400	0.283	0.343	0.333	0.373	0.422	0.447	0.490			
0.480	0.281	0.340	0.335	0.373	0.414	0.445				
0.560	0.286	0.344	0.334	0.386	0.411					
0.640	0.292	0.344	0.347	0.387						
0.720	0.294	0.340	0.348							
0.800	0.293	0.345	0.354							
0.880	0.300	0.353								
0.960	0.303'									
1.000	0.308'									
Average value	0.287	0.346	0.342	0.373	0.404	0.436	0.465	0.503	0.581	0.625
SRMS	0.005	0.007	0.008	0.010	0.014	0.011	0.015	0.003	—	—

TABLE IV

Increase in measured viscosity coefficient, $(\eta_s - \eta_0)_M$, and increase in calculated viscosity coefficient, $(\eta_s - \eta_0)_C$, for systems containing both $SnCl_4 \cdot 5H_2O$ and $SnCl_2 \cdot 2H_2O$ dissolved in methanol – carbon tetrachloride

(Carbon tetrachloride and salt concentrations are indicated as moles/liter values. The calculated value is underlined in cases where it is larger than the measured value)

	Sn(IV) concn.	Sn(II) concn.		Carbon tetrachloride concentration												
			0.000		1.029		2.058		3.087		4.116		5.145		6.174	
			Temperature													
			25°C	45°C	25°C	45°C	25°C	45°C	25°C	45°C	25°C	45°C	25°C	45°C	25°C	45°C
0.100	0.080	$(\eta_s-\eta_0)_M$	0.089	0.065	0.114	0.066	0.103	0.067	0.123	0.085	0.131	0.086	0.145	0.095	0.166	0.105
		$(\eta_s-\eta_0)_C$	0.089	0.059	0.120	0.066	0.114	0.069	0.118	0.084	0.127	0.084	0.144	_0.098_	0.157	0.098
0.200	0.160	$(\eta_s-\eta_0)_M$	0.190	0.129	0.221	0.140	0.229	0.142	0.257	0.167	0.281	0.178	0.321	0.208		
		$(\eta_s-\eta_0)_C$	0.185	0.125	_0.230_	0.134	0.216	0.144	0.245	0.162	0.270	0.175	0.299	0.192		
0.300	0.240	$(\eta_s-\eta_0)_M$	0.302	0.201	0.353	0.229	0.360	0.230	0.408	0.263	0.408	0.291				
		$(\eta_s-\eta_0)_C$	0.290	0.196	0.342	0.208	_0.400_	0.229	0.384	0.251	_0.425_	0.274				
0.400	0.320	$(\eta_s-\eta_0)_M$	0.417	0.279	0.486	0.305	0.496	0.327								
		$(\eta_s-\eta_0)_C$	0.399	0.268	0.469	0.293	_—_	0.307								
0.500	0.400	$(\eta_s-\eta_0)_M$	0.561	0.370	0.642	0.399										
		$(\eta_s-\eta_0)_C$	0.517	0.349	0.597	0.364										
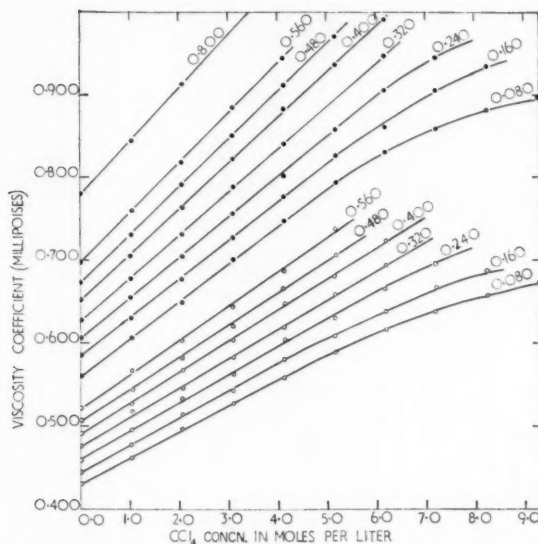
FIG. 3. Viscosity coefficient for $SnCl_2.2H_2O$ – methanol – carbon tetrachloride systems versus concentration of carbon tetrachloride at the indicated temperatures and salt concentrations (moles/liter). ● 25° C; ○ 45° C.

DISCUSSION

Acceptance of the hypothesis that partial reversible association of either covalent or ionic species will lead to a corresponding increase in the molar viscosity of the salt permits an analysis of the new viscosity data which are consistent with earlier conclusions from spectrophotometric and conductance data for the separate and mixed $SnCl_4.5H_2O$ and $SnCl_2.2H_2O$ – methanol – carbon tetrachloride systems. The hypothesis can be justified upon careful consideration of the Stokes' viscosity equation.

Systems with $SnCl_4.5H_2O$ as Solute

The linear dependence of the $SnCl_4.5H_2O$ molar viscosity on salt concentration for solutions with fixed solvent composition and temperature (Fig. 2) may be explained with the supposition that partial reversible dimerization of covalent tin(IV) species occur together with reversible methanolysis of monomeric tin(IV) species. Addition of carbon tetrachloride leads to partial demethanolysis of the monomeric species and a consequent increase in the concentration of the dimeric form. Thus the salt molar viscosity coefficient increases. The increase in positive slope of the straight-line plots in Fig. 2 on addition of carbon tetrachloride supports the competitive dimerization–methanolysis reaction invoked to explain spectrophotometric (1) and conductance (3, 5) data for this system.

Systems with $SnCl_2.2H_2O$ as Solute

As $SnCl_2.2H_2O$ molar viscosity (Table III) is independent of salt concentration for solutions of fixed solvent composition and temperature, partial reversible polymerization of Sn(II) species cannot be significant. There is reversible methanolysis of Sn(II) species. These same conclusions were obtained from spectral (1) and conductance data (3, 5). The gradual increase in the $SnCl_2.2H_2O$ molar viscosity on addition of carbon tetrachloride (Table III) indicates that ion-pair formation and demethanolation may both contribute to the salt molar viscosity.

Systems with $SnCl_4.5H_2O$ and $SnCl_2.2H_2O$ as Solute

If the interaction between tin(IV) and tin(II) species occurs only after demethanolation of the species, the measured $(\eta_s - \eta_o)$ should be greater than the corresponding value calculated with values for the salts in separate solutions. The difference should increase with increased total salt or carbon tetrachloride concentration. Data in Table IV confirm these predictions. Experiments for which the situation is reversed occur because of the relatively small salt molar concentrations and consequent greater experimental error.

Temperature Dependence of Salt Molar Viscosity

As the ratios B and B' are independent of salt concentration for fixed solvent composition for each salt system (Table II) it seems that the salt species in solution behave as Arrhenius–Guzman liquids (9).

ACKNOWLEDGMENT

REFERENCES

1. M. M. DE MAINE and P. A. D. DE MAINE. J. Inorg. & Nuclear Chem. **11**, 13 (1959).
2. P. A. D. DE MAINE. J. Inorg. & Nuclear Chem. **14**, 262 (1960).
3. P. A. D. DE MAINE, M. M. DE MAINE, and G. E. McALONIE. J. Inorg. & Nuclear Chem. **14**, 268 (1960).
4. P. A. D. DE MAINE and M. M. DE MAINE. J. Inorg. & Nuclear Chem. **14**, 142 (1960).
5. P. A. D. DE MAINE and E. J. WALSH. J. Inorg. & Nuclear Chem. In press.
6. P. A. D. DE MAINE and M. M. DE MAINE. J. Inorg. & Nuclear Chem. **11**, 144 (1959).
7. P. A. D. DE MAINE, G. E. McALONIE, and M. M. DE MAINE. J. Inorg. & Nuclear Chem. **14**, 273 (1960).
8. INTERNATIONAL CRITICAL TABLES. McGraw-Hill Book Co., Inc., New York. 1926.
9. S. GLASSTONE. Textbook of physical chemistry. 2nd ed. D. Van Nostrand Company, Inc., New York. 1946.

REARRANGEMENT STUDIES WITH C[14]

## XI. THE FORMOLYSIS OF 2-PHENYLETHYL-1-C[14] p-TOLUENESULPHONATE WITH OR WITHOUT ADDED SODIUM p-TOLUENESULPHONATE-S[35] [1]

J. W. CLAYTON[2] AND C. C. LEE

ABSTRACT

The formolysis of 0.350 M 2-phenylethyl-1-C[14] p-toluenesulphonate (I) was carried out at $74 \pm 0.2°$ C with or without the presence of an equimolar amount of sodium p-toluenesulphonate-S[35] (III). The over-all first-order rate constant, k_1, was found to be 2.6×10^{-5} sec^{-1} and 3.0×10^{-5} sec^{-1}, respectively, for the reaction with and without added III. The determination of the degrees of rearrangement of the C[14]-labeled atoms from the C-1 to the C-2 positions in the 2-phenylethyl p-toluenesulphonate (I_r) recovered from the reaction mixture at various reaction times permitted the evaluation of k^{14}, the rate of return from ionic intermediates to covalent bonding. Using the experimental data, it was possible to calculate k_s and k_Δ, the rates, respectively, for the anchimerically unassisted and assisted solvolysis. As expected, formolysis of I proceeded principally by the anchimerically assisted process. Calculations also showed that the fraction of the anchimerically assisted ionization returning to covalent bonding was about 15% for the reaction in the presence of III, while in the absence of III, the return was about 9%. For the formolysis of I in the presence of III, the extents of incorporation of S[35] in the recovered sulphonate I_r were also determined. The S[35] incorporation in I_r, when considered in conjunction with the C[14] rearrangement in I_r, led to the conclusion that the return from ionic intermediates to covalent bonding during the formolysis of I included both internal and external returns, the extent of external return being the greater of the two.

INTRODUCTION

In earlier publications (1, 2), isotope position rearrangements observed in the solvolysis of 2-phenylethyl-1-C[14] p-toluenesulphonate (I) under various conditions were reported. When acetolysis and formolysis of I were interrupted at about 50% completion, the rearrangement of C[14]-labeled atoms from the C-1 to C-2 positions in the recovered 2-phenylethyl-x-C[14] p-toluenesulphonate (I_r) indicated some return to covalent bonding through the intermediate ethylphenonium ion (II) or its equivalent. Solvolysis of I
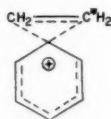
(II)

in the presence of sodium p-toluenesulphonate-S[35] (III) made possible the simultaneous determinations of C[14] rearrangement and S[35] incorporation in the sulphonate I_r recovered from the partially solvolyzed mixture. The data obtained for formolysis (2) indicated that some of the p-toluenesulphonate anions involved in the return to give the isotopically rearranged 2-phenylethyl-2-C[14] p-toluenesulphonate were derived from an intramolecular process, thus pointing to the occurrence of some internal return from an intimate ion pair (3–6) during the formolysis of I.

A drawback in the earlier work (1, 2) has been a lack of any concurrent kinetic data for consideration in conjunction with the observed C^{14} rearrangement and S^{35} exchange. In the present study, the formolysis of I was carried out at 74° C with or without the presence of an equimolar amount of III. At various stages of reaction, the rearrangements of the C^{14}-labeled atoms from the C-1 to C-2 positions were determined in the product, 2-phenylethyl-x-C^{14} formate (IV), and in the 2-phenylethyl-x-C^{14} p-toluenesulphonate (I_r) recovered from the reaction mixture. For the formolysis in the presence of III, the incorporations of S^{35} in I_r were also measured. Concurrent kinetic studies were made by potentiometric titration of the p-toluenesulphonic acid liberated, by isotope dilution of the product, IV, that was formed, and by isotope dilution of the reactant, I_r, that remained.

METHODS AND RESULTS

Formolysis of 2-Phenylethyl-1-C^{14} p-Toluenesulphonate (I) without Added Sodium
  p-Toluenesulphonate-S^{35} (III)

The reaction was carried out in an all-glass apparatus. The reaction vessel of about 75-ml capacity was provided with a cold-finger condenser at the top and a drain with stopcock at the bottom. The vessel was enclosed in a pyrex jacket which was fitted with a reflux condenser and connected to a pot of boiling liquid. The vapor from the boiling liquid heated the reaction mixture and maintained a constant temperature. The boiling liquid used in the present work was ethyl acetate, giving a jacket temperature of $74\pm0.2°$ C for all experiments.

Fifty-milliliter portions of 0.350 M solution of I in anhydrous formic acid were heated in the reaction vessel at $74\pm0.2°$ C for various lengths of time. Each experiment was stopped by draining the reaction mixture into an ice-cooled receiver. A 2-ml aliquot was pipetted into dry acetic acid for potentiometric titration of the liberated p-toluenesulphonic acid (7). A larger aliquot (40 ml) was added to ice water. Known weights of ordinary 2-phenylethyl formate and 2-phenylethyl p-toluenesulphonate were added as carriers. The diluted reaction product (IV) and remaining reactant (I_r) were isolated as

TABLE I

Date from the formolysis of 0.350 M 2-phenylethyl-1-C^{14} p-toluenesulphonate (I) at $74\pm0.2°$ C with no added salt

Reaction time (min)	From titration HOTs	From isotope dilution:		Corrected‡ initial concn. a (mole/l.)	Mean value of $(a-x)$ (mole/l.)	% C^{14} rearrangement from C-1 to C-2	
		IV*	I_r†			In IV*	In I_r†
51	0.035	0.034	—	0.350	0.315	45.9	0.17
167	0.103	0.104	—	0.351	0.247	45.0	0.76
275	—	0.149	0.199	0.352	0.201	43.9	1.83
600	0.245	0.236	0.131	0.354	0.119	46.0	3.37
600	0.244	0.235	0.136	0.354	0.122	46.1	3.30
900	0.293	0.275	0.073	0.355	0.071	—	5.78
1155	0.320	0.327	0.043	0.357	0.036	44.8	8.60
1200	0.317	—	0.043	0.357	0.041	45.0	8.88
						45.2§	

*IV is the formolysis product, 2-phenylethyl-x-C^{14} formate.
†I_r is the recovered reactant, 2-phenylethyl-x-C^{14} p-toluenesulphonate.
‡Corrected for decrease in volume due to decomposition of HCOOH.
§Mean value.

described previously (2). By isotope dilution calculations, the concentrations of IV and I_r were then ascertained. The results are tabulated in Table I.

Let a be the initial concentration of I, x the concentration at time t of the products, p-toluenesulphonic acid and IV, then $(a-x)$ would be the concentration of the recovered reactant I_r. From the titration and isotope dilution data, three separate values of $(a-x)$ could be calculated. In these calculations, a small correction on a was made because prolonged heating caused slight decreases in volume due to decomposition of the formic acid. For example, one of the reactions, stopped at a reaction time of 600 minutes, showed, by titration, a p-toluenesulphonic acid concentration of 0.245 M. From an independent trial, heating of the formolysis mixture at $74\pm0.2°$ C for 600 minutes caused a decrease in volume from 500 to 494 ml. The effective value of a for the aliquot titrated at 600 minutes of reaction time would be $(500/494)\times0.350 = 0.354$ M. Hence $(a-x)$ from potentiometric titration was $0.354-0.245 = 0.109$ M. Similarly, isotope dilution calculations showed that the concentration of IV was 0.236 M. Thus $(a-x)$ would be 0.354 $-0.236 = 0.118$ M. Again from isotope dilution, the concentration of I_r was 0.131 M. Correcting for the decrease in volume, $(a-x)$ would be $(0.350/0.354)\times0.131 = 0.129$ M. The mean value for $(a-x)$ is therefore $(0.109+0.118+0.129)/3 = 0.119$ M. Such mean values of $(a-x)$ corresponding to various reaction times are also given in Table I. From a semilogarithmic plot of the mean $(a-x)$ values vs. t (Fig. 1), a straight line was obtained
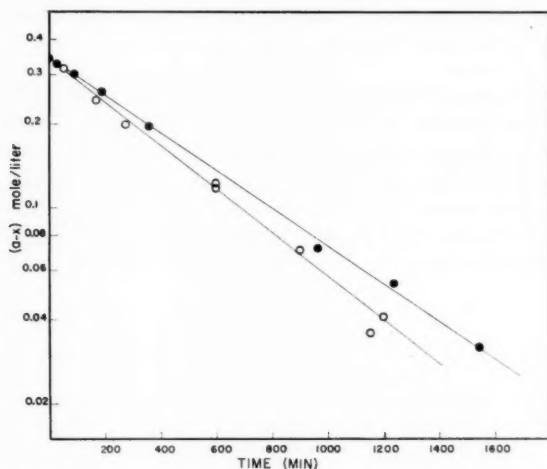

FIG. 1. Rate of formolysis of 2-phenylethyl-1-C^{14} p-toluenesulphonate. Open and closed circles, respectively, represent reaction without and with added sodium p-toluenesulphonate-S^{35}.

indicating a first-order reaction. The first-order specific rate constant, k_1, derived from Fig. 1 is 3.0×10^{-5} sec^{-1}.*

Besides the isotope dilution studies, the rearrangements of the C^{14} label from C-1 to C-2 were determined in the recovered reactant I_r, and in the product IV (2). Treatment of I_r with sodium iodide in acetone gave 2-phenylethyl-x-C^{14} iodide which was oxidized

*Winstein and co-workers (8) reported a k_1 of 3.59×10^{-5} sec^{-1} at $74.62°$ C for 0.074 M initial concentration of the sulphonate. The agreement appears satisfactory since other data given by these authors (8) showed that at a given temperature, an increase in initial concentration decreased k_1.

with potassium permanganate (1) to yield benzoic acid whose activity gave a measure of the C^{14} content in the C-2 position of I$_r$. For the reaction product IV, alkaline permanganate oxidation also yielded benzoic acid whose activity showed the degree of rearrangement of C^{14} to the C-2 position of IV. The C^{14} rearrangements in I$_r$ and IV corresponding to various reaction times are included in Table I.

Formolysis of 2-Phenylethyl-1-C^{14} p-Toluenesulphonate (I) with Added Sodium p-Toluenesulphonate-S^{35} (III)

p-Toluenesulphonic acid-S^{35} was prepared by sulphonation of toluene with concentrated sulphuric acid containing S^{35} (2). Instead of a simple neutralization as a means of obtaining the sodium salt (2), the following series of reactions was used to synthesize III so as to eliminate any possible presence of impurities. p-Toluenesulphonic acid was converted to the sulphonyl chloride. Reaction of the latter with ethanol in pyridine (9) gave ethyl p-toluenesulphonate-S^{35}, which, in turn, was treated with sodium iodide in acetone to give the desired sodium salt, III.

The formolysis was carried out in a reaction vessel of about 600-ml capacity enclosed in a pyrex jacket as described earlier. Five hundred milliliters of anhydrous formic acid solution, 0.350 M in I and in III, was heated in the reaction vessel by the vapor of refluxing ethyl acetate. At zero time, when the jacket temperature first reached 74±0.2° C, and at various time intervals thereafter, aliquots of the reaction mixture were withdrawn for potentiometric titrations of p-toluenesulphonic acid, for isotope dilution determinations of the concentrations of I$_r$ and IV, and for the measurements of C^{14} rearrangement in I$_r$ and IV as outlined in the previous section. In addition, the degrees of incorporation of S^{35} in the various samples of recovered reactant I$_r$ were measured. The procedure (2) was based on the treatment of I$_r$ with sodium iodide in acetone, which gave, besides 2-phenylethyl-x-C^{14} iodide, sodium p-toluenesulphonate whose S^{35} content represented the amount of S^{35} incorporated in I$_r$. The results obtained from formolysis of I in the presence of an equimolar amount of III are summarized in Table II. A semilogarithmic

TABLE II

Data from formolysis of 0.350 M 2-phenylethyl-1-C^{14} p-toluenesulphonate (I) at 74±0.2° C with the presence of 0.350 M sodium p-toluenesulphonate-S^{35} (III)

Reaction time (min)	Mean value of $(a-x)^*$ (mole/l.)	Extent of reaction (%)	% C^{14} rearrangement from C-1 to C-2		% S^{35} incorporated in I$_r$‖	Calc. % S^{35} in I$_r$ for external return
			In IV†	In I$_r$‡		
0	0.347	0.9	—	0.16	—	—
31	0.329	6.0	—	0.47	0.78	0.91
92	0.301	14.0	42.8	1.20	2.22	2.24
186	0.260	25.8	48.2	2.52	4.28	4.46
357	0.197	43.8	48.2	4.15	6.79	6.81
965	0.072	79.4	48.4	10.3	14.3	14.7
1238	0.054	84.6	46.8	13.6	15.3	19.1
1543	0.032	90.8	46.8	16.8	18.6	23.1
			46.9§			

*Mean of two or three values calculated from the concentration of p-toluenesulphonic acid determined by titration; the concentration 2-phenylethyl-x-C^{14} formate and the concentration 2-phenylethyl-x-C^{14} p-toluenesulphonate determined by isotope dilution.
†IV is the formolysis product, 2-phenylethyl-x-C^{14} formate.
‡I$_r$ is the recovered reactant, 2-phenylethyl-x-C^{14} p-toluenesulphonate.
§Mean value.
‖(Specific activity of sodium p-toluenesulphonate-S^{35} derived from I$_r$/specific activity of sodium p-toluenesulphonate-S^{35} added to the reaction mixture)×100. The specific activity of the added sodium p-toluenesulphonate-S^{35} is about 4000 c.p.m. per infinitely thick sample counted.

plot of $(a-x)$ vs. t (Fig. 1) also gave a straight line from which k_1 was calculated to be 2.6×10^{-5} sec^{-1}.

DISCUSSION

With reference to the results tabulated in Tables I and II, the fact that there was rearrangement of the C^{14}-labeled atoms from the C-1 to C-2 positions in every sample of 2-phenylethyl-x-C^{14} p-toluenesulphonate (I_r) recovered from partially solvolyzed reaction mixtures definitely confirmed the earlier conclusion (2) that there was some return to covalent bonding involving an intermediate ethylphenonium ion (II) or its equivalent. The C^{14} rearrangement in I_r could be regarded as a simple isotopic exchange reaction, the rate of exchange being proportional to $Y_\infty - Y$, where Y is the fraction exchanged at time t, and Y_∞ the fraction exchanged at infinite time. This treatment has been applied by Jenny and Winstein (6) in the consideration of data from the solvolysis of 2-p-methoxyphenylethyl-1-C^{14} p-toluenesulphonate.

Thus

$$[1] \qquad \frac{d(\%\ \mathrm{C_2}^{14})}{dt} = k^{14}(\%\ \mathrm{C_{2\infty}}^{14} - \%\ \mathrm{C_2}^{14})$$

where $\%\ \mathrm{C_2}^{14}$ and $\%\ \mathrm{C_{2\infty}}^{14}$ are, respectively, percentage rearrangement of C^{14} to C-2 at time t and at infinite time. Using the maximum rearrangement of 50% as $\%\ \mathrm{C_{2\infty}}^{14}$, integration gave

$$[2] \qquad k^{14}t = 2.303 \log \frac{50}{50 - \%\ \mathrm{C_2}^{14}} .$$

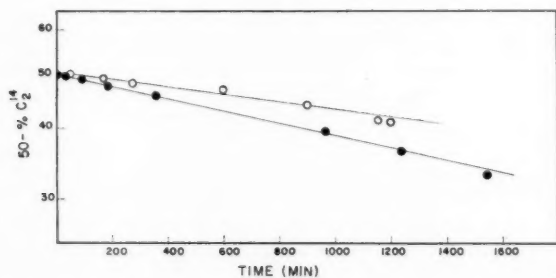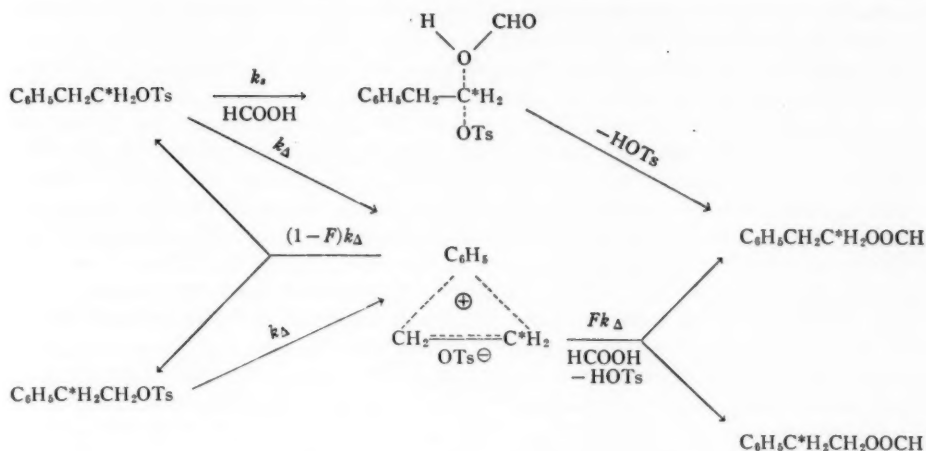From semilogarithmic plots of $50 - \%\ \mathrm{C_2}^{14}$ vs. t (Fig. 2), k^{14} could be evaluated. Values

FIG. 2. Rate of C^{14} rearrangement in 2-phenylethyl p-toluenesulphonate recovered from partially solvolyzed mixtures. Open and closed circles, respectively, represent formolysis without and with added sodium p-toluenesulphonate-S^{35}.

of 4.2×10^{-6} sec^{-1} and 2.5×10^{-6} sec^{-1} were obtained, respectively, for k^{14} for formolysis of I with and without the presence of an equimolar quantity of III.

Using the symbolism of Winstein, with k_s and k_Δ designating, respectively, the anchimerically unassisted and assisted solvolysis, the following scheme may be written:

$$
\begin{array}{c}
\text{H} \qquad \text{CHO} \\
\diagdown \; | \; \diagup \\
\text{O} \\
| \\
\text{C}_6\text{H}_5\text{CH}_2\text{-}\overset{}{\text{C}^*}\text{H}_2 \\
| \\
\text{OTs}
\end{array}
$$

$$
\text{C}_6\text{H}_5\text{CH}_2\text{C}^*\text{H}_2\text{OTs} \quad \xrightarrow[\text{HCOOH}]{k_s} \quad
$$

k_Δ

$-\text{HOTs}$

$\text{C}_6\text{H}_5\text{CH}_2\text{C}^*\text{H}_2\text{OOCH}$

$(1-F)k_\Delta$

$$
\begin{array}{c}
\text{C}_6\text{H}_5 \\
\oplus \\
\text{CH}_2 \text{------} \text{C}^*\text{H}_2 \\
\text{OTs}^\ominus
\end{array}
$$

k_Δ

Fk_Δ

HCOOH
$-\text{HOTs}$

$\text{C}_6\text{H}_5\text{C}^*\text{H}_2\text{CH}_2\text{OTs}$

$\text{C}_6\text{H}_5\text{C}^*\text{H}_2\text{CH}_2\text{OOCH}$

In this scheme, F is that fraction of the anchimerically assisted ionization which leads to solvolysis products, and $(1-F)$ is that fraction which returns to covalent bonding. With the aid of equations [3], [4], and [5], k_s, k_Δ, and F can be calculated (6). The results, together with values of k_1 and k^{14} derived from Figs. 1 and 2, are summarized in Table III.

[3] $$k_1 = Fk_\Delta + k_s$$

[4] $$k^{14} = (1-F)k_\Delta$$

[5] $$\frac{k_\Delta}{k_s} = \frac{\text{mean \% rearrangement in formate IV}}{50 - \text{mean \% rearrangement in formate IV}}$$

TABLE III

Summary of rate data for the formolysis of 2-phenylethyl-1-C14
p-toluenesulphonate (I) with or without the presence of an equimolar
amount of sodium p-toluenesulphonate-S35 (III)

NaOTs-S35	$10^5 k_1$ (sec^{-1})	$10^5 k^{14}$ (sec^{-1})	$10^5 k_s$ (sec^{-1})	$10^5 k_\Delta$ (sec^{-1})	F
None	3.0	0.25	0.4	2.9	0.91
Equimolar	2.6	0.42	0.2	2.8	0.85

From Table III, it may be noted that the relative values of k_s and k_Δ showed that the reaction proceeded chiefly by anchimerically assisted ionization as one would expect for solvolysis in formic acid, a highly ionizing solvent. The over-all formolysis rate, k_1, was some 13% slower when the reaction was carried out with added III. This could be explained on the basis of the so-called mass-law effect (10) with the common p-toluene-sulphonate ion causing a rate depression. The data also demonstrated that this rate depression was attributable to a greater degree of return to covalent bonding when an excess of p-toluenesulphonate ion was present during the formolysis. This was indicated by a greater k^{14} for the formolysis in the presence of III. From the calculated F values, it can also be seen that the fraction of the anchimerically assisted ionization returning to

covalent bonding was some 15% for the reaction in the presence of III as compared with a return of only 9% when III was absent.

In connection with returns to covalent bonding, it may also be of interest to point out that in a study of the rates of solvolysis of 2-phenylethyl-1,1-d_2 and 2-phenylethyl-2,2-d_2 p-toluenesulphonates (I_b and I_c), Saunders and co-workers (11) noted the absence of any drift of the rate constants toward a common value and concluded that "internal return from a phenonium–tosylate ion pair cannot be appreciable, since in its presence I_b and I_c would be interconverted and their rate constants would drift toward a common value as the reaction proceeded". This conclusion would be valid only if the rate of the return process were great enough to cause an almost complete scrambling of the C-1 and C-2 positions in I_r before the product-forming reaction proceeded to completion. Inspection of the data in Table I shows that after a reaction time of 1200 minutes (about 88% completion), the C^{14} rearrangement in I_r was 8.88%, far from a 50% rearrangement expected for a complete scrambling of the C-1 and C-2 positions. Thus the interconversion of I_b and I_c was not great enough during the formolysis of these compounds to cause an observable drift towards a common rate constant. The fraction $(1-F)$ from the present data indicated that a return to covalent bonding did occur to the extent of about 9% of the anchimerically assisted ionization.

The processes of return from ionic intermediates to covalent bonding may be differentiated as internal and external returns, with internal return designating return from the "intimate ion pair" and external return designating return from the "solvent-separated ion pair" or dissociated ions (4, 5). In such a differentiation, internal return would be pictured as an intramolecular process. It was hoped that the inclusion of S^{35}-labeled sodium p-toluenesulphonate (III) in the formolysis studies might provide data which could shed some light on the extent, if any, of the intramolecular return.

The degrees of incorporation of S^{35} in the various samples of I_r are given in Table II. These results could not be treated kinetically as data for a simple exchange reaction between 2-phenylethyl p-toluenesulphonate (I) and sodium p-toluenesulphonate-S^{35} (III) because one of the reactants, I, was being continually converted to 2-phenylethyl formate (IV). Moreover, the S^{35} incorporated in I_r, besides arising from external return, might have resulted also from a direct displacement reaction between I and the added p-toluenesulphonate-S^{35} anion, and (or) by exchange between the labeled p-toluenesulphonate anion and the p-toluenesulphonate anion of the intimate ion pair. However, a qualitative consideration of the S^{35} incorporation in I_r in conjunction with the C^{14} rearrangement in I_r can be made (2). If the C^{14} rearrangement in I_r were to arise entirely from reaction between ethylphenonium ions (II) and the added p-toluenesulphonate-S^{35} anions, in other words entirely from external return, the percentage of S^{35} incorporated in I_r would be twice the percentage of C^{14} rearrangement in I_r. A correction should be made because the added p-toluenesulphonate-S^{35} anions would be progressively diluted by the p-toluenesulphonic acid liberated from I during the course of the reaction. The S^{35} in I_r would be decreased by this dilution effect. For example, for a reaction stopped at 10% completion, on the average, the incorporation of S^{35} would be decreased by a factor of $100/(100+10/2)$. The values obtained from $[100/(100+\% \text{ reaction}/2)]$ $(2\times\% \ C^{14}$ rearrangement in $I_r)$ would be the calculated percentage of S^{35} in I_r if the return process were only external or intermolecular. These calculated values are given in column 7 of Table II. Compared with the observed percentage of S^{35} in I_r (column 6, Table II), it can be seen that during the earlier stages of the reaction, the observed S^{35} in I_r were slightly lower than the calculated S^{35} for pure external return, while at the later stages

of reaction, the observed S^{35} in I_r were considerably lower than the calculated values. Since the observed S^{35} in I_r should be the sum of the S^{35} incorporated via external return, via direct displacement between I and the added p-toluenesulphonate-S^{35}, and possibly even via return from an intimate ion pair containing some exchanged p-toluenesulphonate-S^{35} anions, if the return process were only intermolecular between II and p-toluene-sulphonate-S^{35}, one would expect the observed S^{35} in I_r to be at least equal to, or possibly greater than the calculated % S^{35} in I_r for pure external return. The fact that the observed percentage of S^{35} in I_r were smaller than the calculated values, even though only slightly smaller, indicated that very probably some intramolecular return also took place. It may, therefore, be concluded that the return from ionic intermediates to covalent bonding during the formolysis of I included both internal and external returns, with external return accounting for the major portion of the return processes.

ACKNOWLEDGMENTS

REFERENCES

1. C. C. LEE, G. P. SLATER, and J. W. T. SPINKS. Can. J. Chem. **35**, 1417 (1957).
2. C. C. LEE, R. TKACHUK, and G. P. SLATER. Tetrahedron, **7**, 206 (1959).
3. W. G. YOUND, S. WINSTEIN, and H. L. GOERING. J. Am. Chem. Soc. **73**, 1958 (1951).
4. S. WINSTEIN, E. CLIPPINGER, A. H. FAINBERG, R. HECK, and G. C. ROBINSON. J. Am. Chem. Soc. **78**, 328 (1956).
5. S. WINSTEIN and G. C. ROBINSON. J. Am. Chem. Soc. **80**, 169 (1958).
6. E. F. JENNY and S. WINSTEIN. Helv. Chim. Acta, **41**, 807 (1958).
7. S. WINSTEIN and H. MARSHALL. J. Am. Chem. Soc. **74**, 1120 (1952).
8. S. WINSTEIN, C. R. LINDEGREN, H. MARSHALL, and L. L. INGRAHAM. J. Am. Chem. Soc. **75**, 147 (1953).
9. R. S. TIPSON. J. Org. Chem. **9**, 235 (1944).
10. C. K. INGOLD. Structure and mechanism in organic chemistry. G. Bell & Sons Ltd., London. 1953. pp. 360–370.
11. W. H. SAUNDERS, JR., S. ASPERGER, and D. H. EDISON. J. Am. Chem. Soc. **80**, 2421 (1958).

CONDENSATION OF SPRUCE PERIODATE LIGNIN WITH FORMALDEHYDE[1]

EDGAR EISENBRAUN[2] AND C. B. PURVES

ABSTRACT

The use of 73% sulphuric acid at 41° for 1 hour or less caused the periodate lignin to condense with 32% by weight of formaldehyde, as shown by direct measurement and by employing C^{14}-formaldehyde. Analyses of the product, however, suggested that the elements of water had been expelled during the condensation and that the true yield was about 120%. Up to 106% was recovered as material insoluble in dilute sulphuric acid (Ross–Potter lignin), and about 9% as a more soluble form. The approximate equivalence in weight of the Ross–Potter lignin to the original periodate (or Klason) lignin thus originated in the cancellation of three large errors. Formaldehyde periodate lignin failed to yield vanillin when oxidized in alkali with nitrobenzene or cupric hydroxide. Oxidation with alkaline potassium permanganate, or with iodic acid at not more than 200°, yielded benzenepentacarboxylic acid and perhaps mellitic acid (total, 3.9%) but none of the 1,2,4,5-tetracarboxylic acid recovered (together with the pentacarboxylic acid) from similar oxidations of periodate lignin. Convenient semimicro-scale oxidations with cupric hydroxide and with iodic acid, and the chromatography of the benzene-penta- and -tetra-carboxylic acids on paper, were described.

INTRODUCTION

It is well known that the treatment of wood meal with 72% sulphuric acid near 20°, as in the Klason determination of lignin, soon degrades and dissolves all of the carbohydrates but leaves the lignin as a dark brown, amorphous powder insoluble in all liquids. In 1929, however, Ross and Hill (1) observed that when the wood meal was first soaked in formalin all dissolved in the sulphuric acid, and this solution had to be diluted with water in order to precipitate "formaldehyde lignin". The yield appeared to be quantitative from softwoods, but not from hardwoods, and the products were soluble in alcohol, acetone, or acetic acid containing a little water. Ross and Potter (2) modified the procedure to determine lignin in paper pulps, but the Klason method proved to be more reproducible (3). Since formaldehyde could be expected to condense freely with lignin (a phenolic material) it seemed anomalous that the yield of Ross–Potter lignin was not substantially greater than that of the Klason lignin. The solubility of formaldehyde lignin suggested (2) that the formaldehyde had substituted active centers in the lignin, which normally condensed with each other to form the insoluble Klason lignin. The present research was planned to gain information on these possibilities.

Borisek and Polcin (4) determined the amount of formaldehyde that condensed with sulphite waste liquor solids under various conditions. No condensation occurred in neutral solution, and in alkali the formaldehyde underwent the Cannizzaro reaction. In sulphuric acid, the amount condensed increased as the concentration of the acid was increased to 27%, and 2 hours were sufficient for the reaction. Samples pretreated with sulphurous or sulphuric acid failed to react under the conditions tried. The lignin used on the present occasion was isolated by alternately oxidizing spruce wood meal with sodium periodate near pH 4, and extracting the oxidized polysaccharides with cold, dilute alkali. Although free of carbohydrates and dissolving at almost the normal rate during a calcium bisulphite cook of the type used in pulping wood, the periodate lignin was somewhat oxidized. Nevertheless, it served as a good model substance for lignin

in situ. Periodate lignin, when saturated with formalin, proved to be completely soluble at 41° in sulphuric acid provided the concentration of acid in the final mixture was at least 69% by weight.

The simplest way of isolating the main product (method (a)) was to pour this solution into a large volume of cold water, which was kept near neutrality by the simultaneous addition of sodium hydroxide, and to purify the precipitated formaldehyde periodate lignin by dialysis. The yield was 104% by weight. To recover the soluble products, dialysis was avoided in method (b), in which the neutralized, concentrated liquors were freed of sodium sulphate by dilution with ethanol and acetone. Evaporation of the mother liquor gave a yellow glass highly contaminated with inorganic material and formaldehyde polymer, but extraction with organic solvents recovered 9% of product, which with 106% for the main fraction raised the total yield to 115%, free of ash and moisture. This figure was accepted as being close to the yield actually formed in the condensation. Both the major and the minor fractions retained ultraviolet absorption spectra in 0.1% solution of the type characteristic of most lignins, with a broad, prominent maximum near wave length 280 mμ. A third attempt at isolation (method (c)) involved pouring the original sulphuric acid solution into an excess of acetic anhydride and anhydrous sodium acetate more than sufficient to combine with all the water and acid present. After isolation by precipitation into water followed by dialysis, the acetylated periodate formaldehyde lignin was recovered in 92% yield as a dark, hard resin.

The consumption of formaldehyde in the condensation was estimated, by difference, from the initial and final amounts. The results showed that 100 g of the lignin condensed with 32 g of formaldehyde, but the true amount might be as high as 35 g, since Freuden-berg and Sohns (5) obtained 2 to 3% of formaldehyde by distilling various lignins with sulphuric acid. Thus the expected yield of formaldehyde periodate lignin was at least 132% by weight, whereas 115% was the most that was ever recovered. According to the book by Walker (6), the strongly acidic conditions necessary to cause the condensation of formaldehyde with simple phenolic ethers or with ethylenic compounds were usually, although not always, sufficient to condense the hydroxymethyl derivatives initially formed to cyclic acetals, to ethers, or to derivatives of diphenylmethane. The above discrepancy in the yield of formaldehyde periodate lignin might thus originate in the condensation of hydroxymethyl groups with loss of the elements of water.

To investigate this possibility, the composition of an adduct from 100 parts by weight of periodate lignin and 32 parts of formaldehyde was calculated as shown in Table I, line C. A loss in weight of this adduct in the ratio 132:120 (instead of the observed ratio, 132:115) would result in the calculated composition given in line D, although the figures were no longer percentages. Comparison of line D with line E, the observed percentage composition of formaldehyde periodate lignin, showed that the latter retained all of the original carbon atoms and methoxyl groups but had lost hydrogen and oxygen in the ratio 1:8 characteristic of the composition of water. These calculations were approximate, because they were based on the major Ross–Potter fraction of the formaldehyde periodate lignin rather than on the entire amount, and ignored a sulphur content of 1% derived from the sulphuric acid used in the condensation.

Comparison of columns 4 and 5 in Table I showed that periodate lignin failed to respond to a methylation attempted with diazomethane, and therefore contained no hydroxyl groups of a phenolic nature; the increase of 1.8% observed in a similar methylation of the formaldehyde periodate lignin (line E) suggested that a few phenolic groups had been formed in the condensation, probably by the hydrolytic action of the 73% sulphuric

TABLE I

Composition of spruce periodate lignin and of its formaldehyde derivative

	%C	%H	%O[a]	%OCH₃	Methylated %OCH₃[b]		Acetylated % acetyl
					CH_2N_2	Me_2SO_4	
A. Periodate lignin (obs.)	62.2	5.6	32.2	12.2	—	17.6	—
				12.5[c]	13.1[c]	17.8[c]	5.0[c]
				11.5[d]	11.2[d]	—	
B. Formaldehyde (obs.)	40.0	6.7	53.3	0	0	0	0
C. Adduct, 100 g A:32 g B[e]	56.8	5.9	37.3	9.2	(~10.0)	(13.3)	(3.8)
D. Adduct C condensed 132 g to 120 g[f]	62.5	6.5	41.0	10.1	(~11.0)	(14.8)	(4.2)
E. Formaldehyde periodate lignin (obs.)[g]	62.4	5.4	32.2	9.9	11.7	15.2	3.9[h]

[a]By difference. All analyses corrected for ash and moisture.
[b]Diazomethane in dry ether; dimethyl sulphate in 30% sodium hydroxide.
[c]Data from Wieckowski (ref. 7); acetylation in pyridine.
[d]Data from Cabott and Purves (ref. 8).
[e]Calculated from A and B by method of mixtures. Formaldehyde contributed 17.2% of the carbon content.
[f]Calculated, but not as percentage composition.
[g]Major fraction, 105% by weight, uncorrected for 1% of sulphur.
[h]Acetylated with anhydrous sodium acetate.

acid. Methylation with dimethyl sulphate caused practically the same increase (17.6–12.2%) and (15.2–9.9%) in the methoxyl contents of the two lignins (columns 4 and 6), and thus both had the same total number of phenolic and aliphatic hydroxyl groups. Since the formaldehyde periodate lignin seemed to contain a few phenolic groups, its content of aliphatic hydroxyl groups was probably less than that of the periodate lignin. The acetyl contents of the two acetylated lignins (column 7, lines A and E) also suggested that aliphatic hydroxyl groups had been diminished, rather than increased, by the condensation with formaldehyde.

Two small-scale condensations were carried out with radioactive C^{14}-formaldehyde to determine, by an independent method, the proportion of carbon in formaldehyde periodate lignin which was contributed by the formaldehyde. The procedure of Das Gupta and Nair (9) was adapted to oxidize the various samples quantitatively by combustion to carbon dioxide, the activity of which was measured after conversion to barium carbonate. The count rates given by layers of the carbonate varying in thickness were plotted in Fig. 1 to eliminate the self-absorption factor, and to give comparison for samples of identical superficial density. Individual measurements deviated from the plots by not more than 10%. The open and filled circles (upper plot, left-hand ordinates) represented duplicate combustions of the original C^{14}-formaldehyde, and yielded a single smooth plot. When the ordinate scale shown at the right of Fig. 1 was chosen, the data from duplicate combustions of one C^{14}-formaldehyde periodate lignin sample fitted the same plot (open and filled triangles). It followed that 900/6000, or 15% of the carbon in this sample was derived from the formaldehyde. The values obtained for the second preparation of C^{14}-formaldehyde periodate lignin (crosses) corresponded to 16% of C^{14}.

Downes (16), however, found that C^{14}-formaldehyde condensed with dimedon to form the insoluble bismenthone, $C_{17}H_{24}O_4$, at only 0.93 times the rate displayed by the C^{12} isotope; if a similar effect occurred in the condensation with lignin, the above results would become 16% and 17%, respectively. In the present experiments, some of the C^{14}-formaldehyde was converted quantitatively to the bismenthone to eliminate the isotope effect, and the carbon in the product was recovered as barium carbonate before being counted. The results (Fig. 1, lower plot, open and half-filled circles) showed that 5.0 to
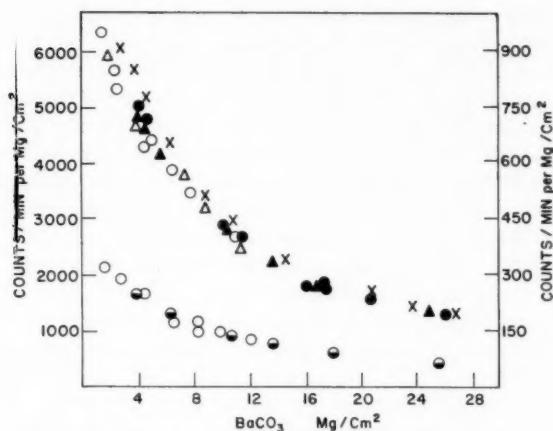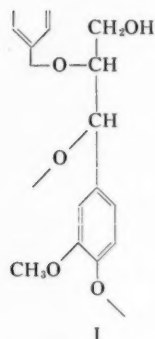
FIG. 1. Activity of C^{14}-compounds as mg barium carbonate per sq. cm. Left-hand ordinates, upper plots, open and filled circles, formaldehyde. Right-hand ordinates, open and filled triangles, formaldehyde periodate lignin; crosses, a duplicate preparation of the lignin; lower plot, open and half-filled circles, duplicate preparations of formaldehyde bismenthone.
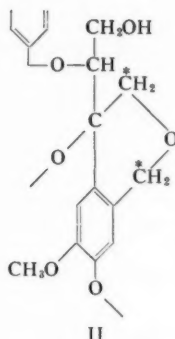
5.4% of the carbon was derived from the C^{14}-formaldehyde, whereas the value calculated for the bismenthone, 5.9%, was higher by about one-tenth. The cause of this discrepancy was not determined. Whether the C^{14}-formaldehyde count or that of its bismenthone derivative was accepted as the primary standard, the amount of C^{14} in the C^{14}-formaldehyde periodate lignin appeared to be between 15% and 18% of the total carbon content. This result agreed well with the value of 17.2% assumed in Table I.

Since the detailed structure of the lignin macromolecule remained unknown, that of the formaldehyde derivative could only be surmised. The greater part of the macromolecule, however, is currently supposed to resemble structure I, in which the ether links in the phenylpropane side chains were assigned to arbitrary positions (11, 12). Cross links rendered the lignin insoluble in all chemically indifferent liquids, but were not numerous enough to prohibit swelling. The action of sulphuric acid by itself would be to cleave some of the ether bonds, but autocondensation would simultaneously yield the insoluble, and presumably more highly cross-linked, Klason lignin. A loss of the elements of water probably occurred in such condensations (13). Perhaps the alpha positions in the side chains and the sixth positions in the nucleii were among those involved in condensation, because the former were probably sulphonated when lignin was heated in aqueous sodium bisulphite (12) and the latter could be chlorinated. A preferential condensation of each of these reactive sites with 1 mole of formaldehyde would increase the base molecular weight of the lignin from about 187 to about 247, or in the ratio 100:132 by weight, and the formaldehyde would contribute 16.7% of the carbon in the adduct. The loss of a molecule of water would lead to a new ether link (structure II) and reduce the yield by weight in the ratio 132:122. These figures were close to those observed. Carbon atoms originating as formaldehyde were denoted by asterisks in this and subsequent structures.
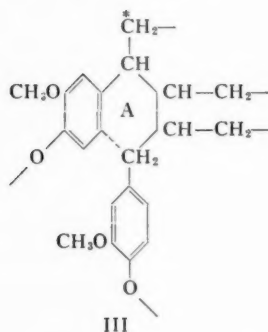
The ready solubility of formaldehyde lignin in several liquids suggested that condensation with formaldehyde did not bring about cross linking, and an intramolecular arrangement of the new ether group was chosen for structure II. Wherever this group was located, its existence reduced the number of the free hydroxyl groups to the original number, as
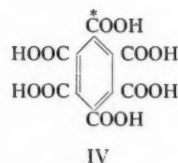
CH₂OH
O—CH
CH
O
CH₃O
O

I

Base molecular weight ∼187

CH₂OH
O—CH
*CH₂
C
O
*CH₂
CH₃O
O

II

Base molecular weight ∼229

*CH₂—
CH
CH₃O
A
CH—CH₂—
CH—CH₂—
CH₂
CH₃O
O

III

*COOH
HOOC COOH
HOOC COOH
COOH

IV

Mellitic acid

was found. Most lignins, including Klason lignin (14) and periodate lignin (15), when heated with nitrobenzene and alkali yielded vanillin, presumably by oxidative cleavage at the alpha carbon atom in structure I. The nitrobenzene could be replaced with cuprous hydroxide (16), whose use was adapted to a convenient semimicro scale. Neither oxidant produced a trace of vanillin from the Ross–Potter fraction, or the acid-soluble fraction, of formaldehyde periodate lignin, and attempts to isolate a carboxyvanillin from the oxidation liquor also failed. These failures were not inconsistent with structure II, since substitution of the alpha positions by formaldehyde might render the molecule more resistant at this point to oxidative cleavage.

Samples of the Ross–Potter fraction were then thoroughly oxidized with potassium permanganate in hot aqueous alkali to carbon dioxide, acetic acid, oxalic acid, and a mixture of benzenepolycarboxylic acids (17). Since the oxalic acid was radioactive when C^{14}-formaldehyde periodate lignin was used, the formaldehyde had formed a C—C bond, rather than a C—O—C bond, with the lignin, as shown in structure II. All aromatic rings directly substituted with oxygen, however, were known to be destroyed in this oxidation, and structure II would yield no benzenecarboxylic acids. As previously discussed (17), the production of these acids suggested that a minor part of the lignin macromolecule consisted of lignan elements in which the β-carbon atoms of the phenyl-propane units were directly joined. Substitution of a hydroxymethyl group in the α-position of the lignan, followed by cyclization as shown by the broken line (structure

III), would yield a cyclohexene ring (A) entirely substituted by carbon atoms. Benzene-hexacarboxylic (mellitic) acid (IV) would result when this ring was oxidized, and also benzenepentacarboxylic acid by partial decarboxylation. A new paper chromatographic technique was used to isolate the benzenepentacarboxylic acid in a pure condition, but the mellitic acid, if present, stayed on the starting line, and no benzenetetracarboxylic acids were present. When C^{14}-formaldehyde periodate lignin was oxidized, the supposed mellitic acid had some activity, but the pentacarboxylic acid had none.

Although parallel oxidations of spruce Klason lignin yielded about the same amount, 4%, of benzenepolycarboxylic acids as did the formaldehyde periodate lignin, the mixture consisted exclusively of benzenepentacarboxylic acid and the 1,2,4,5-tetracarboxylic acid, and mellitic acid was absent (17). This sharp difference between the two lignins strongly supported the view that some of the formaldehyde substituted the alpha positions of the phenylpropane units of structure III, as well as those in structure I. Mellitic acid, benzene-penta-, -1,2,4,5-tetra-, and -1,2,3,5-tetra-carboxylic acid were oxidized to the extent of only 0.7, 2.2, 1.9, and 5.0%, respectively, by iodic acid in concentrated sulphuric acid at 180° to 190°, although Kleinert and Dlouhy (18) recently showed that these acids were quantitatively oxidized at 220° to carbon dioxide. Oxidation at the lower temperature proved to be a simple method of recovering the benzenepolycarboxylic acids from periodate and formaldehyde periodate lignin.

. Another aldehyde capable of condensing with lignin was chloral hydrate in the presence of a little hydrochloric acid. Ogait (19) extracted most of the lignin from spruce wood meal with this reagent, and recovered about half as a thermoplastic "chloral lignin" soluble in chloroform and containing about 15% of chlorine. A repetition of this work with spruce periodate lignin yielded a "chloral periodate lignin" with only 9.2% of chlorine and soluble in acetone, but the results were otherwise too similar to those of Ogait to justify detailed reproduction here. They served to show, however, that the cleavage of lignin–carbohydrate bonds was not an essential step in the production of chloral lignin (19), since the periodate lignin was free of carbohydrates.

EXPERIMENTAL

Materials and Methods

Woodmeal of 20–30 mesh fineness was prepared from a log of black spruce which was free of bark and about 30 years old. The oxidation of a 2160-g batch with 660 g of sodium paraperiodate in 18 liters of water adjusted to pH 3.6–4.0 with acetic acid, and the subsequent extraction of the oxidized carbohydrates with cold 0.1 N sodium hydroxide, were as previously described (15, 20). After four or five oxidation–extraction cycles, the water-wet, gelatinous periodate lignin was solvent-exchanged first into acetone, which yielded a free-flowing, easily filterable suspension, and then through methyl ethyl ketone into ligroin, b.p. 30°–60°. Final drying, *in vacuo* over phosphorus pentoxide and solid paraffin, had to be thorough. Found: C (21), 60.1; H (21), 5.4; OCH$_3$ (22), 11.9; ash (21), 2.5; Klason lignin (23), 87%; holocellulose (24), trace. The product, and also samples isolated by freeze-drying the water-wet mass, were light-colored powders of low density, whereas samples dried directly from water were hard, darker resins. Periodate lignin had a low but noticeable cation-exchange capacity, and the acid form acquired sodium ion from aqueous sodium chloride.

Distilled water and organic liquids of C.P. or equivalent grade were used throughout

the work. Evaporations were performed at not more than 45° in a rotary evaporator under vacuum; often the solutions or suspensions, especially when neutral, produced much froth initially and the pressure had to be reduced gradually. Unless stated otherwise, final drying was *in vacuo* over phosphorus pentoxide, and analyses were in duplicate, the averages of concordant determinations being quoted. Seamless cellulose dialyzer tubing, 0.00072 inch thick, was used in dialyses, which were against large volumes of water. Phenolic compounds were chromatographed on paper with *n*-butanol saturated with 2% aqueous ammonia (16) (solvent A) or with ligroin–dioxane–water in the ratio 4:2:1 by volume (solvent B) as eluents. The spray described by Barton, Evans, and Gardner (25) was made more sensitive by the use of a mixture of 1% ferric chloride, 10 ml; 1% potassium ferricyanide, 6 ml; saturated boric acid solution, 10 ml; and water, 20 ml. The eluent for organic acids was a 10:1:1 mixture of methyl isobutyl ketone, water, and formic acid (solvent C) with bromphenol blue as the spray. Prior to spraying, the paper was dried at 130° *in vacuo* to eliminate formic acid. Yields and analyses were quoted on a moisture- and ash-free basis.

Condensations with Formaldehyde (1, 2)

Many preliminary experiments showed the necessity of immersing the lignin in formalin *before* adding the sulphuric acid, which had to attain at least 69% concentration by weight in the mixture. The required concentration was reached by adding 88.5% sulphuric acid, since the use of the concentrated acid yielded a more highly sulphonated product.

In a typical experiment, 50 g of periodate lignin (47.1 g on a moisture- and ash-free basis) was soaked for 2 hours in changes of commercial 37% formalin, 224 g of which was retained when the swollen mass was recovered on a filter. The moist lignin was mixed in a 1.5-liter beaker with 250 g of solid carbon dioxide, and ice-cold 88.5% sulphuric acid (about 700 g) was slowly added with stirring until the final concentration was $73 \pm 1\%$, the composition being: lignin, 47.1 g; formaldehyde, 83 g; sulphuric acid, 620 g; and water, 227 g. The gummy mixture was then maintained near 41° and was worked with a glass rod until a uniform, dark red-brown solution was obtained. No more solid particles could be detected after 30 to 50 minutes; the solution was then cooled and the product isolated in one of the following ways.

Method (a)

The reaction mixture and about 8 liters of cold, 10% aqueous sodium hydroxide were simultaneously poured into 15 liters of cold water so that the pH remained between 5 and 9, the final value being 3.5. The precipitate was separated on a centrifuge and the liquors were extracted at pH 2 with methyl ethyl ketone, which removed 0.3 g of a dark, nonvolatile, brittle solid. This solid was extracted from the ketone by 5% sodium hydroxide. The major product, 74 g including 30% of sodium sulphate, was mixed with 250 ml of water and was dialyzed for 3 days. Acidification of the dialyzate to pH 1.8 and extraction with methyl ethyl ketone removed 1.8% of a gum which was soluble in water and dilute alkali. Found: OCH_3, 9.2; sulphated ash, 3.9%. This gum remained partly on the starting line, and partly in the solvent front, when chromatographed on paper with solvents A or B.

The contents of the dialysis sac, when evaporated at pH 6, yielded 52.5 g of formaldehyde periodate lignin as dark brown lumps which were powdered in a mortar. Found: C, 59.3; H, 5.1; OCH_3, 9.4; S, 1.0; ash, 4.6%. The yield, ash-free, was 104% of the periodate lignin, and the two minor fractions increased this figure to 107.4%.

Method (b)

A solution of formaldehyde periodate lignin in 73% sulphuric acid, made from 9.7 g of periodate lignin, was poured into 400 ml of water at 0°, and the precipitated Ross–Potter lignin was washed on the centrifuge with four 250-ml volumes of water; a little sulphuric acid had to be added in the last washing to obtain a good separation. The liquors were neutralized with sodium carbonate and were evaporated at pH 8 to 700 ml, when crystalline sodium sulphate was removed at 4°. After acidification to pH 0.5 with sulphuric acid, the liquor was alternately concentrated to 50 ml and diluted with water several times to decompose and eliminate most of the formaldehyde polymers. The neutralized liquor, 40 ml, was highly diluted with acetone to precipitate inorganic material, and the portion soluble in dry acetone was recovered as a near-white, dry gum. Yield: 6.53 g. Found: ash, 27.1; loss in weight on heating in air for 70 minutes at 105°, 45.3%.

This loss of weight represented the decomposition of formaldehyde polymer. A suspension of the gum in 80 ml of water was continuously extracted first with ether and then with methyl ethyl ketone at 240 mm pressure. The ether extract yielded 0.57 g of material of which 0.17 g was non-volatile at 105°, while 0.72 g of the 0.76 g recovered from the ketone was non-volatile. Samples of both extracts were hydrolyzed in boiling 16% sulphuric acid and the formaldehyde liberated from the polymer was determined by the sodium sulphite method (4, 26). The aqueous residue from the extractions contained 2.7 g of a white, amorphous solid. Found: OCH_3, 20.5; S, 21.3; ash, 54.6%. Calc. for $H_2C(OCH_3)OSO_3Na$: OCH_3, 18.9; S, 19.5; ash as Na_2SO_4, 43.3%. The substance failed to give a positive test for sulphate ion with aqueous barium chloride, but the ash did so.

The Ross–Potter fraction was dissolved in dilute sodium hydroxide except for an 0.28-g residue with 45% of ash. Acidification of the brown filtrate reprecipitated the main product, which was washed with water and redissolved while still wet in much acetone. A residue separated on the centrifuge yielded 0.17 g of material insoluble in water (ash, 13.7%), and 0.29 g soluble in water (ash, 30.3%). The acetone solution was diluted with water, adjusted to pH 5.7, concentrated, and the product was isolated as a friable, brown powder by freeze-drying. Yield: 10.43 g: ash, 6.1%. The total recovery of organic material, excluding formaldehyde polymer, was (0.17+0.72+0.14+0.15+0.2+9.8 g) 11.2 g, or 115% by weight.

Method (c)

A solution of formaldehyde periodate lignin, prepared in 73% sulphuric acid from 3.2 g of periodate lignin, was mechanically stirred into a mixture of glacial acetic acid, 81 ml; acetic anhydride, 540 ml; and anhydrous sodium acetate, 105 g. Although the flask was cooled externally with solid carbon dioxide, the temperature rose to 51°. The resulting slurry was kept near 2° for 18 hours, when the excess acetic anhydride was cautiously hydrolyzed with water and the liquor was thoroughly dialyzed against water. The non-dialyzed portion was isolated by evaporation at pH 6.5 followed by drying to constant weight. The dark brown resin weighed 3.21 g. Found: OCH_3, 7.8; acetyl (27), 4.2; ash, 13.4%.

Methylations of Ross–Potter Fraction

A portion of the product isolated by method (a) was suspended in dry tetrahydrofuran and an excess of dry diazomethane was added. Twelve hours later, the liquor was evaporated and the residue dried *in vacuo* over phosphorus pentoxide and solid sodium hydroxide. Found: OCH_3, 11.2; ash, 4.5%.

Another portion of the same Ross–Potter fraction was methylated with dimethyl sulphate and 30% sodium hydroxide in aqueous tetrahydrofuran, the atmosphere being oxygen-free nitrogen. Both the acetone-soluble and acetone-insoluble fractions of the product (yields 37% and 46%, respectively) had the same methoxyl content, not increased by remethylation. Found for the acetone-soluble fraction: OCH_3, 15.0; S, 0.44; ash, 2.0%. A sample of periodate lignin was completely methylated in the same way. Found: OCH_3, 17.5; ash, 1.2%.

Consumption of Formaldehyde

The apparatus consisted of a stout-walled glass bomb of 100-ml capacity with a side-arm dipping into water to trap any formaldehyde expelled when pressure increased. The top of the bomb was connected by a short piece of rubber hose to an air-tight, mercury-sealed stirrer consisting of a stout glass rod reaching almost to the bottom. The flexible connection made it possible to work the particles of lignin into solution. Paraformaldehyde, 42 g, and 68 ml of 0.05 N hydrochloric acid were boiled under reflux and the almost clear solution, when analyzed by the steam distillation – sodium sulphite method (4, 26), contained 36.2, 36.1% formaldehyde by weight. Three grams (2.86 g ash-free) of periodate lignin and 15 g of the formaldehyde solution were weighed into the apparatus; next day 44.8 g of 88% sulphuric acid was added and the condensation completed as previously described.

The resulting solution was cooled, diluted with water, and quantitatively transferred to a 1-liter flask arranged for steam distillation. The suspension, 400 ml, was kept just below the boiling point for 50 minutes to hydrolyze formaldehyde polymers, and was then steam-distilled for 3 to 4 hours, the distillate being exactly 1 liter. Aliquots, 100 ml, of the distillate were then analyzed by the sodium sulphite method, which employed N hydrochloric acid and a thymolphthalein indicator in the final titration (26). Found: CH_2O, 4.30, 4.26 g, whereas a blank containing no lignin yielded 5.28, 5.27 g. The difference, 0.99 g, had therefore condensed with 2.86 g of periodate lignin, or in the proportion of 34.5:100. Since any trace of sulphuric acid carried into the distillate would have registered as formaldehyde, independent experiments were carried out in which the distillates were neutralized to thymolphthalein before the determination of formaldehyde. Found: CH_2O, 4.38, 4.32 g, and 5.29, 5.26 g in the blank. In this case, 32 g of formaldehyde condensed with 100 g of the lignin. The still residues yielded 3.07, 3.09 g of the Ross–Potter fraction, or 104, 105%, and a further 0.22 g or 7.8% of formaldehyde periodate lignin was recovered from the mother liquors after removal of sulphate ion as the barium salt. The removal of sulphate ion by the cation-exchange resin "Amberlite IR-120" reduced the recovery of the acid-soluble lignin to 5.7% in the duplicate experiment.

C^{14}-Formaldehyde Periodate Lignin (Fig. 1)

A solution of radioactive formaldehyde was made by heating 18 mg of C^{14}-paraformaldehyde (obtained from Merck Company of Canada, Limited) and 5 g of inert paraformaldehyde with 8.5 ml of 0.05 N hydrochloric acid in a sealed glass bomb at 100° for several hours. Found for the clear solution by the bisulphite (4, 26) method: H_2CO, 35.8, 35.8, 36.2%. This result was checked by precipitating the formaldehyde in 0.5-g samples with 2 g of dimedon in 300 ml of water at pH 4.6. One gram of the bis-menthone was equivalent to 0.1027 g of formaldehyde (26). Found: H_2CO, 35.7, 36.25%. Two batches of C^{14}-formaldehyde periodate lignin were prepared as described in method

(a), each from 2.5 g of the above solution, 0.5 g of periodate lignin, and 8.5 g of 88.5% sulphuric acid. After the dialysis, solutions of the Ross–Potter fractions in dilute sodium hydroxide were filtered through sintered glass to remove insoluble but active material (15 mg or less), thoroughly dialyzed again, and freeze-dried. Yield: 470, 488 mg.

To determine C^{14}-carbon, 50-mg samples were burned to carbon dioxide in a conventional microcombustion furnace (28), those of the original formaldehyde solution being introduced in a fine glass tube sealed at one end. The carrier gas was purified oxygen, and the carbon dioxide was absorbed by passage through each of two 250-ml centrifuge tubes one-third filled with aqueous barium hydroxide free of carbonate. Each tube contained a small magnetic stirrer to make sure that the distribution of C^{14}-carbon in the precipitated barium carbonate would be uniform (29), and some samples were mixed with pulverized potassium dichromate to prevent any loss of carbon dioxide as sodium carbonate during the combustion. The precipitated barium carbonate was recovered by centrifugation and was magnetically stirred with changes of wash water (free of carbon dioxide) and finally exchanged into acetone, giving a fine-grained product suitable for counting.

A suspension of this precipitate in acetone was deposited in varying amounts on tared aluminum pans 3 cm in diameter; drying was under an infrared lamp and all samples were measured over the same area. A gas-flow proportional counter was used whose efficiency, compared with a 2π gas-flow windowless counter, was checked at 13% on several samples. Each measurement for formaldehyde and the Ross–Potter fraction totalled at least 30,000 and, with two exceptions, at least 11,000 for formaldehyde bismenthone. Each measurement was corrected for background, and the sensitivity and window position of the instrument were kept constant throughout.

Oxidations with Nitrobenzene and Cuprous Hydroxide

One gram of the lignin, 2.3 ml of pure benzaldehyde, and 20 ml of 4 N sodium hydroxide were heated together in a stainless steel bomb at 175° for 3 hours (30, 31). The contents were distilled in steam, the still residue was extracted with benzene, acidified to pH 3, and continuously extracted with ether. Portions of the residue from the ether extract were then chromatographed on paper with solvent A.

In the oxidations with cuprous hydroxide (16), 2 g of the lignin, 42 ml of 3 N sodium hydroxide, and 12 g of finely divided cuprous hydroxide were heated at 175° for 3 hours. The suspension was then filtered, and filtrate plus washings were acidified to pH 2 and continuously extracted with ether. When the extract from an oxidation of periodate lignin was re-extracted with saturated aqueous sodium bisulphite, a 20% yield of vanillin was recovered, some of which was isolated with the correct melting point and mixed melting point. Products from formaldehyde periodate lignin yielded ether extracts which deposited insoluble material continuously during extractions with aqueous sodium bisulphite, bicarbonate, or hydroxide. Every attempt to isolate vanillin, a carboxyvanillin, or vanillic acid failed.

The above oxidation was reduced to the semimicro scale previously described for oxidations with nitrobenzene (30), the 5-ml steel bombs being charged with lignin, 50 mg; cuprous hydroxide, 300 mg; and 2 ml of 2 N sodium hydroxide. During the heating in an air oven at 175° for 2.5 hours, the bomb was twice shaken vigorously by hand. The liquor could then be directly spotted on chromatograph paper; when the spots had been dried, they were exposed for a minute to the vapor of acetic acid to neutralize any free alkali and were then developed with solvent A.

Chromatography of Some Benzenepolycarboxylic Acids

Samples, 15 μg, of the authentic, pure acids were spotted on chromatograph paper, and were subsequently developed with solvent C for 4 hours, the spray being bromphenol blue. The R_F values observed were as follows: mellitic acid, 0.0; benzenepentacarboxylic, 0.035; benzene-1,2,3,4-tetracarboxylic acid, 0.12; the 1,2,4,5-isomer, 0.22; and the 1,2,3,5-isomer, 0.24. A mixture of the five acids in equal amount when chromatographed yielded the first three in a pure state, but the separation between the last two was unsatisfactory.

Oxidations with Potassium Permanganate

A suspension of 10 g of the formaldehyde periodate lignin in 1.6 liters of 1% potassium hydroxide was thoroughly oxidized near 97° by a total of 90 g of potassium permanganate added during 4 days. After the product had been isolated, first as barium salts and then as an aqueous solution of the free acids, in the way described (17), crystalline oxalic acid dihydrate was separated. The residual material after reoxidation with boiling, concentrated nitric acid yielded 0.39 g or 3.9% of a pale yellow solid shown by chromatography to contain benzenepentacarboxylic acid but none of the benzenetetracarboxylic acids.

The above oxidation was repeated with 0.8 g of C^{14} formaldehyde periodate lignin, but when the alkaline oxidation liquor was acidified the carbon dioxide was expelled and recovered as barium carbonate. This carbonate was radioactive, and so was the crystalline oxalic acid dihydrate, which had the correct melting point of 101°. Yield 0.14 g or 17.5%. After the final product had been chromatographed on paper, the spot containing the benzenepentacarboxylic acid was excised and placed in a counter, but no activity was observed. Some activity remained at the starting line of the chromatogram.

Oxidations with Iodic Acid (13, 18)

One gram of the lignin was mixed in an open 50-ml flask with 10 ml of a saturated solution of potassium iodate in concentrated sulphuric acid. When the initial violent reaction subsided, 10 g of powdered potassium iodate was cautiously added in small portions, more heat and iodine being evolved. Nitrogen was then bubbled through the solution, which was kept at 180° to 200°, for 40 minutes. An additional 10 ml of concentrated sulphuric acid was added, and 10 minutes later, 50 mg of paraformaldehyde, to reduce any remaining iodic acid. The solution was cooled 20 minutes later, cautiously diluted with 25 ml of water, and then boiled to expel free iodine. A second dilution with water brought the volume to 60 ml, and the solution was extracted continuously with ether. This extract was evaporated with water several times to expel free iodine that formed, and the final liquor, 8 ml, was ready for paper chromatography. Spots of R_F 0.14 and 0.23 to 0.24 indicated the presence of benzenepentacarboxylic acid and benzene-1,2,4,5-tetracarboxylic acid in the product from periodate lignin, but there was no trace of the latter spot in the products from various fractions of formaldehyde periodate lignin.

REFERENCES

1. J. H. Ross and A. C. Hill.   Pulp Paper Mag. Can. **27**, 541 (1929).
2. J. H. Ross and J. C. Potter.   Pulp Paper Mag. Can. **29**, 569 (1930).
3. P. S. Billington, F. A. Simmons, and P. K. Baird.   Paper Trade J. **96**(4), Tappi Section, 258 (1933).
4. R. Borisek and J. Polcin.   Chem. zvesti (Chem. News), **5**, 322 (1951); Chem. Abstr. **46**, 4223 (1952).
5. K. Freudenberg and F. Sohns.   Ber. **66**, 262 (1936).
6. J. F. Walker.   Formaldehyde. 2nd ed. Reinhold Publishing Corporation, New York, N.Y. 1953. pp. 235–270.
7. E. Wieckowski.   Ph.D. Thesis, McGill University, Montreal, Que. 1957.
8. I. M. Cabott and C. B. Purves.   Pulp Paper Mag. Can. **56**(5), 151 (1956).
9. A. K. Das Gupta and C. K. N. Nair.   J. Sci. Ind. Research (India), **15B**, 1 (1956).
10. A. M. Downes.   Australian J. Sci. Research, Ser. A, **5**, 521 (1952).
11. F. Brauns and H. Hibbert.   J. Am. Chem. Soc. **55**, 4720 (1933).
12. B. Leopold.   Pulp Paper Mag. Can. **55**(3), 184 (1954).
13. T. N. Kleinert and E. J. Dostal.   Tappi, **41**, 689 (1958).
14. K. Iwadare.   J. Chem. Soc. Japan, **62**, 1095 (1941); Chem. Abstr. **41**, 3291 (1947).
15. P. F. Ritchie and C. B. Purves.   Pulp Paper Mag. Can. **48**, 74 (1947).
16. I. A. Pearl and D. L. Beyer.   Tappi, **33**, 544 (1950); J. Am. Chem. Soc. **76**, 6106 (1954).
17. D. E. Read and C. B. Purves.   J. Am. Chem. Soc. **74**, 120 (1952).
18. R-M. Dlouhy and T. N. Kleinert.   Holzforschung, **13**(1), 13 (1959).
19. A. Ogait.   Cellulosechemie, **22**, 15 (1944).
20. D. M. Smith and C. B. Purves.   J. Am. Chem. Soc. **81**, 2405 (1959).
21. Schwartzkopf Microanalytical Laboratory.   Woodside, N.Y. U.S.A.
22. F. Vieböck and A. Schwappach.   Ber. **63**, 2818 (1930).
23. Tappi Standards, T 13m-54, Technical Association of the Pulp and Paper Industry, New York. 1950.
24. E. F. Kurth and G. J. Ritter.   J. Am. Chem. Soc. **56**, 2720 (1934).
25. G. M. Barton, R. S. Evans, and J. A. F. Gardner.   Nature, **170**, 249 (1952).
26. J. F. Walker.   Formaldehyde. 2nd ed. Reinhold Publishing Corporation, New York, N.Y. 1953. pp. 382, 390.
27. E. P. Clark.   Ind. Eng. Chem. Anal. Ed. **8**, 487 (1936); **9**, 539 (1937).
28. W. W. Scott.   Standard methods of chemical analysis. 5th ed. Vol. 2. D. van Nostrand Co., Inc., New York. 1939. p. 2475.
29. W. D. Armstrong, L. Singer, S. H. Zbarsky, and B. Dunshee.   Science, **112**, 531 (1950).
30. J. E. Stone and M. J. Blundell.   Anal. Chem. **23**, 771 (1951).
31. K. R. Kavanagh and J. M. Pepper.   Can. J. Chem. **33**, 24 (1955).

CYCLOHEXANE COMPOUNDS

III. THE 1-METHOXY- AND 1-ETHOXY-2-HYDROXY-3-BROMOCYCLOHEXANES[1, 2]

R. A. B. Bannard and L. R. Hawkins

ABSTRACT

1α-Methoxy-2β-hydroxy-3α-bromocyclohexane and 1α-methoxy-2α-hydroxy-3β-bromo-cyclohexane have been prepared by the action of hydrobromic acid on 1β-methoxy-2α,3α-epoxycyclohexane and 1α-methoxy-2α,3α-epoxycyclohexane respectively. Assignment of stereochemical configuration to 1α-methoxy-2β-hydroxy-3α-bromocyclohexane was made by catalytic debromination of the phenyl- and 1-naphthyl-urethanes to derivatives of 2β-methoxy-1α-cyclohexanol. An alternative proof of structure was obtained by de-etherification of the bromohydrin to 3α-bromo-1α,2β-cyclohexanediol, which was catalytically debrominated to 1α,2β-cyclohexanediol and oxidized via periodate to 2-bromoadipaldehyde, isolated as the bis-2,4-dinitrophenylhydrazone. The structure of 1α-methoxy-2α-hydroxy-3β-bromocyclohexane was established by de-etherification to 3β-bromo-1α,2α-cyclohexanediol, which was oxidized by periodate 10 times more rapidly than its isomer. The corresponding ethoxy compounds were prepared and their structures were elucidated in a completely analogous manner.

In an earlier paper (1) the mixtures of bromohydrins resulting from the action of aqueous N-bromosuccinimide on 1-methoxy- and 1-ethoxy-cyclohexene-2 were utilized for synthesis of the stereoisomeric 1-methoxy- and 1-ethoxy-2,3-epoxycyclohexanes I and II (R = CH₃ or C₂H₅) and led ultimately by ammonolysis of the latter to the 1-methoxy- and 1-ethoxy-2-hydroxy-3-aminocyclohexanes III and IV (R = CH₃ or C₂H₅). The formation of two oxides by the action of aqueous sodium hydroxide on each 1-alkoxy-cyclohexene-2 bromohydrin demonstrated the presence in each of at least two trans-oriented bromohydrins (2, 3), but the possibility existed that all four bromohydrins V–VIII were present. Attempts to separate the bromohydrin mixtures by fractionation *in vacuo* were unsuccessful, and attention was, therefore, directed toward preparation of pure bromohydrins from the pure oxides by the action of hydrobromic acid, since it was anticipated that knowledge gained concerning the physical and chemical characteristics of any of the possible components of the mixtures would facilitate the development of a method for separation and identification of all the components.
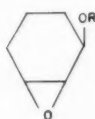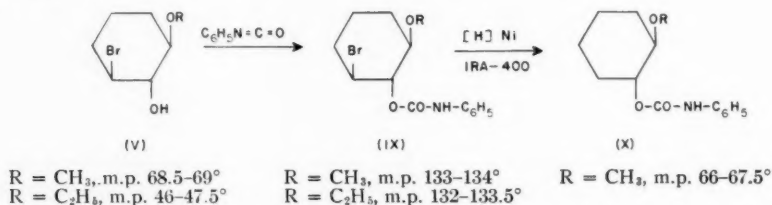

(I)   (II)
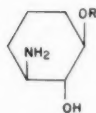
(III)   (IV)
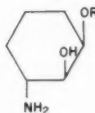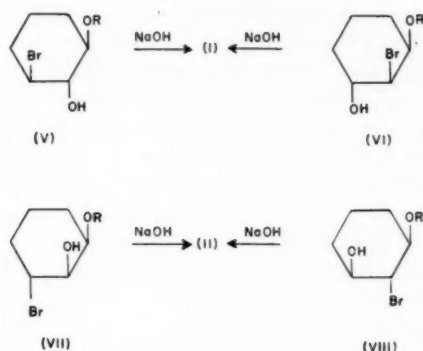
Theoretically, two bromohydrins can be formed from each oxide if ring scission occurs in both possible directions (4). However, our previous experience with ammonolysis of the oxides, in which derivatives of 3-amino-1,2-cyclohexanediol were formed exclusively (1), together with the results obtained by Lemieux, Kullnig, and Moir (5) on methanolysis of the oxides, suggested that 1-alkoxy-2-hydroxy-3-bromocyclohexanes would probably be the only bromohydrins formed. The work now to be described is concerned only with the synthesis and proof of structure of the 1-methoxy- and 1-ethoxy-2-hydroxy-3-bromocyclohexanes. Application of the information gained therefrom to solution of the problem of the composition of the bromohydrin mixtures referred to above is reserved for a subsequent communication.

1β-Methoxy-$2\alpha,3\alpha$-epoxycyclohexane (I, R = CH$_3$) on treatment with hydrobromic acid gave a solid bromohydrin, m.p. 68.5–69°, in 63% yield. The liquid fraction isolated from the reaction was shown to consist of 27% bromohydrin (by isolation of the 1-naphthylurethane, m.p. 185–186°) and 19% of a 1-methoxy-2,3-cyclohexanediol (identified by periodate cleavage followed by isolation of the bis-2,4-dinitrophenyl-hydrazone of 2-methoxyadipaldehyde, m.p. 192–193.5°, and by isolation of a 1-methoxy-2,3-cyclohexanediol bis-1-naphthylurethane, m.p. 224–226°) leaving approximately 50% of the oil unidentified. No further attempt was made to characterize this portion of the product but the suggestion is offered that it could well be a 2-methoxy-3-bromo-cyclohexanol formed by methoxyl migration (6). In support of this suggestion is the observation (see below) that the action of hydrobromic acid on the cis oxide II produces the corresponding bromohydrin in 93% yield with formation of only a very minor quantity of methoxydiol. The absence of a large fraction of unknown structure is to be expected in this instance because facile migration of the methoxyl group is hindered by virtue of the cis relationship of the methoxyl and its neighboring hydroxyl group.
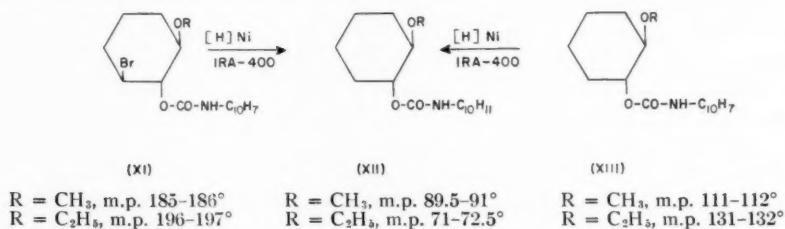
The bromohydrin was characterized by preparation of its phenylurethane, m.p. 133–134° (86%), 1-naphthylurethane, m.p. 185–186° (94%), and its acetyl derivative, m.p. 56–56.5° (90%), and its structure was established as 1α-methoxy-2β-hydroxy-3α-bromo-cyclohexane (V, R = CH$_3$) by the following methods.

The phenylurethane of the bromohydrin (IX, R = CH$_3$) was debrominated according to the method of McCasland and Horswill (7) using hydrogen, Raney nickel, and an anion exchange resin, producing 2β-methoxy-1α-cyclohexanol phenylurethane (X, R = CH$_3$), m.p. 66–67.5°, in 78% yield. The identity of the latter compound was established by comparison with an authentic specimen obtained from 2β-methoxy-1α-cyclohexanol (8).

Prior to use of the debromination method it was shown that no concomitant reduction of the benzene or urethane groups occurred under the conditions employed, since debromination of 2β-bromo-1α-cyclohexanol phenylurethane, m.p. 85–87° (9) gave cyclohexanol phenylurethane, m.p. 83–84.5° (10), in 86.5% yield. The bromine atom must have occupied a position trans to the hydroxyl group in the original bromohydrin since the latter yields the oxide I (R = CH₃) on treatment with alkali (2, 3) and it therefore follows that the bromohydrin must be 1α-methoxy-2β-hydroxy-3α-bromocyclohexane (V, R = CH₃).

R = CH₃,.m.p. 68.5–69°   R = CH₃, m.p. 133–134°   R = CH₃, m.p. 66–67.5°
R = C₂H₅, m.p. 46–47.5°   R = C₂H₅, m.p. 132–133.5°

A similar proof of structure was obtained using the 1-naphthylurethane (XI, R = CH₃) rather than the phenylurethane. During debromination, however, simultaneous reduction of one of the benzenoid rings occurred, leading to the tetralin derivative (XII, R = CH₃). The latter substance was identified by comparison with an authentic specimen prepared by reduction of 2β-methoxy-1α-cyclohexanol 1-naphthylurethane (XIII, R = CH₃) under the same conditions as used for debromination.

R = CH₃, m.p. 185–186°   R = CH₃, m.p. 89.5–91°   R = CH₃, m.p. 111–112°
R = C₂H₅, m.p. 196–197°   R = C₂H₅, m.p. 71–72.5°   R = C₂H₅, m.p. 131–132°

It was also shown that debromination of 2β-bromo-1α-cyclohexanol 1-naphthylurethane by the hydrogen – Raney nickel method leads to a cyclohexanol tetrahydro-1-naphthylurethane identical with that obtained by reduction of cyclohexanol 1-naphthylurethane under the same conditions. These experiments did not establish which benzenoid ring was reduced. However, by analogy with work reported by Papa and Schwenk (11) it seems probable that reduction occurred in the unsubstituted ring.

The urethanes were used rather than the bromohydrin V (R = CH₃) itself to avoid the possibility of intermediate oxide formation, which would invalidate any structural assignment based on the debromination experiments since the oxide I (R = CH₃) could result just as readily from VI as from V (R = CH₃). It will be demonstrated in the sequel, however, that the use of derivatives is unnecessary because oxide formation is readily preventable and, moreover, if it is forced to occur the oxide is not reduced under the conditions of debromination.

De-etherification of the bromohydrin with fuming hydrobromic acid gave a bromodiol, m.p. 98–99°, in 89% yield, which was further characterized via its bis-1-naphthylurethane, m.p. 210–210.5°, and diacetate, m.p. 65.5–66.5°, and was shown to be a

derivative of 1,2-cyclohexanediol, since periodate oxidation followed by treatment with
2,4-dinitrophenylhydrazine gave a 97% yield of the bis-2,4-dinitrophenylhydrazone of
2-bromoadipaldehyde (XV). The steric orientation of the 1,2-diol group was shown to
be trans since debromination in the presence of Amberlite IR-4B (OH) resin gave dl-1α,2β-
cyclohexanediol in 91% yield. Since the bromine and its adjacent hydroxyl group in
the original bromohydrin are in a trans orientation, it follows that the bromodiol must
be dl-3α-bromo-1α,2β-cyclohexanediol (XIV) and the bromohydrin must be dl-1α-
methoxy-2β-hydroxy-3α-bromocyclohexane (V, R = CH$_3$) in agreement with the
structural assignment reached on the basis of debromination of the urethanes. This
proof of structure is based on two assumptions. First, that no inversion of configuration
occurs during de-etherification and second, that elimination of bromine is not assisted
by intermediate oxide formation. The first assumption was shown to be valid by de-
etherification of 2β-methoxy-1α-cyclohexanol under conditions identical with those used
for the bromohydrin, when 1α,2β-cyclohexanediol was obtained in 92% yield. It was
also shown that the oxide cannot be an intermediate in the debromination reaction since
1β-methoxy-2α,3α-epoxycyclohexane and other oxides are not reduced by Raney nickel
and hydrogen under the conditions used. In complete agreement with this result is the
observation that debromination of the bromodiol XIV does not proceed in the presence
of Amberlite IRA-400 (OH) resin, whereas the use of identical conditions with the
phenyl- and 1-naphthyl-urethanes IX and XI (R = CH$_3$) had furnished high yields of
the debrominated compounds X and XII (R = CH$_3$). Debromination of XIV is readily
achieved, however, in the presence of Amberlite IR-4B (OH). This behavior was explained
when the action of the two anion exchange resins on 1α-methoxy-2β-hydroxy-3α-bromo-
cyclohexane (V, R = CH$_3$) was examined. In the presence of the weakly basic resin,
IR-4B, the bromohydrin remains unchanged, but in the presence of the strongly basic
resin it is converted to the oxide I (R = CH$_3$), which does not undergo reduction to
a diol under the conditions used. These results underline the efficacy of the protection
afforded against intermediate oxide formation by the presence of urethane groups in
the earlier debromination experiments in which the strongly basic resin was used.

m.p. 98–99°

R = CH$_3$, m.p. 68.5–69°   m.p. 154–155°
R = C$_2$H$_5$, m.p. 46–47.5°   [H]Ni | IR-4B(OH)

1α,2β-cyclohexanediol
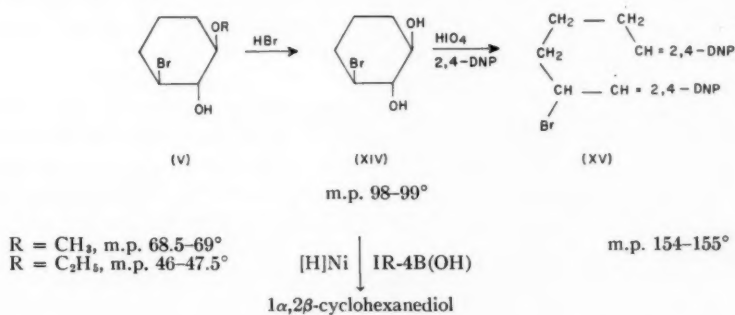
1α-Methoxy-2α,3α-epoxycyclohexane II (R = CH$_3$) on treatment with hydrobromic
acid gave a 93% yield of a liquid bromohydrin VII (R = CH$_3$) b.p. 62–63° at 0.01 mm.
This substance was quite different from the solid bromohydrin V (R = CH$_3$) obtained
from the isomeric oxide, as demonstrated by comparison of their derivatives and infrared
spectra. Conversion of the liquid bromohydrin to a 1-naphthylurethane, m.p. 122–124°,
in 86% yield and to a liquid acetyl derivative, b.p. 63–65° at 0.01 mm in 95% yield

suggested that the compound was sterically pure. The proof of structure of this bromo-hydrin was not as exhaustively pursued as that of its stereoisomer and the simplicity of the de-etherification approach led us to follow this method. Ether cleavage of the bromohydrin gave a bromodiol, m.p. 70.5–71°, in 74% yield together with 8% of un-changed starting material. The new compound gave a liquid diacetyl derivative, b.p. 85–86° at 0.1 mm, in 95% yield and a bis-1-naphthylurethane, m.p. 176–178°, in 95% yield. The bromodiol was shown to be a 3-bromo-1,2-cyclohexanediol since periodate oxidation followed by treatment with 2,4-dinitrophenylhydrazine gave the bis-2,4-dinitrophenylhydrazone of 2-bromoadipaldehyde (XV) which had been obtained earlier from similar treatment of its isomer XIV. The orientation of the hydroxyl groups in the lower-melting bromodiol was shown to be cis since its rate of oxidation by periodate at 20° was 10 times more rapid than that of its isomer. Since the liquid bromohydrin yields the oxide II (R = CH$_3$) on treatment with alkali, it follows (2, 3) that the structure of the bromohydrin must be dl-1α-methoxy-2α-hydroxy-3β-bromocyclohexane (VII, R = CH$_3$) and the corresponding bromodiol must be dl-3β-bromo-1α,2α-cyclohexanediol (XVI).

(VII)   (XVI)
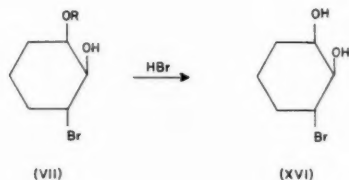
A solid bromohydrin, m.p. 46–47.5°, was obtained in 61% yield by the action of hydrobromic acid on the trans oxide I (R = C$_2$H$_5$) and was further characterized by preparation of the phenylurethane, m.p. 132.5–133.5° (75%), 1-naphthylurethane, m.p. 196–197° (97%), and acetyl derivative, m.p. 29.5–30.5° (92%). Its structure was established as dl-1α-ethoxy-2β-hydroxy-3α-bromocyclohexane (V, R = C$_2$H$_5$) by debromination of the 1-naphthylurethane XI (R = C$_2$H$_5$) to the tetrahydronaphthylurethane of dl-2β-ethoxy-1α-cyclohexanol XII (R = C$_2$H$_5$) in 88% yield and by de-etherification of the bromohydrin to the bromodiol XIV in 86% yield.

As in the case of the cis methoxy oxide II (R = CH$_3$), the action of hydrobromic acid on the ethyl homologue produced a liquid bromohydrin, b.p. 71–72° at 0.01 mm, in 82% yield. This bromohydrin failed to yield a solid 1-naphthylurethane and gave a liquid acetyl derivative, b.p. 72–74° at 0.05 mm, in 90% yield. The substance was assigned the structure 1α-ethoxy-2α-hydroxy-3β-bromocyclohexane VII (R = C$_2$H$_5$) since de-etheri-fication with hydrogen bromide gave the bromodiol XVI in 51% yield together with 26% of unreacted bromohydrin.

The n.m.r. spectra of the bromohydrin acetates and bromodiol diacetates were measured by Dr. R. R. Fraser of Ottawa University. Interpretation of these spectra according to the principles elaborated by Lemieux, Kullnig, Bernstein, and Schneider (12) fully confirmed the structural assignments made above on the basis of chemical evidence. An additional check on the purity of the two liquid bromohydrins (VII, R = CH$_3$ and C$_2$H$_5$) and their corresponding liquid acetyl derivatives was thereby provided, since there were no abnormalities in the spectra indicative of contamination of any of these sub-stances with positional isomers or stereoisomers.

In recent years considerable attention has been focused upon mechanisms of oxide

ring scissions and the mode of addition of nucleophiles to unsymmetrically substituted oxides. The results of these investigations have been summarized by Winstein and Henderson (4) and Parker and Isaacs (13) in extensive review articles, but no unifying theory capable of accurately predicting the products of such reactions has emerged. The stereoisomeric 1-alkoxy-2,3-epoxycyclohexanes I and II ($R = CH_3$ or C_2H_5), which were first prepared by McRae, Moir, and co-workers (14, 15, 16), provided, during and after elucidation of their structures (5, 1), useful models for examination of certain aspects of the mechanisms of oxide ring cleavages by careful product analysis. Investigations by McRae *et al.* (14), Lemieux, Kullnig, and Moir (5), and Bannard and Hawkins (1) made it evident that under alkaline conditions these oxides are attacked by nucleophiles such as methanol, water, and ammonia predominantly at position 3 (yields in excess of 70%). Although some work on the opening of the oxides under acidic conditions by water (17) and *p*-toluenesulphonic acid (5) was also reported earlier, yields of isolated products were not sufficiently high to permit a definite conclusion to be drawn regarding the preferred position of attack. The results of the present work make it quite clear, however, that position 3 is still the preferred point of attack under acidic conditions and that there is apparently no tendency toward reversal of the mode of opening of the oxide ring in 1-alkoxy-2,3-epoxycyclohexanes as has frequently been observed for unsymmetrical oxides of the type XVII (18, 13, 15, 21).

$$R-CH-CH_2$$

(XVII)

In the reactions cited above, opening of the oxide ring was attended by Walden inversion at position 3, which is suggestive that an S_N2 mechanism is operating (19). This result agrees with the majority of evidence in the literature (13, 15, 20, 21), which supports the S_N2 mechanism for oxide scissions. No indication of the presence of products formed by ring opening with retention of configuration was obtained in any of the work summarized above. This observation makes improbable the intervention of an S_N1 process as a major feature of the mechanism (see references 18, 4, 13, 20, 21) since under such circumstances at least some cis-2,3-oriented products would be expected (13, 19, 20, 21). The latter mechanism may occur to a minor extent, however, because in none of the reactions under consideration was a total material balance of completely characterized products obtained. The results of Lemieux, Kullnig, and Moir (5), obtained when the ring was opened with water under alkaline conditions and arrived at by a method of product analysis which was sensitive enough to reveal minor products formed by attack at position 2, suggests that further careful product analysis is required in all these reactions before intervention of the S_N1 mechanism to a minor extent can be ruled out. No clear picture of the role of polar and steric effects in determining the point of attack of nucleophiles on the 1-alkoxy-2,3-epoxycyclohexanes has resulted. On the basis of simple polar effects and the view that the important feature in S_N2 processes is the facilitation of reagent approach (18, 19, 20) (which is adequate for explanation of the mode of addition to oxides of type XVII), it would be predicted that attack should occur at position 2, which is not the case. Lemieux, Kullnig, and Moir (5) have pointed out however, that the observed result is in agreement with prediction if the governing factor in S_N2 mechanisms is ease of development of carbonium ion character in the transition state (22, 13, 20). Also, there is no uniformity in prediction of the position

of attack by the nucleophile on the basis of Angyal's (23) extension of the Fürst–Plattner rule (24) which visualizes the more stable conformer undergoing reaction to produce a chair form by diaxial ring opening. This theory predicts the observed result for the cis oxides but not for the trans oxides. If the view is taken that steric ease of approach of the nucleophile determines the point of attack, the observed products are predicted for the trans oxides because attack at position 2 is inhibited by the presence of the methoxyl group at position 1 in a cis relationship to the entering nucleophile, as indicated by Lemieux, Kullnig, and Moir (5). However, such an effect would be absent from reactions involving the cis oxides and it might have been expected that attack would occur at positions 2 and 3 with equal facility. It seems evident from these observations that much work still remains to be done before the mechanisms of oxide ring openings can be placed on a firm basis.

EXPERIMENTAL*†

dl-1α-Methoxy-2β-hydroxy-3α-bromocyclohexane (V, R = CH₃)

dl-1β-Methoxy-2α,3α-epoxycyclohexane (42.5 g, 0.332 mole) was dissolved in acetone (100 ml) and the solution was cooled with mechanical stirring to $-10°$. Hydrobromic acid (48%, 56.0 g, 0.332 mole) was added dropwise at $-10°$ to $0°$, the solution was allowed to come to room temperature, the excess acid was neutralized by addition of sodium carbonate, the precipitated salt was removed by filtration, and the solution was evaporated to dryness *in vacuo*. The residue was recrystallized from ether, yielding 43.9 g (63.3%) of *dl*-1α-methoxy-2β-hydroxy-3α-bromocyclohexane, as colorless needles, m.p. 68.5–69°. Calc. for $C_7H_{13}O_2Br$: C, 40.22; H, 6.27; Br, 38.22%. Found: C, 40.10; H, 6.25; Br, 38.10%. A liquid fraction (13.1 g), b.p. 65–67° at 0.03 mm, was also obtained which was shown to contain more of the bromohydrin V (R = CH₃) and a 1-methoxy-2,3-dihydroxycyclohexane (see below).

Derivatives of dl-1α-Methoxy-2β-hydroxy-3α-bromocyclohexane

The phenylurethane (IX, R = CH₃) was obtained in 86.1% yield, m.p. 133–134°, after recrystallization from 95% ethanol. Calc. for $C_{14}H_{18}O_3NBr$: C, 51.23; H, 5.53; N, 4.27; Br, 24.35%. Found: C, 51.13; H, 5.35; N, 4.21; Br, 24.72%.

The 1-naphthylurethane (XI, R = CH₃) was obtained in 94.4% yield, m.p. 185–186°, after recrystallization from ether. Calc. for $C_{18}H_{20}O_3NBr$: C, 57.15; H, 5.33; N, 3.70; Br, 21.13%. Found: C, 57.16; H, 5.28; N, 3.91; Br, 21.12%.

The acetyl derivative was obtained in 90.0% yield as colorless needles, m.p. 56–56.5°, after recrystallization from ether–heptane. Calc. for $C_9H_{15}O_3Br$: C, 43.04; H, 6.02; Br, 31.82%. Found: C, 42.99; H, 6.13; Br, 32.08%.

dl-1α-Methoxy-2β,3α-cyclohexanediol Bis-1-naphthylurethane

A sample (1.00 g) of the liquid fraction from preparation of 1α-methoxy-2β-hydroxy-3α-bromocyclohexane was treated with 1-naphthylisocyanate (2.00 g) at 70°. The crude mixture of resultant 1-naphthylurethanes was washed with petroleum ether, then fractionally crystallized from ether, yielding 0.43 g (27%) of *dl*-1α-methoxy-2β-hydroxy-3α-bromocyclohexane 1-naphthylurethane, m.p. 185–186°—identified by mixed melting point and infrared spectrum, and 0.41 g (13%) of *dl*-1α-methoxy-2β,3α-cyclohexanediol bis-1-naphthylurethane, m.p. 224–226°. Calc. for $C_{29}H_{28}O_5N_2$: C, 71.88; H, 5.82; N, 5.78%. Found: C, 71.72; H, 5.84; N, 5.94%.

*All melting points are uncorrected.
†Microanalyses by J. G. Helie of these laboratories.

2-Methoxyadipaldehyde Bis-2,4-dinitrophenylhydrazone

A second portion (1.00 g) of the above-mentioned liquid fraction was dissolved in ethanol (20 ml) and treated with sodium metaperiodate (3 g in 50 ml water). The solution was kept for 4 hours at room temperature, evaporated to dryness *in vacuo*, and extracted with ether. After evaporation, the residue from the ether extract was treated with 2,4-dinitrophenylhydrazine reagent (25). The bis-2,4-dinitrophenylhydrazone of 2-methoxyadipaldehyde separated as a yellow solid and after recrystallization from ethyl acetate had m.p. 192–193.5°. Yield, 0.64 g (19%). Calc. for $C_{19}H_{20}O_9N_8$: C, 45.24; H, 4.00; N, 22.22%. Found: C, 45.31; H, 4.17; N, 21.80%.

Debromination of dl-2β-Bromo-1α-cyclohexanol Phenylurethane

dl-2β-Bromo-1α-cyclohexanol phenylurethane (cf. Bedos (9)), m.p. 85–87° (0.900 g, 3.02×10^{-3} mole), was debrominated by the same method as described below for *dl*-1α-methoxy-2β-hydroxy-3α-bromocyclohexane phenylurethane. The crude product after recrystallization from ethanol–heptane furnished 0.57 g (86.5%) of cyclohexanol phenylurethane, m.p. 83–84.5°, alone and in admixture with an authentic sample (cf. Stengl *et al.* (10)).

dl-2β-Methoxy-1α-cyclohexanol Derivatives

dl-2β-Methoxy-1α-cyclohexanol was prepared by the method of Winstein and Henderson (8) and converted to the phenylurethane in 82% yield, m.p. 66–67.5°, after recrystallization from aqueous ethanol. Calc. for $C_{14}H_{19}O_3N$: C, 67.45; H, 7.68; N, 5.62%. Found: C, 67.40; H, 7.54; N, 5.70%. The 1-naphthylurethane was obtained in 77% yield, m.p. 111–112°, after recrystallization from ether–heptane. Calc. for $C_{18}H_{21}O_3N$: C, 72.22; H, 7.07; N, 4.69%. Found: C, 72.31; H, 7.09; N, 4.74%.

Debromination of dl-1α-Methoxy-2β-hydroxy-3α-bromocyclohexane Phenylurethane

dl-1α-Methoxy-2β-hydroxy-3α-bromocyclohexane phenylurethane (0.900 g, 2.74×10^{-3} mole) was dissolved in ethanol (50 ml), Raney Nickel W-7 (26) catalyst (10 g) and Amberlite IRA-400 (OH) resin (2 ml) were added, and the mixture was shaken for 24 hours at room temperature at 40 p.s.i. hydrogen pressure. The mixture was filtered and the filtrate was evaporated to dryness *in vacuo* yielding a crystalline residue, which, after recrystallization from ether–heptane, furnished 0.53 g (78%) of *dl*-2β-methoxy-1α-cyclohexanol phenylurethane (X, R = CH₃), m.p. 66–67.5°, alone and in admixture with an authentic specimen. The infrared spectra of the two samples (KBr pellet) were also identical.

dl-2β-Methoxy-1α-cyclohexanol Tetrahydro-1-naphthylurethane (XII, R = CH₃)

dl-2β-Methoxy-1α-cyclohexanol 1-naphthylurethane (0.200 g, 6.7×10^{-4} mole) was reduced by the same method as described for *dl*-1α-methoxy-2β-hydroxy-3α-bromocyclohexane phenylurethane except that ethanol–benzene (2:1, v/v; 30 ml) was used as solvent. Recrystallization of the crude product from aqueous ethanol gave 0.199 g (98.5%) of fine colorless needles, m.p. 89.5–91°. Calc. for $C_{18}H_{25}O_3N$: C, 71.25; H, 8.31; N, 4.62%. Found: C, 71.26; H, 8.27; N, 4.67%.

Debromination of dl-1α-Methoxy-2β-hydroxy-3α-bromocyclohexane 1-Naphthylurethane

dl-1α-Methoxy-2β-hydroxy-3α-bromocyclohexane 1-naphthylurethane (1.00 g, 2.65×10^{-3} mole) was debrominated by the same method as given for *dl*-2β-methoxy-1α-cyclohexanol 1-naphthylurethane. The crude product was recrystallized from aqueous ethanol yielding 0.690 g (86%) of *dl*-2β-methoxy-1α-cyclohexanol tetrahydro-1-naphthylurethane,

m.p. 89.5–91°, alone and in admixture with an authentic specimen. The infrared spectra (KBr pellet) of the two substances were also identical.

dl-2β-Bromo-1α-cyclohexanol 1-Naphthylurethane

This compound was obtained in 75% yield from dl-2β-bromo-1α-cyclohexanol (27) after recrystallization from ether, m.p. 177–177.5°. Calc. for $C_{17}H_{18}O_2NBr$: C, 58.63; H, 5.21; N, 4.03; Br, 22.95%. Found: C, 58.54; H, 5.19; N, 4.19; Br, 22.74%.

Cyclohexanol Tetrahydro-1-naphthylurethane

Cyclohexanol 1-naphthylurethane (cf. Bickel and French (28)), m.p. 131–132.5° (1.10 g, 4.07×10^{-3} mole), was reduced by the same method as described for 2β-methoxy-1α-cyclohexanol 1-naphthylurethane. Recrystallization of the crude product from aqueous ethanol gave 1.01 g (90.2%) of cyclohexanol tetrahydro-1-naphthylurethane as fine colorless needles, m.p. 105–106.5°. Calc. for $C_{17}H_{23}O_2N$: C, 74.69; H, 8.48; N, 5.12%. Found: C, 74.77; H, 8.48; N, 5.15%.

Debromination of dl-2β-Bromo-1α-cyclohexanol 1-Naphthylurethane

dl-2β-Bromo-1α-cyclohexanol 1-naphthylurethane (0.340 g, 9.77×10^{-4} mole) was debrominated by the same procedure as described for dl-2β-methoxy-1α-cyclohexanol 1-naphthylurethane. Recrystallization of the crude product from aqueous ethanol gave 0.250 g (93.7%) of cyclohexanol tetrahydro-1-naphthylurethane as colorless needles, m.p. 105–106.5°, alone and in admixture with an authentic specimen. The infrared spectra (KBr pellet) of the two samples were also identical.

Conversion of dl-1α-Methoxy-2β-hydroxy-3α-bromocyclohexane to dl-1β-Methoxy-2α,3α-epoxycyclohexane via Amberlite IRA-400 (OH) Resin

dl-1α-Methoxy-2β-hydroxy-3α-bromocyclohexane (4.18 g, 0.02 mole) was placed in a 500-ml pressure bottle together with Amberlite IRA-400 (OH) resin (40 ml) and ether (200 ml) and the mixture was shaken for 24 hours at atmospheric pressure. The resin was collected, washed with ether (100 ml), and the filtrate and washings dried over anhydrous sodium sulphate. The ether was removed by distillation at atmospheric pressure, after which the residue was fractionated in vacuo yielding 2.18 g (85.1%) of dl-1β-methoxy-2α,3α-epoxycyclohexane as a colorless oil, b.p. 60–61° at 12 mm, n_D^{25} 1.4511. The substance was identified by its infrared spectrum (1).

Attempted Reduction of dl-1β-Methoxy-2α,3α-epoxycyclohexane with Raney Nickel and Hydrogen

dl-1β-Methoxy-2α,3α-epoxycyclohexane (6.00 g, 4.68×10^{-2} mole), dissolved in ether (100 ml), was shaken with Raney nickel catalyst (10 ml) at room temperature under 40 p.s.i. hydrogen pressure for 24 hours. The mixture was filtered, the filtrate was concentrated by removal of the ether at atmospheric pressure, and the residue was distilled in vacuo yielding 5.60 g (93.4%) of unchanged starting material, b.p. 54–55° at 10 mm, which was identified via its infrared spectrum (1).

Action of Amberlite IR-4B (OH) Resin on dl-1α-Methoxy-2β-hydroxy-3α-bromocyclohexane (V, R = CH₃)

dl-1α-Methoxy-2β-hydroxy-3α-bromocyclohexane (1.00 g, 4.78×10^{-3} mole), dissolved in 95% ethanol (100 ml), was shaken for 24 hours with Amberlite IR-4B (OH) resin. The mixture was filtered, and the filtrate was allowed to evaporate to dryness at room temperature in an evaporating dish. The residual crystals were collected, recrystallized from ether, and identified as dl-1α-methoxy-2β-hydroxy-3α-bromocyclohexane by their melting

point of 68–69°, alone and in admixture with an authentic specimen. Recovery, 0.925 g (92.5%).

De-etherification of dl-1α-Methoxy-2β-hydroxy-3α-bromocyclohexane (V, R = CH₃) to dl-3α-Bromo-1α,2β-cyclohexanediol (XIV)

dl-1α-Methoxy-2β-hydroxy-3α-bromocyclohexane (1.05 g, 5.0×10^{-3} mole) was finely ground and heated for 1.5 hours in a sealed tube at 65° with fuming hydrobromic acid (1.0 ml, 68%, 1.57×10^{-2} mole). The pale yellow solution was transferred quantitatively to a 250-ml, round-bottomed flask (in ca. 50 ml of water), the excess acid was neutralized by addition of solid sodium bicarbonate, and the solution was evaporated to dryness *in vacuo*. The residue was transferred to a Soxhlet extractor, extracted for 4 hours with anhydrous ether, and the extract evaporated to dryness. Crystallization of the product from ether gave 0.861 g (88.8%) of dl-3α-bromo-1α,2β-cyclohexanediol as colorless prisms, m.p. 98–99°. Calc. for $C_6H_{11}O_2Br$: C, 36.94; H, 5.68; Br, 40.97%. Found: C, 36.96; H, 5.64; Br, 41.07%.

Derivatives of dl-3α-Bromo-1α,2β-cyclohexanediol (XIV)

The bis-1-naphthylurethane was obtained in 84.5% yield as fine colorless needles, m.p. 210–210.5°, after recrystallization from acetone. Calc. for $C_{28}H_{25}O_4N_2Br$: C, 63.04; H, 4.72; N, 5.25; Br, 14.98%. Found: C, 62.89; H, 4.93; N, 5.49; Br, 14.68%.

The diacetate was obtained in 95.1% yield as fine colorless needles, m.p. 65.5–66.5°, after recrystallization from ether–heptane. Calc. for $C_{10}H_{15}O_4Br$: C, 43.03; H, 5.42; Br, 28.63%. Found: C, 43.17; H, 5.62; Br, 28.73%.

dl-1α,2β-Cyclohexanediol from dl-2β-Methoxy-1α-cyclohexanol

dl-2β-Methoxy-1α-cyclohexanol (0.650 g, 5.0×10^{-3} mole) was heated for 1 hour at 75° with fuming hydrobromic acid (3.0 ml, 68%, 4.70×10^{-2} mole) in a sealed tube. The product was isolated by the same procedure as described for the de-etherification of dl-1α-methoxy-2β-hydroxy-3α-bromocyclohexane, except that final purification was effected by sublimation *in vacuo*. In this manner, 0.533 g (92.0%) of colorless crystals, m.p. 104.5–105.5°, alone and in admixture with an authentic specimen of dl-1α,2β-cyclohexanediol, were obtained.

Debromination of dl-3α-Bromo-1α,2β-cyclohexanediol (XIV)

dl-3α-Bromo-1α,2β-cyclohexanediol (0.400 g, 2.05×10^{-3} mole) was placed in a 500-ml pressure bottle together with ethanol (100 ml), Amberlite IR-4B (OH) resin (3 g), and Raney nickel catalyst and shaken for 24 hours under 40 p.s.i. hydrogen pressure at room temperature. The mixture was filtered and the crystalline residue, which resulted from evaporation to dryness of the filtrate, was sublimed *in vacuo*, yielding 213 mg (90.3%) of colorless crystals, m.p. 104.5–105.5°, alone and in admixture with an authentic specimen of dl-1α,2β-cyclohexanediol. The infrared spectra of the two specimens (KBr pellet) were also identical.

2-Bromoadipaldehyde Bis-2,4-dinitrophenylhydrazone (XV) from dl-3α-Bromo-1α,2β-cyclohexanediol (XIV)

dl-3α-Bromo-1α,2β-cyclohexanediol (1.00 g, 5.12×10^{-3} mole) and sodium metaperiodate (4.18 g, 2×10^{-2} mole) were dissolved in water and the solution was kept overnight at 25°, then evaporated to dryness *in vacuo* at room temperature. The residue was extracted with ether and the latter was removed *in vacuo*. The product was dissolved in ethanol and treated with 2,4-dinitrophenylhydrazine reagent (25). The yellow precipitate

was collected and washed three times with hot ethanol yielding 2.75 g (96.8%) of 2-bromoadipaldehyde bis-2,4-dinitrophenylhydrazone, m.p. 154–155° (with decomposition). Calc. for $C_{18}H_{17}O_8N_8Br$: C, 39.07; H, 3.10; N, 20.25; Br, 14.44%. Found: C, 39.35; H, 3.09; N, 19.90; Br, 14.41%.

dl-1α-Methoxy-2α-hydroxy-3β-bromocyclohexane $(VII, R = CH_3)$

The procedure was identical with that used for the preparation of dl-1α-methoxy-2β-hydroxy-3α-bromocyclohexane (V, R = CH_3) except that the cis oxide II (R = CH_3) (12.0 g, 9.37×10^{-2} mole) was employed as starting material. The crude liquid product was fractionated *in vacuo* yielding 18.3 g (93.3%) of a colorless viscous oil, b.p. 62–63° at 0.01 mm; n_D^{25} 1.5080. Calc. for $C_7H_{13}O_2Br$: C, 40.22; H, 6.27; Br, 38.22%. Found: C, 40.01; H, 6.17; Br, 38.27%.

Derivatives of dl-1α-Methoxy-2α-hydroxy-3β-bromocyclohexane

The 1-naphthylurethane was obtained in 86.5% yield, m.p. 122–124°, after recrystallization from acetone – petroleum ether (65–110°). Calc. for $C_{18}H_{20}O_3NBr$: C, 57.15; H, 5.33; N, 3.70; Br, 21.13%. Found: C, 57.27; H, 5.16; N, 3.80; Br, 20.83%.

The acetyl derivative was obtained in 95.5% yield as a colorless liquid, b.p. 63–65° at 0.01 mm; n_D^{25} 1.4828. Calc. for $C_9H_{15}O_3Br$: C, 43.04; H, 6.02; Br, 31.82%. Found: C, 43.00; H, 5.94; Br, 32.07%.

De-etherification of dl-1α-Methoxy-2α-hydroxy-3β-bromocyclohexane to dl-3β-Bromo-$1\alpha,2\alpha$-cyclohexanediol (XVI)

dl-1α-Methoxy-2α-hydroxy-3β-bromocyclohexane (2.09 g, 1.0×10^{-2} mole) was subjected to ether cleavage under conditions identical with those used for its stereoisomer. The resultant mixture of oil and crystals (1.82 g) was washed with anhydrous ether to dissolve the oil, and recrystallization of the residue from anhydrous ether gave 1.44 g (73.8%) of dl-3β-bromo-$1\alpha,2\alpha$-cyclohexanediol as colorless prisms, m.p. 70.5–71°. This substance was shown to be quite different from its stereoisomer, by comparison of their infrared spectra (KBr pellet). Calc. for $C_6H_{11}O_2Br$: C, 36.94; H, 5.68; Br, 40.97%. Found: C, 37.11; H, 5.43; Br, 40.78%. The oil fraction from this preparation was distilled in an air bath at 25–30° at 0.001 mm pressure yielding 170 mg (8.1%) of colorless oil, n_D^{25} 1.5085, identified via its infrared spectrum as dl-1α-methoxy-2α-hydroxy-3β-bromocyclohexane (VII, R = CH_3).

Derivatives of dl-3β-Bromo-$1\alpha,2\alpha$-cyclohexanediol

The bis-1-naphthylurethane was obtained in 95.3% yield as colorless crystals, m.p. 176–178°, after recrystallization from ethyl acetate. Calc. for $C_{28}H_{25}O_4N_2Br$: C, 63.04; H, 4.72; N, 5.25; Br, 14.98%. Found: C, 63.20; H, 4.73; N, 5.15; Br, 15.14%.

The diacetyl derivative was obtained in 95.0% yield as a colorless viscous oil, b.p. 85–86° at 0.1 mm pressure; n_D^{25} 1.4810. Calc. for $C_{10}H_{15}O_4Br$: C, 43.03; H, 5.42; Br, 28.63%. Found: C, 43.02; H, 5.20; Br, 28.93%.

2-Bromoadipaldehyde Bis-2,4-dinitrophenylhydrazone (XV) from dl-3β-Bromo-$1\alpha,2\alpha$-cyclohexanediol (XVI)

The procedure used was identical with that given for the periodate oxidation and subsequent 2,4-dinitrophenylhydrazone formation from dl-3α-bromo-$1\alpha,2\beta$-cyclohexanediol (XIV). The bis-2,4-dinitrophenylhydrazone was obtained in 95% yield, m.p. 154–155°, and had an infrared spectrum (KBr pellet) identical with that of an authentic specimen of XV.

Periodate Oxidation of dl-3α-Bromo-1α,2β-cyclohexanediol (XIV) and dl-3β-Bromo-1α,2α-cyclohexanediol (XVI)

The experimental procedure used for periodate oxidation of the bromodiols XIV and XVI was identical with that described earlier for oxidation of the *p*-nitrobenzoyl derivatives of the 3-amino-1,2-cyclohexanediols (1), except that the determinations were performed at 20° and 14-mg samples of the bromodiols were used. The results showed uptake of 1 mole of periodate by the cis diol in 15 minutes and by the trans diol in 180 minutes. Comparison of the $t_{\frac{1}{2}}$ values (1.75 minutes for XVI and 18.0 for XIV) indicated that the rate of oxidation of the cis diol is approximately 10 times that of the trans diol.

dl-1α-Ethoxy-2β-hydroxy-3α-bromocyclohexane (V, R = C$_2$H$_5$)

dl-1β-Ethoxy-2α,3α-epoxycyclohexane (I, R = C$_2$H$_5$) (14.2 g, 0.100 mole) on treatment with hydrobromic acid in the same manner as described for its lower homologue gave 13.6 g (61.0%) of *dl*-1α-ethoxy-2β-hydroxy-3α-bromocyclohexane as colorless needles, m.p. 46–47.5°, after recrystallization from ether. Calc. for C$_8$H$_{15}$O$_2$Br: C, 43.07; H, 6.78; Br, 35.82%. Found: C, 42.91; H, 6.58; Br, 35.61%.

Derivatives of dl-1α-Ethoxy-2β-hydroxy-3α-bromocyclohexane

The phenylurethane (IX, R = C$_2$H$_5$) was obtained as fine needles in 75.3% yield, m.p. 132.5–133.5°, after recrystallization from ether–heptane. Calc. for C$_{15}$H$_{20}$O$_3$NBr: C, 52.64; H, 5.89; N, 4.09; Br, 23.35%. Found: C, 52.68; H, 5.84; N, 4.16; Br, 23.38%.

The 1-naphthylurethane (XI, R = C$_2$H$_5$) was obtained in 96.6% yield as fine needles, m.p. 196–197°, after recrystallization from ethyl acetate. Calc. for C$_{19}$H$_{22}$O$_3$NBr: C, 58.17; H, 5.65; N, 3.57; Br, 20.37%. Found: C, 58.32; H, 5.46; N, 3.88; Br, 20.04%.

The acetate was obtained as fine colorless needles in 92.4% yield, m.p. 29.5–30.5°, after recrystallization from *n*-hexane. Calc. for C$_{10}$H$_{17}$O$_3$Br: C, 45.29; H, 6.46; Br, 30.14%. Found: C, 45.28; H, 6.28; Br, 30.31%.

dl-2β-Ethoxy-1α-cyclohexanol 1-Naphthylurethane (XIII, R = C$_2$H$_5$)

dl-2β-Ethoxy-1α-cyclohexanol (b.p. 75–77° at 11 mm; n_D^{25} 1.4538) was prepared in 73% yield by the same method (8) as used for the corresponding methoxy compound (cf. Mousseron *et al.* (29)) and was converted in 94.2% yield to the 1-naphthylurethane, which was obtained as fine needles, m.p. 131–132°, after recrystallization from ethyl acetate. Calc. for C$_{19}$H$_{23}$O$_3$N: C, 72.81; H, 7.40; N, 4.47%. Found: C, 73.08; H, 7.39; N, 4.67%.

dl-2β-Ethoxy-1α-cyclohexanol Tetrahydro-1-naphthylurethane (XII, R = C$_2$H$_5$)

dl-2β-Ethoxy-1α-cyclohexanol 1-naphthylurethane (0.830 g, 2.66×10^{-3} mole) was reduced by the same method as described for *dl*-2β-methoxy-1α-cyclohexanol 1-naphthylurethane. Recrystallization of the crude product from aqueous ethanol gave 0.760 g (90.3%) of fine colorless needles, m.p. 71–72.5°, of the tetrahydro-1-naphthylurethane. Calc. for C$_{19}$H$_{27}$O$_3$N: C, 71.88; H, 8.57; N, 4.41%. Found: C, 71.80; H, 8.67; N, 4.58%.

Debromination of dl-1α-Ethoxy-2β-hydroxy-3α-bromocyclohexane 1-Naphthylurethane (XI, R = C$_2$H$_5$)

dl-1α-Ethoxy-2β-hydroxy-3α-bromocyclohexane 1-naphthylurethane (0.900 g, 2.88×10^{-3} mole) was debrominated by the same method as described for *dl*-2β-methoxy-1α-cyclohexanol 1-naphthylurethane. The crude product was recrystallized from aqueous ethanol yielding 0.640 g (87.9%) of *dl*-2β-ethoxy-1α-cyclohexanol tetrahydro-1-naphthylurethane as colorless needles, m.p. 71–72.5°, alone and in admixture with an authentic sample. The infrared spectra (5% in carbon tetrachloride) were also identical.

dl-3α-Bromo-1α,2β-cyclohexanediol (XIV) from dl-1α-Ethoxy-2β-hydroxy-3α-bromocyclo-hexane (V, R = C₂H₅)

dl-1α-Ethoxy-2β-hydroxy-3α-bromocyclohexane (1.12 g, 5.0×10^{-3} mole) was subjected to ether cleavage under conditions identical with those described for the lower homologue. The crude product was recrystallized from ether yielding 831 mg (85.7%) of colorless prisms, m.p. 98–99°, alone and in admixture with an authentic specimen of dl-3α-bromo-1α,2β-cyclohexanediol.

dl-1α-Ethoxy-2α-hydroxy-3β-bromocyclohexane (VII, R = C₂H₅)

dl-1α-Ethoxy-2α,3α-epoxycyclohexane (II, R = C₂H₅) (14.2 g, 0.100 mole) was treated with hydrobromic acid in the same manner as described for dl-1β-methoxy-2α,3α-epoxy-cyclohexane. The crude liquid product was fractionated *in vacuo* yielding 18.3 g (82.0%) of dl-1α-ethoxy-2α-hydroxy-3β-bromocyclohexane, b.p. 70–71° at 0.01 mm; n_D^{25} 1.4971. Calc. for $C_8H_{15}O_2Br$: C, 43.07; H, 6.78; Br, 35.82%. Found: C, 43.11; H, 6.85; Br, 35.69%.

dl-1α-Ethoxy-2α-acetoxy-3β-bromocyclohexane

dl-1α-Ethoxy-2α-hydroxy-3β-bromocyclohexane (2.23 g, 1.00×10^{-2} mole) was heated under reflux for 1 hour with acetic anhydride (10 ml). The excess anhydride was removed by distillation *in vacuo* and the residue was distilled *in vacuo* yielding 2.39 g (90.2%) of colorless mobile oil, b.p. 64–64.5° at 0.01 mm; n_D^{25} 1.4760. Calc. for $C_{10}H_{17}O_3Br$: C, 45.29; H, 6.46; Br, 30.14%. Found: C, 45.13; H, 6.13; Br, 30.25%.

De-etherification of dl-1α-Ethoxy-2α-hydroxy-3β-bromocyclohexane to dl-3β-Bromo-1α,2α-cyclohexanediol (XVI)

dl-1α-Ethoxy-2α-hydroxy-3β-bromocyclohexane (2.23 g, 1.0×10^{-2} mole) was subjected to ether cleavage under conditions identical with those described for its homologue, yielding a mixture of oil and crystals (1.67 g) which, after recrystallization from anhydrous ether, gave 988 mg (50.6%) of colorless prisms, m.p. 70.5–71°, alone and in admixture with an authentic sample of dl-3β-bromo-1α,2α-cyclohexanediol (XVI). The residual oil was distilled in an air bath at 28–33° at 0.001 mm pressure yielding 588 mg (26.4%) of colorless oil, n_D^{25} 1.4981, which was identified as dl-1α-ethoxy-2α-hydroxy-3β-bromo-cyclohexane (VII, R = C₂H₅) via its infrared spectrum.

ACKNOWLEDGMENTS

REFERENCES

1. R. A. B. BANNARD and L. R. HAWKINS. Can. J. Chem. **36**, 1241 (1958).
2. P. D. BARTLETT. J. Am. Chem. Soc. **57**, 224 (1935).
3. D. H. R. BARTON, D. A. LEWIS, and J. F. McGHIE. J. Chem. Soc. 2907 (1957).
4. S. WINSTEIN and R. B. HENDERSON. *In* Heterocyclic compounds. Vol. 1. John Wiley & Sons, Inc., New York. 1950. p. 29.
5. R. U. LEMIEUX, R. K. KULLNIG, and R. Y. MOIR. J. Am. Chem. Soc. **80**, 2237 (1958).
6. S. WINSTEIN and L. L. INGRAHAM. J. Am. Chem. Soc. **74**, 1160 (1952).
7. G. E. McCASLAND and E. C. HORSWILL. J. Am. Chem. Soc. **75**, 4020 (1953).
8. S. WINSTEIN and R. B. HENDERSON. J. Am. Chem. Soc. **65**, 2196 (1943).
9. P. BEDOS. Bull. soc. chim. France, **39**, 252 (1926).
10. H. STENGL, F. FICHTER, and H. ARNI. Helv. Chim. Acta, **19**, 392 (1936).
11. E. SCHWENK and D. PAPA. U.S. Patent No. 2,475,718 (July 12, 1949); Chem. Abstr. **43**, 7510*i* (1949).

12. R. U. Lemieux, R. K. Kullnig, H. J. Bernstein, and W. G. Schneider.   J. Am. Chem. Soc. **80**, 6098 (1958).
13. R. E. Parker and N. S. Isaacs.   Chem. Revs. **59**, 737 (1959).
14. J. A. McRae, R. Y. Moir, J. W. Haynes, and L. G. Ripley.   J. Org. Chem. **17**, 1621 (1952).
15. R. Y. Moir.   M.A. Thesis, Queen's University, Kingston, Ont. 1942.
16. S. W. Fenton.   M.Sc. Thesis, Queen's University, Kingston, Ont. 1946.
17. R. Y. Moir.   Ph.D. Thesis, McGill University, Montreal, Que. 1948.
18. R. G. Kadesch.   J. Am. Chem. Soc. **68**, 41 (1946).
19. C. K. Ingold.   Structure and mechanism in organic chemistry. Cornell University Press, Ithaca, New York. 1953.
20. E. S. Gould.   Mechanism and structure in organic chemistry. Henry Holt & Co., New York. 1959. Chap. 8.
21. A. A. Frost and R. G. Pearson.   Kinetics and mechanism. John Wiley & Sons, Inc., New York. 1953. Chap. 11.
22. A. Streitweiser.   Chem. Revs. **56**, 571 (1956).
23. S. J. Angyal.   Chem. & Ind. (London), 1230 (1954).
24. A. Fürst and Pl. A. Plattner.   Abstracts of Papers, 12th International Congress of Pure and Applied Chemistry, New York. 1951. p. 405.
25. R. L. Shriner, R. C. Fuson, and D. Y. Curtin.   *In* The systematic identification of organic compounds. 4th ed. John Wiley & Sons, Inc., New York. 1956. p. 111.
26. H. Adkins and H. R. Billica.   J. Am. Chem. Soc. **70**, 695 (1948).
27. C. O. Guss and R. Rosenthal.   J. Am. Chem. Soc. **77**, 2549 (1955).
28. V. T. Bickel and H. E. French.   J. Am. Chem. Soc. **48**, 747 (1926).
29. M. Mousseron, R. Granger, and A. Merle.   Bull. soc. chim. France, 459 (1947).

NOTES

DIFFUSION OF Zn IN ZnO

E. A. Secco

INTRODUCTION

The experimental results reported in the literature on the diffusion of Zn in ZnO appear conflicting and cannot be fitted to a single conventional defect model. There is also a discrepancy between the parabolic rate constant for zinc oxidation and the diffusion of Zn in ZnO if the Wagner equation (3, 17)

$$K = \int_{a_1}^{a_2} D \, d \ln a$$

relating the parabolic rate constant K and the diffusion coefficient D of the zinc metal is accepted. The diffusion of zinc has been suggested to occur via the interstitial sites. However, the apparent disagreement among the experimental results obtained to date, reviewed elsewhere (1, 2, 3), and reproduced in Table I in simple equation form, has led

TABLE I

		Temp., $^\circ K$	Ref.
Oxidation	Parabolic rate equation		
	$K = 3.3 \times 10^{-7} \exp(-29.0 \text{ kcal}/RT) \text{ cm}^2 \text{ sec}^{-1}$	648–673	Moore and Lee (4)
	$K = 1.1 \times 10^{-5} \exp(-35.0 \text{ kcal}/RT) \text{ cm}^2 \text{ sec}^{-1}$	873–973	Krupkowski and Balicki (5)
	$K = 2.5 \times 10^{-7} \exp(-25.0 \text{ kcal}/RT) \text{ cm}^2 \text{ sec}^{-1}$	703–752	Gebhardt (6)
Exchange	Diffusion equation		
	$D = 4.8 \exp(-73 \text{ kcal}/RT) \text{ cm}^2 \text{ sec}^{-1}$	1183–1300	Secco and Moore (7)
	$D = 1.8 \times 10^5 \exp(-89 \text{ kcal}/RT) \text{ cm}^2 \text{ sec}^{-1}$	1180–1540	Spicar (8)
	$D^* = 30 \exp(-75 \text{ kcal}/RT) \text{ cm}^2 \text{ sec}^{-1}$	1180–1540	Moore (3)
	$D = 1.7 \times 10^2 \exp(-76 \text{ kcal}/RT) \text{ cm}^2 \text{ sec}^{-1}$	1073–1463	Lamatsch (9)
	$k_e = 4.0 \times 10^5 \exp(-40 \text{ kcal}/RT) \text{ sec}^{-1}$	993–1113	Secco (14)
	$D = 10 \exp(73.0 \text{ kcal}/RT) \text{ cm}^2 \text{ sec}^{-1}$	993–1113	Secco (14)
Tracer	Diffusion equation		
	$D = 1.3 \exp(-74 \text{ kcal}/RT) \text{ cm}^2 \text{ sec}^{-1}$	1073–1600	Lindner (10)
	$D = 1.3 \times 10^{-5} \exp(-44 \text{ kcal}/RT) \text{ cm}^2 \text{ sec}^{-1}$	1273–1463	Moore and Williams (11)
Conductivity	Diffusion equation		
	$D = 1.6 \times 10^{-2} \exp(-39 \text{ kcal}/RT) \text{ cm}^2 \text{ sec}^{-1}$	973–1603	Pohl (12)
	$D = 1.5 \times 10^{-2} \exp(-39 \text{ kcal}/RT) \text{ cm}^2 \text{ sec}^{-1}$	1100–1370	Arneth (13)

*This diffusion coefficient is obtained from the one above it by correcting to constant zinc pressure on the basis of $D \propto P_{Zn}^{1/2}$.

to the speculation of other structural defects, such as oxide vacancies and Frenkel defects.

Recently, the exchange of zinc vapor with polycrystalline zinc oxide has been studied in a static system under different conditions of temperature and pressure (14). Plots of $\log_{10} \alpha^*$ (exchange fraction) versus time revealed two processes at the temperatures studied, 720°–840° C. The initial process was a rapid simple exchange whose data were fitted to a first-order rate law with the Arrhenius expression given by

$$k_e = 4.0 \times 10^5 \exp(-40 \text{ kcal}/RT) \text{ sec}^{-1}.$$

This first-order rate law was found to persist to a depth of 20–25 molecular thicknesses

at 720° C, i.e. one half of particle radius, and to increasing depths at the higher temperatures. A second, slower process, which appeared to be diffusion-controlled, with the diffusion equation expressed by $D = 10 \exp (73.0 \text{ kcal}/RT)$ cm² sec⁻¹, followed the initial process. This diffusion equation is in agreement with diffusion equations obtained in other exchange studies using single crystals.

Close examination of the above data reveals that the diffusion coefficient as obtained from the exchange studies is equal to, within the limits of experimental uncertainty, the product of the parabolic rate constant or the diffusion coefficient from conductivity studies and the exchange constant k_e from polycrystalline studies. That is, the diffusion coefficient in the exchange work appears to be a composite quantity consisting of a mobility term and an exchange term, $D_e = D_1 k_e$, namely, an interstitialcy type of diffusion mechanism.

Let us consider an interstitial particle of the non-Frenkel type (interstice occupied by a particle without the existence of a corresponding vacancy) diffusing through a lattice. From Fick's law the diffusion coefficient for the interstitial atom D_1 is $D_1 = \nu_1 \lambda^2 \exp (-E_1/RT)$ cm² sec⁻¹ where λ is the distance between the adjacent interstitial positions, and ν_1 is the frequency of vibration or the number of attempts per second made by the interstitial atom to cross the energy barrier E_1. For diffusion of this type the over-all diffusion coefficient may be expressed as $D = D_1 f_1$ where f_1 = fraction of interstices available for occupancy by a mobile interstitial atom, i.e. $f_1 = (N_1 - n_1)/N_1$ where N_1 = number of *effectively* available interstices and n_1 = number of interstices occupied by atoms. The diffusion coefficient becomes $D = ((N_1 - n_1)/N_1)D_1$. Under conditions of unsaturation, it is assumed that $n_1 \ll N_1$, the diffusion coefficient becomes identical with the interstitial mobility, $D = D_1$. Whereas under equilibrium conditions, when $n_1 \approx N_1$, the diffusion coefficient becomes zero, $D = 0$, which means that the simple interstitial mechanism of diffusion is impossible when all available interstices are occupied. Essentially, this condition is visualized when the direct interstice-to-interstice movement becomes energetically unfeasible because of the narrowing in the constriction separating the interstices at saturation caused by the large difference in radii, 1.4 Å for Zn atom and 0.7 Å for the octahedral interstice. Provided the latter condition obtains, the only other alternative would be a diffusion mechanism of the coupled, interstitial-lattice type.

An inspection of the ZnO lattice shows that an interstitial zinc has the same energy barrier E_1, judging solely from lattice dimensions, by the direct interstice path or via a vacant lattice site. In each case the interstitial atom must move through a similar constriction of the atoms constituting the host lattice. In the case of the interstitialcy mechanism the interstitial must possess an additional energy E_e if the lattice site is occupied. That is, the over-all energy required would be $E_e + E_1$. Now, if the rate of exchange of lattice atoms is given by $k_e = \nu_e \exp (-E_e/RT)$, and the interstitial mobility by $D_1 = \nu_1 \lambda^2 \exp (-E_1/RT)$, then the interstitialcy diffusion coefficient would be expected to be $D = \nu_1 \nu_e \lambda^2 \exp ((E_1 + E_e)/RT) = D_1 k_e$, where $\nu_1 \nu_e$ represents the frequencies of vibration of the interstitial and lattice atoms. Thus diffusion occurs when the normal modes of vibration, with adequate energy, of the interstitial and lattice atoms come sufficiently into phase to give the vital configuration for its critical push. The diffusion equation would be $D = \nu_0 \lambda^2 \exp (-(E_e + E_1)/RT)$ where ν_0 is the over-all frequency of the linked process. Thus, the interstitialcy diffusion coefficient becomes $D = 10^{-2} - 10^{-1} \exp (-(E_e + E_1)/RT)$ cm² sec⁻¹ for $\nu_0 = 3 \times 10^{13}$ sec⁻¹ and $\lambda = 3 \times 10^{-8}$ cm for the case of ZnO.

On the basis of the above discussion the interpretation to be given to the two processes observed in the exchange studies on polycrystalline zinc oxide is that the exchange reaction and zinc diffusion via interstices occur simultaneously. But if the interstitial mobility of the zinc is more rapid the exchange process predominates. As soon as the *effectively* available interstices become filled the transport or diffusion step becomes rate-controlling and supersedes the simple exchange process. The critical experiment to check the above hypothesis and empirical relationship is evidently the exchange reaction between zinc oxide, previously saturated with inactive zinc, and active Zn^{65} vapor.

EXPERIMENTAL

The polycrystalline ZnO used in this work was from the batch previously reported (14). The zinc oxide was exposed to excess inactive zinc vapor, ca. 0.15 atm, at 760° C for 5 hours. The exchange runs using this saturated zinc oxide were carried out in a static system which has already been described.

RESULTS

In Fig. 1 is given a plot of the logarithm of the exchange reaction against time for
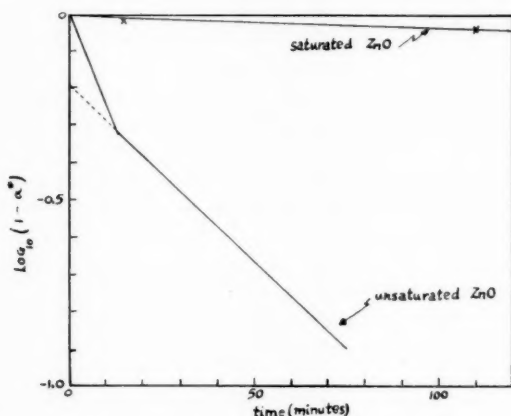
FIG. 1. Plot of logarithm of the unexchanged fraction versus time at 760° C; saturated ZnO curve from present work, unsaturated ZnO from work already reported (14).

Zn^{65} exchange with the saturated ZnO and for Zn^{65} exchange with untreated ZnO, at 760° C. Figure 2 shows the plot of the non-dimensional (Dt/a^2) as a function of time for Zn^{65} exchange with the pretreated ZnO at temperatures 760° and 800° C. The values of Dt/a^2 were taken from Crank (16). The diffusion coefficients were evaluated as the product of the slope of the straight line in Fig. 2 and the square of the particle radius, a^2. The diffusion equation as obtained from these two temperatures is $D = 0.40$ exp $(-76.5 \text{ kcal}/RT)$ cm² sec⁻¹, which is in agreement with existing exchange data on zinc oxide.

It was thought in the pretreatment of ZnO with zinc vapor that sintering could have occurred resulting in a diminution of the surface area and hence increased particle size. The surface area of the oxide used could not be measured but another sample of oxide from the same batch heated in air at 760° C for 2 hours was found to drop from an original
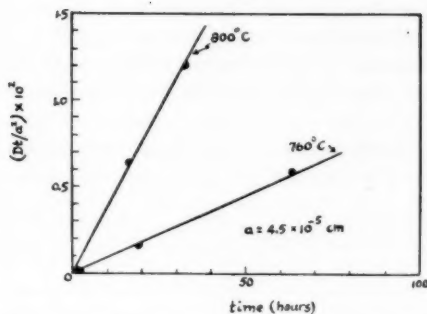
Fig. 2.   Plot of non-dimensional (Dt/a^2) versus time at 760° and 800° C.

value of 3.50 m^2/g to 1.20 m^2/g. The change in surface area is negligible compared to the decrease observed in the exchange reaction rate.

DISCUSSION

It can be concluded that the hypothesis set forth in the introduction of this paper has been verified. The results, therefore, give strong support to the empirical relationship, $D_e = D_1 \cdot k_e$, obtained from the reported data in Table I and the interstitialcy model of diffusion described above. The pre-exponential term for $D_e = D_1 \cdot k_e$, using the mobility term from conductivity measurements, is at variance with the theoretical model by a factor of 10^3. D_1 as calculated from the conductivity data is based on the assumption that the decay in conductivity was due solely to diffusion of interstitial zinc. The latter assumption may or may not be valid. A better fit to the theoretical interstitialcy model is obtained with the mobility term from the parabolic oxidation data.

If the sequence of rate-controlling steps as postulated for the observed processes in the exchange reaction on polycrystalline oxide were correct, then it is possible to calculate the diffusion coefficient of zinc via interstices if the time required for saturation of the oxide with interstitial zinc is taken as that time up to the onset of the interstitialcy diffusion (14). For temperatures 720°, 740°, 760°, and 780° C and using the simple relationship of $a^2 = 2Dt$, where a is the radius of the particle, the diffusion equation $D_1 = 3 \times 10^{-7} \exp(-25 \text{ kcal}/RT)$ cm^2 sec^{-1} was obtained. This equation is concordant with the parabolic rate data, hence the mobility term.

An alternative interpretation of the data in Table I and the results reported herein could be given in terms of zinc vacancies. The existence of zinc vacancies would fit the theoretical model presented, where the mobility term would be diffusion via zinc vacancies under unsaturated conditions, while the exchange reaction under saturated conditions (no Zn vacancies) would consist of an interstitialcy mechanism. This interpretation would demand zinc oxide to be p-type instead of n-type semiconductor as observed. Furthermore, the diffusion constant would show an inverse dependence on zinc pressure, which is not the case.

The parabolic rate and diffusion equations as observed in the oxidation and conductivity studies are explained on the basis of a simple interstitial mechanism. Here, it is assumed that the diffusion coefficient was measured or determined while the excess zinc was diffusing through an unsaturated oxide lattice (oxidation) or out of a saturated oxide (conductivity). In the exchange experiments the diffusion coefficient on the other

hand was determined while the zinc was diffusing through a saturated oxide lattice. The widely divergent results of Lindner on compressed sintered polycrystalline pellets of zinc oxide and of Moore and Williams on single crystals of zinc oxide are explained in a similar manner. That is, the drastic preannealing in the sintering stages of Lindner's experiments permitted saturation of the oxide powder by decomposition of the oxide as already reported (15), while the very moderate preannealing procedure by Moore and Williams produced only a very small concentration of interstitial zinc.

1. G. HEILAND, E. MOLLWO, and F. STOCKMANN. Solid State Phys. **8**, 191 (1959).
2. G. HEILAND and E. MOLLWO. Discussions Faraday Soc. **28**, 123 (1959).
3. W. J. MOORE. Progress Report U.S. Atomic Energy Commission. Indiana University, Bloomington, Indiana. August 1, 1958.
4. W. J. MOORE and J. K. LEE. Trans. Faraday Soc. **47**, 501 (1951).
5. A. KRUPKOWSKI and S. BALICKI. Métaux & corrosion, **12**, 89 (1937).
6. E. GEBHARDT. Z. Metallk. **37**, 87 (1946).
7. E. A. SECCO and W. J. MOORE. J. Chem. Phys. **26**, 942 (1957).
8. E. G. SPICAR. Dissertation, University of Stuttgart, Germany. 1956.
9. H. LAMATSCH. Diplomarbeit, University of Erlangen, Germany. 1958.
10. R. LINDNER. Acta Chem. Scand. **6**, 457 (1952).
11. W. J. MOORE and E. L. WILLIAMS. Discussions Faraday Soc. **28**, 86 (1959).
12. R. POHL. Z. Physik, **155**, 120 (1959).
13. R. ARNETH. Diplomarbeit, University of Erlangen, Germany. 1955.
14. E. A. SECCO. Discussions Faraday Soc. **28**, 94 (1959); Fourth International Symposium on the reactivity of solids, Amsterdam, 1960. In press.
15. E. A. SECCO. Can. J. Chem. **38**, 596 (1960).
16. J. CRANK. The mathematics of diffusion. Clarendon Press, Oxford, 1956. p. 90.
17. C. WAGNER. Atom movements. Am. Soc. Metals, Cleveland, 1953. p. 153.

CONNAISSANCE DES *tert*-BUTYL-4 NITROMÉTHYL-1 CYCLOHEXANOLS-1 *cis* ET *trans*

H. FAVRE ET D. GRAVEL

L'étude de la désamination nitreuse d'α-aminoalcools et plus particulièrement celle de la réaction de Tiffeneau (1) nous ont amenés à préparer les *tert*-butyl-4 nitrométhyl-1 cyclohexanols-1 *cis* (Ia) et *trans* (IIa) et à déterminer leurs configurations respectives. Nous posons que le groupe *tert*-butyle adoptera la conformation équatoriale (2, 3) dans les molécules étudiées.

Ia   R = CH_2NO_2 IIa   III
Ib   R = CH_2NH_2
Ic   R = $CH_2NC_5H_{10}$
Id   R = CH_3 IId

L'action du nitrométhane sur la *tert*-butyl-4 cyclohexanone, en présence d'éthylate de sodium (4), conduit aux deux nitroalcools isomères I*a* et II*a*. Nous avons pu séparer facilement du mélange, par crystallisation fractionnée, l'isomère prédominant p.f. 86–87° et, plus difficilement, l'isomère p.f. 56–57°, qui ne représente que quelques pour-cents du mélange.

Nous attribuons la configuration cis au nitroalcool p.f. 86–87° après l'avoir transformé en méthyl-1 *tert*-butyl-4 cyclohexanol-1 *cis* (I*d*), p.f. 93–95°, en passant par l'α-amino-alcool I*b* et l'époxyde III. Cross et Witham (5) viennent de décrire l'action de l'iodure de méthylmagnésium sur la *tert*-butyl-4 cyclohexanone et d'attribuer la configuration cis à leur isomère p.f. 89–90° et la configuration trans à l'isomère p.f. 70°; ils signalent toutefois que l'isomère cis n'est pas très pur. Dans nos mains les deux isomères purs fondent à 97–98° et 69–70°; nous leur attribuons les configurations cis et trans respective-ment, après avoir mesuré les vitesses de saponification de leurs *p*-nitrobenzoates, à la manière de Hennion et O'Shea (3).

Le passage du nitroalcool I*a* à l'alcool I*d* s'est fait de la manière suivante. L'amino-alcool I*b*, obtenu de I*a* par réduction par le nickel de Raney (4), a été désaminé par l'acide nitreux; le produit brut de désamination a été réduit par l'hydrure de lithium et d'alu-minium, puis oxydé par l'acide chromique et chromatographié: on isole la *tert*-butyl-4 cycloheptanone et l'alcool I*d*. Ces résultats font du produit de désamination de l'amino-alcool I*b* un mélange de *tert*-butyl-4 cycloheptanone et de l'époxyde III.[1] Cet époxyde n'a pas été isolé; outre sa transformation en alcool tertiaire I*d*, qui prouve son existence dans les produits de la désamination de I*b*, il a été caractérisé par un pipéridinoalcool (6) dont la formule probable est I*c*, à l'image de l'ouverture des époxydes dissymétriques par les amines (7, 8). La *tert*-butyl-4 cycloheptanone,[2] produit majeur de la désamination, a été caractérisée par sa dinitro-2,4 phénylhydrazone.

Pour que la preuve de configuration avancée ici soit valable il faut qu'il n'y ait aucune inversion de configuration en passant de I*a* à I*b* à III à I*d*. Les étapes I*a* → I*b* et III → I*d* n'offrent pas de difficultés d'interprétation; elles se font avec rétention de configuration; pour le passage de I*b* à III, nous avançons un mécanisme retenant la configuration, à l'image de la formation des époxydes dans l'agrandissement de cycle des cyclanones par le diazométhane (11) et dans la désamination nitreuse d'aminoalcools axiaux chez les stéroïdes (12, 13, 14).

PARTIE EXPÉRIMENTALE[3]

1. *tert*-Butyl-4 nitrométhyl-1 cyclohexanols-1 cis et trans (Ia et Ib)

En suivant fidèlement les indications opératoires de Dauben *et al.* (4) 25 g de *tert*-butyl-4 cyclohexanone conduisent à 25.8 g (74%) du mélange des deux nitroalcools, I*a* et I*b*, p.f. brut 65–75°. Après une recristallisation dans de l'éther de pétrole on isole 20 g de *tert*-butyl-4 nitrométhyl-1 cyclohexanol-1 *cis* (I*a*) (prismes incolores), p.f. 86–87°. Calculé pour $C_{11}H_{21}O_3N$: C, 61.37; H, 9.83; N, 6.51. Trouvé: C, 61.29; H, 9.91; N, 6.46%. L'isomère trans (II*a*) (paillettes incolores, 400 mg) p.f. 56–57°, s'obtient par 10 recristal-lisations fractionnées du résidu. Trouvé: C, 61.39; H, 9.84; N, 6.49%.

---

[1]*Il est bien connu que la cétone agrandie est le produit majeur de la désamination des aminométhyl-1 cycla-nols-1 (1). Overberger et Katchman (9) ont signalé la formation d'époxydes dans la série hétérocyclique.*

[2]*Nozoe et ses collaborateurs (10) ont obtenu cette cétone en agrandissant la tert-butyl-4 cyclohexanone par le diazométhane.*

[3]*Les points de fusion (p.f.) ont été déterminés en tubes capillaires, avec un thermomètre étalonné avec des substances pures de p.f. connu, en provenance du Bureau des Standards de Washington.*

2. tert-Butyl-4 aminométhyl-1 cyclohexanol-1 cis (Ib)

En suivant fidèlement le mode opératoire de Dauben *et al.* (4) 25 g du nitroalcool I*a*, p.f. 86–87°, conduisent à 21.6 g (84%) du chlorhydrate du *tert*-butyl-4 aminométhyl-1 cyclohexanol-1 *cis* (I*b*), p.f. 235–236°. Calculé pour $C_{11}H_{24}ONCl$: C, 59.57; H, 10.91; N, 6.32. Trouvé: C, 59.40; H, 10.91; N, 6.37%.

3. Désamination du tert-butyl-4 aminométhyl-1 cyclohexanol-1 cis

À 1.2 g de chlorhydrate de *tert*-butyl-4 aminométhyl-1 cyclohexanol-1 *cis* dans 20 ml d'eau on ajoute 5.5 ml de soude 0.1 N pour libérer l'amine de son sel et 9.3 ml d'acide acétique glacial. La petite quantité de chlorure de sodium ne nuit pas à la réaction.

Le mélange est refroidi à 0° et une solution de 1.12 g de nitrite de sodium dans 4.5 ml d'eau est ajoutée goutte à goutte, en 45 minutes. Le mélange est ensuite agité à 0° pendant 2 heures, puis neutralisé par addition d'une solution de soude à 20%, sans que la température ne s'élève au dessus de 0°. On doit cesser l'addition de la soude au moment où l'amino-alcool non-réagi commence à se séparer sous forme de précipité blanc. On ajoute assez d'acide acétique glacial pour redissoudre le précipité, puis 15 gouttes en excès.

La solution acide est extraite à l'éther. Les solutions éthérées sont lavées au bicarbonate de sodium à 5%, à l'eau saturée de chlorure de sodium puis réunies, séchées et évaporées. On obtient une huile jaune pesant 795 mg. Des eaux acides on retire, à la manière habituelle l'aminoalcool qui n'a pas réagi (70 mg). Le produit brut de la réaction (795 mg) est repris par 10 ml de méthanol et 1 ml de pipéridine, puis chauffé à reflux pendant 2 heures. Le solvant est évaporé sous vide à 50°. Le résidu est repris par 100 ml d'éther anhydre; cette solution éthérée est lavée par de l'eau jusqu'à neutralité puis extraite par trois portions de 10 ml d'acide chlorhydrique aqueux 10%.

On examine (A) les solutions aqueuses et (B) la solution éthérée.

(A) Les solutions aqueuses acides sont réunies et évaporées sous vide. On obtient ainsi 82 mg de chlorhydrate de *tert*-butyl-4 pipéridinométhyl-1 cyclohexanol-1 *cis*, p.f. 242–243°. Calculé pour $C_{16}H_{32}ONCl$: C, 66.29; H, 11.13; N, 4.83. Trouvé: C, 66.18; H, 10.92; N, 4.87%.

(B) La solution éthérée est lavée au bicarbonate de sodium à 10%, à l'eau saturée de chlorure de sodium puis séchée et évaporée. On obtient ainsi 768 mg de *tert*-butyl-4 cycloheptanone sous forme d'huile jaune que l'on caractérise par sa dinitro-2,4 phényl-hydrazone p.f. 146–147°. Calculé pour $C_{17}H_{24}O_4N_4$: C, 58.61; H, 6.94; N, 16.08. Trouvé: C, 58.58; H, 6.92; N, 16.19%.

4. Méthyl-1 tert-butyl-4 cyclohexanols-1 cis et trans (Id et IId)

Une solution de 10 g de *tert*-butyl-4 cyclohexanone dans 50 ml d'éther anhydre est traitée à 0° par de l'iodure de méthylmagnésium (préparé à partir de 2.37 g de magnésium et de 23.9 g d'iodure de méthyle dans 160 ml d'éther anhydre) à la façon habituelle. Le mélange des alcools tertiaires est un solide blanc (10.9 g) p.f. 40 à 58°.

Une partie du produit (9.7 g) est mise en solution dans 100 ml d'éther de pétrole (p. éb. 30–43°) et chromatographiée sur 388 g d'alumine Merck pour chromatographie. L'élution de la colonne donne: (*a*) par de l'éther anhydre, une trace de cétone non réagie, identifiée par son spectre infrarouge; (*b*) par un mélange éther 95% – chloroforme 5%, 4.06 g de méthyl-1 *tert*-butyl-4 cyclohexanol-1 *trans* p.f. 69–70° (après sublimation); Cross et Whitham donnent (5) p.f. 70°; (*c*) par un mélange chloroforme 90% – méthanol 10%, 4.16 g de méthyl-1 *tert*-butyl-4 cyclohexanol-1 *cis* p.f. 97–98° (recristallisation dans l'éther de pétrole). Calculé pour $C_{11}H_{22}O$: C, 77.58; H, 13.02. Trouvé: 77.47; H, 13.20%.

Les résultats de cette chromatographie montrent que l'isomère cis et l'isomère trans se sont formés dans un rapport de 1:1.

p-Nitrobenzoates des méthyl-1 tert-butyl-4 cyclohexanols-1 cis et trans

Préparation selon Hennion et Barrett (15).

Cis: p.f. 128–129° (EtOH–eau). Trouvé: C, 67.72; H, 7.94; N, 4.50%.

Trans: p.f. 115–116° (EtOH–eau). Trouvé: C, 67.66; H, 7.91; N, 4.48%. Calculé pour $C_{18}H_{25}O_4N$: C, 67.69; H, 7.89; N, 4.39%.

5. Preuve de configuration du nitroalcool Ia

Le produit brut (1.9 g) obtenu à la suite de la désamination nitreuse de 2.5 g de chlorhydrate du *tert*-butyl-4 aminométhyl-1 cyclohexanol-1 p.f. 235–236° (voir section 3) est immédiatement réduit par 1.9 g d'hydrure de lithium et d'aluminium dans 50 ml d'éther. Le produit de réaction est une huile incolore.

Une solution de 1.0 g de cette huile dans 25 ml d'acide acétique glacial est traitée, à 15°, par 500 mg d'anhydride chromique, ajoutée par petites portions. Le mélange est agité à la température de la pièce pendant 48 heures, puis versé dans 300 ml d'eau glacée et extrait par de l'éther de pétrole (p. éb. 30–43°). La couche organique est lavée par $NaHCO_3$ 10% et à l'eau, puis séchée et évaporée. Le produit brut de la réaction (600 mg) est chromatographié sur 15 g d'alumine Merck pour chromatographie. L'élution de la colonne par un mélange éther de pétrole – éther, donne la *tert*-butyl-4 cycloheptanone, identifiée par son spectre infrarouge et l'élution par de l'éther anhydre donne un solide blanc, p.f. 93–95°, dont le spectre infrarouge est identique à celui du méthyl-1 *tert*-butyl-4 cyclohexanol-1 *cis*, p.f. 97–98°. Point de fusion mixte avec un échantillon authentique: 95–96°.

6. Configuration des alcools tertiaires Id et IId

La configuration des alcools tertiaires est déterminée par l'étude des taux de saponification des *p*-nitrobenzoates à 24.8° dans le mélange acétone–eau, 4–1. La méthode employée est celle utilisée par Hennion et O'Shea (3).

Le *p*-nitrobenzoate de méthyl-1 *tert*-butyl-4 cyclohexanol-1 *trans*, p.f. 115–116°, a donné (deux essais): $k_2 = 4.9 \times 10^{-4}$ et 4.6×10^{-4}, moyenne: 4.75×10^{-4} litre mole^{-1} sec^{-1}. L'isomère cis, p.f. 128–129°, a donné (deux essais): $k_2 = 20.8 \times 10^{-4}$ et 19.5×10^{-4}; moyenne 20.2×10^{-4} litre mole^{-1} sec^{-1}.

1. P. A. S. SMITH et D. R. BAER. Organic reactions. Vol. XI. John Wiley & Sons, Inc., New York 1960. p. 157.
2. S. WINSTEIN et N. J. HOLNESS. J. Am. Chem. Soc. **77**, 5562 (1955).
3. G. F. HENNION et F. X. O'SHEA. J. Am. Chem. Soc. **80**, 614 (1958).
4. H. J. DAUBEN, JR., H. J. RINGOLD, R. H. WADE et A. G. ANDERSON, JR. J. Am. Chem. Soc. **73**, 2359. (1951).
5. B. CROSS et G. H. WHITHAM. J. Chem. Soc. 3892 (1960).
6. E. MOSETTIG et A. BURGER. J. Am. Chem. Soc. **52**, 3456 (1930).
7. S. WINSTEIN et R. B. HENDERSON. Heterocyclic compounds. Vol. 1. John Wiley & Sons, Inc., New York. 1950. p. 33.
8. M. TIFFENEAU, P. WEILL et B. TCHOUBAR. Compt. rend. **205**, 54 (1937).
9. C. G. OVERBERGER et A. KATCHMAN. J. Am. Chem. Soc. **78**, 1965 (1956).
10. T. NOZOE, H. KISHI et A. YOSHIKOSHI. Proc. Japan Acad. **27**, 149 (1951).

11. R. ROBINSON et L. H. SMITH.   J. Chem. Soc. 371 (1937).
12. M. MOUSSERON.   Bull. soc. chim. France, 1008 (1956).
13. R. J. W. CREMLYN, D. L. GARMAISE et C. W. SHOPPEE.   J. Chem. Soc. 1847 (1953).
14. F. WINTERNITZ et S. LADABAUM.   Bull. soc. chim. France, 597 (1960).
15. G. F. HENNION et S. O. BARRETT.   J. Am. Chem. Soc. 79, 2148 (1957).

A CHEMILUMINESCENT REACTION*

H. W. HOLDEN† AND K. O. KUTSCHKE

Recently, Vasil'ev *et al.* (1) observed weak chemiluminescence during the thermal decomposition of certain compounds. Several hydroperoxides were decomposed in their preparative solutions; benzoyl peroxide and azobisisobutyronitrile were studied in chlorobenzene solution. The temperature dependence of the luminescent intensity led the authors to suggest that the emission arose as a rare event which occurred during the combination of radicals. While the evidence for this interpretation is not yet conclusive, it has the corollary that stabilization by emission should be a more probable event in the gas phase where deactivating collisions occur less frequently.

We wish to report here the observation of luminescence in a system containing gaseous ethyl hyponitrite, undergoing thermal decomposition, upon the addition of acetaldehyde. The light was observed with a 1P21 photomultiplier tube in an Eldorado PH200 photometer at signal-to-noise ratios as high as 20 to 1 under some experimental conditions. The system was chosen since it was anticipated that it would contain large concentrations of acetyl radicals produced by the thermal reactions

$$C_2H_5ONNOC_2H_5 \rightarrow 2C_2H_5O + N_2, \tag{1}$$

$$C_2H_5O + CH_3CHO \rightarrow C_2H_5OH + CH_3CO. \tag{2}$$
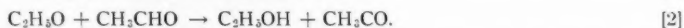
In general terms it was hoped to produce the low-lying triplet state of biacetyl, which possesses a high phosphorescent efficiency (2), by the combination of acetyl radicals formed in [2]. The triplet state is well known in the photochemistry of biacetyl; details of the latter have been reviewed in considerable detail (3).

Ethyl hyponitrite was prepared by Partington and Shah (4) by the esterification of silver hyponitrite with ethyl iodide; they reported a rapid decomposition at 70° C. In our preparation a liberal excess (25–30 mole%) of the silver salt was used (we are indebted to Dr. L. C. Leitch for a supply of silver hyponitrite); this was required because of difficulties encountered in removing ethyl iodide from earlier preparations. The ester, dried over CaCl₂, was introduced into the vacuum system along with a small residue of ether solvent. While the ester was being outgassed at −85° C, it was observed to solidify gradually as the ether was removed. The ester was distilled at −10° C to a storage tube held at −85° C and was stored behind a mercury cutoff. It was crystalline in appearance and melted at a temperature slightly above the −85° C storage temperature.

The cell system consisted of a Pyrex vessel of 8-cm³ capacity having a thinned window. It was contained in an oven and connected by 6 mm i.d. tubing to a magnetically

operated glass circulation pump, a manometer, and a mercury cutoff. Earlier attempts were made to observe the luminescence in a cell designed for measurements of the photo-excited fluorescence. These attempts consumed reagent wastefully since about 75% of the cell system was heated to the decomposition temperature whereas only a small volume could be observed by the photocell.

Measurements of the luminescent intensity were made at several temperatures in the range 56 to 72° C; these yield an apparent activation energy of about 30 kcal/mole. This may be interpreted, following Vasil'ev *et al.* (1), as the activation energy for the decomposition of the ester. At least one alternative explanation involving the reactions

$$R + R \rightarrow R_2^*$$
$$R_2^* + B \rightarrow B^*$$
$$B^* \rightarrow B + h\nu$$
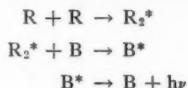
cannot be eliminated on the basis of measurements made thus far. Here R_2^* represents the initially excited dimer of the radicals R (which might be acetyl), and B and B^*, the unexcited and excited states of the product biacetyl. Much more intensive study is required, including identification of the emitting species, before a mechanism can be considered seriously.

The hyponitrite is a difficult compound with which to work and very little is known of the mechanism of its decomposition. The kinetics of the pyrolysis of ditertiarybutyl peroxide are well known. First trials with this initiator were unsuccessful, however, presumably because of the instability of acetyl radicals at the temperature necessary for its rapid decomposition (above 150° C), or because of the instability of the triplet state of biacetyl at that temperature (3).

It is hoped to follow this preliminary investigation with a more complete study in an attempt to determine the mechanism of the phenomenon.

1. R. F. VASIL'EV, O. N. KARPUKHIN, and V. YA. SHLYAPINTOKH. Doklady Akad. Nauk S.S.S.R. **125**, 106 (1959).
2. J. W. SIDMAN and D. S. MCCLURE. J. Am. Chem. Soc. **77**, 6461 (1955). G. M. ALMY and P. R. GILLETTE. J. Chem. Phys. **11**, 188 (1943).
3. W. A. NOYES, JR., G. B. PORTER, and J. E. JOLLEY. Chem. Revs. **56**, 49 (1956). J. HEICKLEN. J. Am. Chem. Soc. **81**, 3863 (1959). R. M. HOCHSTRASSER and G. B. PORTER. Quart. Revs. (London), **14**, 146 (1960).
4. J. F. PARTINGTON and C. C. SHAH. J. Chem. Soc. 2589 (1932).

THE SYNTHESIS OF 17α-FLUOROPROGESTERONE

R. DEGHENGHI AND R. GAUDRY

The biological activity of progesterone can be enhanced by the presence of appropriate substituents in positions α to the 20-carbonyl group. Thus 21-fluoro- and 17α-bromo-progesterone were shown to be twice as active as the natural hormone (1, 2). It was of interest therefore to prepare 17α-fluoroprogesterone and to compare its activity with that of the chloro and bromo analogues.

A previous attempt to introduce a fluorine in position 17 by opening a suitable 16,17-epoxypregnane with hydrogen fluoride, was reported to be unsuccessful (3); we chose, therefore, to investigate the reaction of a 20-cyano-17,20-epoxypregnane (I) with hydrogen halides. The latter pathway was recently used for the preparation of 17α-fluoro-11-dehydrocorticosterone acetate (4). Starting from 17α-bromopregnenolone we prepared readily the corresponding cyanoepoxide (I, R = H) by the action of alcoholic potassium cyanide at room temperature (5, 6). A proof of structure of (I) was obtained by its conversion to the known (7) 17α-chloropregnenolone acetate (III, R = Ac).
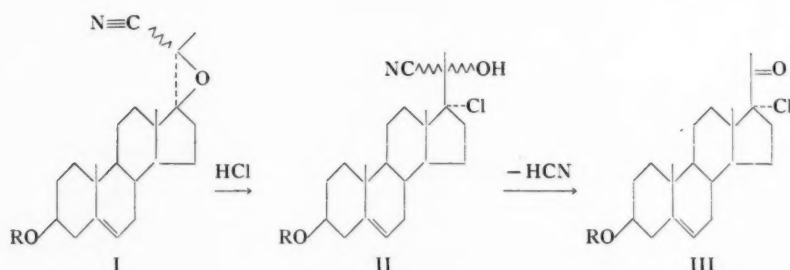
When 17α-bromoprogesterone was similarly allowed to react with potassium cyanide, a crystalline cyanoepoxide was obtained in high yield, the α,β-unsaturated 3-ketone being inert under our reaction conditions. This cyanoepoxide (IV), however, proved to be remarkably stable towards the action of anhydrous HF under the reaction conditions previously described in the 11-oxygenated series (4). It would seem that an 11-oxygen function facilitates the acid-catalyzed opening of the epoxide ring in 17,20 by anhydrous HF. In our case we found that treatment of IV with aqueous HF in a heterogeneous system resulted in the formation of the desired 17α-fluoro-20-cyanohydrin (V), smoothly and in good yield.

The resulting cyanohydrin (V) was found to be stable in non-hydroxylated solvents like ether, but it readily lost the elements of hydrogen cyanide when dissolved in an aqueous alcohol. Alternatively the regeneration of the 20-ketone function was effected by heating the cyanohydrin in organic bases, such as collidine, in a more conventional but less satisfactory manner. A proof of structure for the resulting 17α-fluoroprogesterone was obtained by removal of hydrogen fluoride upon prolonged treatment with refluxing dimethylformamide in the presence of LiBr and Li$_2$CO$_3$ (8), providing the known 16-dehydroprogesterone.
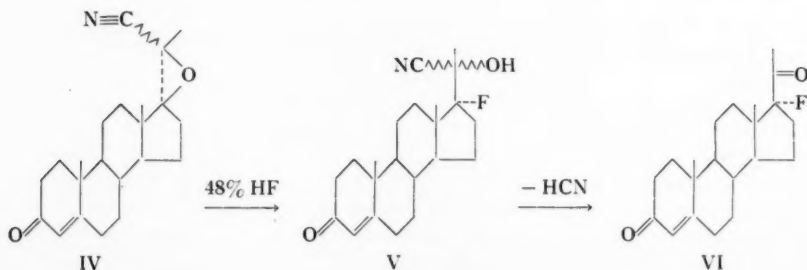
It was interesting to note that a substitution of fluorine at position 17α causes a positive increment in the rotation[1] (see Table I), contrary to the effect of a chlorine or bromine substituent. A hypsochromic displacement of the 20-ketone frequency in the infrared was observed due to the axial fluorine atom. There is only a slight shift with a 17α-chloro substituent, and no effect at all with a 17α-bromine atom. These shifts parallel those observed for an 11-ketone in the 9α-halogenated series (9). 17α-Fluoroprogesterone is slightly less active, in the Clauberg subcutaneous test, than the parent natural hormone.

TABLE I

	$[\alpha]_D$ CHCl$_3$	M_D	ΔM_D	$\Delta\nu$ 20-C=O CHCl$_3$ (cm^{-1})
Progesterone	$+202°$	$+635$	—	—
17α-Br-progesterone (2)	$+ 20°$	$+ 80$	-555	—
17α-Cl-progesterone (7)	$+ 51°$	$+180$	-455	$+ 5$
17α-F-progesterone	$+196°$	$+650$	$+ 15$	$+20$

EXPERIMENTAL[2]

Reaction between 17α-Bromopregnenolone and KCN

17α-Bromopregnenolone (5.00 g) (m.p. 158–159° C) was dissolved in 310 ml of 95% ethanol. A solution of 1.50 g of KCN and 2.20 g potassium acetate in 40 ml water was added and the resulting clear solution was stirred at room temperature for 19 hours. The product (4.0 g) was isolated by pouring the solution into 2 l. of ice water and filtering.

A 2-g portion of the crude bromine-free precipitate was suspended in benzene and chromatographed over 100 g of silica gel. Ethyl acetate – benzene 10:90 eluted 1 g of amorphous material, the infrared spectrum of which was consistent with the *cyanoepoxide* structure I (R = H): ν_{nujol} 3350 cm^{-1} (OH), 2240 cm^{-1} (—CN).

Increasing quantities of EtOAc in benzene eluted crystalline substances whose infrared spectra indicated the presence of a cyanohydrin group, m.p. 250–255° decomp., raised by crystallization from ethanol to 267–298° decomp. A sample was crystallized for analysis, m.p. 290° decomp. According to Barton's suggestions in the corresponding 11-oxygenated series (4) we assign to this substance the structure of a cyclopropanone cyanohydrin VII (or its epimer), intermediate in a Favorski rearrangement. Calc. for

VII
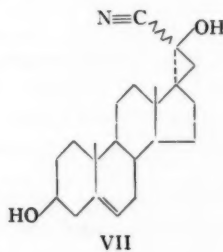
$C_{22}H_{31}O_2N$: C, 77.37; H, 9.15; N, 4.10%. Found: C, 77.67; H, 8.98; N, 3.91%. ν_{nujol} 3440 and 3240 cm^{-1} (OH), 2240 cm^{-1} (C≡N), 1053 cm^{-1} (C—O). Both hydroxyl groups were acetylated by acetic anhydride in pyridine at room temperature.

[1]*Professor Carl Djerassi kindly informed us that he observed a positive Cotton effect for 17α-fluoropregnenolone, prepared independently by Dr. Jensen of the University of Chicago.*
[2]*Melting points were determined in evacuated capillaries and corrected.*

17α-Chloropregnenolone Acetate (III, R = Ac)—Proof of Structure I

The amorphous cyanoepoxide I (0.500 g) was dissolved in 10 ml acetic acid. Anhydrous HCl was bubbled through the solution at room temperature for 30 minutes. A reddish-brown color developed. Ice water was added and the precipitate was collected on a filter and air-dried to give 0.514 g of a solid with a positive Beilstein test. One-half gram of this precipitate (II, R = Ac) was refluxed for 1 hour with 10 ml of toluene and 1 ml of a toluene solution containing 2.3% of collidine. The cooled solution was extracted with CH_2Cl_2, washed with iced dilute HCl, $NaHCO_3$ solution, and water, dried, and the solvent removed to give 0.495 g of a yellow oil which was reacetylated overnight at room temperature with 10 ml of pyridine and 2 ml of acetic anhydride. The usual working up gave 0.472 g of a crude product which was chromatographed on silica gel. EtOAc–benzene 3:97 eluted crystalline fractions (300 mg) which were recrystallized from ether–methanol for analysis, m.p. 142–144° C (III, R = Ac). Calc. for $C_{23}H_{33}ClO_3$: C, 70.30; H, 8.46; Cl, 9.02%. Found: C, 70.52; H, 8.01; Cl, 9.54%. This substance did not depress the melting point of an authentic sample of 17α-chloropregnenolone acetate (7). The infrared spectra were identical.

20-Cyano-17β,20-epoxy-4-pregnene-3-one (IV)

To 17α-bromoprogesterone (20.0 g) in 1200 ml commercial ethanol, there was added a mixture of 5.8 g KCN and 8.5 g CH_3COOK in 150 ml of water. The resulting solution was stirred at room temperature for 24 hours. At the end of this time 3.0 g of 20-cyano-17β,20-epoxy-4-pregnene-3-one crystallized out and was collected on a filter. The alcoholic filtrate was poured into ice water and the precipitate collected on a filter and washed with water. The combined dried precipitate weighed 17.0 g representing crude cyanoepoxide IV, m.p. 230–240° C. A sample was crystallized three times for analysis, m.p. 246–250° C (methanol). $[\alpha]_D^{25}$ +21.3 (CHCl₃ 1%); λ_{max} 241 mμ, ε 17,400. Calc. for $C_{22}H_{29}O_2N$: C, 77.84; H, 8.61; N, 4.13%. Found: C, 77.81; H, 8.46; N, 4.06%. ν_{CHCl_3} 2250 cm⁻¹ (C≡N), 1665 and 1620 cm⁻¹ (3-ketone-Δ⁴). The structure of this substance was proved by conversion to the known 17α-chloroprogesterone (7), m.p. 165–167° C. The infrared spectra were identical and no depression of the melting point with an authentic sample was observed.

17α-Fluoroprogesterone (VI)

20-Cyano-17β,20-epoxy-4-pregnene-3-one (IV), 2.4 g, was slurried with 30 g of 48% aqueous HF at room temperature for 1 hour. The resulting oily substance was taken up in ether and washed to neutrality with $NaHCO_3$ solution and water. Evaporation of the solvent gave 2.45 g of a white solid, which crystallized from ether, m.p. 210–211° decomp. ν_{CHCl_3} 3360 cm⁻¹ (OH), 2240 cm⁻¹ (C≡N), 1663 and 1619 cm⁻¹ (3-keto-Δ⁴). When this substance, representing crude 17α-fluoro-4-pregnene-3-one-20-cyanohydrin, was refluxed in aqueous methanol overnight, HCN gas was evolved and crude 17α-fluoroprogesterone was recovered by evaporation of the solvent. Alternatively the cyanohydrin, 1.0 g, was refluxed for 1 hour in 5 ml of collidine. After the usual working up, 0.98 g of a yellow oil was obtained which was chromatographed on neutral alumina (Woelm III). The petroleum ether – benzene eluates contained 0.450 g of 17α-fluoroprogesterone, m.p. 170–174° C. A sample was recrystallized from acetone–hexane for analysis, m.p. 177–179° C, $[\alpha]_D$ +195.7° (CHCl₃). Calc. for $C_{21}H_{29}O_2F$: C, 75.87; H, 8.79; F, 5.71%. Found: C, 76.08; H, 8.85; F, 5.90%. ν_{CHCl_3} 1718 cm⁻¹ (20-ketone, 17α-fluoro), 1665 and 1620 cm⁻¹ (3-ketone-Δ⁴).

Dehydrofluorination

To 17α-fluoroprogesterone, 130 mg, dissolved in 10 ml of dimethylformamide, there was added 130 mg of LiBr and 130 mg Li_2CO_3. The mixture was refluxed under N_2 for 24 hours. Usual working up gave 80 mg of a yellow oil which crystallized from acetone. The melting point did not depress upon admixture with an authentic sample of 16-dehydroprogesterone, m.p. 184–186° C. The infrared spectrum showed the characteristic Δ^{16} band at 1591 cm^{-1}.

Attempted Reaction of IV with Anhydrous HF

The cyanoepoxide IV, 5.0 g, was dissolved in 100 ml of dry tetrahydrofuran. To this solution, cooled into a dry ice – acetone bath, there was added 20 g of anhydrous HF. The resulting solution was stirred at room temperature for 18 hours. The usual working up (4) gave 5.0 g of a solid which crystallized from ether, m.p. 225–236° decomp. The infrared spectrum was identical with that of IV.

ACKNOWLEDGMENTS

1. P. TANNHAUSER and E. V. JENSEN. J. Am. Chem. Soc. **78**, 2658 (1956).
2. CH. R. ENGEL and H. JAHNKE. Can. J. Biochem. Physiol. **35**, 1047 (1957).
3. E. L. SHAPIRO, M. STEINBERG, D. GOULD, M. J. GENTLES, H. L. HERZOG, M. GILMORE, W. CHARNEY, E. B. HERSHBERG, and L. MANDELL. J. Am. Chem. Soc. **81**, 6483 (1959).
4. H. L. HERZOG, M. J. GENTLES, H. M. MARSHALL, and E. B. HERSHBERG. J. Am. Chem. Soc. **82**, 3691 (1960).
5. R. JUSTONI and M. TERRUZZI. Gazz. chim. ital. **78**, 155 (1948).
6. R. GERBAUX. Bull. acad. roy. Belg. (V) **24**, 88 (1938).
7. D. J. MARSHALL and R. GAUDRY. Can. J. Chem. **38**, 1495 (1960).
8. R. JOLY and J. WARNANT. Bull. soc. chim. France, 367 (1958).
9. A. H. NATHAN, B. J. MAGERLEIN, and J. A. HOGG. J. Org. Chem. **24**, 1517 (1959).

SOME REMARKS ON AGGREGATION OF POLYTHENE IN SOLUTION

H. P. SCHREIBER

INTRODUCTION

In a recent article Trementozzi (1) noted serious differences in the weight-average molecular weights, $\overline{M_w}$, obtained for high- and low-pressure polythene samples from light scattering in α-chloronaphthalene (α-CN) and tetralin solutions. He suggested that these differences were due to association of polythene molecules in α-CN solutions at the temperatures in question (∼100–140° C). Thus, the α-CN data presumably gave the dimension of aggregates of polythene chains, rather than that of the average molecular chain. The suggested association was supported by data showing a decrease in $\overline{M_w}$ values obtained for one high-pressure polythene as the temperature of the α-CN solutions rose from 95–141° C. Subsequently Tung (2) noted similar differences in $\overline{M_w}$ values

obtained for low-pressure polythenes from light scattering in α-CN solution and from calculations involving their intrinsic viscosities, $[\eta]$, in tetralin solution. Tung postulated the existence of long-chain branches in the supposedly linear polythenes used in his work. Long branching would reduce values of the intrinsic viscosity of the polymers (3) and result in calculations of erroneously low $\overline{M_w}$ values from an equation established on the basis of calibration data obtained for linear polythenes. This postulate gives internal consistency to the results, but does not explain the results of the earlier work (1), in which light scattering in α-CN and tetralin solutions of high-pressure polythenes (which are generally assumed to contain long-chain branches) also resulted in large $\overline{M_w}$ differences.

The possible aggregation of polythene in α-CN solution would cast doubt on a considerable body of published molecular weight data. Consequently comparisons of the temperature coefficients of intrinsic viscosity of two polythenes in α-CN and tetralin solutions were carried out to test further the possibility of association. This article reports the results of these comparisons.

THEORETICAL

The well-known theoretical treatment of Flory and Fox (4) gives the intrinsic viscosity $[\eta]$ of a polymer solution as

$$[1] \qquad\qquad\qquad [\eta] = KM^{\frac{1}{2}}\alpha^3$$

where M is the molecular weight of the polymer, K is a temperature-dependent parameter, and α is the linear expansion coefficient which depends on the configuration of the polymer molecule in a specified solution.

The temperature dependence of $[\eta]$, discussed in detail by Flory (5) and more recently by Kawai and Ueyama (6), is due to the temperature coefficients of K and α in equation [1]. In general, K tends to decrease as the temperature rises, but its temperature dependence is generally small compared with that of α. The temperature dependence of α may be shown (5, 6) to reflect the solvent–polymer interaction in any system, the sign being settled by the heat of dilution in the pertinent system. As a rule, for nonpolar polymer–solvent systems this is positive (5). Thus in polythene solutions, α may be expected to increase with increasing temperature, especially in the vicinity of θ, the critical temperature for miscibility of the infinite polymer homologue in a given solvent.

If, in the investigated temperature range 100–150° C, appreciable association between polythene molecules occurs in α-CN solutions as compared with tetralin solutions, then the degree of solvent–solute interaction in α-CN is appreciably less than in tetralin solutions. The α-CN solutions are consequently closer to their characteristic θ temperatures and the temperature coefficient of $[\eta]$ in α-CN should be positive and significantly greater than that in tetralin. Further, if the assumption of aggregation is true, the greater tendency for expansion of the polythene molecules in tetralin solutions must result in $[\eta]_t > [\eta]_{\alpha\text{-CN}}$ at comparable temperatures (the subscript t is used to denote tetralin solution). These experimental consequences seem necessary to support the contention of association, although they are not sufficient to establish this behavior unequivocally.

EXPERIMENTAL

Materials

Two unfractionated polythenes were used in this work. One was a low-pressure linear polythene L, the other a high-pressure branched polythene B. Some of their physical properties are summarized below. Methyl group contents for the two samples were

	Density (g/cc)	CH$_3$/1000 carbons	$\overline{M_w}$
Polythene L	0.960	1.1	13.5×10^4
Polythene B	0.920	22.7	12.8×10^4

obtained from infrared spectrophotometry and attest to the essential linearity of sample L, and the presence of branches in B. The $\overline{M_w}$ values were obtained from light-scattering measurements in α-CN solution at 120° C using a modified Bryce-Pheonix apparatus. In view of the uncertainty of the meaning of the values, however, the quoted molecular weights are not considered to be absolute. The two samples were in fact chosen because of similarities in their melt viscosities over an appreciable shear-stress range, which suggested that their molecular weights were not greatly different.

Viscosity Measurements

Solution viscosity measurements were carried out in modified Ubbelohde viscometers described by Schulken and Sparks (7), and no kinetic energy or shear corrections were applied. In the investigated range, 100–150° C, temperatures were controlled to about ±0.05° C. Polythene samples used to make up appropriate solutions were stabilized against oxidation by incorporating 0.1% by weight of a commercial antioxidant on a two-roll mill. Viscosity measurements on the redistilled solvents showed these to be thermally stable over periods which were long compared with the working life of a given solution. Minimum exposure of solutions to air was ensured by carrying out all viscosity determinations in a nitrogen atmosphere. Intrinsic viscosities were obtained from extrapolation to zero concentration (c) of plots of η_{sp}/c vs. c and ln η_r/c vs. c, where η_{sp} is the specific viscosity and η_r the relative viscosity of the solution. These plots were found to be linear in the range $0.1 < c < 0.6$ g/100 ml. Values of [η] so obtained had a high degree of internal consistency, the precision being not less than ±2%.

RESULTS

The pertinent intrinsic viscosity data are given in Table I. The temperature coefficient

TABLE I
Intrinsic viscosities of polythene solutions at various temperatures

Temp. (°C)	[η] (dl g^{-1})			
	Polymer L		Polymer B	
	Tetralin	α-CN	Tetralin	α-CN
100	1.91		1.21	
110		1.43		1.00
120	1.94	1.47	1.23	1.02
140	1.94	1.56	1.21	1.05
150	1.92	1.60	1.19	1.07

of [η] in α-CN is positive and substantially greater for both polythenes than the corresponding coefficients in tetralin solutions. Further, the [η] values in tetralin for both polymers are significantly greater than the corresponding α-CN values. This indicates a greater tendency for polymer expansion in tetralin, which is therefore thermodynamically the better solvent. The results are in keeping with the theoretical development outlined above; consequently they are consistent with the supposition of solute aggregation in α-CN solutions of polythene (1).

DISCUSSION

Differences between the $[\eta]$–temperature relationships of polythenes L and B are more readily seen from a plot of $[\eta]$ versus T, such as given in Fig. 1. The temperature
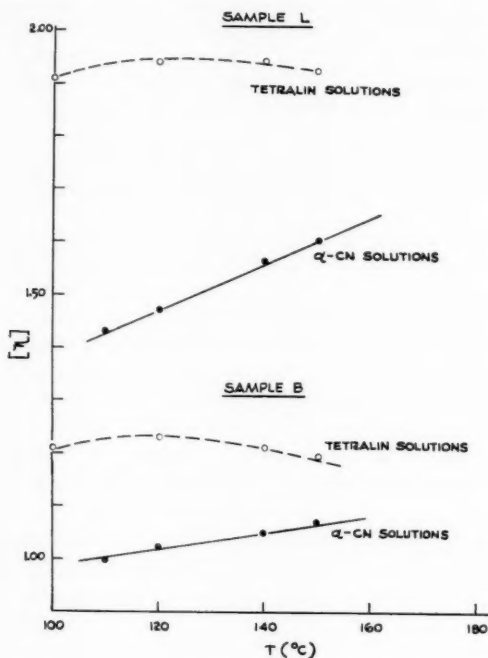
FIG. 1.   Temperature dependence of intrinsic viscosity in polythene solutions.

coefficient of $[\eta]_{\alpha\text{-CN}}$ for polythene L is substantially greater than for polythene B, the respective slopes of the linear plots being 2.1×10^{-3} and 1.2×10^{-3}. Since the apparent $\overline{M}_w$ of these samples is roughly equivalent, it is suggested that the polymer L – α-CN pair may be closer to its characteristic θ temperature than the pair polymer B – α-CN at the temperatures involved in these experiments. In terms of a solute-association hypothesis, the molecules of polymer L thus have a greater tendency for aggregation than do those of polymer B. In view of the generally held opinion that linear polymers are more subject to segmental entanglements (8) than are branched polymers, an aggregation in α-CN solution could result simply from the inability of the weak solvent to disrupt these entanglements. The aggregation should therefore be increasingly evident with rising molecular weight, lowered temperature (in line with the findings of Trementozzi (1) and Tung (2)), and increasing linearity of the polythene, but should be partially reduced or eliminated in thermodynamically better solvents such as tetralin.

The $[\eta]_t$ values appear to attain a maximum near 120° C, more noticeably so for polythene B. Kawai and Ueyama (6) have recently suggested such a maximum to be generally expected in high-polymer systems and have noted its occurrence in polythene–xylene. The temperature at which this maximum occurs increases with the flexibility

of the polymer chain (6); since the maximum for sample L should then occur at a somewhat higher temperature than that of sample B, its more pronounced manifestation in polythene B may be understood. The weak temperature coefficient of $[\eta]_t$ indicates a general balance of thermal effects due to changes in K and α of equation [1] and, as previously noted, suggests an appreciably stronger solvent–solute interaction than in the α-CN solution systems.

The temperature at which the solute molecule appears to expand to the same extent in α-CN as it does in a corresponding tetralin solution may be estimated from the $[\eta]$–T relationships in Fig. 1. Thus, if $[\eta]_t$ is assumed to attain a maximum near 120° C for both polythenes, then the linear $[\eta]_{\alpha\text{-CN}}$–$T$ plots may be extrapolated to the appropriate maximum value of $[\eta]_t$. For polythene L the temperature for "solvent equivalence" appears to be about 230° C; for B about 270° C. This admittedly gross procedure suggests that light-scattering experiments using α-CN solutions of polymers L and B at the above temperatures, and tetralin solutions at 120° C, should yield equal values of $\overline{M_w}$ for each of the two resins. Both of the suggested temperatures for α-CN experimentation would, of course, be well beyond limits of practicability.

CONCLUSIONS

Tetralin is thermodynamically a superior solvent for polythene than α-CN. At the temperatures normally utilized for light-scattering measurements of $\overline{M_w}$, α-CN solutions of polythene seem closer to their characteristic θ temperatures, and would therefore be the preferred solution systems for such measurements, provided no solute aggregation occurred. The present results, however, are fully consistent with the suggestion of polythene aggregation in α-CN solutions (1), although they do not unequivocally establish its existence. In view of this, further critical experimentation into the state of the polymer molecule in α-CN solution would appear to be called for.

1. Q. A. TREMENTOZZI. J. Polymer Sci. **36**, 113 (1959).
2. L. H. TUNG. J. Polymer Sci. **46**, 409 (1960).
3. B. H. ZIMM and R. W. KILB. J. Polymer Sci. **37**, 19 (1959).
4. P. J. FLORY and T. G. FOX, JR. J. Am. Chem. Soc. **73**, 1904 (1951).
5. P. J. FLORY. Principles of polymer chemistry. Cornell University Press, Ithaca, New York. 1953. Chap. XIV.
6. T. KAWAI and T. UEYAMA. J. Appl. Polymer Sci. **3**, 227 (1960).
7. R. M. SCHULKEN and M. L. SPARKS. J. Polymer Sci. **26**, 227 (1957).
8. F. BUECHE. J. Chem. Phys. **20**, 1959 (1952).

NOTES TO CONTRIBUTORS

Canadian Journal of Chemistry

MANUSCRIPTS

General.—Manuscripts, in English or French, should be typewritten, double spaced, on paper $8\frac{1}{2}\times11$ in. **The original and one copy are to be submitted.** Tables and captions for the figures should be placed at the end of the manuscript. Every sheet of the manuscript should be numbered. Style, arrangement, spelling, and abbreviations should conform to the usage of recent numbers of this journal. Greek letters or unusual signs should be written plainly or explained by marginal notes. Characters to be set in bold face type should be indicated by a wavy line below the characters. Superscripts and subscripts must be legible and carefully placed. Manuscripts and illustrations should be carefully checked before they are submitted. Authors will be charged for unnecessary deviations from the usual format and for changes made in the proof that are considered excessive or unnecessary.

Abstract.—An abstract of not more than about 200 words, indicating the scope of the work and the principal findings, is required, except in Notes.

References.—These should be designated in the text by a key number and listed at the end of the paper, with the number, in the order in which they are cited. The form of the citations should be that used in this journal; in references to papers in periodicals, titles should not be given and only initial page numbers are required. The names of periodicals should be abbreviated in the form given in the most recent *List of Periodicals Abstracted by Chemical Abstracts*. All citations should be checked with the original articles and each one referred to in the text by the key number.

Tables.—Tables should be numbered in roman numerals and each table referred to in the text. Titles should always be given but should be brief; column headings should be brief and descriptive matter in the tables confined to a minimum. Vertical rules should not be used. Numerous small tables should be avoided.

ILLUSTRATIONS

General.—All figures (including each figure of the plates) should be numbered consecutively from 1 up, in arabic figures, and each figure referred to in the text. The author's name, title of the paper, and figure number should be written in the lower left corner of the sheets on which the illustrations appear. Captions should not be written on the illustrations.

Line drawings.—Drawings should be carefully made with India ink on white drawing paper, blue tracing paper, or co-ordinate paper ruled in blue only; any co-ordinate lines that are to appear in the reproduction should be ruled in black ink. Paper ruled in green, yellow, or red should not be used. All lines must be of sufficient thickness to reproduce well. Decimal points, periods, and stippled dots must be solid black circles large enough to be reduced if necessary. Letters and numerals should be neatly made, preferably with a stencil (**do NOT use typewriting**), and be of such size that the smallest lettering will not be less than 1 mm high when the figure is reduced to a suitable size. Many drawings are made too large; originals should not be more than 2 or 3 times the size of the desired reproduction. Wherever possible two or more drawings should be grouped to reduce the number of cuts required. In such groups of drawings, or in large drawings, full use of the space available should be made; the ratio of height to width should conform to that of a journal page ($5\frac{1}{2}\times7\frac{1}{4}$ in.), but allowance must be made for the captions. **The original drawings and one set of clear copies (e.g. small photographs) are to be submitted.**

Photographs.—Prints should be made on glossy paper, with strong contrasts. They should be trimmed so that essential features only are shown and mounted carefully, with rubber cement, on white cardboard, with no space between those arranged in groups. In mounting, full use of the space available should be made. **Photographs are to be submitted in duplicate;** if they are to be reproduced in groups one set should be mounted, the duplicate set unmounted.

REPRINTS

A total of 100 reprints of each paper, without covers, are supplied free. Additional reprints, with or without covers, may be purchased at the time of publication.

Charges for reprints are based on the number of printed pages, which may be calculated approximately by multiplying by 0.5 the number of manuscript pages (double-space typewritten sheets, $8\frac{1}{2}\times11$ in.) and including the space occupied by illustrations. Prices and instructions for ordering reprints are sent out with the galley proof.

Contents